

SCOURGE OF THE EMPIRE? ANCIENT PATHOGEN GENOMICS AND
THE BIOSOCIAL CONTEXT OF MALARIA IN IMPERIAL PERIOD
SOUTHERN ITALY (1st-4th C. A.D.)

SCOURGE OF THE EMPIRE? ANCIENT PATHOGEN GENOMICS AND
THE BIOSOCIAL CONTEXT OF MALARIA IN IMPERIAL PERIOD
SOUTHERN ITALY (1st-4th C. A.D.)

By

STEPHANIE-MARIE MARCINIAK, H.BSc., M.A.

A Thesis Submitted to the School of Graduate Studies in Partial Fulfillment of the
Requirements for the Degree Doctor of Philosophy

McMaster University © Stephanie-Marie Marciniak, September 2016

DOCTOR OF PHILOSOPHY (2016)

McMaster University

(Anthropology)

Hamilton, Ontario

TITLE: Scourge of the Empire? Ancient Pathogen Genomics and the Biosocial Context of Malaria in Imperial Period Southern Italy (1st-4th c. A.D.)

AUTHOR: Stephanie-Marie Marciniak, H.BSc. (University of Toronto), M.A. (Trent University)

SUPERVISOR: Dr. Hendrik N. Poinar

NUMBER OF PAGES: 289

Abstract

The complementarity of ancient DNA lends itself to integration with paleopathological inquiries of disease, particularly in scenarios where there is limited or conflicting historical, skeletal, and archaeological information in a given spatio-temporal context. This thesis expands on molecular approaches applied to the detection of “invisible” pathogens associated with non-catastrophic morbidity and mortality that are embedded in a unique biosocial context of the disease experience. Presented in ‘sandwich-thesis’ format, I explore the historical narrative surrounding malaria in Imperial period Italy (1st-4th c. A.D.) using a molecular approach that is integrated with an ecosocial framework, as well as addressing the methodological challenges of identifying pathogens in contexts without *a priori* knowledge or incongruous evidentiary sources. My research presents the first partial mitochondrial genome for *P. falciparum* recovered from two adults (prioritized from a subset of 58 individuals) in disparate ecological and social localities in Imperial period Italy. This provides a timestamp for this ancient protozoan parasite, with an emphasis on a multi-faceted approach to frame the human-parasite-vector-environment interactions in the studied localities. Additionally, I successfully applied an in-solution hybridization capture technique designed to detect over 1,000 human pathogens in archaeological samples, both of known and unknown pathogen constituents. This technique qualitatively and quantitatively assesses the likelihood of low abundance pathogenic targets that are present, in order to prioritize candidates to further pursue with downstream

analyses, as well as beginning to explore the synergistic landscape of pathogen-pathogen interactions. In combination, the research outlined in this thesis emphasizes the molecular and biosocial experience of disease as interconnected elements in dynamic epidemiological environments of the past.

Acknowledgements

This thesis was a journey of stubborn perseverance – a “never tell me the odds!” strategy. With vast uncertainty, I was able to pursue ideas for the sake of knowledge and curiosity. This would not have been possible without the support of family, friends, and the mentorship of my supervisory committee.

My supervisory committee is the most amazing trifecta of people assembled. These past five (!) years went by in a blink, and this process was enriched by each of you. Ann, you are truly inspiring and have richly influenced my approach to integrated anthropological research. Tracy, the guidance that you provided helped me to explore research avenues that challenged my own thinking. Hendrik, as a supervisor, the dedication and commitment you have to your students is unrivalled. I am exceedingly fortunate to have been mentored by you as the ultimate Obi-Wan (à la Alec Guinness).

This research is also a testament to the collaborative and creative atmosphere embodied by the current and past members of the McMaster Ancient DNA Centre. I am immensely grateful for the years of assistance and feedback as this research went from an amorphous blob to an actualized project (with results!).

Naturally, heartfelt appreciation goes to my parents, and sister, Marinna, who supported me at every stage, and reminded me to keep a “work”-life balance.

A special thanks is extended to the collaborators that contributed to elements of this work. I am grateful for the financial support provided by the Department of Anthropology, Ontario Graduate Scholarship, and the Social Sciences and Humanities Research Council of Canada.

Mischief managed.

Table of Contents

Title Page	i
Descriptive Notes.....	ii
Abstract.....	iii
Acknowledgements.....	v
Table of Contents	vi
List of Tables	ix
List of Figures	xi
List of Abbreviations	xiii
Statement of Academic Achievement.....	xiv
CHAPTER 1: INTRODUCTION.....	1
The Antiquity of Malaria’s Association with Humans	2
Framing Health and Disease in the Empire	5
Contextualizing the “Roman Malaria”	8
Integrating Ancient DNA in the Detection of Pathogens	11
Study Context.....	16
Theoretical and Methodological Framework.....	18
Research Questions	22
Thesis Format.....	26
CHAPTER 2: <i>PLASMODIUM FALCIPARUM</i> MALARIA IN 1ST-2ND C. A.D. SOUTHERN ITALY.	32
References.....	40
Supplemental Information	42
Supplementary Appendix Figures.....	69
Supplementary Appendix Tables.....	83

CHAPTER 3: A MULTI-FACETED APPROACH TO FRAMING MOLECULAR SIGNATURES OF <i>PLASMODIUM FALCIPARUM</i> MALARIA IN IMPERIAL PERIOD SOUTHERN ITALY (1ST-4TH C. A.D.)	107
Abstract	108
Introduction.....	109
Pathogenesis and post-mortem detection of malaria	113
Malaria in ancient Rome.....	117
Materials and Methods.....	120
Context of the Imperial period Italian cemeteries	120
Results.....	126
Discussion.....	132
The anthropogenic context for malaria in Imperial Italy.....	133
Conclusions.....	144
Acknowledgements.....	146
Literature Cited	148
CHAPTER 4: PARALLEL HYBRIDIZATION CAPTURE OF MULTIPLE PATHOGENS IN ARCHAEOLOGICAL SAMPLES: TOWARDS INTEGRATED PALEOPATHOLOGICAL INVESTIGATIONS	161
Abstract	162
Introduction.....	163
Pathogen detection strategies.....	166
Pathogen capture overview	170
Methods.....	173
Results.....	175
Discussion.....	196
References.....	199
Supplementary Appendix.....	204
Supplementary Methods	205
Supplementary Results.....	208
A. Taxonomic distributions for select samples.....	208
B. LLNL and HTS analysis	208
Supplementary References.....	232

CHAPTER 5: DISCUSSION AND CONCLUSIONS	234
Catastrophic Malaria and the Molecular Evidence	237
Malaria pathogenesis impacts its post-mortem recovery.....	238
Reconciling the genomic evidence with the historical record	242
The Epidemiological Context of Malaria in Imperial Southern Italy	246
Malaria intensification under a burgeoning Empire	248
A) Intensification of the agricultural economy.....	250
B) Spatial heterogeneity framing exposure	252
C) “Preventative” measures of malaria.....	256
D) “Local” and “non-local” individuals’ vulnerability to malaria	256
Synergistic Pathogen Interactions and Ancient DNA.....	259
Conclusions.....	266
Future Research Directions.....	269
REFERENCES.....	272

List of Tables

CHAPTER 2: *PLASMODIUM FALCIPARUM* MALARIA IN 1ST-2ND C. A.D. SOUTHERN ITALY

Supplemental Table

Supplemental Table S1. <i>P. falciparum</i> capture summary	65
---	----

Supplementary Appendix Tables

Table 1. Sequences included in <i>Plasmodium</i> spp. mitochondrial baits design	83
Table 2. Sets of <i>Plasmodium</i> spp. enriched libraries	84
Table 3. Blocking oligonucleotide sequences.....	85
Table 4. Metagenomic assessment of prioritized Imperial Italian samples	86
Table 5. <i>P. falciparum</i> capture summary.....	87
Table 6. LG20-LV13 <i>P. falciparum</i> coverage metrics	89
Table 7. <i>Plasmodium</i> spp. combined mapped data metrics	90
Table 8. <i>Plasmodium</i> spp. and Apicomplexan mtDNA conservation	91
Table 9. <i>P. falciparum</i> SNP identification.....	93
Table 10. LG20-LV13 SNPs and amino acid translation	96
Table 11. <i>Plasmodium</i> spp. used in the phylogenetic analysis.....	97
Table 12. Human mitochondrial genome SNP identification.....	99
Table 13. Human mitochondrial genome coverage metrics	105
Table 14. LG20 and LV13 haplogroup comparisons to rCRS database matches	106

CHAPTER 3: A MULTI-FACETED APPROACH TO FRAMING MOLECULAR SIGNATURES OF *PLASMODIUM FALCIPARUM* MALARIA IN IMPERIAL PERIOD SOUTHERN ITALY (1ST-4TH C. A.D.)

Table 1. Metagenomic analysis of the prioritized samples.....	128
Table 2. Estimated endogeneity of the prioritized Imperial Italian shotgun sequenced data	129
Table 3. <i>P. falciparum</i> coverage metrics for LG20 and LV13	130
Table 4. LG20-LV13 coverage metrics for <i>P. falciparum</i> and human mtDNA.....	131

CHAPTER 4: PARALLEL HYBRIDIZATION CAPTURE OF MULTIPLE PATHOGENS IN ARCHAEOLOGICAL SAMPLES: TOWARDS INTEGRATED PALEOPATHOLOGICAL INVESTIGATIONS

Table 1. Pre-capture shotgun data for primary pathogen constituents	179
Table 2. Post-capture summary for “known” samples	180
Table 3. Post-capture summary for “unknown” samples	181
Table 4. Summary of probe hits for Black Death specimen (P06BD)	191
Table 5. Summary of probe hits for cholera specimen (P20CH).....	194
Supplementary Appendix Tables	
Table S1. Family-level probes identified from alignments to the sequence data, full results	214
Table S2. Taxonomic assessment of sequence data, full results	225

List of Figures

CHAPTER 2: *PLASMODIUM FALCIPARUM* MALARIA IN 1ST-2ND C. A.D. SOUTHERN ITALY

Figure 1a. Burial of individual F234 at Vagnari.....36

Figure 1b. Maximum likelihood phylogenetic tree38

Supplemental Figure

Figure S1. Composite of the map of the cemeteries, fragment length distribution, damage profiles, and phylogenetic tree63

Supplementary Appendix Figures

Figure 1a. *P. falciparum* mtDNA (LG20-LV13) fragment length distribution.69

Figure 1b. *P. falciparum* fragment length distribution for LV13.70

Figure 1c. LG20 human mtDNA fragment length distribution71

Figure 1d. LV13 human mtDNA fragment length distribution.72

Figure 2a. *P. falciparum* mtDNA (LG20-LV13) damage profile (min 24bp, MQ 30, with stacks).....73

Figure 2b. *P. falciparum* mtDNA (LG20-LV13) damage profile (min 30bp, MQ 30, with stacks).....74

Figure 2c. *P. falciparum* mtDNA (LG20-LV13) damage profile (min 30bp, MQ 30, stacks removed).....75

Figure 2d. LG20 human mtDNA damage profile (min 30bp, MQ 30)76

Figure 2e. LV13 human mtDNA damage profile (min 30bp, MQ 30).....77

Figure 3. Examples of stacked and repetitive regions78

Figure 4a. Randomized LG20 human mtDNA damage profile to approximate *P. falciparum* (with stacks).....79

Figure 4b. Randomized LV13 human mtDNA damage profile to approximate *P. falciparum* (with stacks).....80

Figure 4c. Randomized LG20 human mtDNA damage profile to approximate *P. falciparum*81

Figure 4d. Randomized LV13 human mtDNA damage profile to approximate *P. falciparum*82

CHAPTER 3: A MULTI-FACETED APPROACH TO FRAMING MOLECULAR SIGNATURES OF *PLASMODIUM FALCIPARUM* MALARIA IN IMPERIAL PERIOD SOUTHERN ITALY (1ST-4TH C. A.D.)

Figure 1a. Map of the cemeteries in Imperial period Italy113
Figure 1b. Overlay of Luigi Torelli’s identification of malarious areas in Italy (1882, “Carta della malaria dell’Italia”) constituting the “malaria belt”126
Figure 2. Contextualization of malaria in Imperial Italy133

CHAPTER 4: PARALLEL HYBRIDIZATION CAPTURE OF MULTIPLE PATHOGENS IN ARCHAEOLOGICAL SAMPLES: TOWARDS INTEGRATED PALEOPATHOLOGICAL INVESTIGATIONS

Figure 1. Workflow summary.....175
Figure 2. Number of reads taxonomically identified to respective primary targets for "known" samples177
Figure 3. Number of reads taxonomically identified for "unknown" samples.....178
Figure 4. Number of reads taxonomically identified for reagent controls and sediment samples178
Figure 5. Post-capture comparisons for primary pathogenic targets in the known samples.....185
Figure 6. Microbial profile for Imperial Italian (Vagnari) juvenile.....186
Figure 7. Post-capture microbial profile for the Italian child mummy187
Figure 8. Post-capture comparison of sediments188
Figure 9. CLiMax algorithm applied to Black Death sample (P06BD)192
Figure 10. CLiMax algorithm applied to cholera sample (P20CH)195

Supplementary Appendix Figures

Figure S1. Maritime Archaic adult post-capture microbial profile.209
Figure S2. Plague of Justinian #2 post-capture microbial profile.....210
Figure S3. Italian adult mummy post-capture microbial profile_210
Figure S4. Italian child mummy #2 post-capture microbial profile211
Figure S5. Imperial Italian adult post-capture microbial profile.212
Figure S6. Vagnari juvenile post-capture microbial profile.212
Figure S7. Troy sediment post-capture microbial profile.....213

List of Abbreviations

aDNA	Ancient DNA
AD	Anno Domini
bp	Base pair
BC	Before Christ
BWA	Burrows-Wheeler Aligner
blast	Basic Local Alignment Search Tool
DDT	Dichlorodiphenyltrichloroethane
DNA	Deoxyribonucleic acid
DTT	Dithiothreitol
EDTA	Ethylenediaminetetraacetic acid
FLD	Fragment Length Distribution
G6PD	Glucose-6-phosphate dehydrogenase
Hg	Human genome
LLNL	Lawrence Livermore National Laboratory
LLMDA	Lawrence Livermore Microbial Detection Array
MQ	Mapping Quality
ML	Maximum Likelihood
MEGAN	MEtaGenome ANalyzer
mtDNA	Mitochondrial deoxyribonucleic acid
PTB	N-phenacylthiazolium bromide
PCR	Polymerase Chain Reaction
PVPD	Polyvinylpyrrolidone
rCRS	Revised Cambridge Reference Sequence
RPM	Revolutions per Minute
rRNA	Ribosomal ribonucleic acid
SNP	Single Nucleotide Polymorphism
sp.	Single species
spp.	Multiple species
Tris-HCl	Tris hydrochloride

Statement of Academic Achievement

I am the main contributor to the three articles that comprise this thesis. Chapter 2 “*Plasmodium falciparum* malaria in 1st-2nd c. A.D. southern Italy” is a co-authored paper accepted as a Correspondence to Current Biology, and Chapter 3 “A multi-faceted approach to framing molecular signatures of *Plasmodium falciparum* malaria in Imperial period southern Italy (1st-4th c. A.D.)” is also a co-authored paper situating the genomics in an anthropological context, submitted to the American Journal of Physical Anthropology. For these two papers, I am the first author, conducting all laboratory work and analyses, with collaboration on the phylogenetic analyses from my co-authors. Further to Chapter 3, collaboration from co-authors assisted in gathering bioarchaeological information on the cemeteries. I wrote the first draft, prepared the figures and tables, and collaborated with co-authors for subsequent revisions. Chapter 4 “Parallel hybridization capture of multiple pathogens in archaeological samples: towards integrated paleopathological investigations” is a co-authored paper for submission to Nature Scientific Reports. As first author, I performed all laboratory work and subsequent analyses, with collaboration from co-authors on the algorithmic analyses and interpretations. I wrote the first draft, prepared the figures and tables, with feedback from co-authors for revisions.

CHAPTER 1: INTRODUCTION

Malaria presence in ancient Rome represents a paradox, as the pathogen is accorded a significant role in rupturing the fabric of the Empire (1st-5th c. A.D.), exacting a toll on health, life expectancy, social relations, and the economy (Sallares, 2002; Scheidel, 2009; Soren, 2003); however, the evidentiary support remains a patchwork woven from the writings of ancient scholars and modern parallels drawn from recent urban settings. In the discourse of malaria in ancient Rome, inferences imply a fixed rather than dynamic nature of this disease, due to particular factors invoked to substantiate its expected scope and scale in antiquity, ranging from biological (e.g., periodic fevers), social (e.g., urbanization), to environmental (e.g., swamps or marshes).

To address the prevailing narrative of this “Roman malaria”, I focus on contemporaneous Imperial period (1st-4th c. A.D.) cemeteries of varied social and ecological contexts (i.e., coastal port cities and a rural inland estate) in southern Italy (Isola Sacra, Velia, and Vagnari) through a multi-faceted approach. First, using ancient DNA analyses to definitively establish the presence of malaria in human skeletal remains; and second, grounding the molecular results in ecosocial theory (Krieger, 1994, 2001, 2011) to frame the potential spectrum of exposure pathways (e.g., relationships between the pathogen, humans, and environment) by integrating elements of the historical record (e.g., ancient literary sources) and archaeological evidence (e.g., paleoenvironment). The only existing molecular evidence for malaria in Imperial period Italy is an 89-base pair *P. falciparum* 18S

rRNA fragment from one infant in Lugnano (central Italy, 450 A.D.) (Sallares & Gomzi, 2001). The dearth of molecular investigations of malaria in Imperial Italy since 2001 requires a critical re-evaluation of the degree to which an integrated ancient DNA and anthropological approach is applicable to evaluate the distribution of this parasite alongside the human experience of this disease in the past.

The Antiquity of Malaria's Association with Humans

By framing malaria within an ecosocial framework, the emphasis remains on the active interaction between an individual in a given spatio-temporal context where a complex interplay between social, biological, and ecological factors influence the distribution of disease (Krieger, 1994, 2001, 2011). The individual (biological) response to malaria via inoculation by the *Anopheles* vector is variable, due to the spectrum of clinical responses to this haematogenous infection (i.e., asymptomatic to lethal), with influences from the *Plasmodium* parasite (e.g., virulence or parasitization rate of susceptible host cells) and vector biology (e.g., intensity of host-feeding to transmit infection) (Ali et al., 2008; Crompton et al., 2014). This biological response is further embedded within the social and ecological context, as demographic factors (e.g., population growth, movement or migration), technological changes (e.g., urbanization, changing land use patterns) or cultural experiences (e.g., medical belief systems related to causation and prevention) impact the distribution of this disease in ways that are unpredictable not only contemporarily (Packard & Brown, 1997), but in antiquity.

The challenge of inferring the distribution of malaria in antiquity is confounded by the limited evidentiary sources available, which is predominantly molecular genomics and the literary record. *Plasmodium* species are presumed to predate hominids, with divergence from other Apicomplexans several hundred million years ago (Rich & Ayala, 2006). The overarching consensus is *P. falciparum* became a threat to human health 6,000-8,000 years ago during the Neolithic Revolution in Africa (as part of a series of transitions to agriculture occurring in different regions across various timescales), where the confluence of optimum climate, increased population density, and anthropogenic modifications, enhanced the diversification and specialization of anthropophilic vectors that ultimately created a sustainable scenario for malaria (Armelagos & Harper, 2005; Tishkoff et al., 2001). This is indirectly supported by recent signatures of selection in the human genome for the protective polymorphisms of sickle cell, thalassemia, and glucose-6-phosphate dehydrogenase (G6PD) mutations arising 1,500-10,000 years ago, where geographic distributions coincide with regions previously or currently malarious (different populations developing independent responses) (Carter & Mendis, 2002; Hartl, 2004; Tishkoff et al., 2001).

However, there are disparate views on *Plasmodium* population history itself, ranging from a recent expansion 10,000 years ago leading to low genetic diversity of the genome (e.g., Conway et al., 2000; Joy et al., 2003; Rich et al., 1998) while others (e.g., Hughes & Vierra, 2001; Mu et al., 2002) suggest hundreds of thousands of years resulting in high genetic diversity of the genome.

It is presumed that malaria existed prior to the advent of agriculture, while the “African origin” *P. falciparum* malaria parasite population (arising from a cross-species transmission from a gorilla) transformed to virulent strains under the mutually reinforcing factors of agricultural expansion, thereby spreading to North Africa, the Near East, and regions beyond (Hartl, 2004; Kwiatkowski, 2005; Loy et al., 2016; Tishkoff et al., 2001). Overall, the phylogenetic picture does not preclude human *Plasmodium* in the Mediterranean; however, the timing of its entry to Europe is uncertain, (broadly generalized as the Holocene), while its historical distribution is unknown.

The post-Africa malaria migration is extended by the writings of ancient scholars, although there is incomplete knowledge about malaria in antiquity. Various literary sources such as the Nei Ching (China, 5th c. B.C.), Vedic and Brahmanic scriptures (Indus Valley, 4th to 2nd c. B.C.), Sumerian and Egyptian texts (5th c. B.C.) as well as the Hippocratic Corpus (Greece, 5th c. B.C.) note the “classic” malaria symptomology of febrile paroxysms (i.e., chills, fever, sweating) and enlarged spleens, with connections to the environment (e.g., marshes) or seasons (e.g., late summer and early autumn) (Carter & Mendis, 2002). Most critically, descriptions in ancient texts do not permit definitive identification of a causative malaria species; however, contemporary scholars (e.g., Grmek, 1991; Jones, 1909; Sallares, 2002; Scheidel, 2003) infer “benign or mild tertian fevers” as *P. vivax*, “malignant tertian” as *P. falciparum*, and “quartan” as *P. malariae*. The fragmentary survival of an extensive literary record, although suggestive of

malaria broadly in the Near East and Mediterranean regions, does not provide a lens to specifically situate malaria in a given location, at a specific moment in historical time. Paleopathological evidence supporting malaria in antiquity is also lacking, due to the absence of skeletal involvement during infection (Kindt et al., 2007), with assessments relying on non-specific manifestations of physiological stress (e.g., lesions on the cranial vault or orbits identified as porotic hyperostosis and cribra orbitalia, respectively) that are of increased prevalence in presumably malarious environments in the past, such as Egypt (e.g., Nerlich et al., 2008; Rabino Mass et al., 2000; Smith-Guzman, 2015) or Imperial Rome (e.g., Gowland & Garnsey, 2010).

Based on the historical and lasting effect of malaria on the human genome, is it possible to detect its influence in more recent human history, such as Imperial Italy, where the confluence of ecological, social, and biological factors presume a scenario of sustainability for this parasite? Can the local factors contributing to the malaria story in Imperial Italy be untangled with an integrated ancient DNA and anthropological approach? The following sections will frame these questions.

Framing Health and Disease in the Empire

The precise demographic conditions of ancient Rome “are remarkably poorly known” (Scheidel, 2009: 2), which affects the scope of inferring disease distribution, as population density and quality of infrastructure are critical determinants of health (Dyson, 2010; Nutton, 2004). There is an emphasis on drawing parallels from recent urban settings, such as pre-industrial London

(Scheidel, 2009), while Nutton (2004) generalizes that health conditions in antiquity were likely similar to a contemporary third-world country with high mortality rates for children and low life expectancies for adults (ages 30-40 years) with localized outbreaks of infectious disease. The picture of disease is framed by chronic infections (e.g., tuberculosis, leprosy), acute diseases (e.g., smallpox, cholera, malaria), and opportunistic infections (e.g., gastroenteritis attributed to *Salmonella* spp., *Staphylococcus* spp.) (e.g., Grmek, 1991; Nutton, 2004; Sallares, 2002; Scheidel, 2003, 2009).

Despite the range of potential circulating diseases, a question remains – how healthy was the populace in Italy beyond the Roman capital during antiquity? The predominant discourse focuses on the city of Rome, while much remains unknown regarding other parts of the Roman world. As a result, the disparate perspectives on health result from the limited evidence and the manner of interpretation (Morley, 2005). One model argues physiological stressors of “urbanization” (particularly in cities), such as poor nutrition, crowded living conditions and “unsanitary” practices (e.g., absence of sanitary facilities in dwellings, improper corpse disposal, ineffective sewage and wastewater removal) created substandard living conditions (Dyson, 2010; Sallares, 2002; Scheidel, 2003, 2009; Scobie, 1986). For example, the sewage system is argued to have functioned as a drain (rather than carrying waste away), with aqueducts creating overflows, and perpetual surface cesspools of gastroenteritis and helminth infections (Dyson 2010; Hansen, 1983; Scheidel, 2003, 2009). The converse

conceptualization argues the urban environment of the city in terms of town planning (e.g., location of houses or ceremonial complexes) and public facilities (e.g., bathhouses, latrines, or piped water) provided a measure of health for the inhabitants, in a relatively pleasant environment (Morley, 2005). Similarly, relative health in rural areas in the absence of “unhealthy” city conditions is presumed, where for example, field drainage may remove reservoirs for water- or vector-borne diseases (Dyson 2010). Rather than life as “nasty, brutish and short” (Dyson, 2010: 5), it is critical to emphasize health is not simply an absence of disease (Morley, 2005), but a confluence of factors (e.g., social, biological, ecological) that manifest dynamically, whether in urban, suburban or rural locales.

In light of these discordant scenarios of life in the Empire, there is an absence of evidence (e.g., historical, literary or skeletal) on the constitution of health and disease in areas beyond the city of Rome. There are Roman period skeletal assemblages (e.g., Beauchesne, 2012; Cucina et al., 2006; Eckardt, 2010; Facchini et al., 2004; Gowland & Garnsey, 2010; Killgrove, 2010), indicating stressors associated with life during this time (e.g., cribra orbitalia, porotic hyperostosis, linear enamel hypoplasia); while inferences of the infectious disease burden remain limited. The complexity of morbidity and mortality patterns requires exploring how diseases structured life in this period (Oerlemans & Tacoma, 2014).

Contextualizing the “Roman Malaria”

It is within this scenario of presumed high mortality and poor life expectancy that the prevalence and pathogenicity of malaria, particularly *P. falciparum*, is posited to have intensified over time in ancient Rome, becoming a threat in the early Imperial period (1st to 2nd c. A.D.) due to population expansion, agricultural practices, and economic activity alongside increased travel and extensive trading networks (Bruce-Chwatt & de Zulueta, 1980; Brunt, 1971; Sallares et al., 2004; Scheidel, 2009). The basis for inferences of malaria in ancient Rome is predominantly drawn from the literary record, which poses unique challenges in inferring the Roman experience of disease, with one outstanding question – are the “fevers” noted by various writers equivalent to “malaria”?

Inferences about health and disease in the Roman context are embedded within the Hippocratic medical philosophy that persisted until the 17th century A.D. (Cruse, 2004; Scarborough, 1969). In this system of thought, the humours (blood, phlegm, yellow and black bile) and elemental qualities determine individual health and susceptibility to disease (Cruse, 2004; Nutton, 2004). Health is a balanced mixing of elements (*eukrasia*) whereas disturbances in the balance of one or more humours create excess or deficiency, resulting in disease (*dyskrasia*) (Cruse, 2004; Jouanna, 1999; Nutton, 2004). There is no single causal explanation for disease, with the result that many illnesses were attributed to noxious odours (bodily or religious pollution rather than infection) acting on an

individual's constitution through climate or geography (Jouanna, 1999; Langholf, 1990). The doctrine of critical days explains disease progression through the crisis (*krisis*) as a point of recovery or death on particular days alongside certain symptoms (Langholf, 1990; Nutton, 2004). For example, sweats in febrile diseases, were favourable “on the third, fifth, seventh, ninth, eleventh, fourteenth, seventeenth, twenty-first, twenty-seventh and thirty-fourth day” in restoring humoral balance (Hippocrates, *Aphorisms, IV*, in Adams, 1891).

Accordingly, the Greek and Roman literary record is the main source that supports malaria as present in ancient Greece as early as the 5th century B.C., with entry into southern Italy by the 3rd to 2nd centuries B.C. (Sallares, 2002; Sallares et al., 2004). From the time of Hippocrates (5th c. B.C.), Celsus (1st c. A.D.), and Galen (2nd c. A.D.), fevers were considered a disease (embodying a range of illnesses) rather than a symptom where causation was attributed to: an imbalance or noxious build-up of the humours; the blockage of bodily pores, trapping heat; overheating due to travel, stress or anger; breathing putrefied vapours in the air near stagnant water; or divine origins (e.g., the goddess Febris, dragons or demons) (Cunha & Cunha, 2008; Neghina et al., 2010). The classification of fevers based on the periodicity of paroxysms (chills, fevers, sweats, exacerbation) and remissions (e.g., tertian, semi-tercian, quartan, quotidian) connect health to the uniformity of nature and the cosmos (e.g., four humours, four elements, four seasons, four fevers) (Cunha & Cunha, 2008; Jones, 1909; Jouanna, 1999). Although the environment is recognized as one of many

factors influencing health, the causal mechanisms behind disease (i.e., bacteria or parasites) are not part of the Roman nosological experience, which limits specific inferences on the geographic extent of malaria (as understood today).

The social, political, and economic consequences of malaria in ancient Rome is also inferred by retrospective applications of morbidity and mortality characterizing Italy's 20th century struggles with malaria (see Snowden, 2008). For example, an observed 60% mortality rate among 20-50 year olds in Grosseto (Tuscany) is linked to funerary inscriptions from 4th and 5th century A.D. Rome, where 38% of the recorded 4,000 deaths occurred during the late summer and early autumn (August to October), which is presumed as typical of *P. falciparum* seasonal mortality (Baldari et al., 1998; Sallares, 2002; Scheidel, 2003, 2009). Similarly, the geographic distribution of malaria during this contemporary period as along the Tiber River and into Tuscany (Sallares, 2002; Sallares et al., 2004), provides a modern counterpart from which scholars infer distribution in Roman antiquity; however, the presumption of homogeneous responses (e.g., biological, ecological, social) are not coincident with the dynamism of malaria infection. In the absence of demographic data for ancient Rome (Morley, 2013; Shaw, 1996), a comparative framework is beneficial for reconstructing a presumptive scenario of malaria distribution, with the recognition that host and pathogen interactions are inherently complex.

Ultimately, the narrative of malaria in ancient Greece and Rome is “cumulative” (Jones, 1909: 175) where the entirety of disparate accounts rather

than the details supports inferences of its presence; however, its scope and scale remain uncharacterized throughout the duration of its presumed influence during the Imperial period (1st-5th c. A.D.).

Integrating Ancient DNA in the Detection of Pathogens

The application of molecular techniques to recover DNA from fossils, museum specimens, and human skeletal or archaeological remains characterizes the field of ancient DNA (aDNA). Previous research successfully identified pathogen DNA in the absence of skeletal lesions, for example in tuberculosis (Baron et al., 1996) and recently, genomic signatures of acute infections (not inducing skeletal responses) are retrievable, such as *Yersinia pestis* associated with the 14th c. A.D. Black Death pandemic (Bos et al., 2011; Drancourt et al., 1998; Raoult et al., 2000), and the Plague of Justinian (541-543 A.D.) (Wagner et al., 2014); an 1849 A.D. pandemic strain of *Vibrio cholerae* (Devault et al., 2014a); and *P. falciparum* malaria (5th c. A.D.) (Sallares & Gomzi, 2001).

The integration of ancient DNA complements skeletal, archaeological or historical evidence; however, there are unique challenges in confirming the presence of disease-associated pathogens in antiquity through this approach. Primarily, molecular and chemical degradation accumulating over time non-specifically fragments the DNA into an abundance of short sequences (30 to 60 base pairs or bp) (Molak & Ho, 2011; Orlando, Gilbert & Willerslev, 2015; Pääbo et al., 2004). These fragments are embedded in a pool of exogenous (contaminant) DNA that may characterize up to and exceed 90% of the molecular constituents

(e.g., environmental, microbial, or modern sources) with only 0-5% endogenous DNA (Burbano et al., 2010; Carpenter et al., 2013; Molak & Ho, 2011; Orlando, Gilbert & Willerslev, 2015). Further, as part of the endogenous DNA component, the human pathogen fraction is typically of even lower abundance (Rollo & Marota, 1999) and often far less than 1% of the overall molecular constituents (e.g., less than 0.008% in Devault et al., 2014b), but exceptional specimens, such as calcified nodules (e.g., Devault et al., n.d.; Kay et al., 2014), may contain a rich pathogen fraction. Ultimately, the use of robust techniques to capture this minute portion, to the exclusion of all other molecules from a dynamic microbial pool requires specific molecular targets to maximize pathogen recovery.

The recovery of surviving ancient pathogen DNA also depends on understanding pathogenesis, essentially the localization or dissemination of microbes throughout infection to sample from the most appropriate site (as influenced by immune responses and physiological factors affecting post-mortem pathogen survivability). Early research by Faerman and colleagues (1997) demonstrated direct evidence of bacilli is obtainable in teeth or bones upon haematogenous spread. For acute infections or those that do not leave skeletal signatures, the ability to recover DNA depends on the degree of bacteremia (dissemination of pathogens via the blood), to optimize recovery in bone marrow or teeth (dental pulp and tooth roots). Successful detection of such acute infections from teeth was demonstrated for *Yersinia pestis* (14th c. A.D. Black Death pandemic) (Bos et al., 2011; Drancourt et al., 1998; Raoult et al., 2000;

Schuenemann et al., 2011). As malaria is a blood-borne pathogen, the potential exists for its recovery from dental pulp or bone marrow (Drancourt & Raoult, 2005), although it has yet to be attempted. Pathogens also variably persist in ancient tissues after death, where for example, *Y. pestis* was recovered from five of 46 tooth samples from the East Smithfield Black Death epidemic cemetery (Bos et al., 2011). Similarly, some pathogens are notoriously challenging to retrieve, such as *Treponema pallidum*, attributed to the low pathogen load in the tertiary stage of the disease (bone involvement) (Bouwman & Brown, 2005; Kindt et al., 2007; von Hunnius et al., 2007). The interpretation of positive or negative molecular results remains a challenge, as neither outcome provides absolute answers as pathogenic remnants may not be present in detectable amounts (Donoghue & Spigelman, 2006).

The scope of previous biomolecular investigations of malaria in antiquity (predominantly in Egypt) focused on the immunological detection of *P. falciparum* targets (e.g., histidine-rich protein 2, antigenic variants) or *Plasmodium*-specific enzymes (e.g., Bianucci et al., 2008; Fornaciari et al., 2010; Hawass et al., 2010; Miller et al., 1994; Nerlich et al., 2008; Rabino Massa et al., 2000) as well as PCR-based detection of singular genomic regions, such as 18S rRNA (e.g., Sallares & Gomzi, 2001; Taylor et al., 1997; Zink et al., 2001). However, short DNA fragments remain untargeted with PCR methods due to amplification biases, while the detection of antigens may lead to misdiagnoses as the techniques are not necessarily optimized for degraded samples, with limits of

detection sensitivity and confounding effects of diagenesis (Knapp & Hofreiter, 2010; Setzer, 2010; Tran et al., 2011). For example, Taylor et al. (1997) were unable to confirm *P. falciparum* DNA via PCR-based detection from previously positive antigen results in Egyptian mummies by Miller et al. (1994). PCR and immunological approaches confound the robust detection of non-*P. falciparum* species, which is a critical limitation as *P. vivax* historically contributed to morbidity or mortality (e.g., early 20th c. A.D. England in the marshy areas of Kent and Essex as described by Dobson, 1997); while *P. malariae* and *P. vivax* are also presumed to co-circulate with *P. falciparum* in Roman antiquity based on inferences from literary and climatological evidence (Bruce-Chwatt & de Zulueta, 1980; Sallares et al., 2004). There are no recent applications of hybridization capture (sequestration of DNA targets through binding to known DNA probes or baits) to specifically detect human *Plasmodium* parasites, which is a significant oversight, as genome-scale data is only retrievable with this approach.

Malaria as a human pathogen embodies the challenges of identifying paleopathological signatures of a disease process, owing to its pathogenesis, which complicates connecting this parasitic infection to skeletal assemblages. As such, the integration of DNA in the detection of ancient pathogens, complements limitations of associating skeletal lesions with specific pathological processes, as not only is there a spectrum of responses to infectious agents (e.g., immunity and susceptibility), but few diseases result in skeletal manifestations that are diagnostic in presentation (e.g., Ortner, 2011; Roberts & Manchester, 2005; Wood

et al., 1992). Similarly, it is exceedingly rare for multiple evidentiary sources (e.g., skeletal, historical, or archaeological) to provide a consensus on the association of a specific pathogen to a given archaeological assemblage. It is at this crossroads where ancient DNA can be used to prioritize candidate pathogens from the complex background of environmental and post-mortem molecules that characterize a specimen's surviving DNA constituents.

The shift towards integrating molecular methods in paleopathological studies is part of an anthropological holism aimed at elucidating the pathways and contexts of human disease-associated pathogens. A multi-faceted approach is capable of revealing the complex evolutionary trajectories of pathogens (Maixner et al., 2016; Wagner et al., 2014), screening for primary and co-infecting pathogens in diverse assemblages (e.g., Bos et al., 2015; Devault et al., 2014b), and exploring the relationship between the human microbiome and host immunity (e.g., Tito et al., 2012; Warinner et al., 2014). The emphasis is not only on pathogens as shaping the epidemiological landscape, but also on the influences of the biosocial context in the causal pathways of disease.

Accordingly, the scope and scale of human malaria is uncharacterized and bound by direct (i.e., biomolecular) and indirect (i.e., non-specific skeletal lesions, literary records) evidence. My research contributes to rendering the invisibility of pathogens visible, beyond a static dimension of presence (as yielded with ancient DNA) but integrating the molecular in the biosocial context that structures the experience of disease.

Study Context

The molecular investigation of malaria using ancient DNA is ideal because it is the only approach that can positively detect traces of these blood-borne parasites in human remains. As malaria is argued to have reached its zenith in the Imperial period (Brunt, 1971; Sallares, et al., 2004; Scheidel, 2009), samples associated with this time are necessary to evaluate the presumption of rampant malaria throughout southern Italy. In particular, the historical record (e.g., literary sources) and archaeological assemblages do not indicate catastrophic burials attributed to malaria from this period, nor is the distribution or spatial range of malaria known for Italy. Accordingly, as only the time period is relatively “known” for malaria, samples from the cemeteries of Isola Sacra (1st-3rd c. A.D.) (n=20), Velia (1st-2nd c. A.D.) (n=20), and Vagnari (1st-4th c. A.D.) (n=18) are used to evaluate malaria presence in southern Italy.

Velia is a coastal settlement on a small promontory (with river valleys to the north and south) (Crowe et al., 2010). As a port city, Velia was integral in supplying the surrounding population and Roman capital with foodstuffs (i.e., cereals and olives) and timber, as well as building and servicing boats (Craig et al., 2009; Crowe et al., 2010, Greco, 1999). The city was built on a terraced landscape, and the topography dictated the architecture of the residential blocks, roads, and cultivable land scattered across distinct districts (Cicala, 2013; Greco & Krinzinger, 1994). The surrounding coastal plains are argued as suitable for marshes, which were noted to have encroached upon the settlement after the

Classical period (Craig et al., 2009). The cemetery was used during the Imperial period (1st-2nd c. A.D.) and 330 burials have been excavated to-date (Craig et al., 2009, Crowe et al., 2010; Fiammenghi, 2003).

Isola Sacra is a cemetery situated on an artificial island between Ostia and Portus Romae, with use from the 1st to 3rd centuries A.D. by the inhabitants of Portus, with 2,000 individuals excavated to-date (Prowse et al., 2007). Portus functioned as the main port and warehouse for Rome, with a highly mobile and diverse population (e.g., merchants, traders, migrants) (Keay et al., 2005; Prowse et al., 2004, 2007). The ecology of Portus is also unique, with coastal marshes and lagoons, alongside intense anthropogenic modification of the environment through the construction of its artificial harbour and canals (Keay et al., 2005; Prowse et al., 2007).

As a rural inland estate, Vagnari represents over 3.5 hectares within the Basentello valley (Gravina in Puglia), bisected by a ravine and surrounded by plateaus of land (Prowse et al., 2010; Small, 2011, 2014). The cemetery was in use from the 1st to 4th centuries A.D. with 108 burials excavated to-date, and the inhabitants were likely slaves, freedman and/or freed tenants participating in industrial processing activities (e.g., iron-working, tile-making) and intensified agriculture alongside transhumance (Prowse et al., 2010; Small, 2011, 2014).

Broad indicators of physiological stress are evident in samples previously analyzed from these cemeteries (e.g., linear enamel hypoplasia, cribra orbitalia, and porotic hyperostosis) among the individuals at Vagnari (Prowse et al., 2014),

Velia (Beauchesne, 2012), and Isola Sacra (Gowland & Garnsey, 2010; Sperduti, 1995); however, the burden of infectious diseases (as manifested via pathological skeletal indicators) are unclear.

The coastal geomorphology of Velia (hills, coastal plains, marshes, cliffside location – Amato et al., 2010) and Portus (coastal woodland, marshes, lagoons, dunes – Di Rita et al., 2010; Keay & Paroli, 2011) contrasts to inland Vagnari (river valley with lowland hills and plateaus – Small, 2011). Velia, Portus, and Vagnari are ideal to explore the potential range of malaria, as the *Anopheles* vectors are potentially capable of occupying the fresh- and salt-water habitats of the swamps, lagoons, and marshes in such ecologically diverse locations (Jetten & Takken, 1994). These heterogeneous landscapes enable the exploration of malaria as part of a dynamic and local ecology within the social, cultural, and economic context of the Imperial period.

Theoretical and Methodological Framework

The theoretical framework encompassing my research draws on ecosocial theory and ecosystem health (Krieger, 2001, 2011; Rapport et al., 1998; Sutherst, 2004) complemented by an integrated ancient DNA methodology. Broadly, the anthropology of infectious disease (Inhorn & Brown, 1990) as applied to bioarchaeology, emphasizes a biocultural approach to studying disease where integrating molecular techniques within a humanistic and scientific perspective enables contextualization of the dynamism between humans, health, and the environment. For example, through sequencing *Y. pestis*, Bos et al. (2011)

demonstrate the pathogen's virulence was due to combined factors of ecology, social conditions, as well as host and vector biology, rather than solely genetic mutations.

The ecosocial approach to health integrates the inexorable linkages between humans and the biological, social, and economic environments with disease functioning as a constraint in the embodiment of individual health (Krieger, 2011; Lebel, 2003; Waltner-Toews, 2001). The stability and sustainability of an ecosystem directly influences population health as its resilience to natural or human stressors determines the degree to which imbalances in the human-vector-pathogen-environment relationship mitigate or facilitate the risk of disease (Rapport et al., 1998; Sutherst, 2004). This creates a framework for the identification of factors potentially proliferating or limiting disease. Krieger's (2011, p. 215) concept of the "lived experience of disease" guides the identification of ecological factors affecting the retrospective burden of disease in antiquity. Drawing from these frameworks, critical ecological components impacting the proliferation of disease(s) and causative agents include: climate; landscape (type of soil, sediment, or vegetation); geomorphology (topography changes, coastline formations); water bodies (lagoons, swamps, lakes); and extreme events (flooding, periods of aridity).

The manifestation of disease is further structured within sociocultural and political realms (Krieger, 2008). The dynamic approach of ecosocial health theory emphasizes humans "are shaped by and shape their environment" (Krieger, 2011,

p. 208), where the specific spatio-temporal and analytical scale (e.g., global, national, regional), historical and geographical contexts produce the observed patterns of disease (Krieger, 1994, 2001). The differential susceptibility to disease requires elucidating ecological, economic, and social forces with humans as active agents in directly or indirectly influencing the distribution of disease (Krieger, 1994, 2008, 2011). This approach considers the impact of anthropogenic processes (e.g., urbanization, agricultural practices, construction activities, trade, and migration) as active modifiers of disease ecology and the resultant disease burden (Krieger, 2011).

The application of an ecosocial epidemiological and ecosystem health approach within a genomics scope is applicable to exploring multi-level disease dynamics. For example, *Yersinia pestis* associated with the Plague of Justinian (541-543 A.D.) (Wagner et al., 2014) represents a terminal strain whereas *Yersinia pestis* from the medieval Black Death is the ancestor of subsequent plague strains (e.g., Bos et al., 2011; Haensch et al., 2010). This further argues for dynamic infectious disease transmission patterns, particularly heightened dissemination in a given socio-political and environmental context of medieval London.

The biosocial context of disease is also informed by Grmek's (1969) concept of pathocenosis for highlighting the interplay of the pathogen-pathogen interaction in the synergistic landscape of disease. This embodies the dynamics of infectious diseases as influenced by ecological and human factors (Grmek, 1969,

1991). Grmek (1969, p. 1476) framed pathocenosis as the frequency and distribution of disease depends not only biological factors (e.g., infectivity and virulence) or ecological factors (e.g., climate, urbanization), but the frequency and distribution of all other existing diseases in that population. In this manner, Grmek (1969, 1991) examined the European pathocenosis over two millennia, identifying a succession of diseases: where plague succeeded leprosy, and then was followed by syphilis, smallpox, cholera, and tuberculosis (Gonzalez et al., 2010). This represents the scope of integrating ancient DNA as part of an anthropological approach to contextualize the biosocial pathways of disease in a more static dimension, without the multi-level integration of ecosocial theory.

As part of the biocultural approach to exploring disease in the past, the Greek and Roman literary record represents a cornerstone for situating the human experience of disease as developed through the ecosocial and anthropological framework. Literary evidence (e.g. chronicles, histories, epics, manuscripts, or biographies) provides a means of accessing ancient historical realities by enabling diverse methodological inquiries (e.g., historical, anthropological or medical). Limitations associated with integrating such evidence are that texts represent cultural products from specific contexts of experiencing and understanding disease (Leven, 2004; Rosenberg, 1992); surviving material is generally fragmentary (Cunha & Cunha, 2008; Nutton, 2004); and translating ancient descriptions to modern terminology risk inaccuracy (Cunha & Cunha, 2008; Mitchell, 2011). For example, modern epidemic typhus existed as a multi-vocal

word in ancient Greek (as smoke, vapour, conceit, vanity, or stupor) demonstrating a broad framing of the disease, as in “*On Internal Affections*” (Hippocrates) where five types of burning fever suggestive of typhus are mentioned but only one is accompanied by the modern diagnostic symptom translated as “stupor” (Arrizabalaga, 2002, p. 58). Discrepancies in reconstructing ancient nosology through a modern understanding of a particular disease entity challenges the unequivocal identification of diseases in antiquity, thereby benefitting from integrative humanistic and scientific approaches.

The purposeful integration of an ecosocial epidemiological framework alongside a biocultural lens of exploring infectious disease is critical to form the foundation for the integration of ancient DNA with additional lines of evidence from the historical and archaeological records. Krieger (2008, 2011) emphasizes geographical contexts as the focal point of specific social, cultural, political, and economic influences in affecting disease pathways. Accordingly, ancient DNA although representing the story of the pathogen, requires contextualization from the historical space it represents. In this manner, I situate ancient DNA within multiple pathways of disease manifestation that are amenable to inferences from diverse sources (e.g., archaeological, literary, and skeletal).

Research Questions

To address the evidentiary patchwork of malaria in Imperial Italy alongside the challenges of paleopathological disease inquiries, the following questions constitute the research streams of this thesis:

1. Is the presumption of catastrophic malaria in Imperial period Italy (1st-5th c. A.D.) amenable to investigation using molecular evidence from different localities in the southern peninsula? If so, is it possible to identify a causative species? The primary aim is evaluating whether *Plasmodium* spp. genomic signatures are detectable in ancient tissues, as there are uncertainties regarding where this parasite localizes during infection (DeBarry, Fatumo & Kissinger, 2013) and, its survivability over time; however, the haematogenous nature of this infection suggests recovery is possible (Drancourt & Raoult, 2005). There is no research on the recovery of *P. falciparum* DNA from adult human skeletal remains in Imperial period Italy, and previous molecular or immunological approaches are limited in comprehensively detecting the four human *Plasmodium* species. Accordingly, my research uses hybridization capture as it is an established technique for recovering minute pathogen fractions from a background of exogenous (non-target) molecules (see Burbano et al., 2010; Carpenter et al., 2010; Enk et al., 2014). In addition, the capture strategy employed to address this question is robust, as it includes all four species of *Plasmodium* that infect humans (*P. ovale*, *P. malariae*, *P. falciparum*, and *P. vivax*) alongside two non-human host species (*P. cynomolgi*, *P. knowlesi*).

2. To what degree is it possible to identify factors contributing or hindering the emergence and maintenance of malaria within specific localities in Imperial southern Italy? Disease is a multi-faceted process, with influences from the biocultural environment, ecology, and humans as active modifiers of disease

ecology (Krieger, 1994, 2011; Singer, 2010). As such, it is critical to integrate molecular data within the human experience of disease and the ecological parameters contributing to a dynamic pathogen burden. Malaria influences morbidity and mortality by its interactions with other pathogens (e.g., Faure, 2014; Sallares, 2005) and is responsive to anthropogenic activity (e.g., deforestation, agriculture, infrastructure development) and local ecology (e.g., temperature fluctuations, floods) (Sallares, 2002; Sallares et al., 2004; Scheidel, 2009). My research situates malaria as part of a dynamic biosocial landscape to elucidate the scope of its interactions at Vagnari, Velia, and Portus Romae.

3. How effective is ancient DNA for assisting researchers to address pathogen-pathogen interactions for a range of endemic (or acute) diseases under conditions of non-catastrophic morbidity and mortality? The paleopathological investigation of disease is complicated by limited evidence, whether it is historical, skeletal or archaeological, that links a specific disease to a given burial assemblage. Skeletal markers of infectious disease are diagnostic at times (e.g., chronic disease processes related to tuberculosis or leprosy); however, there is a spectrum of responses to pathogenic agents (e.g., non-specific skeletal lesions or an absence of such) due to heterogeneous vulnerability and susceptibility (Ortner, 2011; Wood et al., 1992; Wright & Yoder, 2003). The challenge of associating skeletal responses to specific pathogens is complemented by the inclusion of a molecular approach capable of prioritizing contextually relevant disease-associated pathogens. The approach is grounded in Grmek's (1969, 1991) concept

of pathocenosis (the interaction of all pathogens influence the presence of one another), in order to explore the biosocial interactions contributing to the disease burden. My research evaluates a technique of parallel pathogen capture as a means of providing a methodological approach to qualitatively and quantitatively prioritize the suite of low abundance pathogens represented in a single archaeological specimen.

These questions are examined in three papers for publication that constitute the body of this thesis. The first paper, entitled “*Plasmodium falciparum* malaria in 1st-2nd c. A.D. southern Italy” presents the first genome-scale data for *P. falciparum* in two adults from Vagnari (1st-2nd c. A.D.) and Velia (1st-2nd c. A.D.). The second paper, entitled “A multi-faceted approach to framing molecular signatures of *Plasmodium falciparum* malaria in Imperial period southern Italy (1st-4th c. A.D.)” frames the *P. falciparum* genomic data in the specific epidemiological contexts of the studied Imperial Italian localities, to show malaria as a parasite that dynamically interacts within social, cultural, and ecological networks. The third paper, “Parallel hybridization capture of multiple pathogens in archaeological samples: towards integrated paleopathological investigations” evaluates parallel pathogen capture as a means of prioritizing low abundant pathogens from the complex pool of DNA in archaeological human remains alongside reconstructing the microbial burden.

Through these analyses aimed at framing the biosocial context of disease in the past, points of debate are raised in the evaluation of malaria as a critical

pathogen in the epidemiological landscape of Imperial Italy: how is the ancient DNA evidence for *P. falciparum* reconcilable with the historical presumption of widespread malaria within an ecosocial epidemiological framework? In exploring the landscape of disease in the past, are ancient DNA approaches (single or multiple pathogen capture) amenable to integration with higher order epidemiological frameworks (e.g., pathocenosis, ecosocial theory, and the biosocial context of disease) (e.g., Krieger, 1994, 2011; Grmek, 1969)?

Thesis Format

This thesis is comprised of four chapters where three are standalone (Chapters 2-4) for submission to scholarly journals (Current Biology, the American Journal of Physical Anthropology, and Nature Scientific Reports). The organization is as follows:

Chapter 2: Paper 1: *Plasmodium falciparum* malaria in 1st-2nd c. A.D. southern Italy.

By: Stephanie Marciniak, Tracy L. Prowse, D. Ann Herring, Jennifer Klunk, Melanie Kuch, Ana T. Duggan, Luca Bondioli, Edward C. Holmes, Hendrik N. Poinar

Chapter 2 represents the culmination of the molecular work in retrieving genomic signatures of *P. falciparum* in two adult skeletal samples of southern Italy (Velia, 1st-2nd c. A.D., and Vagnari, 1st-2nd c. A.D.). The experimental methods are outlined in the Supplemental Information that was also submitted with this publication. Screening the Imperial Italian samples through a metagenomic approach (sequencing the entire microbial content) prioritized

putative specimens with *Plasmodium* spp. or Apicomplexan taxa for downstream hybridization capture. Approximately 50.8% of a *P. falciparum* genome was recovered, with phylogenetic analyses showing the association of this Imperial Italian malaria to *P. falciparum* (strains from diverse geographical locations). This paper exclusively presents the genomic side of malaria in the southern Italian localities studied, outlining the specific methods and protocols alongside bioinformatic processing of the resultant data to demonstrate the authenticity of the results. I performed all of the laboratory work and analyses of the sequence data, and worked with H.N. Poinar and E.C. Holmes for the phylogenetic analyses. Further to this, I wrote the first draft of the paper and all co-authors reviewed subsequent drafts to provide feedback. This paper was accepted in September 2016 to *Current Biology* as a Correspondence.

Chapter 3: Paper 2: A multi-faceted approach to framing molecular signatures of *Plasmodium falciparum* malaria in Imperial period southern Italy (1st-4th c. A.D.)

By: Stephanie Marciniak, D. Ann Herring, Alessandra Sperduti, Roberto Macchiarelli, Luca Bondioli, Hendrik N. Poinar, Tracy L. Prowse

Chapter 3 represents the contextualization of the *P. falciparum* molecular results within Imperial period Italy, as the scope of the paper in Chapter 2 was focused on the genomic results. This work is inspired by and framed through Krieger's (1994, 2011) ecosocial health framework to situate malaria as a dynamic human pathogen. The focus is the meaning of this ancient DNA data in consideration of the presumption of malaria presence in Imperial southern Italy.

The overall contribution is to highlight the complexity of malaria as a pathogen that interacts not only with its human hosts, but associated *Anopheles* vector, with its resultant distribution or intensity as an outcome of entangled ecological and anthropogenic factors within a particular socio-political context. I performed all of the laboratory work and analyses, wrote the first draft of the paper, created the figures and tables, with subsequent revisions informed by feedback from co-authors. This paper was submitted to the American Journal of Physical Anthropology.

Chapter 4: Paper 3: Parallel hybridization capture of multiple pathogens in archaeological samples: towards integrated paleopathological investigations

By: Stephanie Marciniak, Ana T. Duggan, Shea Gardner, Crystal Jaing, Jonathan Allen, Kevin McLoughlin, Monica Borucki, Tracy L. Prowse, Hendrik N. Poinar

Chapter 4 evaluates a hybridization capture technique targeting multiple pathogens all at once as an approach to characterize microbial constituents within archaeological assemblages. The specific significance of this work is addressing the challenges of multiple evidentiary sources (e.g., skeletal, historical, or archaeological) in providing a consensus on disease-associated pathogens within a given burial, as such scenarios are exceedingly rare. This work uses previously verified human pathogens (*Yersinia pestis*, *Vibrio cholerae*, *Staphylococcus saprophyticus*) to demonstrate the success of pathogen capture and includes an array of unknown samples (from Imperial period and medieval Italy, as well as North America) to show the versatility of this approach. The application of a highly stringent algorithm (through collaboration with the Lawrence Livermore

National Laboratory), facilitates identifying the likelihood of target presence in these archaeological samples. Under the umbrella of this technique is the connection to the Osteological Paradox (Wood et al., 1992; Wright & Yoder, 2003), particularly heterogeneous vulnerability and susceptibility to the skeletal manifestation of disease. In this sense, parallel pathogen capture is capable of addressing synergistic disease interactions, informed by contextually relevant factors (e.g., ecological, social or biological sources). I performed all laboratory work and analyses and wrote the first draft of the paper, and our collaborators at LLNL performed algorithmic assessments. This paper will be submitted to Nature Scientific Reports with a Supplementary Appendix detailing the methods and results.

Chapter 5: Discussion and Conclusions

My research contributes to ongoing methodological and theoretical challenges in the integration of ancient DNA with the historical and archaeological records to connect “invisible” pathogens to the biosocial context in which each is embedded. The recovery of *P. falciparum* within the time of its presumed zenith of the Imperial period (1st-2nd c. A.D.) indicates the promise and success of a combined ancient DNA and anthropological approach. Two critical issues emerge from this work and are further discussed in this section. First, exposure to a pathogen does not always result in disease, which means the molecular detection of a pathogen (similar to skeletal manifestations) may misrepresent the scope of those “infected” with a pathogen(s). This speaks to the

underpinnings of the Osteological Paradox (heterogeneity and frailty) (Wood et al., 1992; Wright & Yoder, 2003) and pathocenosis (Grmek, 1969) that are intertwined with ancient DNA investigations of disease.

The second issue focuses on the potential discord between evidence for ancient *P. falciparum* (i.e., recovered from two individuals in disparate social and ecological localities in southern Italy) and the overarching narrative that stresses the significance of this human parasite to Imperial Rome. I apply ecosocial health theory to the ancient DNA results as part of the historical and archaeological records to propose particular biosocial pathways that frame the context for malaria at Vagnari, Velia, and Portus Romae. This exploration leads to a discussion of the degree to which ancient DNA techniques are increasingly applicable to exploring pathogen-pathogen interactions as contributing factors to a multi-faceted disease experience, essentially moving beyond “single disease-single pathogen” investigations. By recognizing multiple pathogens create the landscape of disease, I emphasize ancient DNA as an avenue to reconstruct these interactions as part of an interconnected web with other pathogens, human hosts, and the environment (biological, cultural, physical).

Future research in the parallel pathogen detection can elucidate the interactions in a given spatiotemporal context by expanding the scope and scale of such strategies in population-level samples. With respect to malaria in Imperial Italy, having demonstrated the recovery of malaria DNA in ecologically and socially distinct localities, it is arguable that further molecular investigations of

this parasite should expand the range of sites to investigate the distribution across the Empire (particularly in Egypt), and also situate this data as part of the dynamic landscape of sociopolitical and economic change of this historical period.

**CHAPTER 2: *PLASMODIUM FALCIPARUM* MALARIA IN 1ST-2ND C.
A.D. SOUTHERN ITALY.**

By: Stephanie Marciniak ^{1,2}, Tracy L. Prowse², D. Ann Herring ², Jennifer Klunk^{1,3}, Melanie Kuch ¹, Ana T. Duggan ^{1,2}, Luca Bondioli ⁴, Edward C. Holmes ⁵ and Hendrik N. Poinar ^{1,2,3,6,7}

Accepted to Current Biology, September 2016.

¹McMaster Ancient DNA Centre, Department of Anthropology, McMaster University, Hamilton, ON, L8S 4L9 Canada.

²Department of Anthropology, McMaster University, Hamilton, ON, L8S 4L9, Canada.

³Department of Biology, McMaster University, Hamilton, ON, L8S 4L9, Canada.

⁴Polo Museale del Lazio, Museo Nazionale Preistorico Etnografico “Luigi Pigorini”, Sezione di Bioarcheologia, P.le G. Marconi 14, 00144, Rome, Italy

⁵Marie Bashir Institute for Infectious Diseases and Biosecurity, Charles Perkins Centre, School of Life and Environmental Sciences and Sydney Medical School, The University of Sydney, Sydney, NSW 2006, Australia.

⁶DeGroot Institute for Infectious Disease Research, McMaster University, Hamilton ON, L8S 4L9, Canada.

⁷ Humans & the Microbiome Program, Canadian Institute for Advanced Research, Toronto, Ontario M5G 1Z8, Canada.

The historical record attests to the devastation malaria exacted on ancient civilizations, particularly the Roman Empire [1]. However, evidence for the presence of malaria in Imperial period Italy (1st-5th c. A.D.) is based on indirect sources (e.g., historical, epigraphic, or skeletal), and although crucial for revealing the context of this disease cannot establish the causative species of *Plasmodium*. Importantly, definitive evidence for the presence of malaria is now possible through the implementation of ancient DNA (aDNA) technology. As malaria is presumed to have been at its zenith during the Imperial period [1], we selected first or second molars from 58 adults from three cemeteries from this time: Isola Sacra (associated with Portus Romae, 1st-3rd c. A.D.), Velia (1st-2nd c. A.D.), and Vagnari (1st-4th c. A.D.). We performed hybridization capture using baits designed from the mitochondrial (mtDNA) genomes of *Plasmodium* spp. on a prioritized subset of 11 adults (informed by metagenomic sequencing). The mtDNA sequences generated provided compelling phylogenetic evidence for the presence of *P. falciparum* in two individuals. This is the first genomic data directly implicating *P. falciparum* in Imperial period southern Italy in adults from multiple localities.

The story of malaria in Imperial Italy is drawn from a rich historical narrative (e.g., Hippocrates' "*On Epidemics*", Celsus' "*De Medicina*", or Galen's "*De Morborum Temporibus*") that describes the classic fever periodicity (e.g., tertian, semi-tertian, quartan or quotidian) since the 5th c. B.C. Despite this, the timing and geographical range of malaria remains uncertain, as only a broad northward spread is thought to have occurred across Italy from 500 B.C. to 1000 A.D. [2]. The inability to connect malaria to a precise historical and geographical space in antiquity is further complicated by its pathogenesis, as this infection does not cause distinct pathological changes to the human skeleton, although non-specific skeletal indicators of physiological stress are prevalent in malarious environments [3]. Furthermore, the existing molecular evidence for malaria in Imperial Italy currently comprises a single PCR product detection of *P. falciparum* in an infant from 5th c. A.D. Lugnano (Umbria) [4]. The prevalence and influence of malaria among adults in southern Italy therefore remains unknown.

Malaria is responsive to climate, topography, human activity, and ecology on a local scale, so there is likely no single mortality profile that is applicable to all of Imperial period Italy [1,2]. Accordingly, we used ecologically diverse coastal and rural localities to determine the presence of *Plasmodium* through aDNA technology: Velia, a coastal promontory between alluvial plains [5]; Portus Romae (Isola Sacra), a low-lying basin of woodlands near the Tiber River

alongside marshes and lagoons [6]; and inland Vagnari, a wooded river valley with lowland hills [7] (Fig. S1a).

We detected *P. falciparum* mitochondrial DNA fragments from two individuals, LV13 (Velia) and LG20 (Vagnari) dating to the 1st-2nd centuries A.D. (Fig. 1a), with no positive results from the Portus Romae samples (Supplemental Information, Table S1). Through an RNA-bait set designed from four human and two non-human *Plasmodium* species, we were able to enrich a total of 3,033 base pairs (bp) (120 reads total) or 50.8% of the 5,967 bp *P. falciparum* mitochondrial genome when reads from LG20 and LV13 were combined. Separately, LG20 yielded 300 bp (seven reads) and LV13 had 2,901 bp (113 reads). Although our baits will enrich for *P. vivax* and *P. malariae*, which may have co-circulated with *P. falciparum*, we did not detect any reads matching these species. Importantly, *Plasmodium* species rely on host (mosquito and human) cellular machinery for survival and are species-specific, with parasites restricted to particular hosts [8]. These factors preclude environmental reservoirs of infection and hence contamination of the skeletal remains from surrounding sediments.

Figure 1a. The burial of individual F234 at Vagnari (adult male, approximately 35.2 ± 9.4 years of age). Velia individual 186 (not pictured) is also an adult male, approximately 20-25 years of age. © T.L. Prowse.

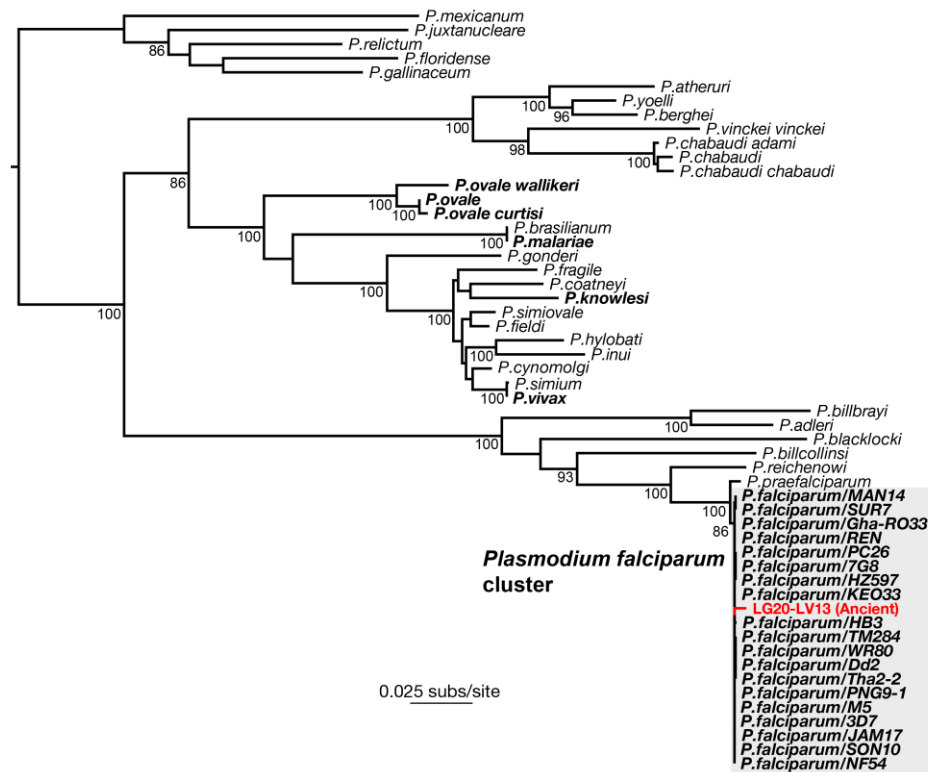


The sequence reads mapping to *P. falciparum* averaged 51 bp, with damage patterns characteristic of aDNA (C>T at the 3' and 5' termini) (Supplemental Information, Fig. S1b and S1c). Low coverage data required using human mitochondrial reads from individuals LG20 and LV13 as a proxy for quantitative assessments of aDNA damage (Supplemental Information, Fig. S1d and S1e). The positive, but low, *P. falciparum* signal is perhaps unsurprising considering the idiosyncrasies of recovering pathogen DNA and the nature of parasite pathogenesis that includes differential expression of the parasite's mitochondrion that varies with infective stage (e.g., one to eight organelles each containing up to 20 copies of the genome) [9], the recurrence of infection (i.e., re-

infection, recrudescence), and the spectrum of host-parasite interactions (i.e., asymptomatic to lethal).

Phylogenetic analyses of LG20-LV13 combined with mtDNA genomes from diverse *Plasmodium* spp. (n=53) place our Imperial period strain within a clade of exclusively *P. falciparum* sequences (n=19) with strong support (86%; 100% bootstrap support linking the *P. falciparum* cluster with its closest non-human relative, *P. praefalciparum* from gorillas) (Fig. 1b and related Fig. S1f). However, due to the fragmentary nature of the LG20-LV13 sequence it was not possible to resolve evolutionary relationships within the *P. falciparum* cluster nor determine the time-scale of *P. falciparum* evolution through molecular clock dating.

Figure 1b. Maximum likelihood phylogenetic tree of 54 *Plasmodium* spp. including the Imperial period Italian sequence obtained here shown in red (the ancient LG20-LV13 sequences were combined for this analysis). *Plasmodium* species that infect humans are shown in bold. Bootstrap support values (>80%) are shown for key nodes.



Our results are compatible with Sallares and Gomzi’s (2001) identification of *P. falciparum* from central Italy [4], but predate their detection of the parasite by several centuries. Detecting signatures of *P. falciparum* in individuals from Vagnari and Velia, but not Portus Romae (a presumably ideal ecological context), as well as the recovery of *P. falciparum* among adults at these disparate localities, and in infants [4], means that the nature of malaria (i.e., endemic, epidemic, or sporadically imported) in Imperial Italy remains unclear. Indeed, it is possible that malaria exhibited complex population dynamics at the localities studied here,

reflecting the variable impact of demography (e.g., population movement, migration), economic activities (e.g., trade, resource use), social circumstances (e.g., urbanization, land use patterns), and parasite biology (e.g., regional variation among strains or vectors) [10].

In sum, these data provide a key reference point for the antiquity of *P. falciparum* in humans. Ancient DNA therefore lends a materiality to the existence of malaria in Imperial Italy, complementing the multi-faceted narrative of “malarial fevers” told by authors thousands of years ago.

SUPPLEMENTAL INFORMATION

Supplemental information including experimental procedures and acknowledgements along with a figure and table can be found with this article.

References

1. Sallares, R. (2002). *Malaria and Rome: A History of Malaria in Ancient Italy* (Oxford: Oxford University Press).
2. Sallares, R., Bouwman, A., and Anderung, C. (2004). The spread of malaria to southern Europe in antiquity: new approaches to old problems. *Med. Hist.* 48, 311-328.
3. Gowland, R., and Garnsey, P. (2010). Skeletal evidence for health, nutritional status and malaria in Rome and the Empire. In *Roman Diasporas: Archaeological Approaches to Mobility and Diversity in the Roman Empire*, H. Eckardt, ed. (Portsmouth: *Journal of Roman Archaeology*, Supplement 78), pp. 131-156.
4. Sallares, R., and Gomzi, S. (2001). Biomolecular archaeology of malaria. *Anc. Biomol.* 3, 195-213.
5. Amato, L., Bisogno, G., Cicala, L., Cinque, A., Romano, P., Ruello, M.R., and Russo Ermolli, E. (2010). Palaeo-environmental changes in the archaeological settlement of Elea-Velia: climatic and/or human impact signatures? In *Scienze naturali e archeologia. Il paesaggio antico: interazione uomo ambiente ed eventi catastrofici*, A. Ciarallo, M.R. Senatore, eds. (Rome: Aracne Editrice), pp. 13-16.
6. Keay, S.J., and Paroli, L., eds. (2011). *Portus and its Hinterland: Recent Archaeological Research* (London: British School at Rome).

7. Small, A.M., ed. (2011). *Vagnari. The village, the industries the imperial property* (Italy: Edipuglia).
8. Paul, A. S., Egan, E. S., and Duraisingh, M. T. (2015). Host-parasite interactions that guide red blood cell invasion by malaria parasites. *Curr. Opin. Hematol.* 22, 220–226.
9. Krungkrai, J. (2004). The multiple roles of the mitochondrion of the malarial parasite. *Parasitol.* 129, 511-524.
10. Martens, P. (2002). Of malaria and models: challenges in modeling global climate change and malaria risk. In *The Contextual Determinants of Malaria*, E.A. Casman, H. Dowlatabadi, eds. (Washington: RFF Press), pp. 14-26.

Supplemental Information

Plasmodium falciparum malaria in 1st-2nd c. A.D. southern Italy

Stephanie Marciniak, Tracy L. Prowse, D. Ann Herring, Jennifer Klunk, Melanie Kuch, Ana T. Duggan, Luca Bondioli, Edward C. Holmes, Hendrik N. Poinar

Supplemental Experimental Procedures

Malaria in the Archaeological Record

A retrospective identification of malaria in ancient human remains is complicated by its “invisibility” in the archaeological record, which is due to the following: *Plasmodium* spp. parasites are localized within the bloodstream and organs (e.g., spleen, liver), with limited persistence in host tissues, which challenges the recovery of this haematogenous infection post-mortem (i.e., after thousands of years); and, immune-induced rupture of parasitized and non-parasitized red blood cells contributes to hemolytic anemia [S1, S2] that may manifest skeletally as porotic hyperostosis (porosity of the cranial vault), cribra orbitalia (porosity of the orbital roof) [S3] or a suite of cribrotic lesions on various skeletal elements [S4]. However, these indicators have a multifactorial etiology (e.g., anemia, infection, trauma, metabolic disease, nutritional deficiency) [S5] which is not irrefutable evidence of malaria. It is also worth noting that bioarchaeological analyses indicate a high prevalence of such non-specific cribrotic stressors in presumptively malarious environments of the Roman and Egyptian periods [S6, S7], alongside potentially deleterious interactions (i.e., malnutrition, parasitic or bacterial infections) [reviewed by Faure, 2014, in ref. S8]. Previous molecular and immunological investigations of malaria in Egyptian mummies from diverse chronological periods similarly demonstrate success in the recovery of *P. falciparum*-specific functional gene fragments (i.e., 18S rRNA, chloroquine-resistance transporter) (e.g., Taylor et al., 1997 in ref. S9; Zink et al., 2001 in ref. S10; Nerlich et al., 2008 in ref. S11); and protein fragments [e.g., apical membrane antigen 1 (AMA1), merozoite surface protein (MSP), subtelomeric variable open reading frame (STEVAR), histidine-rich protein 2 (PfHRP-2)] (e.g., Miller et al., 1994 in ref. S12; Rabino Massa et al., 2000 in ref. S13; Bianucci et al., 2008 in ref. S14; Hawass et al., 2010 in ref. S15; Lalremruata et al., 2013 in ref. S16).

Ultimately, the inability to select samples based on visible pathological lesions for our analyses required a random selection of skeletal material from diverse ecological localities in Imperial period Italy, integrated with a broad molecular approach to prioritize those putatively infected with *Plasmodium* spp. For a comprehensive review of the paleopathological identification of malaria in

antiquity the reader is directed to Bianucci et al. (2015) [S17] and Setzer (2014) [S18].

Sample Sites: Context of the Imperial Period Italian Cemeteries

Figure S1a indicates the locations of the cemeteries used in this study. Vagnari is over 400-km southeast of Rome, characterized as a rural estate participating in industrial processing activities as indicated by archaeological evidence of tile kilns, iron-working, alongside agricultural production [S19, S20]. In terms of Vagnari's connection to the Empire at large, the site likely consisted of slaves, freedmen, and/or free tenants contributing to the activities of an Imperial estate [S21]. The cemetery at Vagnari is located on the southern part of the site, away from the main habitation area, and the 108 burials excavated mainly date between the 1st to 4th centuries A.D. [21].

Velia is over 350-km south of Rome, and is considered a minor port city, with archaeological evidence of fortified city walls enclosing residential blocks and a thriving urban centre (e.g., workshops, bathhouse, villas, ceremonial complex) [S22, S23, S24]. Alongside agricultural output, economic activities included a fishing industry, and harvesting timber for the building and servicing of boats at the port facilities [S22, S23, S24]. The cemetery itself was used from the 1st to 2nd centuries A.D., with more than 330 scattered burials excavated (inhumations and cremations) beyond the city walls [S25].

Isola Sacra is a necropolis (1st-3rd c. A.D.) 20-km southwest of Rome, situated on an artificial island between the cities of Ostia and Portus Romae. The cemetery was used by residents of Portus Romae (23-km southwest of Rome) and approximately 2,000 individuals have been recovered to date, mostly consisting of commingled remains from monumental tomb excavations [S26]. At the beginning of the Imperial period, Portus functioned as the main port and warehouse for Rome, characterized as a highly mobile and varied population (i.e., merchants, traders, migrants, slaves or freedmen) of relatively recent immigrants from other areas of the Empire [S27, S28].

Broad indicators of health stress are evident (e.g., linear enamel hypoplasia, cribra orbitalia, and porotic hyperostosis) among the individuals at Vagnari, Velia, and Isola Sacra [S29, S30, S31]. However, the burden of infectious diseases (as manifested via skeletal indicators of pathology) is unclear.

Sampling Strategy

We obtained teeth (first or second molars) randomly selected from 58 adult individuals across the three Imperial period cemeteries (Velia, n=20; Isola Sacra, n=20; Vagnari, n=18) with an additional set of nine teeth (deciduous molars) from juveniles (1.5-14 years of age) buried at Vagnari as an *ad hoc* assessment of whether *Plasmodium* genomic signatures offered a greater chance of recovery in this age group (cognizant of the small sample size), due to the potential for increased susceptibility to malaria. Aside from the Imperial period Italian adults and juveniles, control samples from a Maritime Archaic population (North

American cultural complex) dated from 5,000-4,000 B.C. (Newfoundland, Canada) were included, as no previous or contemporary exposure to malaria is evident in the historical record [S32].

All manipulation of the samples, associated DNA extracts, and downstream products was performed at the McMaster Ancient DNA Centre (Hamilton, ON, Canada), which includes clean room facilities dedicated to the pre-PCR processing of ancient material (sampling, extraction, PCR set-up, library preparation) and physically separated “modern” facilities (PCR amplification, enrichment, re-amplification). Importantly, the laboratory procedures were performed in facilities with no prior exposure to modern *Plasmodium* spp. DNA.

The workspace and associated subsampling tools (e.g., Dremel collar parts, cutting wheel, pulverizing components) were cleaned prior and between the subsampling of individual specimens with a bleach solution followed by UV-irradiated double-distilled water. A portion of the dental root was removed from each specimen with a Dremel rotary tool using a thin diamond wheel, with a focus on preserving the integrity of the tooth structure and morphology. The removed portion was then pulverized with a hammer and transferred to a small weighing boat. For the specimens that were subsampled a second time (LG20 and LV13), the pulp cavity was accessed from the previously subsampled root with a grout attachment and the Dremel on the lowest speed setting. The subsequent dental powder was then transferred to 1.5-mL MAXYMum Recovery PCR tubes with storage at -20°C for enzymatic extraction.

DNA Extraction

Extractions were performed with a modified protocol [S33, S34] on the 58 adult teeth from the three cemeteries and nine juveniles from Vagnari. Extractions for 50- to 125-mg of the pulverized dental material first proceeded with demineralization by incubation for 24 hours in EDTA (pH 8.0, 0.5M) while shaken at 1,000 rpm in a Thermomixer at 22°C (room temperature), with subsequent removal and storage of the supernatant at -20°C. This was followed by enzymatic digestion in a buffer [20 mM Tris-HCl pH 8.0, 5 mM calcium chloride, 50mM dithiothreitol (DTT), 2.5 mM N-phenacylthiazolium bromide (PTB), 1% polyvinylpyrrolidone (PVPD), 0.5% sarcosyl, 20 mg/mL Proteinase K and nuclease-free water] incubated for 24 hours in a Thermomixer at 25°C shaken at 1,000 rpm. The supernatant was removed and stored at -20°C. Three rounds of demineralization and digestion of the contents were performed, removing the supernatant each time with subsequent storage in 2.0-mL MAXYMum Recovery PCR tubes at -20°C. One reagent control was included for every seven samples.

Organic extraction of the demineralisation/digestion supernatant mixtures followed the phenol-chloroform method for the 58 Imperial period Italian adults [S35]: 500-µL of phenol-chloroform were added to 1000-µL of supernatant mixtures, centrifuged for 6-10 minutes at 13,100 rpm (retaining the aqueous phase), followed by an addition of 500-µL chloroform (CHCl₃) to the sequestered aqueous phase with centrifugation (6-10 minutes at 13,100 rpm). Column

ultrafiltration with 10 kDa cut-off (10K Amicon Ultra-0.5mL; Millipore, MA) of the extraction products proceeded in a stepwise manner. After priming the filters with 450- μ L of 0.1xTE (20mM Tris-HCl pH 8.0 and 0.5M EDTA pH 8.0) to minimum retention, the extracted material was applied to the column (450- μ L increments) and spun to minimum retention (50- μ L) for the entire sample tube contents. Two washes of 450- μ L 0.1x TE were then applied to the column and spun to minimum retention. The extracted DNA solution obtained a final volume of 50- μ L and was removed via pipette in order to purify the concentrate with the Qiagen MinElute PCR Purification Kit according to the standard protocol, but with two washes of 750- μ L Buffer PE, eluting to a final volume of 50- μ L with 0.1x TE + 0.05% Tween (for long-term storage).

The supernatant mixtures from the re-sampled specimens LG20 and LV13 as well as the Vagnari juveniles were subjected to organic extraction and purification according to an ultra-short DNA retention protocol [S36] with modifications. 1.0-mL of the supernatant was added to a binding buffer solution consisting (in final concentrations) of 5M guanidine hydrochloride, 40% (vol/vol) isopropanol, 0.05% Tween-20, and 90 mM sodium acetate (pH 5.2) in a Roche nucleic acid column. The solution was spun for 4 minutes at 1,500 x g, rotated 90 degrees then spun again for 2 minutes at 1,500 x g. This process was repeated for the second 1.0-mL of the supernatant. The column was removed from the reservoir, placed in a clean 2.0-mL MAXYMum recovery tube, followed by a dry spin at 3,300 x g for 1 minute (flow through discarded). Two washes of 750- μ L PE Buffer (Qiagen) were performed, centrifuging at 3,300 x g (flow through discarded), with two dry spins at 16,100 x g (rotating the tube 180 degrees after the first spin) and placed in a new 1.7-mL collection tube. For elution, 25- μ L of buffer EBT (15.0-mL of Buffer EB from Qiagen, plus 7.5- μ L of Tween-20) was added to the silica membrane, incubated for five minutes at room temperature and centrifuged for 30 seconds at maximum speed. This step was repeated twice for a total of 50- μ L of DNA extract, which was then stored at -20°C.

Library Preparation

Following an established protocol [S37] with recommended modifications [S38], 25- μ L of each DNA extract (n=58), re-sampled specimens LG20 and LV13 (n=4), extraction blank controls (one for every seven samples) and water blanks, were converted into Illumina sequencing libraries. One negative library preparation control (UV-irradiated double-distilled water) was included for every 20 samples. Two libraries were prepared from each individual extract in the following manner: a) blunt end repair with Uracil-DNA Glycosylase (UDG) and Endonuclease VIII (EndoVIII) treatment to remove deaminated cytosine residues; and b) blunt end repair without removal of cytosine residues (non-UDG/EndoVIII). Instead of SPRI bead clean-up, MinElute PCR Purification (Qiagen) with the modifications described above was applied between library preparation steps (blunt-end repair, adapter ligation, and adapter fill-in). Heat deactivation (80°C for 20 minutes) was performed after the fill-in stage instead of an additional purification step. The

final library volume was 40- μ L, which was then used directly as templates in the subsequent indexing and quantification applications.

Post-Library Indexing and Quantification

A unique P5 and P7 index combination was added to each library in parallel 50- μ L reactions following established protocols for double indexing amplification [S38]. The reaction component concentrations and volumes for the UDG/EndoVIII-treated libraries followed the Agilent Technologies Herculase II Fusion DNA polymerase protocol, with modifications of 150 nM of each indexing primer and 20- μ L of each library. The amplification conditions were: 95°C denaturation (2 minutes), amplified until samples reached plateau at 95°C (15 seconds), 60°C (20 seconds), 72°C (30 seconds) with a final 72°C (3 minutes). Indexed products for each library were purified via MinElute (Qiagen), and then eluted in 20- μ L EB.

The double-indexing real-time reactions for the non-UDG/EndoVIII libraries and re-sampled libraries (LG20 and LV13) were each 50- μ L reactions that included library inputs of 20- μ L, indexing primers at 150 nM, and KAPA SYBR® FAST qPCR Master Mix (2X). The samples were amplified for 10 cycles or until reaching plateau, with the following conditions: 95°C denaturation (5 minutes), 95°C (30 seconds), 60°C (45 seconds), and a final 60°C (3 minutes). Indexed products for each library were purified via MinElute PCR Purification Kit (Qiagen) with the modifications described above, and eluted in 30- μ L EB.

To quantify the total DNA in all of the indexed libraries, parallel 10- μ L real-time PCR reactions used the primer combination IS5_long_amp.P5 (5'-AATGATACGGCGACCACCGA-3') and IS6_long_amp.P7 (5'-CAAGCAGAAGACGGGCATACGA-3'), KAPA SYBR® FAST qPCR Master Mix (2X) and 1:1,000 dilutions of each library with a 425 bp-525 bp PhiX Control (Illumina) standard serially diluted from 1 nM to 0.0625 pM, to infer the concentration of the libraries. The qPCR conditions were the following: 200 nM of each primer, 1X KAPA SYBR® FAST qPCR Master Mix (2X), 1:1,000 library dilutions (4- μ L), PhiX serial dilutions (4- μ L) alongside two water blanks and two EBT blanks. Amplification proceeded as the following: 95°C activation (5 minutes), followed by 35 cycles of 95°C (30 seconds), 60°C (45 seconds), and a melt curve 60-95°C, ending with 8°C (30 seconds).

Plasmodium spp. Capture Baits Design

An in-solution bait set was designed incorporating the diversity within the mitochondria of *Plasmodium* species (human and non-human host species) (MYcroarray, Ann Arbor, MI) using the following GenBank accession numbers: *Plasmodium falciparum* (NC_002375), *Plasmodium vivax* (Sal-1) (NC_007243), *Plasmodium malariae* (AB_354570), *Plasmodium ovale* (AB_354571), *Plasmodium knowlesi* (NC_007232), and *Plasmodium cynomolgi* (AB_434919). These genomic targets ranged in size from 5,957 to 5,990 bp; and the probes were tiled at one 80-mer bait per 20 bp (distributed contiguously across genomic regions) for a total of 3,267 bait sequences.

The bait set was redesigned after the first two enrichment experiments showed non-specific reads: a) near the 3' termini of the *COXIII* gene for *P. falciparum* (1,522-1,557), *P. vivax* (2,790-2,824), *P. malariae* (2,732-2,766), *P. ovale* (2,721-2,756), *P. knowlesi* (2,779-2,813), and *P. cynomolgi* (2,788-2,822); and b), positions within the intergenic and rRNA regions of *P. falciparum* (5,707-5,754), *P. vivax* (1,012-1,077), *P. malariae* (954-1,016), *P. ovale* (943-1,007), *P. knowlesi* (1,010-1,074) and *P. cynomolgi* (1,009-1,074).

***Plasmodium* spp. Enrichment**

In-solution enrichment was performed three separate times: set 1 included specimens prioritized from the metagenomic data for initial evaluation of human *Plasmodium* presence (n=11 adult specimens and nine juveniles, using one library from each), set 2 included the original and re-sampled high priority specimens identified from set 1 (multiple libraries from three specimens – LG20, LV13, and Vagnari juvenile JV05) and set 3 included the re-sampled and original specimens for LG20 and LV13 (multiple libraries from the two specimens). Reagent blanks (e.g., extraction blanks, library preparation blanks) and control samples (Maritime Archaic libraries) were also included during each capture. Refer to Table S1 for the capture metrics.

In-solution enrichment was performed on sets 1, 2, and 3 according to the manufacturer's protocol (MYcroarray, Ann Arbor, MI) with modifications for maximizing sensitivity to ensure high target complexity in capture (e.g., 55°C hybridization temperature, 16-24h hybridization capture, bait concentration from 50-200 ng), rather than reducing complexity in order to increase the proportion of target captured (e.g., increasing temperature or bait concentration) [S39]. All samples were enriched with the *Plasmodium* mitochondrial bait set; however, the baits were redesigned to remove non-specific stacking in the regions previously indicated and this revised bait set was used on set 3. Set 2 samples were enriched with the original *Plasmodium* bait set, but included blocking oligonucleotides designed to prevent the capture of non-specific stacked regions observed with the set 1 enrichment. *Plasmodium* blocking oligonucleotides were PBO.1 (5'-CTA AGG TAG CAA AAT TCC TTG TCG GGT AAT CTC CGT CCT G/3SpC3/-3'); PBO.2 (5'-TGG GTT AAG AAC GTC TTG AGG CAG TTT GTT CCC TAT CT/3SpC3/-3'); and PBO.3 (5'-AAT TTG CGT GAC GAG CGG TGT GTA CAA GGC /3SpC3/-3'). Blocking oligonucleotides (from Integrated DNA Technologies, Inc.) were used for set 1 enrichment to prevent hybridization of adapter sequences (for universal adapters P5 and P7), using four forward blocking oligonucleotides. The sequences of these forward blocking oligonucleotides were: a) 5'-AGA TCG GAA GAG CAC ACG TCT GAA CTC CAG TCA C /3Phos/-3'; b) 5'-ATC TCG TAT GCC GTC TTC TGC TTG /3Phos/-3'; c) 5'-AAT GAT ACG GCG ACC ACC GAG ATC T /3Phos/-3'; and d) 5'-ACA CTC TTT CCC TAC ACG ACG CTC TTC CGA TCT /3Phos/-3'. The published MYbaits protocol was followed for each set with two rounds of enrichment, alongside modifications to bait concentration, hybridization temperature, and blocking

agents used (except for sets 2 and 3 that used the MYbaits Blocking Agent 3 for Illumina-prepared libraries).

For all sets, the hybridization temperatures remained at 55°C for both rounds of enrichment. For set 1, the bait concentration was 50 ng per reaction and four forward blocking oligonucleotides were used at 2 µM (BO1.P5.part1.F, BO1.P5.part2.F, BO3.P7.part1.F, BO3.P7.part2.F) instead of Blocking Agent 3. For set 2, the bait concentration was 500 ng per reaction and the three *Plasmodium* blocking oligonucleotides were used (PBO.1 at 2.30 µM, PBO.2 at 2.25 µM, and PBO.3 at 2 µM) along with MYbaits Blocking Agent 3. For set 3, the bait concentration was 200 ng per reaction and Blocking Agent 3 was used according to the MYbaits (v3) manual. Additionally, 20-µL of resuspended beads per reaction was used for sets 1 and 3, while 70-µL of resuspended beads per reaction was used for set 2. The reamplification after each round of enrichment used the primer combination IS5_long_amp.P5 and IS6_long_amp.P7 (150 nM each), and KAPA SYBR® FAST qPCR Master Mix (2X). The parameters of the thermal program for all reamplifications were the following: 95°C activation (5 minutes), followed by 11-13 cycles of 95°C (30 seconds), 60°C (45 seconds), ending with 60°C (3 minutes). Following this amplification, each sample was purified with the modified MinElute PCR Purification (Qiagen) protocol described previously, and eluted in 18-µL of EB for sets 1, 2, and 3.

Sequencing

Direct shotgun sequencing was performed on all indexed libraries (UDG/EndoVIII-treated and non-UDG/EndoVIII-treated) to characterize the constituents of each sample and facilitate detection of *Plasmodium* or Apicomplexan reads. Sequencing of the shotgun and *Plasmodium*-enriched libraries was performed on the Illumina HiSeq 1500 platform at the Farncombe Family Digestive Health Research Institute (McMaster University, Hamilton ON, Canada). The samples were pooled in equimolar ratios and sequenced using 2 x 90 bp read chemistry.

Shotgun Library Processing

CASAVA processed reads for the Imperial period Italian libraries (n=58 adults, n=9 juveniles) were trimmed and merged with leeHom [S40] [<https://github.com/greanod/leeHom>], using ancient DNA parameters (--ancientdna). Reads in unmapped bam files were then converted to a fasta file for blastn-megablast analysis (v.2.2.29) [S41]. Each BLAST (Basic Local Alignment Search Tool) output was parsed using MEGAN5 (v.5.11.3) [S42] to assign a taxon and enable prioritization of libraries with putative Apicomplexan or *Plasmodium* spp. reads.

The 11 Imperial period Italian libraries identified as candidates to move forward to *Plasmodium* spp. mitochondrial enrichment had 5-7 reads (from 25,000 to 183,000 assigned reads across the libraries) identified as Apicomplexa or *Plasmodium* taxa (0.006-0.01% of all taxonomically identifiable reads). One

Imperial period adult specimen from Velia (LV33) was included as a “control” during the subsequent enrichments (not showing Apicomplexa or *Plasmodium* taxa in the metagenomic analysis).

In addition, as described below, the shotgun libraries were also mapped with a modified version of BWA [S43] [<https://github.com/udo-stenzel/network-aware-bwa>] to the four human *Plasmodium* mitochondrial genomes. The number of *Plasmodium* spp. reads that mapped in these non-enriched shotgun samples ranged from 0-1 from a total of 544,000 to 3,000,000 processed (trimmed and merged) reads. Non-specific 25-30 bp reads in rRNA and intergenic regions were indicated in Portus Romae (Isola Sacra) libraries LS02, LS06, and LS07, which were not successful during capture, as shown in Table S1; while no reads mapped in LG20 and LV13. Relative estimates of the “endogenous” portion were obtained via mapping to the human mitochondrial (NC_012920) and nuclear genomes [hg38.fa.gz, soft-masked, UCSC Genome Browser, <http://hgdownload.cse.ucsc.edu/goldenPath/hg38/bigZips>] using the parameters described below. The results demonstrate variable “preservation” of human (nuclear) DNA (0.03-15.90%) and mitochondrial DNA (0.0006-0.027%). For LG20, 13.51% and 0.026% of the sequences mapped to the nuclear and mitochondrial genomes (respectively), while for LV13, 1.081% and 0.0025% were also respectively mapped.

***Plasmodium* spp. genome assembly**

CASAVA processed reads for the *Plasmodium*-enriched libraries were trimmed and merged with leeHom [S40] [<https://github.com/greinaud/leeHom>], using ancient DNA parameters (--ancientdna), then mapped with a modified version of BWA [S43] [<https://github.com/udo-stenzel/network-aware-bwa>] with a maximum edit distance of 0.01 (-n 0.01), allowing a maximum of two gap openings (-o 2) and with seeding effectively disabled (-l 16500). Mapped reads were further filtered to those which were either merged or unmerged but properly paired [<https://github.com/greinaud/libbam>] as well as unique based on both 5’ and 3’ coordinates [<https://github.com/udo-stenzel/biohazard>]. The resulting files were collapsed by indexed library removing molecules with identical 5’ and 3’ coordinates [<https://github.com/udo-stenzel/biohazard>]. The collapsed reads were imported into Geneious (v. 7.1.2) (<http://www.geneious.com>) [S44], with the previously noted stacking removed. For all further analyses, we restricted reads to those where the minimum length of inserts was 30 bp and mapping quality (MQ) of 30.

Human mitochondrial genome assembly

The shotgun data and *Plasmodium*-enriched libraries (UDG and non-UDG) for LG20 and LV13 were processed and mapped to the human mitochondrial genome (revised Cambridge Reference Sequence or rCRS, NC_012920), collapsed by indexed library, with duplicate molecules removed within and between libraries, as noted previously. The goal was to generate as complete a human mitochondrial

genome as possible (since enrichment for this target was not performed) as a means to authenticate the data (e.g., internal consistency). Contamination of the rCRS mapped reads was also assessed using schmutzi [S45] [<https://github.com/greanau/schmutzi>]. For the combined non-UDG treated libraries, LG20 had an estimated contamination rate of 0.08 (range of 0.01-0.15), while LV13 was below the threshold of assessment.

Phylogenetic inference

To determine the phylogenetic position of the data generated from our ancient samples within the diversity of *Plasmodium* spp., we combined the read data from both LG20 and LV13 (min 30 bp, MQ 30) with the complete mitochondrial genome sequences of 53 other *Plasmodium* species from various hosts (birds, reptiles, rodents, and primates) including 19 that covered the full range of diversity currently sequenced within *P. falciparum* selected from the National Center for Biotechnology Innovation (NCBI) database.

These data were aligned using multiple rounds of MAFFT (v.7.017) [S46] and MUSCLE (v.3.5) [S47] alignment within Geneious (v. 7.1.2) (<http://www.geneious.com>) [S44], resulting in an aligned data set 7,366 bp in length. However, due to the non-overlapping nature of some the sequences and the presence of indels, all ambiguously aligned regions were removed using Gblocks [S48]. This resulted in a final data set of 4,570 bp that was used for the main phylogenetic analysis. Phylogenetic trees of these data were inferred using the maximum likelihood (ML) method available within PhyML [S49], assuming the GTR+ Γ model of nucleotide substitution and a combination of Nearest-Neighbour Interchange (NNI) and sub-tree pruning and regrafting (SPR) branch-swapping. The relevant parameters for the 4,570 bp data set were $\Gamma = 0.682$ and $I = 0.478$. The degree of support for each node on the tree was then determined using a second ML phylogenetic analysis in which 1,000 bootstrap replicates were estimated utilizing NNI branch-swapping and the same model of nucleotide substitution as defined above. An ML tree of the full 7,366 bp alignment prior to Gblocks [48] pruning was also inferred and is shown in Figure S1f.

In both trees it is notable that LG20-LV13 clearly clusters within the phylogenetic diversity of *P. falciparum* with strong bootstrap support. However, there was no strong bootstrap support linking LG20-LV13 with any individual strain of *P. falciparum*, such that these data do not provide sufficient phylogenetic resolution at this scale. It is also notable that the branch leading to the LG20-LV13 data in all phylogenies is longer than that seen in other strains of *P. falciparum*. This increased branch length is due to the presence of SNPs unique to LG20-LV13 that may contain both damage and sequencing errors (see below).

P. falciparum and human mitochondrial genome validation

i. Fragment length distributions. We generated fragment length distributions (FLDs) for the *P. falciparum* and human mitochondrial genomes for LG20 (Vagnari specimen F234) and LV13 (Velia specimen 186) from reads >30 bp and

with minimum mapping quality (MQ) of 30. The FLDs when mapped to the *P. falciparum* mitochondrial genome (NC_002375) showed patterns typical of ancient DNA fragmentation (i.e., abundance of short fragments), while reagent blanks and associated controls (e.g., Maritime Archaic libraries) did not have the same distribution. In addition, using a custom RStudio (ggplot2) [S50] script, read length distributions were generated for LG20 and LV13 as mapped to the *P. falciparum* (NC_002375) and human mitochondrial (rCRS, NC_012920) genomes, with an additional overlay of LV13 *P. falciparum* reads and LV13 human mitochondrial reads (Figure S1b).

ii. *Misincorporation rates.* To estimate damage in our ancient extracts we used mapDamage [S51] (v.0.3.6) [<http://ginolhac.github.io/mapDamage>], on non-UDG/EndoVIII indexed library reads once mapped to the *P. falciparum* (NC_002375) and human mitochondrial genomes (rCRS, NC_012920). Multiple libraries sequenced for samples LG20 and LV13 were merged into a single data set in the following manner: from the three *Plasmodium* capture experiments each similarly indexed library was combined using SAMtools merge with duplicates collapsed by indexed library to remove molecules with identical 5' and 3' coordinates using bam-rmdup [<https://github.com/udo-stenzel/biohazard>]. The resulting files for all libraries were then merged into a single bam file, and duplicates collapsed between the libraries [<https://github.com/udo-stenzel/biohazard>], with restrictions on read length and mapping quality. Accordingly, the combined data set for LG20-LV13 (min 24 bp MQ 30 and min 30 bp MQ 30) that mapped to *P. falciparum* (NC_002375) were then put into mapDamage [S51], with and without stacks removed (Figure S1c). As described above (in the Supplemental Experimental Procedures) “*Plasmodium* spp. Capture Baits Design” section, the stacked regions represented the capture of repetitive non-specific reads of diverse species (e.g., Bacteria, Eukaryota) in rRNA and intergenic regions, and were removed so as to not bias downstream analyses (Table S1 provides mapped data with and without these stacked regions).

Using the same approach, but mapping to the human mitochondrion (rCRS, NC_012920), multiple (non-UDG) libraries for LG20 and LV13 were separately merged from the capture experiments as well as shotgun libraries using SAMtools merge, with duplicates collapsed by indexed library to remove molecules with identical 5' and 3' coordinates using bam-rmdup [<https://github.com/udo-stenzel/biohazard>]. The resulting files for LG20 and LV13 were each merged into a single bam file, with duplicates collapsed [<https://github.com/udo-stenzel/biohazard>], with restriction to a minimum length of 30 bp and mapping quality of 30 to generate damage profiles (Figure S1d).

As the total number of reads mapping to *P. falciparum* (NC_002375) (LG20-LV13 combined) was low, the frequency of C>T and G>A substitutions was also low, yet still showed a deamination signal as expected of ancient DNA damage (also supported by a manual count of these substitutions that indicated a higher number of G>A changes). Accordingly, to simulate our estimates of

damage and authenticity of the samples, we randomly selected a similar number of reads mapping to the human rCRS (NC_012920) from the LG20 and LV13 libraries (min 30 bp, MQ 30, non-UDG shotgun and enriched) that approximated the number of reads and maximum length of the *Plasmodium*-enriched LG20-LV13 combined non-UDG libraries (min 30 bp, MQ 30) with stacks (116 reads, 76 bp max) and stacks removed (51 reads, 76 bp max). Although the damage patterns were broadly similar between the human mtDNA and *P. falciparum* genome, they were not surprisingly low; emphasizing the challenge of bioinformatic authentication of low endogenous aDNA damage signals (refer to Figure S1e for an example).

iii. *Sequence validation per sample and combined*

A) LV13 (Velia 186)

LV13 has 2,901 bp covered by 113 reads, composed of reads ranging from 30 bp to 161 bp, with a mean coverage of 1.0X (up to a maximum coverage 6X), with 48.6% of the *P. falciparum* genome covered.

B) LG20 (F234, Vagnari)

LG20 has 300 bp covered by 7 reads, ranging from 42 bp to 106 bp, with a mean coverage of 0.1X (up to a maximum coverage 2X) that were scattered across the genome in the *COI* and *CYTB* genes, as well as intergenic regions, with 5.0% of the *P. falciparum* genome covered. Five of the LG20 reads were highly specific to *P. falciparum* when evaluated via mapping and blastn-megablast analysis (v.2.2.29) [S41], while two are non-specific 30 bp reads.

The combined *P. falciparum* data set (LG20-LV13, min 30 bp, MQ 30) merged the separate indexed libraries from the three capture experiments of the multiple libraries for LG20 and LV13, removing duplicate molecules both within and between libraries as described in the Supplemental Experimental Procedures section. The justification for pooling the *Plasmodium*-mapped reads from LG20 and LV13 was the presumption that genetically similar strain(s) are likely to circulate in the study populations, particularly given the known genetic diversity of *P. falciparum* mtDNA within individual geographic localities (e.g., Conway et al., 2000 in ref. S52; Joy et al., 2003 in ref. S53; Tyagi et al., 2014 in ref. S54), as well as to maximize genome coverage and hence phylogenetic resolution and certainty. The merged data for LG20-LV13 (with stacks removed) at minimum 30 bp and mapping quality 30 resulted in 120 reads (3,033 bp) mapping to *Plasmodium falciparum* (average fragment length 51 bp, and maximum fragment length 161 bp), with 50.8% of the reference covered at a mean coverage of 1X with a maximum 7X coverage.

The merged data for LG20-LV13 at the same parameters (min 30 bp, MQ 30) (with stacks removed) was mapped to other *Plasmodium* species in the baits set. Although reads map to other *Plasmodium* species, these demonstrate

similarity to *P. falciparum*, with the overall numbers reduced. For example, the number of reads assembled to the other human *Plasmodium* genomes (*P. vivax*, *P. malariae*, and *P. ovale*) ranged from 66-67, with 0.5-0.6X coverage, average fragment lengths of 43.8-45.2 bp, and ultimately only represent 24.6-25.9% coverage of the respective genomes. This lends credence to the genus level identification of these reads and bolsters the evidence for specific detection of *P. falciparum* in the Imperial period Italian skeletal remains.

To evaluate the specificity of the LG20-LV13 sequence reads and to rule out, to the greatest extent possible, contamination of the remains from related genera among the Apicomplexans we similarly processed reads to *Leucocytozoon* species [*L. fringillinarum* (NC_012451), *L. majoris* (NC_012450), *L. sabrazei* (NC_009336), *L. caullyeri* (NC_015304)], *Haemoproteus columbae* (NC_012448), *Hepatozoon catesbiana* (KF894962), *Parahaemoproteus vireonis* (NC_012447), *Babesia bovis* (NC_009902), *Babesia microti* (NC_019570), *Theileria annulata* (NT_167255), *Theileria parva* (Z23263), and *Neospora caninum* (JX473252)] and other *Plasmodium* species of various hosts (e.g., birds, rodents, and primates including the gorilla clade) used in the phylogenetic analysis. The results indicate conserved *P. falciparum* reads from LG20-LV13 map to these genomes as well, with 0-108 reads shared with various *Plasmodium* species (*P. reichenowi* is the highest with 108 reads, followed by *P. billcollinsi* with 84 reads) and 0-38 reads are shared with the selected Apicomplexa (*Haemosporida*) predominantly in the *Leucocytozoon* and *Haemoproteus* species. The similarity is expected due to the high degree of conservation with *Plasmodium* spp. mitochondrial genomes and *Haemosporida* in general, which is well-characterized [S55], but does not suggest that the signal here is derived from these non-human *Plasmodium* species.

We identified 21 unique SNPs within the consensus of LG20-LV13 where 15 SNPs were invariant (i.e., not present in any *Plasmodium* species, indicated by an “*”) : 200 C>T, 301 A>C*, 314 A>C*, 489 A>G*, 546 G>A, 610 C>T*, 831 T>A*, 2298 C>T, 2338 C>T*, 2357 C>T*, 2362 C>T*, 2763 C>T, 2822 G>A*, 2858 T>C*, 3193 T>C*, 3539 C>T, 3856 C>T*, 3860 C>T*, 3938 A>T*, 4426 C>T*, 4527 C>T. Of these invariant SNPs, four were in rRNA and intergenic regions, with 11 in the *COXIII*, *COI* and *CYTB* genes (8 non-synonymous and 3 synonymous mutations that were predominantly artefacts of damage, such as C>T and G>A substitutions). All of these SNPs were excluded from the final tree in Figure 1b of the main text (i.e., following Gblocks pruning) such that the short branch leading to LG20-LV13 is defined by 6 SNPs. However, the removal of these 15 SNPs made no difference to the phylogenetic analysis as the Gblocks-pruned tree (4,570 bp; Figure 1b of the main text) is topologically identical to the 7,366 bp tree (Fig. S1f) that contains all of the LG20-LV13 SNPs.

Of the 6 unique SNPs evident in Figure 1b of the main text, 2 occur in the *COI* gene (synonymous C>T mutations), 2 occur within the *CYTB* gene (1 synonymous and 1 non-synonymous C>T mutation). A single SNP (C>T) is evident in the intergenic region, while there was a G>A (invariant) substitution in

the RNA region. While 4 of these SNPs occur in regions that are not highly variable in current *Plasmodium* strains (e.g., *COI* and *CYTB*) these are likely to be due to damage or sequence errors, but we were hesitant to call them as such given they were predominantly third position synonymous changes. Ultimately, for the bulk of the SNPs, the non-synonymous mutations were attributed to sequence errors and/or damage-induced substitutions, as the conserved *Plasmodium* spp. mitochondrial genomes predominantly exhibit synonymous mutations in protein-coding genes with only a few polymorphic sites [S55].

iv. Human mitogenome

We also evaluated SNPs in our reconstructed human mitochondrial genomes. All SNPs were called by Geneious (v. 7.1.2) (<http://www.geneious.com>) [S44] at 5X coverage and 90% minimum variant frequency and also interpreted via HaploGrep2 [S56], with mutations indicated (i.e., absent, expected, private). The haplogroup of each individual was determined using HaploGrep2 [S56] from a consensus fasta file generated from the mitochondrial alignments, with the resultant SNP calls compared between HaploGrep2 [S56] and PhyloTree Build 17 [S57]: the haplogroup for sample LG20 is consistent with T2c1e (88.16% quality score) and LV13 is consistent with haplogroup T2b29 (62.17% quality score). The rCRS metrics are as follows: LG20, has a combined 2,811 reads (min 30 bp, MQ 30), mean coverage 10.6X, average fragment length 62.6 bp, and 99.4% of the reference covered; while LV13 has 922 reads (min 30 bp, MQ 30), mean coverage 3X, average fragment length 53.5 bp, and 85.3% of the reference covered. Using a local human mitochondrial database (updated from GenBank 2016-02-05), we recovered additional published mtDNA genomes that shared the same haplogroups as LV13 and LG20 [using rCRS data from refs. S58, S59, S60, S61, and S62] and found them to originate from individuals in Europe and the Mediterranean.

All datasets are available upon request.

Author contributions

SM and HNP conceptualized the study, and SM performed all laboratory work. LB and TLP provided the skeletal samples. SM, TLP, DAH and HNP designed the study. SM, HNP, and ECH analyzed the data. SM, ATD, HNP, and ECH assisted in data interpretation. All authors vouch for the data and analysis. SM, HNP, and ECH wrote the first draft, and co-wrote subsequent drafts with all other co-authors. All co-authors approved the paper.

Acknowledgements

We would like to thank D. Poinar, and all members of the McMaster Ancient DNA Centre for their contribution to this manuscript. In addition, we would like

to thank all contributing members of the archaeological excavations. Funding for this project was provided by The Australian, National Health and Medical Research Council to EH and HNP, and the Canada Research Chairs Program to HNP. A Social Sciences and Humanities Research Council of Canada Doctoral Fellowship (#752-2014-1849) was awarded to SM. The authors declare no conflicting financial interests.

Supplemental References

- S1. Kindt, T.J., Goldsby, R.A., and Osborne, B.A. (2007). *Kuby Immunology*, Sixth edition (New York: WH Freeman and Company).
- S2. Sherman, I.W., ed. (1998). *Malaria: parasite biology, pathogenesis, and protection* (Washington: ASM Press).
- S3. Roberts, C., and Manchester, K. (2005). *The Archaeology of Disease* (Ithaca: Cornell University Press).
- S4. Smith-Guzman, N.E. (2015). The skeletal manifestation of malaria: An epidemiological approach using documented skeletal collections. *Am. J. Phys. Anthropol.* 158, 624-635.
- S5. Walker, P.L., Bathurst, R.R., Richman, R., Gjerdrum, T., and Andrushko, V.A. (2009). The causes of porotic hyperostosis and cribra orbitalia: A reappraisal of the iron-deficiency-anemia hypothesis. *Am. J. Phys. Anthropol.* 139, 109-125.
- S6. Gowland, R., and Garnsey, P. (2010). Skeletal evidence for health, nutritional status and malaria in Rome and the Empire. In *Roman Diasporas: Archaeological Approaches to Mobility and Diversity in the Roman Empire (Supplement 78)*, H. Eckardt, ed. (Portsmouth: Journal of Roman Archaeology), pp. 131-156.
- S7. Smith-Guzman, N.E. (2015). Cribra orbitalia in the ancient Nile Valley and its connection to malaria. *Int. J. Paleopathol.* 10, 1-12.
- S8. Faure, E. (2014). Malarial pathocoenosis: beneficial and deleterious interactions between malaria and other human diseases. *Front. Physiol.* 5, 441-454.
- S9. Taylor, G.M., Rutland, P., and Molleson, T. (1997). A sensitive polymerase chain reaction method for the detection of *Plasmodium* species DNA in ancient human remains. *Anc. Biomol.* 1, 193-203.
- S10. Zink, A., Haas, C.J., Herberth, K., and Nerlich, A.G. (2001). PCR amplification of *Plasmodium* DNA in ancient human remains. *Anc. Biomol.* 3, 293.
- S11. Nerlich, A.G., Schraut, B., Dittrich, S., Jelinek, T.H., and Zink, A. (2008). *Plasmodium falciparum* in Ancient Egypt. *Emerg. Infect. Dis.* 14, 1317–8.

- S12. Miller, R.L., Ikram, S., Armelagos, G.J., Walker, R., Harer, W.B., Shiff, C.J., Baggett, D., Carrigan, M., and Maret, S.M. (1994). Diagnosis of *Plasmodium falciparum* infections in mummies using the rapid manual ParaSight-F Test. *Trans. R. Soc. Trop. Med. Hyg.* 88, 31–32.
- S13. Rabino Massa, E., Cerutti, N., and Savoia, A.M.D. (2000). Malaria in ancient Egypt: paleo-immunological investigations in predynastic mummified remains. *Chungara (Arica)* 32, 7–9.
- S14. Bianucci, R., Mattutino, G., Lallo, R., Charlier, P., Jouin-Spriet, H., Peluso, A., Higham, T., Torre, C., and Rabino Massa, E. (2008). Immunological evidence of *Plasmodium falciparum* infection in an Egyptian child mummy from the Early Dynastic Period. *J. Archaeol. Sci.* 35, 1880-1885.
- S15. Hawass, Z., Gad, Y.Z., Ismail, S., Khairat, R., Fathalla, D., Hasan, N., Ahmed, A., Elleithy, H., Ball, M., Gaballah, F., and Wasef, S. (2010). Ancestry and pathology in King Tutankhamen’s family. *J. Am. Med. Assoc.* 303, 638-647.
- S16. Lalremruata, A., Ball, M., Bianucci, R., Welte, B., Nerlich, A.G., Kun, J.F., and Pusch, C.M. (2013). Molecular identification of falciparum malaria and human tuberculosis co-infections in mummies from the Fayum depression (Lower Egypt). *PLoS ONE* 8, e60307.
- S17. Bianucci, R., Araujo, A., Pusch, C.M. and Nerlich, A.G. (2015). The identification of malaria in paleopathology—An in-depth assessment of the strategies to detect malaria in ancient remains. *Acta Tropica* 152, 176-180.
- S18. Setzer, T.J. (2014). Malaria detection in the field of paleopathology: a meta-analysis of the state of the art. *Acta Tropica* 140, 97-104.
- S19. Small, A.M., ed. (2011). *Vagnari. The village, the industries the imperial property* (Italy: Edipuglia).
- S20. Small, A.M., ed. (2014). *Beyond Vagnari: New Themes in the Study of Roman South Italy* (Italy: Edipuglia).
- S21. Prowse, T.L., Barta, J.L., von Hunnius, T.E., and Small, A.M. (2010). Stable isotope and mtDNA evidence for geographic origins at the site of Vagnari, south Italy. In *Roman Diasporas: Archaeological Approaches to Mobility and Diversity in the Roman Empire*, H. Eckardt, ed. (Portsmouth: *Journal of Roman Archaeology, Supplement* 78), pp. 175-198.

- S22. Sperduti, A., Bondioli, L., and Garnsey, P. (2012). Skeletal evidence for occupational structure at the coastal towns of Portus and Velia (1st-3rd c. AD). In *More Than Just Numbers? The Role of Science in Roman Archaeology*, I. Schrufer-Kolb, ed. (Portsmouth: Journal of Roman Archaeology, Supplement 91), pp.53-70.
- S23. Craig, O.E., Biazzo, M., O'Connell, T.C., Garnsey, P., Martinez-Labarga, C., Lelli, R., Salvadei, L., Tartaglia, G., Nava, A., Renò, L., Fiammenghi, A., Rickards, O., and Bondioli, L. (2009). Stable isotopic evidence for diet at the Imperial Roman coastal site of Velia (1st and 2nd centuries AD) in Southern Italy. *Am. J. Phys. Anthropol.* 139, 572-583.
- S24. Crowe, F., Sperduti, A., O'Connell, T.C., Craig, O.E., Kirsanow, K., Germoni, P., Macchiarelli, R., Garnsey, P., and Bondioli, L. (2010). Water-related occupations and diet in two Roman coastal communities (Italy, first to third century AD): correlation between stable carbon and nitrogen isotope values and auricular exostosis prevalence. *Am. J. Phys. Anthropol.* 142, 355-366.
- S25. Fiammenghi CA. 2003. La Necropoli di Elea-Velia: qualche osservazione preliminare. In *Elea-Velia. Le Nuove ricerche*, L. Cicala, G. Greco, eds. (Quaderni del Centro Studi Magna Grecia 1: Naus Editoria), pp. 49-61.
- S26. Prowse, T.L., Schwarcz, H.P., Saunders, S.R., Macchiarelli, R., and Bondioli, L. (2005). Isotopic evidence for age-related variation in diet from Isola Sacra, Italy. *Am. J. Phys. Anthropol.* 128, 2-13.
- S27. Prowse, T.L., Schwarcz, H.P., Garnsey, P., Knyf, M., Macchiarelli, R., and Bondioli, L. (2007). Isotopic evidence for age-related immigration to imperial Rome. *Am. J. Phys. Anthropol.* 132, 510-19.
- S28. Keay, S., Millett, M., Paroli, L., and Strutt, K., eds. (2005). *Portus: An Archaeological Survey of the Port of Imperial Rome*. London: Archaeological Monographs of the British School at Rome.
- S29. Prowse, T.L., Nause, C., and Ledger, M. (2014). Growing up and growing old on an imperial estate: preliminary palaeopathological analysis of skeletal remains from Vagnari. In *Beyond Vagnari: New Themes in the Study of Roman South Italy*, Small, A.M., ed. (Italy: Edipuglia), pp. 111-122.

- S30. Beauchesne, P.D. (2012). *Physiological Stress, Bone Growth and Development in Imperial Rome*. University of California, Berkley, unpublished PhD dissertation.
- S31. Sperduti, A. (1995). *I resti scheletrici umani della necropoli di età romano imperiale di Isola Sacra (i-iii sec. d. C.): analisi paleodemografica*. PhD dissertation.
- S32. Fisk, G.H. (1931). Malaria and the Anopheles mosquito in Canada. *Can. Med. Assoc. J.* 25, 679-683.
- S33. Schwarz, C., Debruyne, R., Kuch, M., McNally, E., Schwarcz, H., Aubrey, A.D., Bada, J., and Poinar, H. (2009). New insights from old bones: DNA preservation and degradation in permafrost preserved mammoth remains. *Nucleic Acids Res.* 37, 3215–29.
- S34. Wagner, D.M., Klunk, J., Harbeck, M., Devault, A., Waglechner, N., Sahl, J.W., Enk, J., Birdsell, D.N., Kuch, M., Lumibao, C., Poinar, D., Pearson, T., Fourment, M., Golding, B., Riehm, J.M., Earn, D.J., DeWitte, S., Rouillard, J.M., Grupe, G., Wiechmann, I., Bliska, J.B., Keim, P.S., Scholz, H.C., Holmes, E.C., and Poinar, H. (2014). *Yersinia pestis* and the plague of Justinian 541-543 AD: a genomic analysis. *Lancet Infect. Dis.* 14, 319-326.
- S35. Hagelberg, E., and Clegg, J.B. (1991). Isolation and characterization of DNA from archaeological bone. *Proc. R. Soc. Lond. B Biol. Sci.* 244, 45-50.
- S36. Dabney, J., Knapp, M., Glocke, I., Gansauge, M.T., Weihmann, A., Nickel, B., Valdiosera, C., García, N., Pääbo, S., Arsuaga, J.L. and Meyer, M. (2013). Complete mitochondrial genome sequence of a Middle Pleistocene cave bear reconstructed from ultrashort DNA fragments. *Proc. Nat. Acad. Sci. USA* 110, 15758-63.
- S37. Meyer, M., and Kircher, M. (2010). Illumina sequencing library preparation for highly multiplexed target capture and sequencing. *Cold Spring Harb. Protoc.* 2010, pdb prot5448.
- S38. Kircher, M., Sawyer, S., and Meyer, M. (2012). Double indexing overcomes inaccuracies in multiplex sequencing on the Illumina platform. *Nucleic Acids Res.* 40, e3.

- S39. Enk, J. (2016). Target capture for ancient DNA: temperature, time, and tiling density. 81st Annual Meeting of the Society for American Archaeology (Orlando, FL).
- S40. Renaud, G., Stenzel, U., and Kelso, J. (2014). leeHom: adaptor trimming and merging for Illumina sequencing reads. *Nucleic Acids Res.* *42*, e141.
- S41. Altschul, S.F., Gish, W., Miller, W., Myers, E.W., and Lipman, D.J. (1990). Basic local alignment search tool. *J. Mol. Biol.* *215*, 403–10.
- S42. Huson, D.H., Auch, A.F., Qi, J., and Schuster, S.C. (2007). MEGAN analysis of metagenomic data. *Genome Res.* *17*, 377-386.
- S43. Li, H., and Durbin, R. (2009). Fast and accurate short read alignment with Burrows–Wheeler transform. *Bioinformatics* *25*, 1754-60.
- S44. Kearse, M., Moir, R., Wilson, A., Stones-Havas, S., Cheung, M., Sturrock, S., Buxton, S., Cooper, A., Markowitz, S., Duran, C. and Thierer, T. M. (2012). Geneious Basic: an integrated and extendable desktop software platform for the organization and analysis of sequence data. *Bioinformatics* *28*, 1647-1649.
- S45. Renaud, G., Slon, V., Duggan, A.T., and Kelso, J. (2015). Schmutzi: estimation of contamination and endogenous mitochondrial consensus calling for ancient DNA. *Genome Biol.* *16*, 1-18.
- S46. Katoh, K., and Standley, D.M. (2013). MAFFT multiple sequence alignment software version 7: improvements in performance and usability. *Mol. Biol. Evol.* *30*, 772-780.
- S47. Edgar, R.C. (2004). MUSCLE: multiple sequence alignment with high accuracy and high throughput. *Nucleic Acids Res.* *32*, 1792-97.
- S48. Talavera, G., and Castresana, J. (2007). Improvement of phylogenies after removing divergent and ambiguously aligned blocks from protein sequence alignments. *Syst. Biol.* *56*, 564-77.
- S49. Guindon, S., Dufayard, J.F., Lefort, V., Anisimova, M., Hordijk, W., and Gascuel, O. (2010). New algorithms and methods to estimate maximum-likelihood phylogenies: assessing the performance of PhyML 3.0. *Syst. Biol.* *59*, 307-321.
- S50. RStudio. Integrated Development for R. Boston: RStudio, Inc., 2015. <http://www.rstudio.com/>.

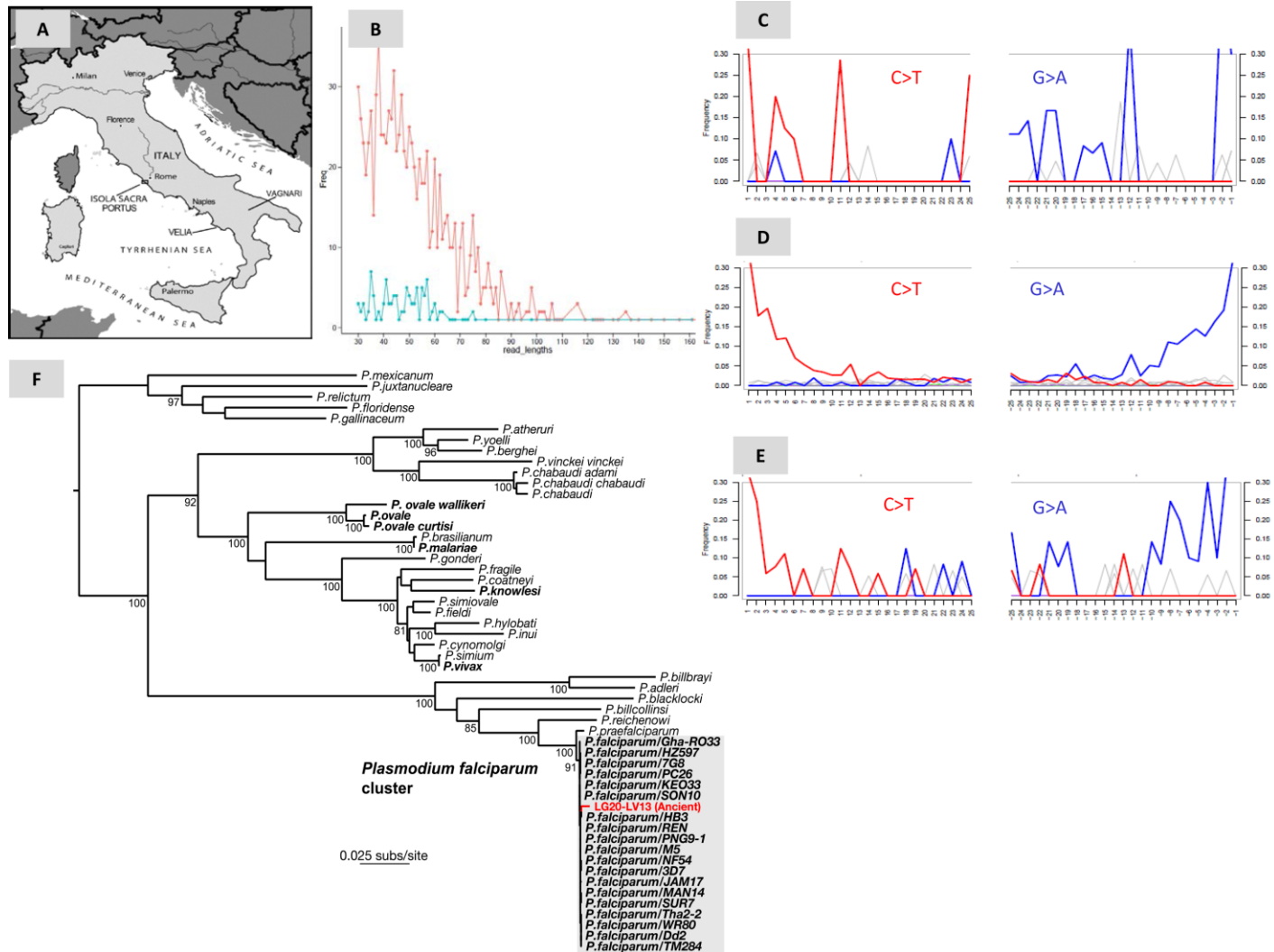
- S51. Ginolhac, A., Rasmussen, M., Gilbert, M.T.P., Willerslev, E., and Orlando, L. (2011). mapDamage: testing for damage patterns in ancient DNA sequences. *Bioinformatics* 27, 2153-2155.
- S52. Conway, D.J., Fanello, C., Lloyd, J.M., Ban, M.S., Baloch, A.H., Somanath, S.D., Roper, C., Oduola, A.M., Mulder, B., Povoia, M.M. and Singh, B. (2000). Origin of *Plasmodium falciparum* malaria is traced by mitochondrial DNA. *Mol. Biochem. Parasitol.* 111, 163-171.
- S53. Joy, D.A., Feng, X., Mu, J., Furuya, T., Chotivanich, K., Krettli, A.U., Ho, M., Wang, A., White, N.J., Suh, E. and Beerli, P. (2003). Early origin and recent expansion of *Plasmodium falciparum*. *Science* 300, 318-321.
- S54. Tyagi, S., Pande, V., and Das, A. (2014). Mitochondrial genome sequence diversity of Indian *Plasmodium falciparum* isolates. *Mem. Inst. Oswaldo Cruz* 109, 494-498.
- S55. Feagin, J.E., Harrell, M.I., Lee, J.C., Coe, K.J., Sands, B.H., Cannone, J.J., Tami, G., Schnare, M.N. and Gutell, R.R. (2012). The fragmented mitochondrial ribosomal RNAs of *Plasmodium falciparum*. *PLoS ONE* 7, e38320.
- S56. Kloss-Brandstätter, A., Pacher, D., Schönherr, S., Weissensteiner, H., Binna, R., Specht, G. and Kronenberg, F. (2011). HaploGrep: a fast and reliable algorithm for automatic classification of mitochondrial DNA haplogroups. *Hum. Mutat.* 32, 25-32.
- S57. van Oven M. (2015). PhyloTree Build 17: Growing the human mitochondrial DNA tree. *Forensic Sci. Int., Genetics Supp. Series* 5, e392-e394.
- S58. Fernandes, V., Triska, P., Pereira, J.B., Alshamali, F., Rito, T., Machado, A., Fajkošová, Z., Cavadas, B., Černý, V., Soares, P. and Richards, M.B. (2015). Genetic stratigraphy of key demographic events in Arabia. *PLoS ONE* 10, E0118625.
- S59. Family Tree DNA. Genealogy, by Genetics Ltd. Submitted (23-MAY-2015).
- S60. Carossa, V., Ghelli, A., Tropeano, C.V., Valentino, M.L., Iommarini, L., Maresca, A., Caporali, L., La Morgia, C., Liguori, R., Barboni, P. and Carbonelli, M. (2014). A novel in-frame 18-bp microdeletion in MT-CYB

causes a multisystem disorder with prominent exercise intolerance. *Hum. Mutat.* 35, 954-958.

- S61. Behar, D.M., van Oven, M., Rosset, S., Metspalu, M., Loogväli, E.L., Silva, N.M., Kivisild, T., Torroni, A. and Villems, R. (2012). A 'Copernican' reassessment of the human mitochondrial DNA tree from its root. *Am. J. Hum. Genet.* 90, 675-684.
- S62. Pala, M., Olivieri, A., Achilli, A., Accetturo, M., Metspalu, E., Reidla, M., Tamm, E., Karmin, M., Reisberg, T., Kashani, B.H., Perego, U.A., Carossa, V., Gandini, F., Pereira, J.B., Soares, P., Angerhofer, N., Rychkov, S., Al-Zahery, N., Carelli, V., Sanati, M.H., Houshmand, M., Hatina, J., Macaulay, V., Pereira, L., Woodward, S.R., Davies, W., Gamble, C., Baird, D., Semino, O., Villems, R., Torroni, A., and Richards, M.B. (2012). Mitochondrial DNA signals of late glacial recolonization of Europe from near eastern refugia. *Am. J. Hum. Genet.* 90, 915-924.

Supplemental Figure S1 and Table S1

Figure S1. (A) Map of the Imperial period Italian cemeteries (courtesy of L. Bondioli); (B) Read length distribution for LV13 *P. falciparum* (indicated in blue with 113 reads, mean 50.8 bp, and 1.0X average coverage) and human mtDNA (indicated in red with 922 reads, mean 53.5 bp, and 3.0X average coverage); (C) Damage profile for LG20-LV13 *P. falciparum* mitochondrion assembly; (D) Damage profile for LV13 human mitochondrion assembly; (E) Randomized damage profile for LV13 human mitochondrion assembly to approximate LG20-LV13 *P. falciparum* assembly; (F) Phylogenetic relationships of LG20-LV13 and other *Plasmodium* spp. inferred from the full 7,366 bp mtDNA sequence alignment. The tree was rooted on non-mammalian *Plasmodium* sequences and all horizontal branch lengths are drawn to a scale of nucleotide substitutions per site. Bootstrap support values are shown for key nodes with >80% support. The tree presents the same topology as the phylogeny in Figure 1b in the main text.



Supplemental Table S1. *P. falciparum* capture summary.

Set 1 capture metrics

Individual	Library ID	Raw reads	Trimmed and merged reads	Mapped reads	Mapped (24bp, MQ20)	Mapped (30bp, MQ30)	Uniquely mapped (stacks removed, 30bp, MQ30)	% on-target reads	% unique reads
VAG F226, Juvenile, Vagnari	JV01	24,556	13,534	48	45	5	0	0.04	0.0000
VAG F283, Juvenile, Vagnari	JV02	39,782	23,311	24	24	6	0	0.03	0.0000
VAG F282, Juvenile, Vagnari	JV03	1,096	572	1	1	0	0	0.00	0.0000
VAG F297, Juvenile, Vagnari	JV04	5,258	3,272	6	5	0	0	0.00	0.0000
VAG F299, Juvenile, Vagnari	JV05	38,374	21,657	438	161	35	1	0.16	0.0046
VAG F286B, Juvenile, Vagnari	JV06	14,002	7,642	84	80	15	0	0.20	0.0000
VAG F210, Juvenile, Vagnari	JV07	13,518	7,186	80	78	12	0	0.17	0.0000
VAG F55, Juvenile, Vagnari	JV08	1,376	863	6	6	1	0	0.12	0.0000
VAG F43, Juvenile, Vagnari	JV09	510	313	0	0	0	0	0.00	0.0000
Juvenile extraction blank	JV10	16	10	0	0	0	0	0.00	0.0000
SCR 602, Adult, Isola Sacra	LS02	0	0	0	0	0	0	0.00	0.0000
SCR 698, Adult, Isola Sacra	LS03	43,254	24,344	218	83	16	1	0.07	0.0041
SCR 382, Adult, Isola Sacra	LS05	53,162	27,613	172	170	43	0	0.16	0.0000
SCR 526, Adult, Isola Sacra	LS06	157,396	86,210	218	214	62	1	0.07	0.0012
SCR 797, Adult, Isola Sacra	LS07	144,542	78,517	370	124	61	0	0.08	0.0000
Roman extraction blank	LS08	4	2	1	0	0	0	0.00	0.0000
VAG F234, Adult, Vagnari	LG20	6,962	3,695	510	32	7	1	0.19	0.0271
VAG F37, Adult, Vagnari	LG23	94,650	48,914	138	134	21	0	0.04	0.0000
VEL 186, Adult, Velia	LV13	126,838	68,282	492	175	42	6	0.06	0.0088
VEL 205, Adult, Velia	LV14	61,240	33,532	140	127	34	0	0.10	0.0000
VEL82, Adult, Velia	LV33	6,394	3,709	30	28	7	0	0.19	0.0000
VAG F117, Adult, Vagnari	PLG11	58,458	34,110	546	219	53	1	0.16	0.0029
VEL 194, Adult, Velia	PLV06	55,288	31,723	155	150	43	0	0.14	0.0000
NP31, Maritime Archaic, adult	BTK21	7,696	3,936	0	0	0	0	0.00	0.0000
NP51, Maritime Archaic, adult	BTK28	412	213	0	0	0	0	0.00	0.0000
Maritime Archaic extraction blank	BTKB1	50	35	0	0	0	0	0.00	0.0000

Set 1 subset capture metrics

Individual	Library ID	Raw reads	Trimmed and merged reads	Mapped reads	Mapped (24bp, MQ20)	Mapped (30bp, MQ30)	Uniquely mapped (stacks removed, 30bp, MQ30)	% on-target reads	% unique reads
VAG F299, Juvenile, Vagnari	JV05	3,420,644	1,974,996	438	415	90	2	0.0046	0.00010
SCR 698, Adult, Isola Sacra	LS03	378,848	208,883	213	182	42	0	0.0201	0.00000
SCR 526, Adult, Isola Sacra	LS06	2,885,598	1,637,851	359	292	62	0	0.0038	0.00000
Extraction blank	LS08	578	289	1	0	0	0	0.0000	0.00000
VAG F117, Adult, Vagnari	PLG11	2,162,052	1,315,885	543	517	97	0	0.0074	0.00000
VAG F234, Adult, Vagnari	LG20	2,754,418	1,475,992	510	390	81	1	0.0055	0.00007
VEL 186, Adult, Velia	LV13	2,835,460	1,552,249	488	445	89	12	0.0057	0.00077

Set 2 capture metrics

Individual	Library ID	Raw reads	Trimmed and merged reads	Mapped reads	Mapped (24bp, MQ20)	Mapped (30bp, MQ30)	Uniquely mapped (stacks removed, 30bp, MQ30)	% on-target reads	% unique reads
VAG F299, Juvenile, Vagnari	MJV01	1,799,042	953,910	98	72	11	1	0.0012	0.00010
	MJV07	168	92	0	0	0	0	0.0000	0.00000
VAG F234, Adult LG20, Vagnari	MLG02	7,632,046	3,997,873	170	150	17	1	0.0004	0.00003
	MLG03	43,933,816	23,398,604	236	170	33	1	0.0001	0.00000
	MLG08	5,450,830	3,007,552	97	87	18	2	0.0006	0.00007
	MLG09	6,286,326	3,381,400	116	104	14	1	0.0004	0.00003
	MLG14	7,330,436	4,555,869	92	75	9	1	0.0002	0.00002
VEL 186, Adult LV13, Velia	MLV04	6,194,872	4,006,498	38	28	8	5	0.0002	0.00012
	MLV05	7,713,490	4,045,129	205	167	51	39	0.0013	0.00096
	MLV10	8,051,628	5,172,257	64	48	22	21	0.0004	0.00041
	MLV11	15,488,420	7,974,259	126	121	28	16	0.0004	0.00020
	MLV13	9,288,898	4,895,348	189	144	28	17	0.0006	0.00035
Extraction blank	MEB06	2,354,448	1,529,637	19	0	0	0	0.0000	0.00000
Extraction blank	MEB12	5,156,454	3,298,046	27	1	0	0	0.0000	0.00000
Extraction blank	MEB15	10,166	5,349	1	0	0	0	0.0000	0.00000
Extraction blank	MEB16	26	18	0	0	0	0	0.0000	0.00000
NP41, Maritime Archaic, adult	MBT17	1,415,748	1,045,204	0	0	0	0	0.0000	0.00000
NP60D, Maritime Archaic, adult	MBT18	2,220,354	1,414,678	6	4	0	0	0.0000	0.00000
Library blank	MBT19	4	2	0	0	0	0	0.0000	0.00000

Set 3 capture metrics

Individual	Library ID	Raw reads	Trimmed and merged reads	Mapped reads	Mapped (24bp, MQ20)	Mapped (30bp, MQ30)	Uniquely mapped (stacks removed, 30bp, MQ30)	% on-target reads	% unique reads
VAG F234, Adult LG20, Vagnari	MLG01	13,907,570	4,172,962	88	49	1	1	0.0000	0.00002
	MLG02	4,315,542	2,232,153	71	40	4	0	0.0002	0.00000
	MLG05	13,262,960	6,905,638	41	22	3	2	0.0000	0.00003
	MLG06	15,264,738	7,912,346	61	23	1	2	0.0000	0.00003
	MLG11	14,734,854	8,021,915	92	62	9	2	0.0001	0.00002
	MLG13	16,317,848	8,454,929	345	64	9	4	0.0001	0.00005
VEL 186, Adult LV13, Velia	MLV03	8,520,820	4,814,213	39	14	6	5	0.0001	0.00010
	MLV04	10,782,318	5,493,805	143	96	38	38	0.0007	0.00069
	MLV07	15,252,818	8,642,751	80	39	17	17	0.0002	0.00020
	MLV08	56,662,968	28,954,027	92	55	15	15	0.0001	0.00005
	MLV10	3,724,726	1,953,974	106	65	13	12	0.0007	0.00061
	MLV12	14,606,238	7,521,612	274	118	22	15	0.0003	0.00020
Extraction blank	MEB09	1,006	506	0	0	0	0	0.0000	0.0000
Library blank	MEB14	2	1	0	0	0	0	0.0000	0.0000

Supplementary Appendix Figures

Figure 1a. *P. falciparum* mtDNA (LG20-LV13) fragment length distribution.
Ungapped lengths: mean 51.0 bp, standard deviation 18.3. Coverage: mean 1.0,
standard deviation 1.3.

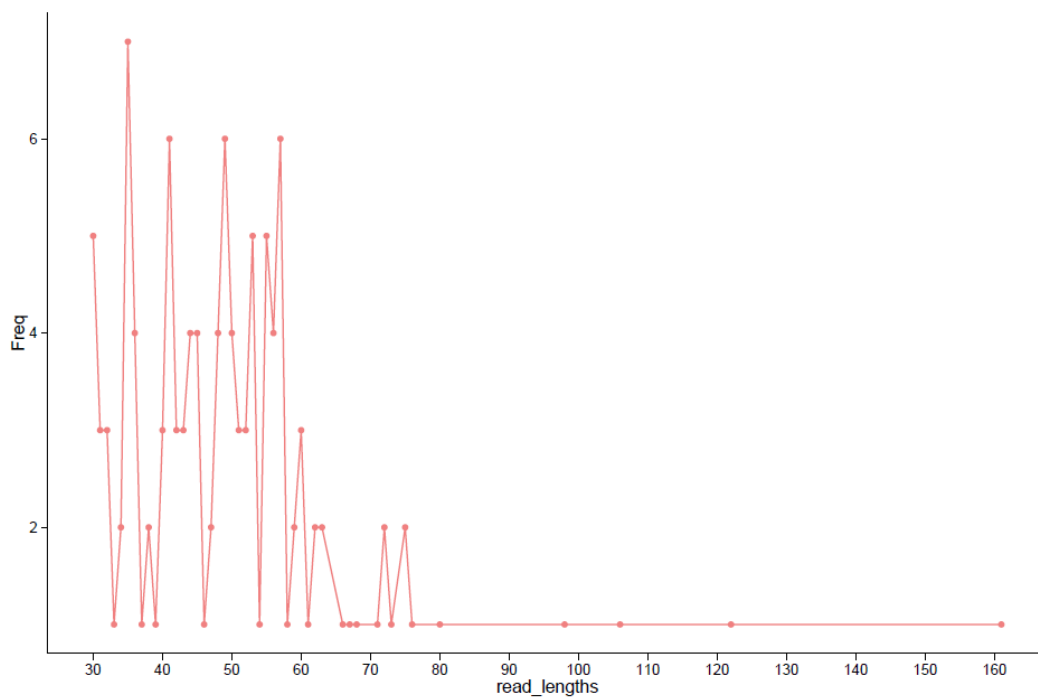


Figure 1b. *P. falciparum* fragment length distribution for LV13. For 113 reads, ungapped lengths: mean 50.8 bp, standard deviation 17.5. Coverage: mean 1.0, standard deviation 1.3.

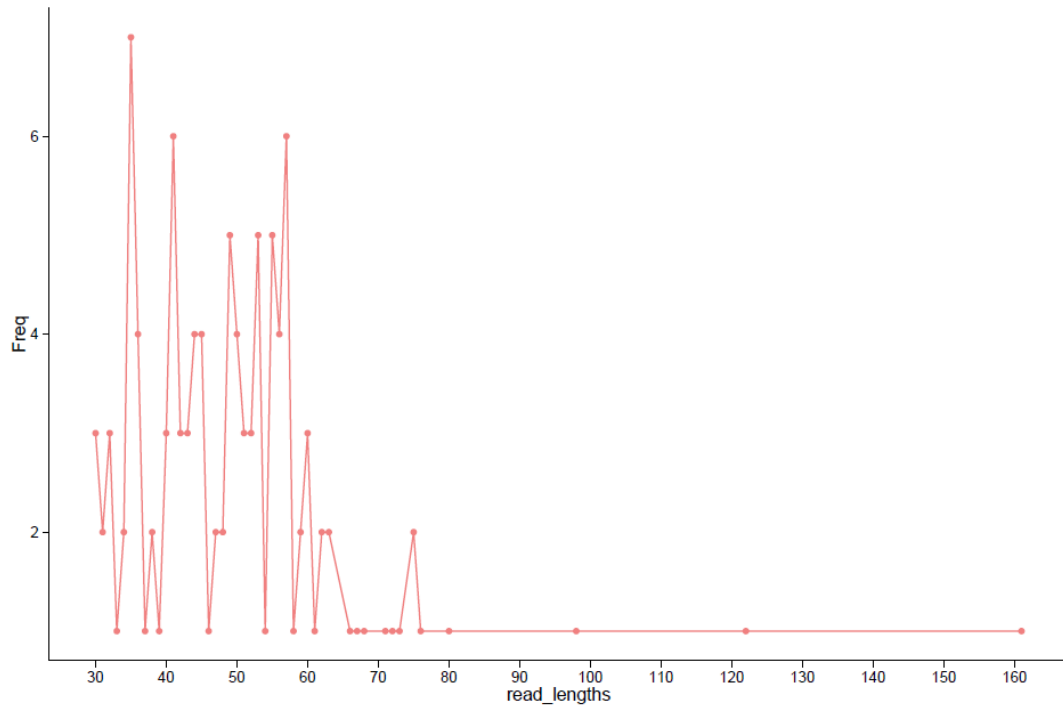


Figure 1c. LG20 human mtDNA fragment length distribution. For 2,811 reads, ungapped lengths: mean 62.6 bp, standard deviation 25.8. Coverage: mean 10.6, standard deviation 14.6.

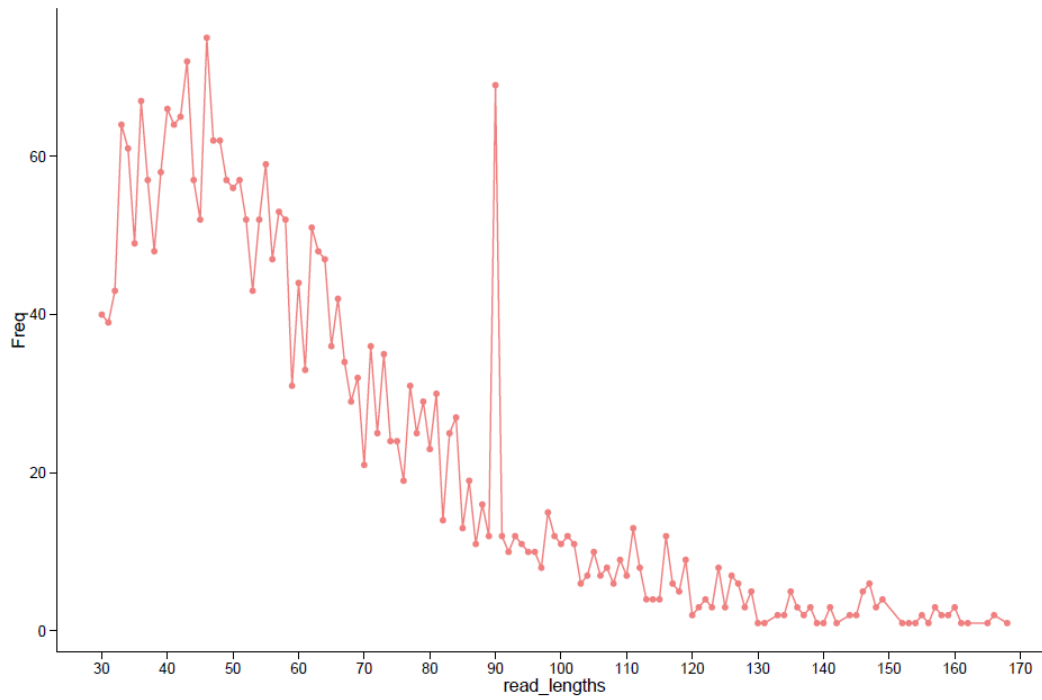


Figure 1d. LV13 human mtDNA fragment length distribution. For 922 reads, ungapped lengths: mean 53.5 bp, standard deviation 19.7. Coverage: mean 3.0, standard deviation 3.7.

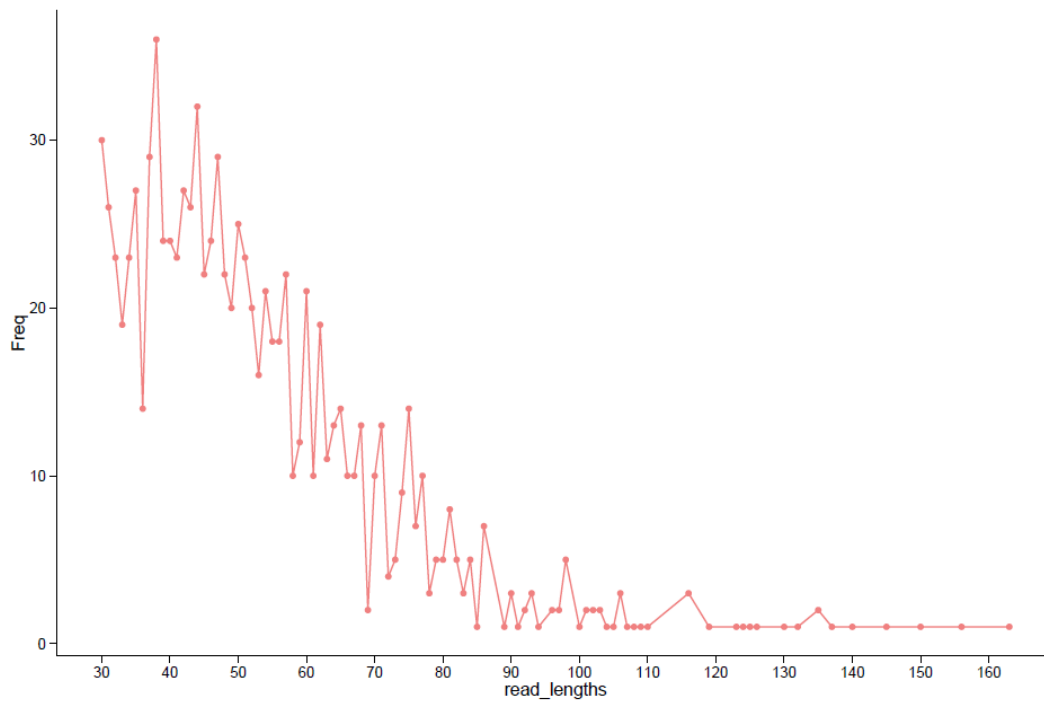


Figure 2a. *P. falciparum* mtDNA (LG20-LV13) damage profile (min 24bp, MQ 30, with stacks). For 227 reads, ungapped lengths: mean 33.6 bp, standard deviation 11.3. Coverage: mean 1.3, standard deviation 7.0.

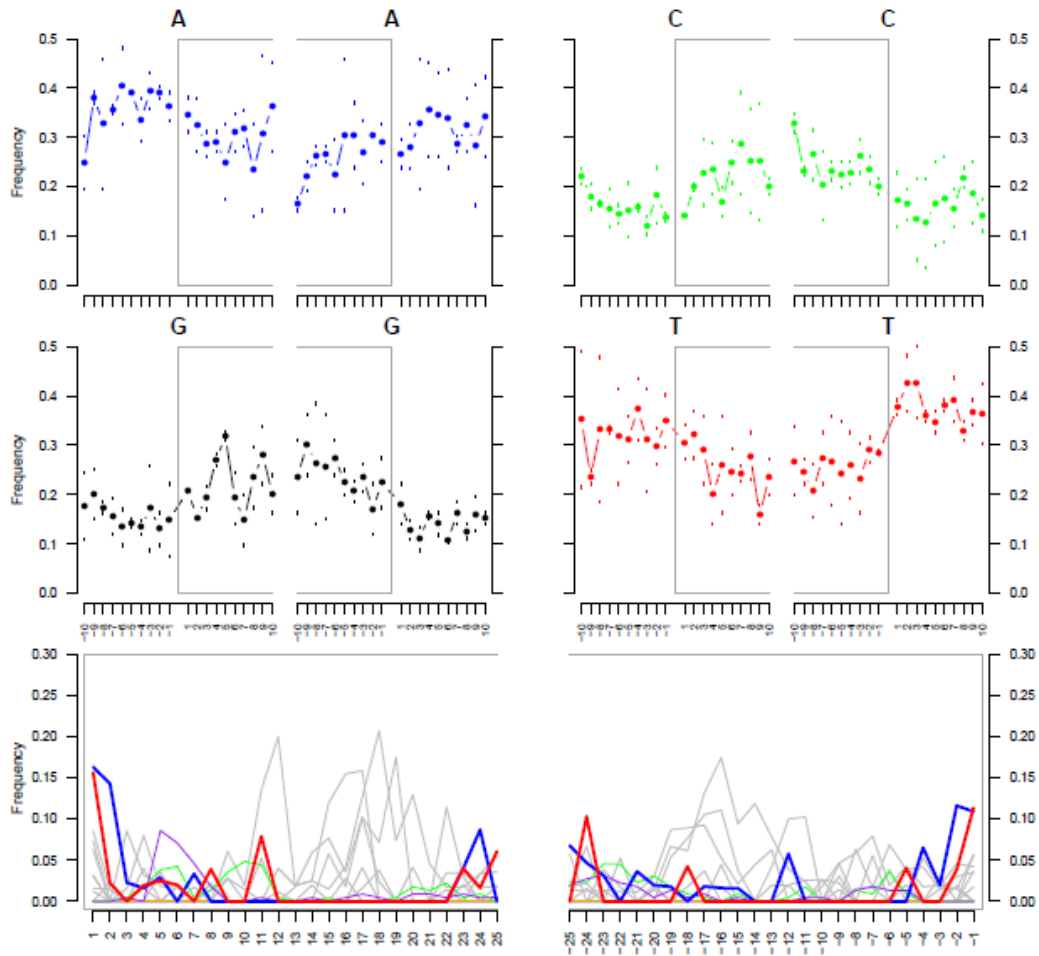


Figure 2b. *P. falciparum* mtDNA (LG20-LV13) damage profile (min 30bp, MQ 30, with stacks). For 116 reads, ungapped lengths: mean 41.0 bp, standard deviation 11.6. Coverage: mean 0.8, standard deviation 3.9.

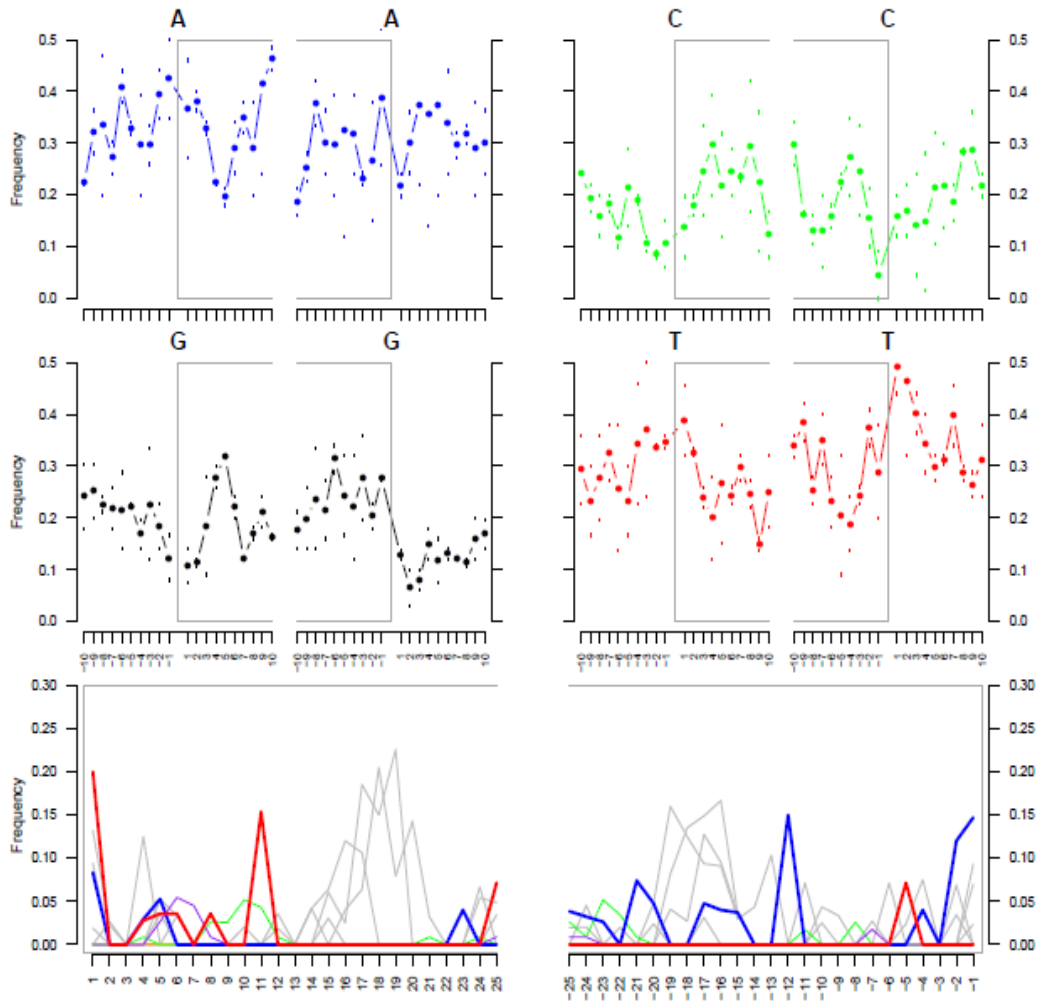


Figure 2c. *P. falciparum* mtDNA (LG20-LV13) damage profile (min 30bp, MQ 30, stacks removed). For 51 reads, ungapped lengths: mean 49.4 bp, standard deviation 12.8. Coverage: mean 0.4, standard deviation 0.8.

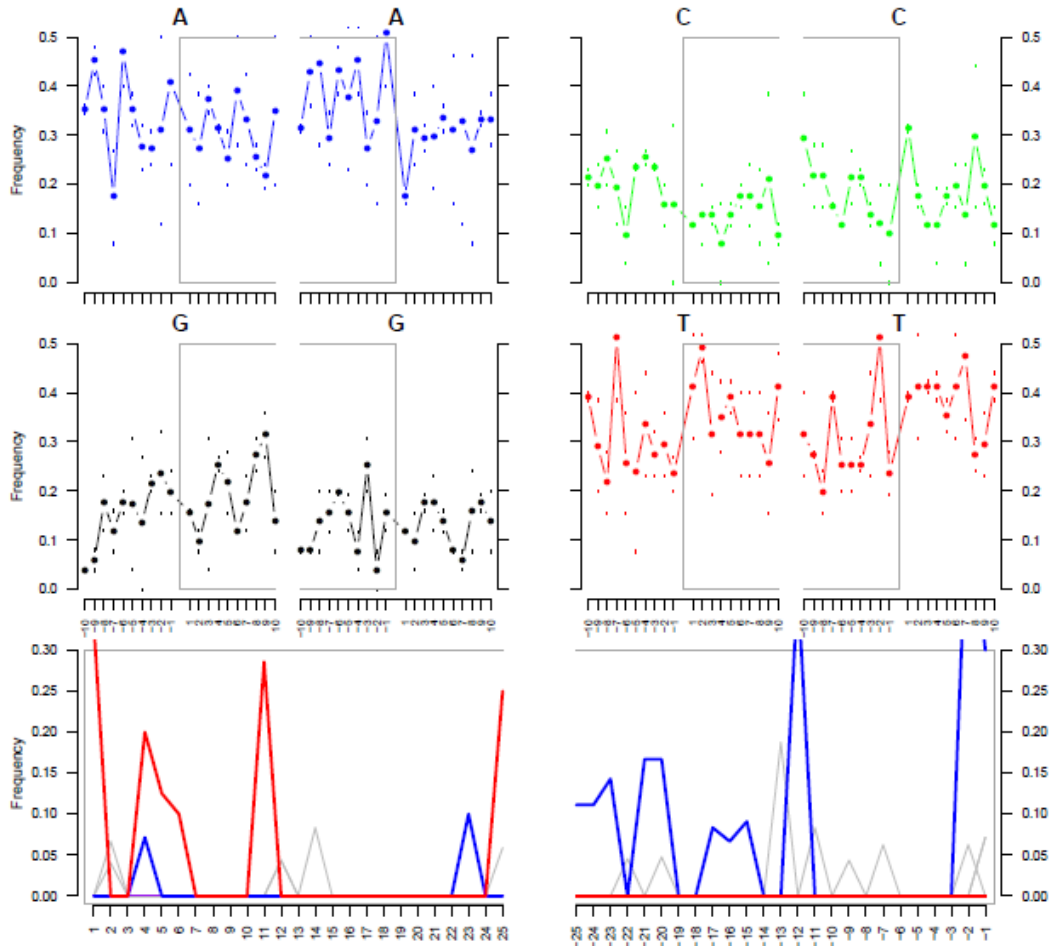


Figure 2d. LG20 human mtDNA damage profile (min 30bp, MQ 30). For 950 reads, ungapped lengths: mean 71.5 bp, standard deviation 29.7. Coverage: mean 4.1, standard deviation 7.8.

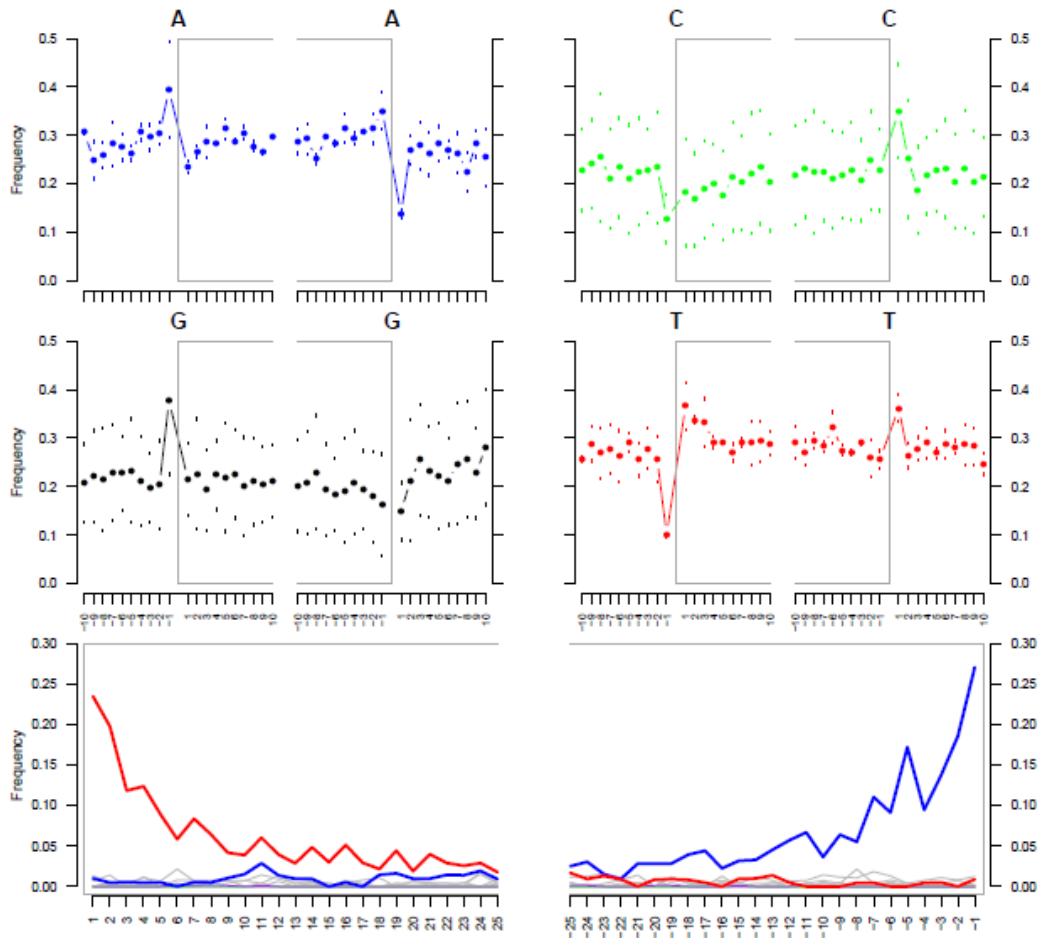


Figure 2e. LV13 human mtDNA damage profile (min 30bp, MQ 30). For 524 reads, ungapped lengths: mean 55.8 bp, standard deviation 22.0. Coverage: mean 1.8, standard deviation 2.4.

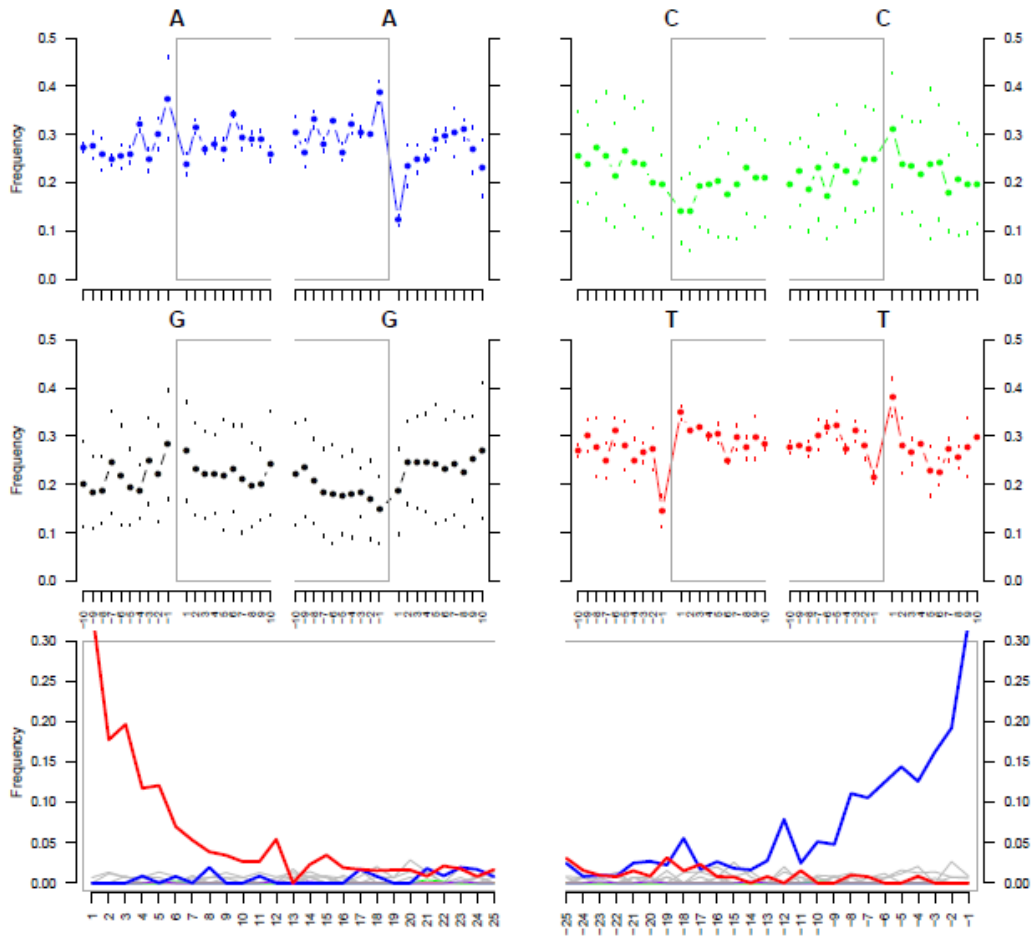


Figure 3. Examples of stacked and repetitive regions captured during *Plasmodium* spp. enrichments.

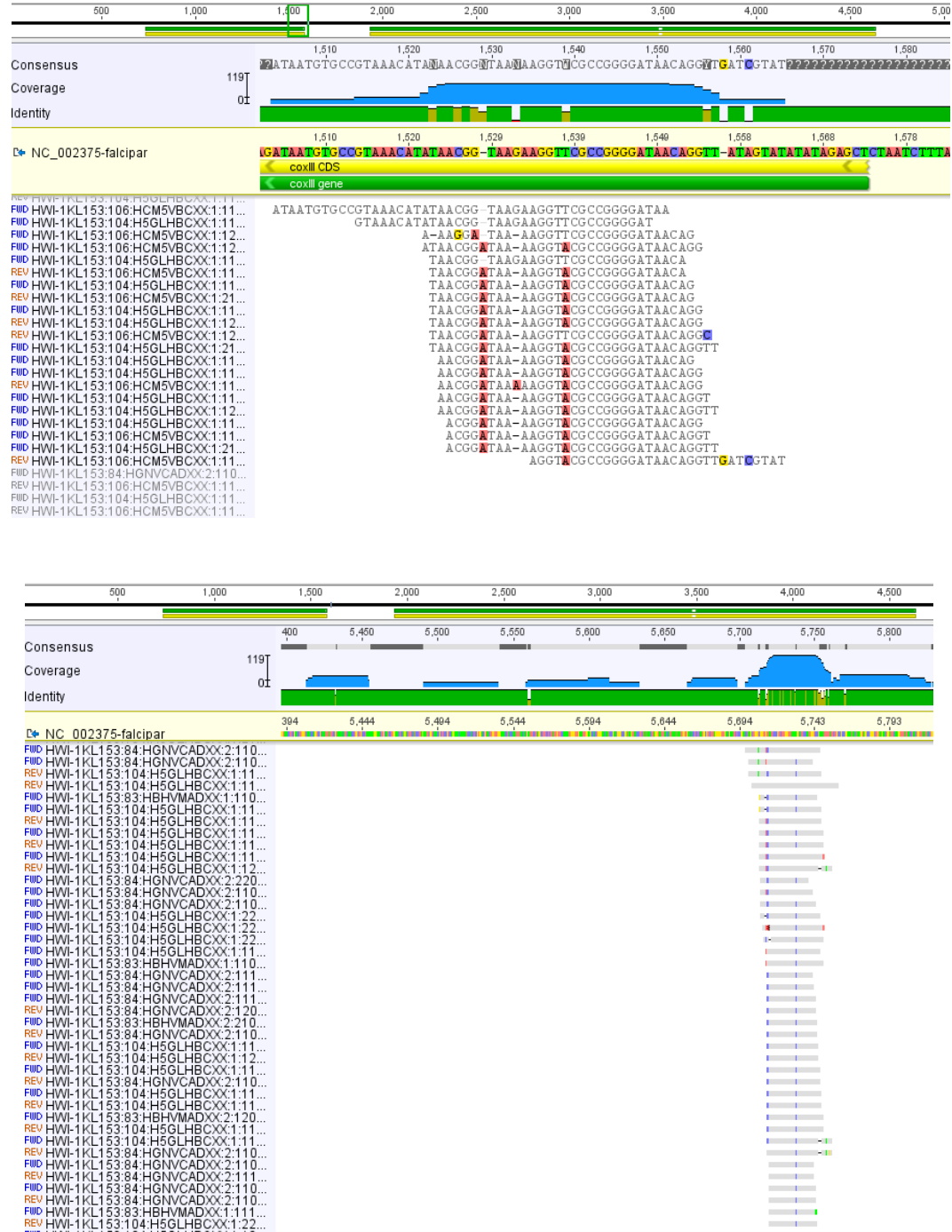


Figure 4a. Randomized LG20 human mtDNA damage profile to approximate *P. falciparum* (with stacks). Random subsample of 116 reads, less than 76bp for the human mitochondrion assembly which is equivalent to the *P. falciparum* assembly (min 30 bp MQ 30, with stacks).

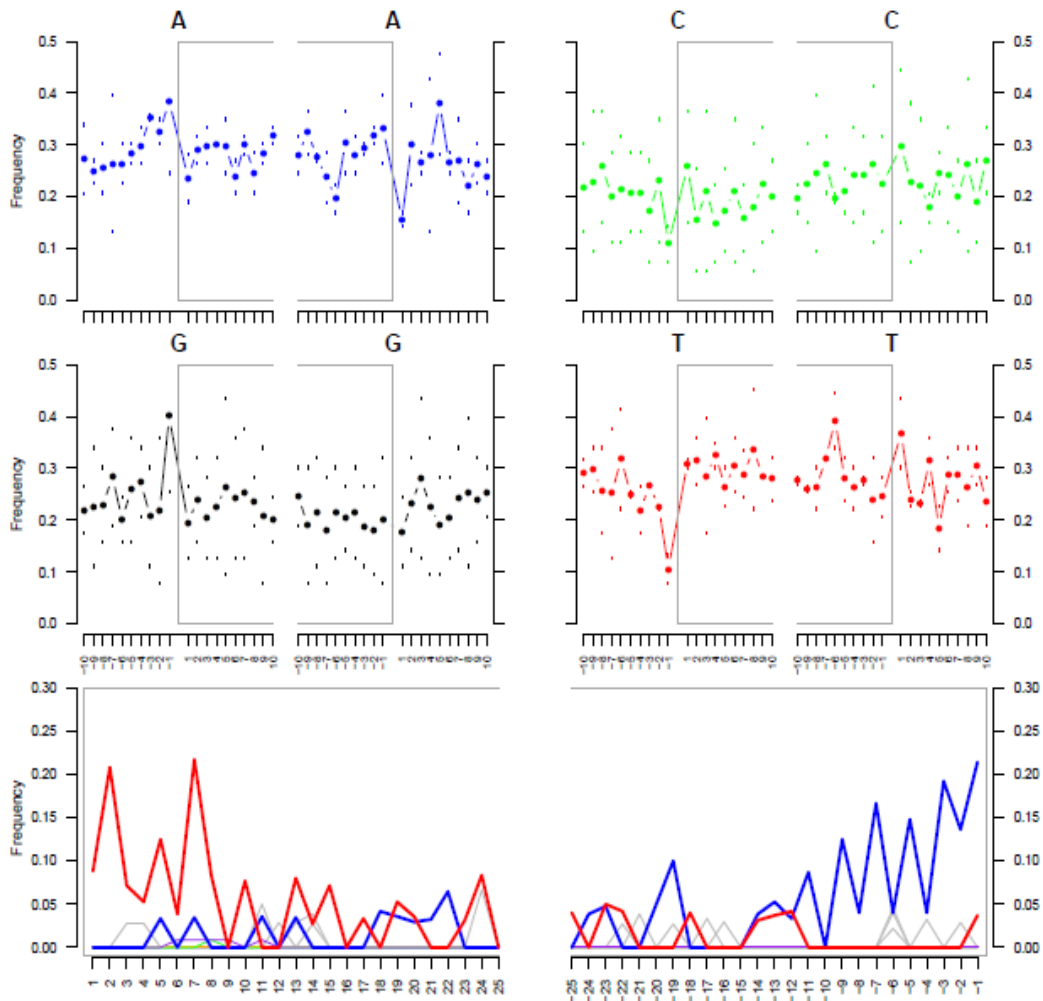


Figure 4b. Randomized LV13 human mtDNA damage profile to approximate *P. falciparum* (with stacks). Random subsample of 116 reads, less than 76bp for the human mitochondrion assembly which is equivalent to the *P. falciparum* assembly (min 30 bp MQ 30, with stacks).

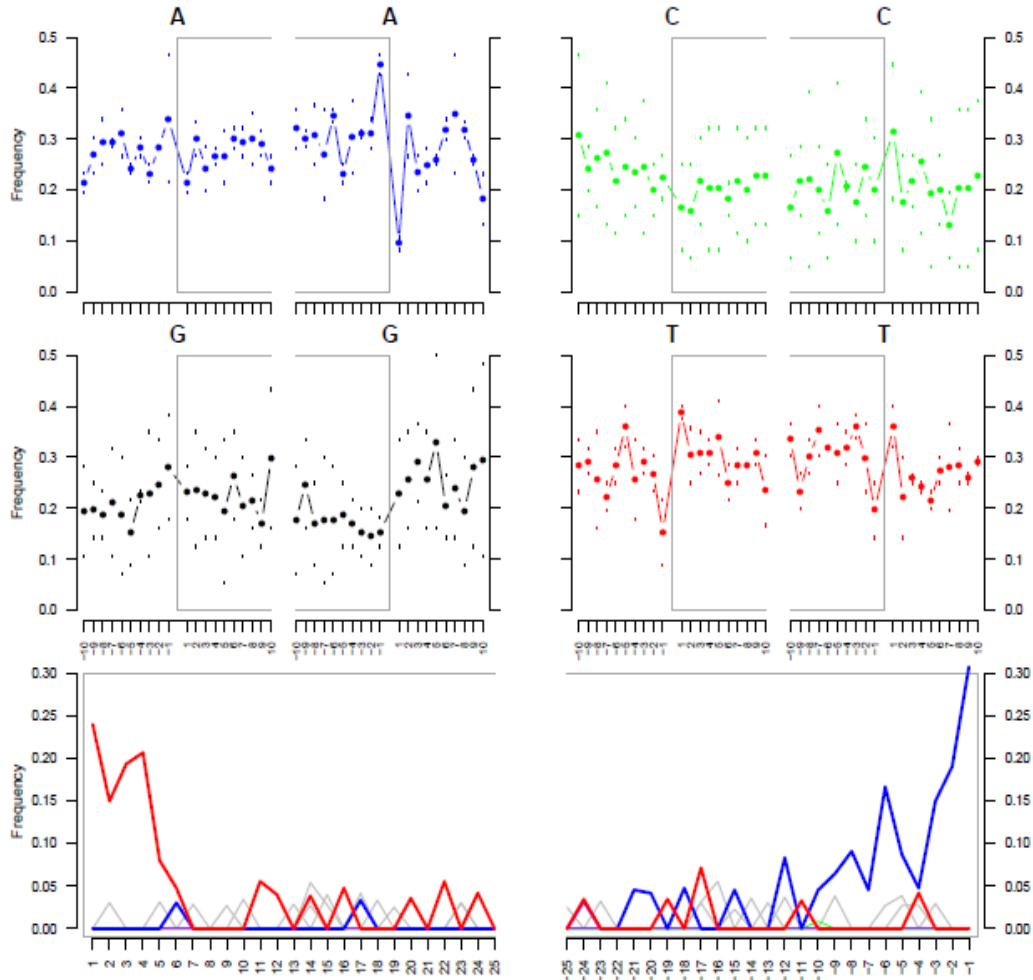


Figure 4c. Randomized LG20 human mtDNA damage profile to approximate *P. falciparum* (stacks removed). Random subsample of 51 reads, less than 76bp for the human mitochondrion assembly which is equivalent to the *P. falciparum* assembly (min 30 bp MQ 30, stacks removed).

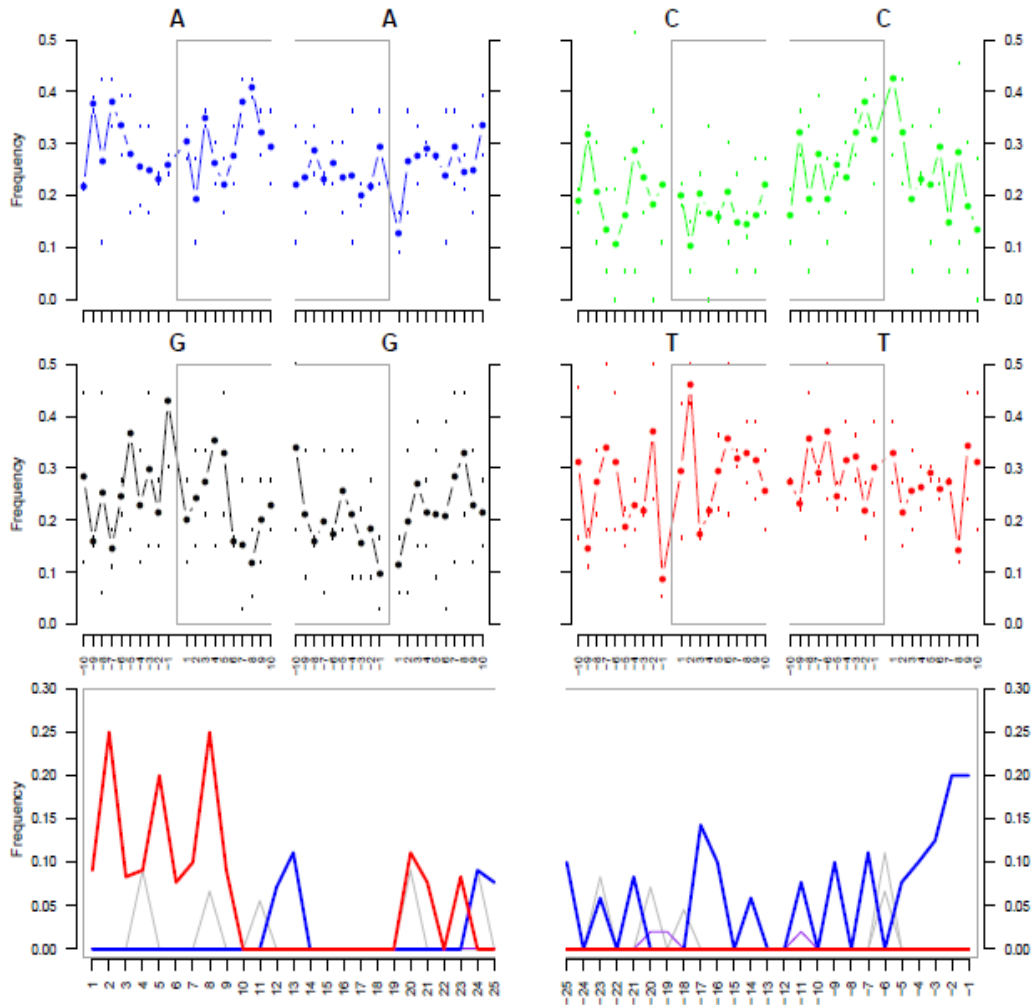
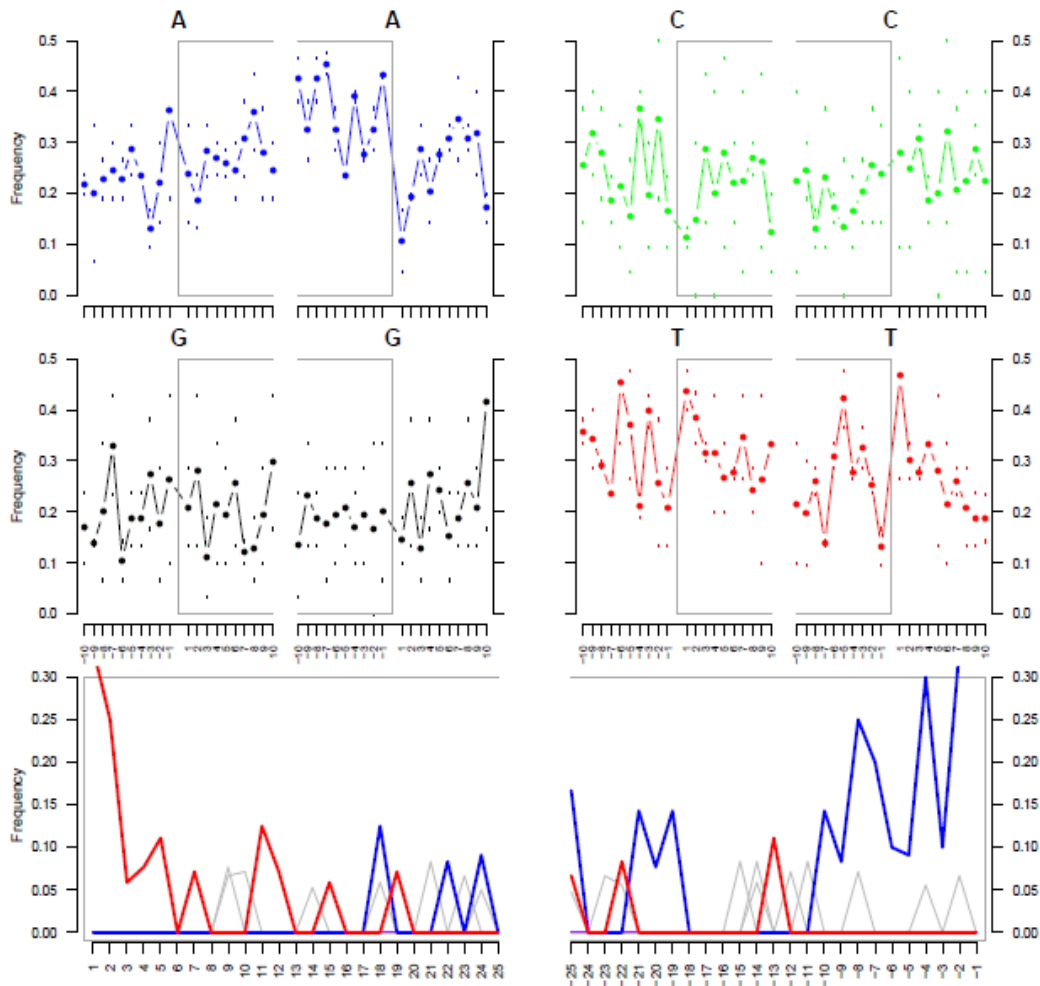


Figure 4d. Randomized LV13 human mtDNA damage profile to approximate *P. falciparum* (stacks removed). Random subsample of 51 reads, less than 76bp for the human mitochondrion assembly which is equivalent to the *P. falciparum* assembly (min 30 bp MQ 30, stacks removed).



Supplementary Appendix Tables

Table 1. Sequences included in *Plasmodium* spp. mitochondrial baits design

Accession	Description	Host species	Length (bp)	% GC
AB_434919	<i>P. cynomolgi</i>	Primate (monkey)	5,983	30.4
NC_007232	<i>P. knowlesi</i>	Primates (monkey), humans	5,957	30.5
NC_002375	<i>P. falciparum</i>	Humans	5,967	31.6
AB_354570	<i>P. malariae</i>	Humans, Primates (monkey)	5,968	29.9
AB_354571	<i>P. ovale</i>	Humans	5,974	30.7
NC_007243	<i>P. vivax</i>	Humans	5,990	30.5

Table 2. Sets of *Plasmodium* spp. enriched libraries

Specimen ID	Library ID
SET 1	
VAG F226, Juvenile, Vagnari	JV01
VAG F283, Juvenile, Vagnari	JV02
VAG F282, Juvenile, Vagnari	JV03
VAG F297, Juvenile, Vagnari	JV04
VAG F299, Juvenile, Vagnari	JV05
VAG F286B, Juvenile, Vagnari	JV06
VAG F210, Juvenile, Vagnari	JV07
VAG F55, Juvenile, Vagnari	JV08
VAG F43, Juvenile, Vagnari	JV09
Juvenile extraction blank	JV10
SCR 602, Adult, Isola Sacra	LS02
SCR 698, Adult, Isola Sacra	LS03
SCR 382, Adult, Isola Sacra	LS05
SCR 526, Adult, Isola Sacra	LS06
SCR 797, Adult, Isola Sacra	LS07
Roman extraction blank	LS08
VAG F234, Adult, Vagnari	LG20
VAG F37, Adult, Vagnari	LG23
VEL 186, Adult, Velia	LV13
VEL 205, Adult, Velia	LV14
VEL82, Adult, Velia	LV33
VAG F117, Adult, Vagnari	PLG11
VEL 194, Adult, Velia	PLV06
NP31, Maritime Archaic, adult	BTK21
NP51, Maritime Archaic, adult	BTK28
Maritime Archaic extraction blank	BTKB1

Specimen ID	Library ID
SET 2	
VAG F299, Juvenile, Vagnari	MJV01
	MJV07
VAG F234, Adult LG20, Vagnari	MLG02
	MLG03
	MLG08
	MLG09
VEL 186, Adult LV13, Velia	MLG14
	MLV04
	MLV05
	MLV10
Extraction blank	MLV11
	MLV13
	MEB06
Extraction blank	MEB12
Extraction blank	MEB15
Extraction blank	MEB16
NP41, Maritime Archaic, adult	MBT17
NP60D, Maritime Archaic, adult	MBT18
Library blank	MBT19

Specimen ID	Library ID
SET 3	
VAG F234, Adult LG20, Vagnari	MLG01
	MLG02
	MLG05
	MLG06
	MLG11
VEL 186, Adult LV13, Velia	MLG13
	MLV03
	MLV04
	MLV07
	MLV08
	MLV10
MLV12	
Extraction blank	MEB09
Library blank	MEB14

Table 3. Blocking oligonucleotide sequences

Blocking oligonucleotide ID	Sequence	Length (bp)
<i>Plasmodium blocking oligonucleotides</i>		
PBO.1	CTA AGG TAG CAA AAT TCC TTG TCG GGT AAT CTC CGT CCT G/3SpC3/	40
PBO.2	TGG GTT AAG AAC GTC TTG AGG CAG TTT GTT CCC TAT CT/3SpC3/	38
PBO.3	AAT TTG CGT GAC GAG CGG TGT GTA CAA GGC /3SpC3/	30
<i>Blocking oligonucleotides for universal adaptors P5 and P7</i>		
EnrichDNA- BO3.P7.1.F	AGA TCG GAA GAG CAC ACG TCT GAA CTC CAG TCA C /3Phos/	34
EnrichDNA- BO3.P7.2.F	ATC TCG TAT GCC GTC TTC TGC TTG /3Phos/	24
EnrichDNA- BO1.P5.1.F	AAT GAT ACG GCG ACC GAG ATC T /3Phos/	25
EnrichDNA- BO1.P5.2.F	ACA CTC TTT CCC TAC ACG ACG CTC TTC CGA TCT /3Phos/	33

Table 4. Metagenomic assessment of prioritized Imperial Italian samples

Library ID	Raw (unprocessed) reads	Processed reads (24bp, MQ 20)	Metagenomic assessment			Endogeneity estimates		Reads mapped to <i>Plasmodium</i> bait set
			MEGAN assigned reads	<i>Plasmodium</i> or Apicomplexa reads	% <i>Plasmodium</i> or Apicomplexa reads	Proportion (%) nuclear DNA	Proportion (%) mtDNA	
LS02	3,373,972	1,644,770	68,482	7	0.01% <i>Plasmodium</i>	1.652	0.0050	1
LS03	1,704,130	868,774	64,581	6	0.009% Apicomplexa	2.255	0.0130	0
LS05	4,807,888	2,436,839	96,971	6	0.004% Apicomplexa	2.881	0.0042	0
LS06	7,650,436	3,911,717	82,719	5	0.006% <i>Plasmodium</i>	0.878	0.0030	1
LS07	5,223,706	2,671,350	83,316	6	0.007% Apicomplexa	15.899	0.0268	0
LG20	5,585,448	1,276,428	128,925	5	0.004% Apicomplexa	13.509	0.0256	0
LG23	7,679,034	3,920,311	172,251	5	0.003% <i>Plasmodium</i>	0.567	0.0023	0
LV13	7,108,588	3,630,379	183,342	5	0.003% <i>Plasmodium</i>	1.024	0.0025	0
LV14	4,054,792	2,064,208	94,230	5	0.005% <i>Plasmodium</i>	1.037	0.0048	0
PLG11	3,325,996	1,698,006	62,482	5	0.008% Apicomplexa	0.031	0.0012	0
PLV06	2,480,602	1,271,588	57,747	6	0.01% Apicomplexa	1.276	0.0033	0
LV33	1,061,550	544,953	25,469	0	Control	0.918	0.0006	0

Table 5. *P. falciparum* capture summary, where the number of "*" indicates the number of capture experiments and sequencing aggregated for totals (without duplicates collapsed)

Individual	Library ID	Raw reads	Processed reads	Mapped (with stacks)	Mapped (no stacks)	% on-target reads	% unique reads
<i>Vagnari, Juveniles</i>							
VAG F226	JV01	24,556	13,534	5	0	0.04	0.0
VAG F283	JV02	39,782	23,311	6	0	0.03	0.0
VAG F282	JV03	1,096	572	0	0	0.0	0.0
VAG F297	JV04	5,258	3,272	0	0	0.0	0.0
***VAG F299	JV05	5,258,228	2,950,655	136	4	0.0	0.00014
VAG F286B	JV06	14,002	7,642	15	0	0.20	0.0
VAG F210	JV07	13,518	7,186	12	0	0.17	0.0
VAG F55	JV08	1,376	863	1	0	0.12	0.0
VAG F43	JV09	510	313	0	0	0.0	0.0
Roman extraction blank	JV10	16	10	0	0	0.0	0.0
<i>Vagnari, Adults</i>							
***VAG F234	LG20	151,198,346	77,517,233	181	18	0.0	0.00002
VAG F37	LG23	94,650	48,914	21	0	0.04	0.0
**VAG F117	PLG11	2,220,510	1,349,995	150	1	0.01	0.00007
<i>Isola Sacra, Adults</i>							
SCR 602	LS02	0	0	0	0	0.0	0.0
**SCR 698	LS03	422,102	233,227	58	1	0.02	0.00043
SCR 382	LS05	53,162	27,613	43	0	0.16	0.0
**SCR 526	LS06	3,043,394	1,724,061	124	1	0.01	0.00006
SCR 797	LS07	144,542	78,517	61	0	0.08	0.0
<i>Velia, Adults</i>							
***VEL 186	LV13	159,249,494	85,026,122	337	212	0.0	0.00025
VEL 205	LV14	61,240	33,532	34	0	0.10	0.0
VEL82	LV33	6,394	3,709	7	0	0.19	0.0
VEL 194	PLV06	55,288	31,723	43	0	0.14	0.0
**Roman extraction blank	LS08	582	291	0	0	0.0	0.0
<i>Reagent controls</i>							
Extraction blank	MEB06	2,354,448	1,529,637	0	0	0.0	0.0
Extraction blank	MEB12	5,156,454	3,298,046	0	0	0.0	0.0
Library blank	MEB15	10,166	5,349	0	0	0.0	0.0
Library blank	MEB16	26	18	0	0	0.0	0.0

Individual	Library ID	Raw reads	Trimmed and merged reads	Mapped (with stacks)	Mapped (no stacks)	% on-target reads	% unique reads
<i>Maritime Archaic, Adults</i>							
NP31	BTK21	7,696	3,936	0	0	0.0	0.0
NP51	BTK28	412	213	0	0	0.0	0.0
NP41	MBT17	1,415,748	1,045,204	0	0	0.0	0.0
NP60D	MBT18	2,220,354	1,414,678	0	0	0.0	0.0
Library blank	MBT19	4	2	0	0	0.0	0.0
Extraction blank	BTKB1	50	35	0	0	0	0

Table 6. LG20-LV13 *P. falciparum* coverage metrics

Specimen	# unique reads	Coverage metrics				Ungapped read length metrics			
		Coverage	Mean Coverage	Standard deviation	Max. coverage	Average fragment length	Min. fragment length	Max. fragment length	Standard deviation
LG20_LV13	120	50.8%	1	1.3	7	51	30	161	18.3

Table 7. *Plasmodium* spp. combined mapped data metrics

a. *Plasmodium* spp. mapped data with stacks

Accession	Description	Host species	Total length (bp)	%GC	LG20-LV13 (min 30bp, MQ30, with stacks)			
					# reads assembled	Average coverage	% reference covered	Average fragment length
AB434919	<i>P. cynomolgi</i>	Primate (monkey)	5,983	30.4	354	2.6	24.9	42
NC_007232	<i>P. knowlesi</i>	Primates (monkey), humans	5,957	30.5	349	2.6	24.3	41.8
NC_002375	<i>P. falciparum</i>	Humans	5,967	31.6	225	1.6	51	42.5
AB354570	<i>P. malariae</i>	Humans, Primates (monkey)	5,968	29.9	360	2.7	26.1	42.2
AB354571	<i>P. ovale</i>	Humans	5,974	30.7	353	2.6	25.6	41.9
NC_007243	<i>P. vivax</i>	Humans	5,990	30.5	317	2.3	24.8	41.3

b. *Plasmodium* spp. mapped data with stacks removed

Accession	Description	Host species	Total length (bp)	%GC	LG20-LV13 (min 30bp, MQ30, stacks removed)			
					# unique reads assembled	Average coverage	% reference covered	Average fragment length
AB434919	<i>P. cynomolgi</i>	Primate (monkey)	5,983	30.4	67	0.5	24.6	44.6
NC_007232	<i>P. knowlesi</i>	Primates (monkey), humans	5,957	30.5	63	0.5	24.1	43.5
NC_002375	<i>P. falciparum</i>	Humans	5,967	31.6	120	1	50.8	51
AB354570	<i>P. malariae</i>	Humans, Primates (monkey)	5,968	29.9	74	0.6	25.9	45.2
AB354571	<i>P. ovale</i>	Humans	5,974	30.7	67	0.5	25.3	43.9
NC_007243	<i>P. vivax</i>	Humans	5,990	30.5	66	0.5	24.6	43.8

Table 8. *Plasmodium* spp. and Apicomplexan mtDNA conservation

Species	# unique reads assembled (LG20-LV13)	# reads shared with LG20-LV13 <i>P. falciparum</i>	% Identity with LG20-LV13 <i>P. falciparum</i>
LG20-LV13 <i>P. falciparum</i>	120	120	100.00
<i>Plasmodium</i> spp.			
<i>P. reichenowi</i>	113	108	95.58
<i>P. billcollinsi</i>	92	84	91.30
<i>P. knowlesi</i>	66	60	90.91
<i>P. relictum</i>	65	59	90.77
<i>P. gonderi</i>	62	56	90.32
<i>Plasmodium</i> sp. Chimpanzee clade	74	66	89.19
<i>Plasmodium</i> sp. Gorilla clade	68	60	88.24
<i>P. chabaudi adami</i>	58	51	87.93
<i>P. fragile</i>	58	51	87.93
<i>P. chabaudi chabaudi</i>	57	50	87.72
<i>P. mexicanum</i>	61	53	86.89
<i>P. hylobati</i>	68	59	86.76
<i>P. ovale</i>	68	59	86.76
<i>P. billbrayi</i>	82	71	86.59
<i>P. vinckei vinckei</i>	57	50	87.72
<i>P. simium</i>	70	60	85.71
<i>P. simiovale</i>	69	59	85.51
<i>P. fieldi</i>	67	57	85.07
<i>P. berghei</i>	59	50	84.75
<i>P. cynomolgi</i>	71	60	84.51
<i>P. coatneyi</i>	64	54	84.38
<i>P. ovale curtisi</i>	63	52	82.54
<i>P. ovale wallikeri</i>	57	47	82.46
<i>P. gallinaceum</i>	65	53	81.54
<i>P. vivax</i>	69	56	81.16
<i>P. juxtannucleare</i>	59	47	79.66
<i>P. inui</i>	70	55	78.57
<i>P. atheruri</i>	55	43	78.18
<i>P. malariae</i>	71	55	77.46
<i>P. yoelli</i>	0	0	0
<i>P. brasilianum</i>	0	0	0
Related Apicomplexan species			
<i>Leucocytozoon fringillarum</i>	30	28	93.33

Species	# unique reads assembled (LG20-LV13)	# reads shared with LG20-LV13 <i>P. falciparum</i>	% Identity with LG20-LV13 <i>P. falciparum</i>
<i>Leucocytozoon majoris</i>	22	19	86.36
<i>Haemoproteus columbae</i>	32	27	84.38
<i>Leucocytozoon sabrazezi</i>	44	35	79.55
<i>Leucocytozoon caulleyeri</i>	39	31	79.49
<i>Parahaemoproteus vireonis</i>	42	30	71.43
<i>Haemoproteus</i> sp. JA27	55	35	63.64
<i>Haemoproteus</i> sp. SEW5141	60	38	63.33
<i>Hepatocystis</i> (cytb only)	2	1	50.00
<i>Hepatozoon catesbiana</i>	7	1	14.29
<i>Babesia bovis</i>	6	0	0
<i>Theileria annulata</i>	1	0	0
<i>Theileria parva</i>	1	0	0
<i>Babesia microti</i>	0	0	0
<i>Neospora caninum</i>	0	0	0

Table 9. *P. falciparum* SNP identification
 SNPs highlighted in yellow indicate *P. falciparum* in the Imperial Italian data.

Gene (NC_002375) rRNA (M76611)	Original Position (in NC_002375)	<i>P. falciparum</i> reference isolates	LG20_LV13 (consensus)	Synonymous or nonsynonymous
Intergenic	74	A	T	
Intergenic	200	C	T	
rnl (206..>222)	208	G	G	
	222	A	A	
Intergenic	230	G	G	
Intergenic	276	G	No coverage	
rnl (283..>389)	301	A	C	N/A – rRNA
	314	A	C	N/A – rRNA
rns (390..>502)	489	A	G	N/A – rRNA
rnl (506..>606)	510	A	A	N/A – rRNA
	546	G	A	N/A – rRNA
	555	A	R	N/A – rRNA
Intergenic	610	C	T	
Intergenic	615	C	C	
Intergenic	725	C	No coverage	
coxIII (734..>1,573)	772	C	C	
	831	T	A	Nonsynonymous
	1122	G	No coverage	
	1339	A	No coverage	
rns gene (1,650..>1,688)	1668	T	Y	N/A – rRNA
	1676		T	Insertion – rRNA
	1678	A	W	N/A – rRNA
Intergenic	1692	G	G	
coI (1,933..>3,471)	2175	T	No coverage	
	2298	C	T	Synonymous

	Original Position (in NC_002375)	<i>P. falciparum</i> reference isolates	LG20_LV13 (consensus)	Synonymous or nonsynonymous
	2338	C	T	Nonsynonymous
	2357	C	T	Nonsynonymous
	2362	C	T	Synonymous
	2685	A	W	Nonsynonymous if T codon, synonymous if A codon
	2763	C	T	Synonymous
	2768	T	T	
	2822	G	A	Nonsynonymous
	2858	T	C	Nonsynonymous
	3004	G	R	Nonsynonymous if codon is A, synonymous if codon is G
	3193	T	C	Nonsynonymous
	3289	G	G	
	3330	A	A	
	3341	C	Y	Nonsynonymous if codon is T, synonymous if codon is C
	3433	T	T	
	3444	T	T	
cytb (3,492.>4,622)	3539	C	T	Synonymous
	3575	C	C	
	3617	A	No coverage	
	3764	T	T	
	3766	A	A	
	3805	C	Y	Nonsynonymous if T codon, synonymous if C codon
	3812-3814		NNN (CCG)	Insertion
	3856	C	T	Nonsynonymous
	3860	C	T	Synonymous
	3868	A	A	
	3938	A	T	Synonymous
	3985	C	No coverage	
	4066	A	M	Nonsynonymous

	Original Position (in NC_002375)	<i>P. falciparum</i> reference isolates	LG20_LV13 (consensus)	Synonymous or nonsynonymous
	4067	T	W	Nonsynonymous
	4179	C	No coverage	
	4352	A	No coverage	
	4353	T	No coverage	
	4420	T	No coverage	
	4426	C	T	Nonsynonymous
	4527	C	T	Nonsynonymous
	4640	A	No coverage	
	4759	T	No coverage	
RNA5 (4,717.>4,802)	4952	T	C	
Intergenic	5485	T	T	
rns (5,447.>5,507)	5554	T	K	N/A – rRNA
RNA14 (5,508.>5,562)	5555	A	W	N/A – rRNA
	5927	G	S	N/A – rRNA
rns (5,855.>5,955)				

Table 10. LG20-LV13 SNPs and amino acid translation

Position in <i>P.falciparum</i> (NC_002375)	SNP type	Base change	Codon change	Ancestral amino acid (NC_002375)	Derived amino acid (LG20-LV13)	Polymorphism type	Read length (bp)	Gene
831	Non-synonymous	A>T	TAT>TTT	Y	F	Transversion	63	coxIII (734..>1,573)
2,298	Synonymous	C>T	TAC>TAT	Y	Y	Transition	72	
2,338	Non-synonymous	C>T	CCT>TCT	P	S	Transition	112	col (1,933..>3,471)
2,357	Non-synonymous	C>T	TCT>TTT	S	F	Transition		
2,362	Synonymous/non-synonymous	C>T	CTG>TTG	L	L/M	Transition		
2,685	Non-synonymous/synonymous	A>W	TTA>TTW	L	L/F	Transversion		
2,763	Synonymous	C>T	TTC>TTT	F	F	Transition	220	
2,822	Non-synonymous	G>A	AGT>AAT	S	N	Transition		
2,858	Non-synonymous	T>C	TTT>TCT	F	S	Transition		
3,004	Non-synonymous/synonymous	G>R	GGT>RGT	G	G/S	Transition	73	
3,193	Non-synonymous	T>C	TTT>CTT	F	L	Transition	112	
3,341	Non-synonymous/synonymous	C>Y	CCT>CYT	P	P/L	Transition	70	
3,539	Synonymous	C>T	TAC>TAT	Y	Y	Transition	61	
3,805	Non-synonymous/synonymous	C>Y	CCA>CYA	P	P/L	Transition	42	cytb (3,492..>4,622)
3,856	Non-synonymous	C>T	GCT>GTT	A	V	Transition	156	
3,860	Synonymous	C>T	TTC>TTT	F	F	Transition		
3,938	Synonymous	A>T	CCA>CCT	P	P	Transversion		
4,066-4,067	Non-synonymous	AT>MW	CAT>CMW	H	?	?	36	
4,426	Non-synonymous	C>T	GCT>NTT	A	?	Transition	57	
4,527	Non-synonymous	C>T	CGA>TGA	R	W	Transition	93	

Table 11. *Plasmodium* spp. used in the phylogenetic analysis

Accession	Description	Host species	Total length	%GC
NC_008288	<i>P. gallinaceum</i>	Avian	6,003	31.8
NC_008279	<i>P. juxtannucleare</i>	Avian	6,014	31.3
AY733090	<i>P. relictum</i>	Avian	5,996	31.4
NC_009961	<i>P. floridense</i>	Reptiles	6,002	31.8
NC_009960	<i>P. mexicanum</i>	Reptiles	5,991	31
LM993670	<i>P. yoelli</i>	Rodents	5,957	31.1
HQ712051	<i>P. atheruri</i>	Rodents	5,851	30.4
NC_015303	<i>P. berghei</i>	Rodents	5,957	31
AB379671	<i>P. chabaudi adami</i>	Rodents	5,949	30.9
AB379669	<i>P. chabaudi chabaudi</i>	Rodents	5,949	30.9
AB599931	<i>P. vinckei vinckei</i>	Rodents	5,948	31
GQ355484	<i>P. brasilianum</i>	Primate (monkey)	5,774	29.7
AB354575	<i>P. coatneyi</i>	Primate (monkey)	5,976	30.5
NC_012369	<i>P. fragile</i>	Primate (monkey)	5,977	30.4
AB434918	<i>P. gonderi</i>	Primate (monkey)	5,989	30
HM032052	<i>P. inui</i>	Primate (monkey)	5,972	30.5
AB434920	<i>P. simiovale</i>	Primate (monkey)	5,987	30.3
NC_007233	<i>P. simium</i>	Primate (monkey)	5,990	30.5
AB354574	<i>P. fieldi</i>	Primate (monkey)	5,983	30.3
AB354573	<i>P. hylobati</i>	Primate (gibbons)	5,973	31
GQ355468	<i>P. billbrayi</i>	Primate (chimpanzee)	5,945	32.1
GQ355479	<i>P. billcollinsi</i>	Primate (chimpanzee)	5,950	31.8
HM235183	<i>Plasmodium</i> sp. chimpanzee (pop. set)	Primate (Chimpanzee)	3,368	33.9
HM235171	<i>Plasmodium</i> sp. gorilla (pop. set)	Primate (Gorilla)	3,374	34.2
AJ276847	<i>P. falciparum</i> 7G8 (Brazil, South America)	Humans	5,967	31.6
AY282930	<i>P. falciparum</i> 3D7 (Europe)	Humans	5,949	31.7
AY282952	<i>P. falciparum</i> Dd2 (Thailand)	Humans	5,949	31.7
NC_017931	<i>P. falciparum</i> HB3 (Central America)	Humans	5,967	31.6
AB570543	<i>P. falciparum</i> (Ghana)	Humans	5,884	31.5
AY282967	<i>P. falciparum</i> HZ5957 (South America)	Humans	5,949	31.6

Accession	Description	Host species	Total length	%GC
KJ569477	<i>P. falciparum</i> JAM17 (Jamshedpur, India)	Humans	5,967	31.6
KT119883	<i>P. falciparum</i> MAN14 (India)	Humans	5,967	31.6
AY282979	<i>P. falciparum</i> M5 (East Africa)	Humans	5,949	31.7
KJ569502	<i>P. falciparum</i> KEO33 (Keonjhar, India)	Humans	5,967	31.6
AJ276844	<i>P. falciparum</i> NF54 (Nigeria, Africa)	Humans	5,967	31.6
AY282995	<i>P. falciparum</i> PC26 (South America)	Humans	5,949	31.6
AY283003	<i>P. falciparum</i> PNG9-1 (Papua New Guinea)	Humans	5,949	31.7
AY283005	<i>P. falciparum</i> REN (Central Africa)	Humans	5,949	31.7
KJ569465	<i>P. falciparum</i> SON10 (Sonapur, India)	Humans	5,967	31.6
KJ569485	<i>P. falciparum</i> SUR7 (Surat, India)	Humans	5,967	31.6
AY283015	<i>P. falciparum</i> Tha2-2 (Thailand)	Humans	5,949	31.7
AY283017	<i>P. falciparum</i> TM284 (Thailand)	Humans	5,949	31.7
AY283019	<i>P. falciparum</i> WR80 (Vietnam)	Humans	5,949	31.7
HQ712052	<i>P. ovale curtisi</i>	Humans	5,851	30.7
HQ712053	<i>P. ovale wallikeri</i>	Humans	5,855	30.6
NC_002235	<i>P. reichenowi</i>	Primate (Gorilla)	5,966	31.7

Table 12. Human mitochondrial genome SNP identification

12a. LG20 human mtDNA SNPs. SNPs highlighted in blue are those called at 5X, 90% variant frequency.

Position	rCRS Reference	LG20	Coverage	Polymorphisms (Expected, Absent, or Private mutation)
73	A	G	4	Expected
146	T	C	10	Expected
152	T	C	8	Local private mutation
225	G	R	1	Ambiguity
263	A	G	4	Expected
321.1	TGG	TGG	10	Global private mutation
709	G	A	4	Expected
750	A	G	7	Expected
1332	A	R	1	Ambiguity
1438	A	G	3	Expected
1632	T	Y	1	Ambiguity
1633	T	Y	1	Ambiguity
1888	G	A	7	Expected
2706	A	G	6	Expected
3171	C	S	1	Global private mutation
3180	A	R	1	Ambiguity
3398	T	C	1	Local private mutation
3442	C	T	1	Local private mutation
4216	T	C	11	Expected
4408	G	R	1	Ambiguity
4456	C	Y	1	Global private mutation
4769	A	G	4	Expected
4917	A	G	50	Expected
6261	G	A	17	Expected
6899	G	R	1	Ambiguity
7028	C	T	6	Expected
7624	T	C	1	Local private mutation
7997	G	R	1	Ambiguity
8239	C	N	No coverage	Global private mutation
8697	G	A	8	Expected
8860	A	G	3	Expected
9999	A	W	1	Global private mutation
10289	A	G	4	Expected

Position	rCRS Reference	LG20	Coverage	Polymorphisms (Expected, Absent, or Private mutation)
10463	T	C	2	Expected
10822	C	T	8	Expected
11251	A	G	12	Expected
11719	G	A	3	Expected
11812	A	G	8	Expected
12185	G	R	2X G, 1X A	Ambiguity
12186	G	R	2X G, 1X A	Ambiguity
13368	G	A	6	Expected
14211	C	Y	2X T, 4X C	Ambiguity
14233	A	G	10	Expected
14766	C	T	6	Expected
14769	A	G	6	Local private mutation
14902	C	T	8	Local private mutation
14905	G	A	8	Expected
15326	A	G	14	Expected
15452	C	A	28	Expected
15607	A	G	13	Expected
15928	G	A	1	Expected
16126	T	T	2	Absent
16196	G	A	1	Global private mutation
16198	T	C	1	Global private mutation
16205	C	T	1	Global private mutation
16292	C	T	2	Expected
16294	C	T	2	Expected
16296	C	T	2	Expected
16391	G	R	2X G, 1X A	Ambiguity
16519	T	C	2	Hotspot

12b. LV13 human mtDNA SNPs. SNPs highlighted in blue are those called at 5X, 90% variant frequency.

Position	rCRS Reference	LV13	Coverage	Polymorphisms (Expected, Absent, or Private mutation)
73	A	G	3	Expected
89	T	A	1	Global private mutation
140	C	Y	1	Ambiguity
141	C	Y	1	Ambiguity
185	G	A	1	Local private mutation
263	A	G	2	Expected
278	A	G	1	Global private mutation
329.1	CAG	CAG	2	Global private mutation
434	C	T	3	Global private mutation
526	G	deletion	-	Global private mutation
527	C	deletion	-	Global private mutation
709	G	A	2	Expected
750	A	G	2	Absent
930	G	N	No coverage	Absent
1004	G	A	2	Global private mutation
1218	A	N	No coverage	Global private mutation
1322	C	T	1	Global private mutation
1377	C	Y	1	Ambiguity
1438	A	G	1	Expected
1563	T	C	1	Global private mutation
1637	C	T	1	Global private mutation
1626	C	d	No coverage	Global private mutation
1646	T	A	1	Global private mutation
1888	G	A	3	Expected
2008	G	R	1	Ambiguity
2144	A	W	1	Global private mutation
2170	G	A	1	Global private mutation
2173	G	A	1	Global private mutation
2394	A	R	1	Ambiguity
2440	G	R	1	Ambiguity
2566	C	T	1	Global private mutation
2706	A	G	3	Expected
2735	G	R	1	Ambiguity
2845	A	N	No coverage	Global private mutation
2885	T	Y	1	Ambiguity

Position	rCRS Reference	LV13	Coverage	Polymorphisms (Expected, Absent, or Private mutation)
2959	G	N	No coverage	Global private mutation
3067	T	d	No coverage	Global private mutation
3090	G	K	1	Global private mutation
3107	N	C	3	Global private mutation
3328	G	N	No coverage	Global private mutation
3522	T	C	5	Global private mutation
4043	C	Y	2X T, 2X C	Ambiguity
4087	A	G	1	Global private mutation
4198	C	T	1	Local private mutation
4216	T	C	3	Expected
4419	A	N	No coverage	Global private mutation
4629	G	R	1	Ambiguity
4769	A	A	3	Absent
4836	C	Y	1	Ambiguity
4917	A	G	15	Expected
5057	C	T	1	Global private mutation
5060	C	T	1	Local private mutation
5061	C	T	1	Global private mutation
5062	C	T	1	Global private mutation
5147	G	A	4	Expected
5380	T	Y	1	Ambiguity
5417	G	R	2X G, 2X A	Ambiguity
5483	T	T	11	Absent
6427	C	Y	2X C, 2X T	Ambiguity
6857	C	Y	1	Ambiguity
6873	C	Y	1	Ambiguity
6955	G	R	1	Ambiguity
7028	C	N	No coverage	Absent
7250	A	G	1	Local private mutation
7716	T	C	1	Global private mutation
8062	C	Y	1	Ambiguity
8152	G	A	1	Local private mutation
8169	A	N	No coverage	Global private mutation
8387	G	R	1	Ambiguity
8407	C	Y	1	Ambiguity
8419	T	Y	1	Ambiguity
8477	T	N	No coverage	Global private mutation
8697	G	N	No coverage	Absent
8860	A	G	1	Absent

Position	rCRS Reference	LV13	Coverage	Polymorphisms (Expected, Absent, or Private mutation)
8881	T	C	1	Global private mutation
8920	G	R	1	Ambiguity
8927	C	Y	1	Ambiguity
9180	A	G	3	Local private mutation
9282	C	T	2	Global private mutation
9480	T	Y	1	Ambiguity
9484	T	Y	1	Ambiguity
9562	C	Y	1	Ambiguity
9648	C	Y	1	Ambiguity
9739	C	Y	1	Ambiguity
9816	C	Y	1	Ambiguity
9860	C	Y	1	Ambiguity
9905	T	Y	1	Ambiguity
10164	C	T	1	Global private mutation
10399	C	A	1	Global private mutation
10463	T	N	No coverage	Absent
10686	G	A	1	Global private mutation
10745	C	Y	3X C, 1X T	Ambiguity
10810	T	Y	1	Ambiguity
11169	G	R	1	Ambiguity
11251	A	G	1	Expected
11266	C	T	1	Local private mutation
11268	C	T	1	Local private mutation
11270	C	T	1	Global private mutation
11719	G	A	6	Expected
11812	A	G	3	Absent
11837	C	T	1	Global private mutation
11896	C	T	2	Global private mutation
12031	C	Y	1	Ambiguity
12034	C	Y	1	Ambiguity
12418	A	R	1	Ambiguity
12735	C	Y	1	Ambiguity
13010	C	Y	1	Ambiguity
13368	G	A	1	Absent
13551	C	Y	1	Ambiguity
13639	C	T	2	Global private mutation
13785	C	Y	1	Ambiguity
14233	A	G	4	Expected
14612	G	N	No coverage	Global private mutation

Position	rCRS Reference	LV13	Coverage	Polymorphisms (Expected, Absent, or Private mutation)
14663	G	R	1	Ambiguity
14673	T	A	1	Global private mutation
14766	C	N	No coverage	Absent
14801	A	N	No coverage	Global private mutation
14905	G	A	2	Expected
15126	C	Y	2X C, 2X T	Ambiguity
15182	A	R	1	Ambiguity
15167	T	Y	1	Ambiguity
15190	C	Y	1	Ambiguity
15326	A	G	9	Expected
15387	A	G	1	Global private mutation
15452	C	A	7	Expected
15529	C	Y	1	Ambiguity
15607	A	G	2	Expected
15928	G	A	2	Expected
16056	C	T	1	Global private mutation
16057	C	T	1	Global private mutation
16096	G	R	1	Ambiguity
16126	T	C	1	Expected
16192	C	A	4	Global private mutation
16294	C	C	1	Absent
16296	C	C	1	Absent
16304	T	T	1	Absent
16311	T	C	1	Local private mutation
16519	T	C	1	Hotspot

Table 13. Human mitochondrial genome coverage metrics

Specimen	# reads assembled	Coverage metrics				Ungapped read length metrics				HaploGrep2 metrics	
		% Coverage	Mean Coverage	Standard deviation	Max. coverage	Average fragment length	Min. fragment length	Max. fragment length	Standard deviation	Haplogroup	Quality
LG20_combined	2,811	99.4%	10.6	14.6	176	62.6	30	168	25.8	T2c1e	88.16%
LV13_combined	922	85.3%	3	3.7	40	53.5	30	163	19.7	T2b29	62.17%

Table 14. LG20 and LV13 haplogroup comparisons to rCRS database matches

Specimen	Haplogroup	GenBank metrics			HaploGrep2 metrics		
		<i>Accession</i>	<i>Haplotype</i>	<i>Origin</i>	<i>Source</i>	<i>Haplogroup</i>	<i>Quality score (%)</i>
LG20	T2c1e	KP317002.1	T2c1b2	Yemen	Ref. S58	T2c1e	95.47
		KP317017.1	T2c1b2	Yemen	Ref. S58	T2c1e	96.30
		KP317036.1	T2c1b2	United Arab Emirates	Ref. S58	T2c1e	96.60
		KR902535.1	T2c1e	Turkey	Ref. S59	T2c1e	97.96
		KF836133.1	T2c1e	Italy	Ref. S60	T2c1e	97.94
		JQ703823	T2c1e	Not identified	Ref. S61	T2c1e	94.34
LV13	T2b29	JQ798080	T2b	Italy	Ref. S62	T2b29	97.58
		JQ798081	T2b	France	Ref. S62	T2b29	99.1

**CHAPTER 3: A MULTI-FACETED APPROACH TO FRAMING
MOLECULAR SIGNATURES OF *PLASMODIUM FALCIPARUM*
MALARIA IN IMPERIAL PERIOD SOUTHERN ITALY (1ST-4TH C.
A.D.)**

By: Stephanie Marciniak^{1,3}, D. Ann Herring³, Alessandra Sperduti^{4,6}, Roberto Macchiarelli⁵, Luca Bondioli⁶, Hendrik N. Poinar^{1,2,3}, Tracy L. Prowse³

Submitted to the American Journal of Physical Anthropology.

¹McMaster Ancient DNA Centre, Department of Anthropology, McMaster University, Hamilton, ON, L8S 4L9 Canada.

²DeGrootte Institute for Infectious Disease Research, McMaster University, Hamilton ON, L8S 4L9, Canada.

³Department of Anthropology, McMaster University, Hamilton, ON, L8S 4L9, Canada.

⁴La Sapienza University of Rome, Piazzale Aldo Moro, 5, 00185, Rome, Italy

⁵University of Poitiers, 15 Rue de l'Hôtel Dieu, 86000, Poitiers, France.

⁶Polo Museale del Lazio, Museo Nazionale Preistorico Etnografico “Luigi Pigorini”, Sezione di Bioarcheologia, P.le G. Marconi 14, 00144, Rome, Italy.

Abstract

Objectives

Plasmodium falciparum is a significant historical pathogen, particularly as a scourge of ancient Rome. We discuss our molecular investigation of malaria in Imperial period (1st-4th c. A.D.) cemeteries in southern Italy as a scenario where the molecular evidence for *P. falciparum* was recovered from adults in Vagnari and Velia, but not from Portus Romae.

Materials and Methods

Due to the limited retrieval of *P. falciparum* molecular signatures it was crucial to frame this pathogen within the specific localities of Velia, Vagnari, and Portus Romae. The biosocial context of disease was explored using literary, epidemiological, and archaeological evidence in order to contextualize relationships between the pathogen, human hosts, *Anopheles* vector, and environment.

Results

It was possible to propose pathways that potentially enabled a multifaceted distribution of malaria at the studied localities, ranging from elements of disease ecology (e.g., climate, landscape, and geomorphology) to human-environment interactions (e.g., land use patterns such as agriculture or infrastructure activities). Although not all of these factors could be disentangled, this represents an approach to identify factors framing the epidemiology of malaria in a given location.

Discussion

As pathogens are embedded in specific historical and geographical contexts, it is important to highlight the synergistic interactions underlying ancient landscapes of disease. Although much remains unknown regarding epidemiological patterns in antiquity, combining ancient DNA with complementary evidentiary sources represents a dynamic strategy to frame the multifaceted experience of disease.

Introduction

The story of a malarious scourge impacting the fabric of Roman civilization has long fascinated a breadth of scholars – from classicists, historians, and anthropologists to geneticists. The framework supporting notions of endemic malaria in ancient Rome is drawn from disparate evidentiary sources, both direct (i.e., biomolecular) and indirect (i.e., skeletal, climatological, textual). For example, the classical paroxysms and febrile symptoms in descriptions from Hippocrates (5th c. B.C.), Celsus (1st c. A.D., *De Medicina*), and Galen (2nd c. A.D., *De Morborum Temporibus*), are entrenched in contemporary biomedicine as evidence of the ancient relationship between humans and this parasitic infection. Roman cultural beliefs also connected the environment to health (i.e., pestilential marshes are isolated from the sea, while healthy ones receive inflows) (Sallares, 2002), which is further interpreted by scholars as indicators of malaria presence, despite the association of “fevers” with noxious vapours rather than mosquitoes. The retrospective application of patterns of morbidity and mortality associated with Italy’s struggles with malaria from 1880-1962 (see Snowden, 2008) to the Imperial period (1st-5th c. A.D.) comparatively highlights the potential social, political, and economic consequences on local populations (e.g., Shaw, 1996; Sallares, 2002; Scheidel, 2003). Yet, there is limited physical evidence to support the widespread presence of this parasite in Imperial Italy, which challenges inferences from contemporary settings due to the disparate temporal and geographic contexts that are embedded within the local determinants of malaria

epidemiology (Mackinnon & Marsh, 2010). The integration of skeletal evidence in this narrative remains problematic, as the complex pathogenesis of the human malaria parasites (e.g., *Plasmodium falciparum*, *Plasmodium vivax*, *Plasmodium malariae*, and *Plasmodium ovale*) do not induce specific skeletal responses. The result is a reliance on the indirect association of non-specific skeletal stressors, such as cribra orbitalia and porotic hyperostosis (e.g., Angel, 1966; Soren and Soren, 1999; Rabino Massa et al., 2000; Gowland and Western, 2012), or a suite of skeletal lesions (Smith-Guzman, 2015a), to infer the presence of the disease. The dynamic interplay between humans, the local environment (e.g., biocultural, ecological), and the *Plasmodium* parasite benefits from a multi-faceted approach to explore malaria in antiquity.

Ancient DNA (aDNA) is an important component of the paleopathological toolkit to investigate the presence of human pathogens in a particular geographical and spatiotemporal context, particularly when associated skeletal changes are not diagnostic. Despite well-appreciated challenges in applying aDNA in the investigation of disease, such as exogenous contamination, variable endogenous DNA preservation, and minute pathogen fractions (see Pääbo et al., 2004; Burbano et al., 2010; Molak and Ho, 2011; Carpenter et al., 2013; Hofreiter et al., 2015), it remains a powerful approach to robustly detect the pathogenic signatures of human *Plasmodium* species.

The application of polymerase chain reaction (PCR) in the recovery of a *P. falciparum*-specific 18S rRNA fragment from an infant in 5th c. A.D. central Italy

by Sallares and Gomzi (2001) remains the singular evidence for the presence of this parasite in Imperial Italy. However, there have been no investigations on the recovery of this protozoan parasite from adults of this time period (1st-5th c. A.D.), or a systematic search for the presence of this pathogen in more than one Imperial period population. A key piece of the “Roman malaria” narrative has yet to be accomplished, that is, the detection of human *Plasmodium* genomic signatures by harnessing targeted capture strategies alongside high-throughput sequencing. Hybridization capture (sequestration of DNA targets through binding to known DNA probes or “baits”) is a highly successful technique for recovering minute pathogen fractions from a background of exogenous (non-target) molecules, and in combination with the capacity to sequence millions of DNA molecules in parallel, renders this as the most robust and stringent molecular strategy (see Burbano et al., 2010; Carpenter et al., 2010; Enk et al., 2014).

The present study frames our previous work on recovering ancient *Plasmodium* genomic signatures using contemporaneous Imperial period (1st-4th c. A.D.) southern Italian cemeteries (Marciniak et al., 2016). We detected *P. falciparum* in one adult from the port city of Velia (1st-2nd c. A.D.) and another adult from Vagnari (1st-2nd c. A.D.), but without molecular evidence from adults at Isola Sacra (associated with Portus Romae) (1st-3rd c. A.D.) (Figure 1a). It was hypothesized that the coastal hub of Portus, which functioned as an integral port and trading centre, would have a greater potential for the presence of malaria due to its location within a “malarious” environment, the influx of immigrants

potentially importing this parasite or being more vulnerable to it upon exposure, in addition to an ecological setting that is conducive to *Anopheles* vector proliferation (e.g., marshes and coastal lagoons). Conversely, Velia as a minor port city and Vagnari as a relatively remote rural site, are distinct by comparison, in terms of population structure (e.g., potentially less dense than Portus), economic activity (e.g., intensified agriculture in both localities with transhumance at Vagnari), and diverse natural landscapes (e.g., forested hills and plateaus of Vagnari, or the coastal plains and promontory of Velia). In consideration of not only the genomic results, but the complexity of malaria epidemiology, it was crucial to integrate this new aDNA evidence within a framework that emphasizes malaria is part of the “lived experience” of health and disease (Krieger, 2011: 215), in order to infer the potential multi-causal biosocial pathway of disease at these diverse localities.

Figure 1a. Map of the cemeteries in Imperial period Italy.



Pathogenesis and post-mortem detection of malaria

The complex life cycle of the *Plasmodium* parasite, existing within the mosquito host, followed by a liver and blood stage in humans, results in varied clinical manifestations from mild to life-threatening with influences from protective genetic polymorphisms (e.g., thalassemia, glucose-6-phosphate-dehydrogenase deficiency or sickle cell), clinical immunity, co-infections confounding mortality (e.g., respiratory or gastrointestinal illnesses) and parasite virulence (e.g., susceptibility in the host or parasite genetic factors) (Sherman, 1998; Carter and Mendis, 2002; Riley et al., 2006; Bei and Duraisingh, 2013).

Malaria parasites have an impressive repertoire of molecular mechanisms to evade detection by the host's immune system in order to facilitate ongoing invasion and release of parasites into the host bloodstream (Miller et al., 2002; Sacks and Sher, 2002; Bei and Duraisingh, 2013). The periodic amplification of the parasites within the human host are associated with the rupture of red blood cells, correlating with febrile paroxysms; although such fevers may also be continuous or intermittent (Kwiatkowski and Nowak, 1991; Sherman, 1998; Faure, 2014). High levels of parasitaemia are obtainable with *P. falciparum* infections (i.e., hyper-parasitaemia with 2-5% erythrocytes parasitized or 250,000 parasites per μL of blood and up to 500,000 parasites or 10% parasitaemia), while *P. vivax* and *P. malariae* are more moderate (i.e., 100,000 parasites per μL of blood or 2% parasitaemia), with the potential for relapse or dormancy (Wilkinson et al., 1994; Hansheid, 1999; Garcia, 2001). Additionally, the excessive host inflammatory response to sequester hemoglobin from the *Plasmodium* parasites and immune-induced rupture of parasitized and non-parasitized red blood cells in later disease stages, contributes to hemolytic anemia and systemic spread (Sherman, 1998; Schofield and Grau, 2005; Riley et al., 2006). There is no skeletal involvement as infection is confined to the bloodstream and organs (e.g., spleen, liver), with limited persistence in host tissues (Riley et al., 2006; Kindt et al., 2007), although physiological perturbations due to anemia may manifest skeletally, as described below.

Despite uncertainties surrounding the localization of malaria parasites in ancient human skeletal remains, the indirect association between skeletal indicators of anemia with malaria infection remain predominant in the retrospective identification of this protozoan parasite. Malaria as a disease is an embodiment of the Osteological Paradox (Wood et al., 1992; Wright and Yoder, 2003; DeWitte and Stojanowski, 2015) in the heterogeneous vulnerability of different members of the population and the problem of associating skeletal lesions to specific pathological processes. Paleopathological approaches to the identification of malaria in the past correlate cribra orbitalia (porosity on the orbital roof) and porotic hyperostosis (porosity of the cranial vault) as non-specific responses to malaria infection (e.g., Angel, 1966; Rabino Massa et al., 2000; Sallares and Gomzi, 2001, Nerlich et al., 2008; Gowland and Western, 2012) alongside polymorphic hemoglobinopathies (i.e., thalassemia, sickle cell) (e.g., Hershkovitz et al., 1997; Henneberg and Henneberg, 1998; Lewis, 2012). The inference of porotic hyperostosis and cribra orbitalia as outcomes of hemolytic anemia due to malaria infection are broadly non-specific indicators with a multifactorial etiology (e.g., infection, trauma, metabolic disease, nutritional deficiency) (Stuart-Macadam, 1992; Holland and O'Brien, 1997; Walker et al., 2009; Oxenham and Cavill, 2010). However, the increased prevalence of these skeletal indicators in presumptively malarious environments of the past [e.g., Imperial Rome in Gowland and Garnsey, 2010; eastern England (410-1050 A.D.) in Gowland and Western, 2012; and the Nile Valley in Smith-

Guzman, 2015b], denote a connection to existing ecological and biological stressors where malaria is potentially one component of a dynamic epidemiological context.

Similarly, the molecular and immunological investigation of malaria in antiquity is represented by an array of approaches, such as confirmation of *Plasmodium*-specific functional genes (e.g., 18S rRNA, chloroquine-resistance transporter) (e.g., Taylor et al., 1997; Sallares and Gomzi, 2001; Zink et al., 2001; Nerlich et al., 2008); and protein fragments [e.g., apical membrane antigen 1 (AMA1), merozoite surface proteins (MSP), subtelomeric variable open reading frame (STEVOR), or histidine-rich protein 2] in mummies (e.g., Miller et al., 1994; Rabino Massa et al., 2000; Bianucci et al., 2008; Hawass et al., 2010; Lalremruata et al., 2013) and skeletal remains (Fornaciari et al., 2010). Yet, applications of polymerase chain reaction (PCR) or immunological assays are limited in the scale of retrievable ancient pathogen genomic data. For example, a limitation with PCR is that the abundant short DNA fragments typical of ancient DNA (e.g., less than 40 bp) are untargeted due to the selective amplification of the fewer longer fragments (e.g., greater than 70 bp) (Knapp and Hofreiter, 2010). Similarly, immunological assays are not necessarily optimized for degraded samples, may be insensitive to low-levels of parassitaemia (e.g., less than 100 parasites per μl of blood) and suffer from false positives (e.g., antigens remaining after parasite clearance) (Moody, 2002; Perandin et al., 2004). It is only through a combined approach of hybridization capture targeting entire *Plasmodium*

genomes that phylogenetic inferences and authentication parameters render it possible to implicate this protozoan parasite at a specific locality in historical time.

Malaria in ancient Rome

The Pleistocene epoch is not compatible with malaria transmission in Italy, due to alternating glacial and interglacial periods within the Mediterranean creating an unsuitable climate and lack of ecological niches for *Anopheles* (Bruce-Chwatt and de Zulueta, 1980; Elenga et al., 2000; Sallares, 2006). The shift in climate and ecology of the Holocene (10,000 years ago) removed Pleistocene barriers to the entry of the *Anopheles maculipennis* complex (Mediterranean and European vectors of malaria), as temperatures approximated those of the present-day subtropical Mediterranean climate, enabling the spread of malaria into southern Europe from North Africa and the Near East alongside human demographic expansions (i.e., Neolithic Revolution) (Bruce-Chwatt and de Zulueta 1980; de Zulueta, 1994; Grove and Rackham 2001). The Hellenistic (323 B.C. – 30 B.C.) and Roman (27 B.C. – 476 A.D.) periods are presumed to be when the *Anopheles* vectors became established in human environments transmitting *P. falciparum*, *P. malariae*, and *P. vivax*, due to the intensity of anthropogenic processes related to socioeconomic activities and population growth, such as facilitating a nautical dispersal of malaria in southern Italy due to maritime trade, or incoming slaves and armies returning from across the Mediterranean (e.g., North Africa, southwest Asia), creating an ideal

epidemiological environment (de Zulueta 1973; Bruce-Chwatt and de Zulueta 1980; Sallares, 2006). *Anopheles* vectors with an exclusive or specialized preference for human blood are increasingly likely to be transported across such geographic distances and physical barriers due to anthropogenic activity (Loiaza et al., 2012). These forms of malaria presumably spread together northward across Italy from 500 B.C. – 1000 A.D. along with the *Anopheles maculipennis* complex vectors (*An. labranchiae* and *An. sacharovi*) based on historical inferences (Sallares et al., 2004).

The antiquity of febrile illnesses presumptively representing “malaria” is long documented in diverse written sources, noting the classical symptomology of malaria infection (e.g., chills, fever, headaches, rigor, sweats, enlarged spleen) from the Nei Ching (China, 5th c. B.C.), Vedic and Brahmanic scriptures from the Indus Valley (4th to 2nd c. B.C.), the Ebers Papyri (3rd c. B.C.) and ultimately, Hippocrates (Greece, 5th c. B.C.) (Carter and Mendis, 2002; Sallares, 2002). There is incomplete knowledge on the history of malaria in Rome during the late Republican (5th -1st c. B.C.), Imperial (1st-5th c. A.D.), and late Antiquity (5th-7th c. A.D.) periods due to limited written documentation regarding outbreaks and epidemics (Scheidel, 2009). The works attributed to Hippocrates, Celsus, and Galen refer to elements of malaria infection (as understood today): 1) periodic fever patterns (i.e., *P. falciparum* as malignant tertian, *P. vivax* as benign tertian, *P. malariae* as quartan, quotidian as multiple *P. falciparum* or *P. vivax* strains causing intermittent fevers, and continuous fevers

as a mixed infection); 2) seasonal mortality patterns (late summer and early fall) associated with the incubation period (up to 30 days) of malaria; and, 3) geography or topography influencing the distribution of malaria (i.e., low-lying areas as prone to such “fevers”) (Carter and Mendis, 2002; Sallares, 2002; Retief and Cilliers, 2004; Sallares et al., 2004; Cunha and Cunha, 2008). *P. ovale* is not expected to be present in ancient Rome, as it is not endemic to the Mediterranean either in the past or currently (Carter and Mendis, 2002; Sallares, 2002). The prevalence and pathogenicity of malaria, particularly *P. falciparum*, is believed to have increased over time in ancient Rome. It became a threat in the early Imperial period (1st to 2nd centuries A.D.) due to population expansion, agricultural practices, and economic activity alongside increased travel and development of extensive trading networks, on a scale not previously reached in earlier Roman periods (Brunt, 1971; Bruce-Chwatt and de Zulueta, 1980; Sallares et al., 2004; Scheidel, 2009). The inference from the literary record is that malaria was not considered a “novel” disease, owing to the continuity of descriptions from the time of Hippocrates in Greece (5th c. B.C.) to the ancient Roman authors (1st c. A.D.) (Sallares, 2002; Retief and Cilliers, 2004; Sallares et al., 2004).

Retrospective applications of morbidity and mortality associated with Italy’s 1880-1962 malaria epidemic and ongoing struggle of eradication (see Snowden, 2008) provides a means to conceptualize the consequences of this parasite on the economic, social, and political realms of the Imperial Italian context. One example is Grosseto (Tuscany) where endemic malaria in the mid-

19th century A.D. (1840-1841) led to a 60% mortality rate in 20-50 year olds, generally perceived as the most resistant age group to infection (Baldari et al., 1998; Sallares, 2002; Scheidel, 2003). This epidemiological pattern of malaria is retrospectively linked to funerary inscriptions in the Late Antique (4th-5th c. A.D.) city of Rome where a *P. falciparum* malaria epidemic is inferred from an increase in seasonal deaths among adults (late summer and early autumn) (Shaw, 1996; Scheidel, 2003, 2009). In drawing parallels from contemporary settings to epigraphic evidence it is critical to recognize that *Plasmodium* pathogenicity, host susceptibility, and dynamic biosocial pathogen interactions contribute to complex mortality patterns in disparate time periods.

Materials and Methods

Context of the Imperial period Italian cemeteries

The acropolis of Velia is a settlement located on a small promontory (with coastal plains to the north and south), 295-km southeast of Rome. Founded in the mid-6th century B.C. as a Greek colony, Velia was under Roman control by the late 3rd century B.C. and functioned as an important maritime hub, with gradual abandonment beginning in the 9th century A.D. that accelerated due to encroaching marshland, as tax registers recorded only 12 households in 1648 (Greco and Krinzinger, 1994; Craig et al., 2009). The precise timing of encroaching marshland is inconclusive, with estimates of the Classical period (3rd-1st c. B.C.) or after the 9th century A.D., as “swamps” are inferred to have surrounded the promontory (Greco and Krinzinger, 1994; Craig et al., 2009).

The acropolis ridge divided the city into northern and southern districts (with fortified walls lining the city), and was linked by paved streets connected to a main road, the *Via di Porta Rosa* (Greco and Krinzinger, 1994; Cicala, 2013). Archaeological evidence indicates the remains of several residential blocks (*insulae* and mudbrick dwellings) scattered across distinct districts, workshops (e.g., milling), an aqueduct drawing spring water, and proxy archaeological evidence of a thriving urban centre (e.g., theatre, porticoes, bathhouse, villas, and ceremonial complex) (Krinzinger, 1986; Greco and Krinzinger, 1994; Cicala, 2013). Agricultural output at the site included cereals, vines, and olives alongside pastures for animal husbandry; further, economic activities included a fishing industry, and harvesting timber for the building and servicing of boats at the port facilities (Greco, 1999; Morel, 1999; Craig et al., 2009; Crowe et al., 2010). Essentially, this minor port city was a maritime trading centre critical in supplying the surrounding population (including the Roman capital), as well as a spa-town for aristocrats (Crowe et al., 2010; Sperduti et al., 2012). However, as the city was built upon a terraced landscape, Velia was prone to flood events (from 1st c. B.C.-5th c. A.D.), as evidenced by stratigraphic alluvial deposits in areas such as the necropolis, the “*Villa degli Affreschi*”, and residential zones (Amato et al., 2010; Cicala, 2013; Ermolli et al., 2014). The cemetery itself was used during the Imperial period (1st-2nd c. A.D.), with more than 330 scattered burials excavated (inhumations and cremations) beyond the city walls (see Fiammenghi, 2003; Craig et al., 2009, Crowe et al., 2010).

The site of Vagnari extends over 3.5 ha within in the Basentello valley near Gravina in Puglia, Bari (over 400-km from Rome), surrounded by plateaus of land (the Murgia) that are ideal for animal husbandry and transhumance (Small, 2011, 2014). The site was likely connected to Rome along the *Via Appia*, one of numerous ancient roads connecting Rome to the coastlines of Italy, and is characterized as a rural village participating in industrial processing activities as indicated by archaeological evidence of tile kilns, iron-working, as well as agricultural production (e.g., cereal crops, viticulture) (Prowse et al., 2010; Small, 2011, 2014). In antiquity, trees surrounded the area and water was supplied by numerous natural springs that characterized the landscape around the site, alongside the Silvium aqueduct (Parise et al., 2000; Small, 2011). In terms of Vagnari's connection to the Empire at large, the site likely consisted of slaves, freedmen, and/or free tenants contributing to the activities of an Imperial estate, land that was owned by the Emperor or his designate (Prowse et al., 2010). The cemetery at Vagnari is located on the southern part of the site, away from the main habitation area, and the 108 burials excavated mainly date between the 1st to 4th centuries A.D. (see Prowse et al., 2010; Small, 2011, 2014).

Isola Sacra is a necropolis (1st-3rd c. A.D.) 20-km southwest of Rome, situated on an artificial island between the cities of Ostia and Portus Romae (Bondioli et al., 1995; Prowse et al., 2004, 2007). The cemetery was used by residents of Portus Romae (23-km southwest of Rome) built near a main road (*Via Flavia Severiana*) and approximately 2,000 individuals have been recovered to

date, mostly consisting of commingled remains from monumental tomb excavations (Prowse et al., 2005, 2007; Sperduti, 1995). At the beginning of the Imperial period, Portus functioned as the main port and warehouse for Rome, until the port fell into decline during the 4th century A.D. (Keay and Paroli, 2011; Keay, 2012). In contrast to Velia, Portus had direct economic ties with the Roman capital through the maritime and river transport of foodstuffs from other regions to the city of Rome via connected docks and quays along the Tiber River (Keay and Paroli, 2011; Keay, 2012). The construction and maintenance of canals in this artificial harbour was critical to accommodate the increased volume of goods and larger sea vessels as the Empire expanded (Keay and Millett, 2005).

The population of Portus is characterized as highly mobile and varied (i.e., merchants, traders, migrants, slaves or freedmen) of relatively recent immigrants from other areas of the Empire, with epigraphic evidence identifying individuals from North West Asia Minor and Egypt; however, there are no textual references to a local aristocracy (Sacco, 1984; Mannucci and Verduchi, 1996; Prowse et al., 2004, 2007). In terms of infrastructure, an aqueduct along the *Via Portuensis* (a road connecting Portus and Rome) brought spring water to the residents, supplemented by local wells and cisterns, in addition to servicing public baths and fountains (Keay et al., 2005). Archaeological excavations of the habitation structures is not possible as the site is privately owned, and previous investigations in the 19th and 20th centuries focused on the harbour system (Prowse et al., 2004). However, paleoenvironmental evidence from the artificial

harbour indicates the structure of the administrative and economic centre of the site. For example, a densely occupied area near the *Canale Traverso* (from 1st c. A.D. to the late Middle Ages) provides a record of an urban sector as evidenced by warehouses and storage areas along the port area, becoming residential near the end of the 3rd c. A.D., with the *Basilica Portuense* built in the mid-5th century A.D. (Paroli, 2005; Salomon et al., 2012). Ecologically, the site is also unique, particularly due to the *Stagno di Maccarese* (2.5-km from Portus), a brackish marsh as indicated by paleobotanical evidence (e.g., riparian trees that grow in saline conditions and saltwater clams) (Keay and Millett, 2005; Giraudi et al., 2009; Sadori et al., 2010; Mazzini et al., 2011). Even nearby Ostia (connected to Portus with the *Via Flavia* road) is associated with a brackish marsh, the *Stagno di Ostia* (2-km from Ostia), as shown by a predominance of salt tolerant weeds and plants (Keay and Millett, 2005; Bellotti et al., 2011). The gradual and seasonal desiccation of such coastal marshes due to isolation from the Tyrrhenian Sea is supported by palynological evidence (ferns and algae), increasing the probability as a potential vector proliferation source for transmitting malaria (Sallares, 2006; Di Rita et al., 2010; Bellotti et al., 2011).

In terms of hypothesizing the presumptive range of malaria, the geographic location of Isola Sacra is ideal, as Portus is located within the “malarial belt” of ancient Rome (Sallares 2002; Scheidel 2003, 2009; Prowse et al., 2007: 512), which is inferred from the distribution of malaria in Italy (1882) (see Figure 1b). For example, immigration to Portus is presumed to be significant

based on the historical evidence for mortality during antiquity (20-25 years of age; Macchiarelli et al., 1998), requiring a continuous influx of recent arrivals to sustain the population (Scheidel, 2003; Prowse et al., 2007). If malaria is presumed as present and exerting a toll on mortality, the newly arrived individuals from areas without malaria or a different strain may be more vulnerable to severe infections (Sallares, 2002; Scheidel, 2003; Prowse et al., 2007). Ecologically, the presence of marshes with seasonal desiccation and extensive modification of the environment at Portus in consideration of its connectivity to the Roman capital as an economic centre, further leads to a presumptive optimal context for malaria sustainability. Comparably, Velia as a minor port city and Vagnari as part of the rural countryside present varied epidemiological environments; however, the settlement of Velia on a terraced promontory alongside coastal plains and the reliance of intensified agriculture or transhumance at Vagnari, also present potential scenarios for malaria proliferation.

Broad indicators of health stress are evident (e.g., linear enamel hypoplasia, cribra orbitalia, porotic hyperostosis) among the individuals at Vagnari (Prowse et al., 2014), Velia (Beauchesne, 2012), and Isola Sacra (Sperduti, 1995; Gowland and Garnsey, 2010); however, the burden of infectious diseases (as manifested via skeletal indicators of pathology) are unclear. As a purposeful line of inquiry, it is integral to use ancient DNA as a means to explore the presence of malaria in these Imperial period Italian cemeteries alongside epidemiological, archaeological, or historical sources to frame pathogen presence

in context. Details surrounding the extraction of DNA from the Imperial Italian adults, conversion of the extracts into double-stranded indexed libraries as well as the parameters of the *Plasmodium* mitochondrial genome capture and phylogenetic analyses are outlined in Marciniak et al. (2016).

Figure 1b. Overlay of Luigi Torelli’s identification of malarious areas in Italy (1882, “Carta della malaria dell’Italia”) constituting the “malaria belt”.



Results

Our approach enabled the successful recovery of a partial *P. falciparum* mitochondrial genome combined from two adults at Velia and Vagnari, with phylogenetic support (outlined in Marciniak et al., 2016). Refer to Table 1 for the metagenomic analysis of the 11 prioritized adult samples from a subset of 58. The

proportion of human DNA as assessed by mapping to the human nuclear and mitochondrial genomes (hg38.fa.gz, soft-masked, UCSC Genome Browser, and NC_012920, respectively) is indicated in Table 2. The summarized capture data for the two individuals from which *P. falciparum* aDNA was recovered – LG20 (VAG234 from Vagnari) and LV13 (Velia 186), is presented in Table 3, with the coverage metrics for *P. falciparum* and the human mitochondrial genomes indicated in Table 4. Details surrounding the authentication of the *P. falciparum* sequence data (e.g., fragment length distribution, damage signal, and internal consistency) are described in Marciniak et al. (2016).

VAG F234 is an adult male, aged 35 years (± 9.4), from the Vagnari necropolis, whose burial is dated to the 2nd century A.D. The skeleton is well-preserved, with evidence of ‘barely discernable’ cribra orbitalia in the right orbit, and ‘barely discernable’ porotic hyperostosis on the left parietal (scored according to criteria in Buikstra and Ubelaker, 1994). The only other evidence of pathological changes on the skeleton is that the spinous process of the fifth lumbar vertebra was not fused to the vertebral body. Velia 186 is an adult male, aged 20-25 years from the Velia necropolis, dated to the 1st-2nd A.D. The skeleton is well-preserved, with a number of developmental anomalies: retention of the metopic suture, unfused scapular acromion (right side), bipartite rib (left side), and bipartite patella (right side). Cribra orbitalia on both orbits are also observed as Type 3 lesions (according to Stuart-Macadam, 1991) and are in a remodeling phase.

Table 1. Metagenomic analysis of the prioritized Imperial Italian samples

Library ID	Processed reads	Taxonomic assignments (no mapping to genomes)					Mapping to reference <i>Plasmodium</i> species						
		MEGAN assigned reads	Apicomplexa reads	Proportion (%) Apicomplexa	<i>Plasmodium</i> reads	Proportion (%) <i>Plasmodium</i>	Total <i>P. falciparum</i> reads	Total <i>P. vivax</i> reads	Total <i>P. malariae</i> reads	Total <i>P. ovale</i> reads	Total <i>P. cynomolgi</i> reads	Total <i>P. knowlesi</i> reads	Proportion (%) <i>Plasmodium</i> spp.
<i>Isola Sacra</i>													
LS02	1,483,348	68,482	N/A	N/A	7	0.0102	1	1	1	1	1	1	0.000067
LS03	826,153	64,581	6	0.0093	N/A	N/A	0	0	0	0	0	0	0
LS05	1,699,223	96,971	6	0.0062	N/A	N/A	0	0	0	0	0	0	0
LS06	2,572,465	82,719	N/A	N/A	5	0.0060	1	1	1	1	1	1	0.000039
LS07	934,052	83,316	6	0.0072	N/A	N/A	0	0	0	0	0	0	0
<i>Vagnari</i>													
LG20	1,276,428	128,925	5	0.0039	N/A	N/A	0	0	0	0	0	0	0
LG23	1,836,150	172,251	N/A	N/A	5	0.0029	0	0	0	0	0	0	0
PLG11	1,698,006	62,482	5	0.0080	N/A	N/A	0	0	0	0	0	0	0
<i>Velia</i>													
LV13	3,437,946	183,342	N/A	N/A	5	0.0027	0	0	0	0	0	0	0
LV14	1,957,091	94,230	N/A	N/A	5	0.0053	0	0	0	0	0	0	0
PLV06	1,271,588	57,747	6	0.0104	N/A	N/A	0	0	0	0	0	0	0
LV33	544,953	25,469	0	N/A	0	N/A	0	0	0	0	0	0	0

Table 2. Estimated endogeneity of the prioritized Imperial Italian shotgun sequenced data as mapped to human mitochondrial and nuclear genomes

Library ID	Raw reads	Processed reads	Human (hg38) reads	Proportion (%) nuclear	Human (mtDNA) reads	Proportion (%) mtDNA
<i>Isola Sacra</i>						
LS02	3,373,972	1,483,348	24,502	1.652	74	0.0050
LS03	1,704,130	826,153	18,629	2.255	107	0.0130
LS05	4,807,888	1,699,223	48,959	2.881	72	0.0042
LS06	7,650,436	2,572,465	22,590	0.878	76	0.0030
LS07	5,223,706	934,052	148,503	15.899	250	0.0268
<i>Vagnari</i>						
LG20	5,585,448	1,276,428	172,437	13.509	327	0.0256
LG23	7,679,034	1,836,150	10,419	0.567	43	0.0023
PLG11	3,325,996	1,698,006	533	0.031	21	0.0012
<i>Velia</i>						
LV13	7,108,588	3,437,946	37,179	1.081	85	0.0025
LV14	4,054,792	1,957,091	20,304	1.037	94	0.0048
PLV06	2,480,602	1,271,588	16,224	1.276	42	0.0033
LV33	1,061,550	544,953	5,001	0.918	3	0.0006

Table 3. *P. falciparum* coverage metrics for LG20 and LV13

Library ID	Raw reads	Processed reads	Mapped (with stacks)	Mapped (stacks removed)	% unique reads
<i>Shotgun_1 metrics</i>					
LV13	7,108,588	1,276,428	0	0	0
LG20	5,585,448	2,879,272	0	0	0
<i>Shotgun_2 metrics</i>					
LV13	1,379,984	718,791	0	0	0
LG20	1,053,742	554,509	0	0	0
<i>Capture set_1 metrics</i>					
LG20	2,754,418	1,475,992	81	1	0.000068
LV13	2,835,460	1,552,249	89	12	0.000773
<i>Capture set_2 LG20 metrics</i>					
MLG02	7,632,046	3,997,873	17	1	0.000025
MLG03	43,933,816	23,398,604	33	1	0.000004
MLG08	5,450,830	3,007,552	18	2	0.000066
MLG09	6,286,326	3,381,400	14	1	0.000030
MLG14	7,330,436	4,555,869	9	1	0.000022
<i>Capture set_2 LV13 metrics</i>					
MLV04	6,194,872	4,006,498	8	5	0.000125
MLV05	7,713,490	4,045,129	51	39	0.000964
MLV10	8,051,628	5,172,257	22	21	0.000406
MLV11	15,488,420	7,974,259	28	16	0.000201
MLV13	9,288,898	4,895,348	28	17	0.000347
<i>Capture set_3 LG20 metrics</i>					
MLG01	13,907,570	4,172,962	1	1	0.000024
MLG02	4,315,542	2,232,153	4	0	0.000000
MLG05	13,262,960	6,905,638	3	2	0.000029
MLG06	15,264,738	7,912,346	1	2	0.000025
MLG11	14,734,854	8,021,915	0	2	0.000025
MLG13	16,317,848	8,454,929	0	4	0.000047
<i>Capture set_3 LV13 metrics</i>					
MLV03	8,520,820	4,814,213	6	5	0.000104
MLV04	10,782,318	5,493,805	38	38	0.000692
MLV07	15,252,818	8,642,751	15	17	0.000197
MLV08	56,662,968	28,954,027	17	15	0.000052
MLV10	3,724,726	1,953,974	13	12	0.000614
MLV12	14,606,238	7,521,612	22	15	0.000199

Table 4. LG20-LV13 coverage metrics for *P. falciparum* and human mtDNA.

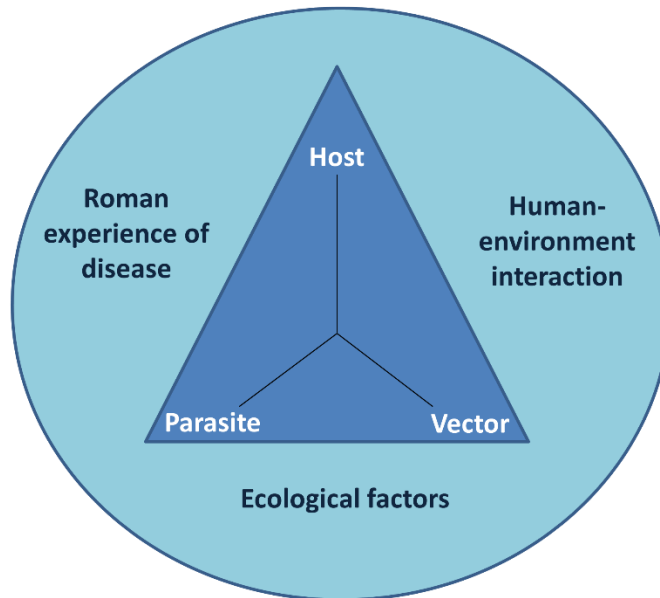
Specimen	Unique reads	Coverage metrics			Read length metrics		Haplogroup metrics	
		Coverage	Mean Coverage	Max. coverage	Average fragment length	Max. fragment length	Haplogroup	Quality
<i>P. falciparum</i> LG20_LV13	120	50.8%	1	7	51	161	N/A	N/A
<i>Human mtDNA</i> LG20	2,811	99.4%	10.6	176	62.6	168	T2c1e	88.16%
LV13	922	85.3%	3	40	53.5	163	T2b29	62.17%

Discussion

The recovery of a partial mitochondrial genome confirming the causative species of *P. falciparum* (to the exclusion of other *Plasmodia*) in two individuals that were prioritized from a set of 58 adults, and from two distinct sites (ecologically and socially) in Imperial period southern Italy has significant implications for the dynamics of malaria at Velia, Vagnari, and Portus. Although the existing literary record is fragmentary and focused in specific geographic regions, such as the Hippocratic Corpus documenting select cases of interest within Thessaly and northern Greece (Jouanna, 1999), our molecular results provide direct evidence of a causative *Plasmodium* species, which is not possible with retrospective diagnoses using textual evidence. The identification of *P. falciparum* in the coastal town of Velia and the rural countryside of Vagnari, but not at Portus Romae, leads to questions surrounding the complexity of malaria in these localities.

As a means of framing this dynamic within the studied localities, as well as at the macroscale of Italy, the integration of an ecosocial health approach (Krieger, 2001, 2008, 2011) is critical to inform evaluations of the multi-causal pathways of malaria (e.g., human-environment-vector-parasite interactions) (Figure 2).

Figure 2. Contextualization of malaria in Imperial Italy (adapted from Breman, 2001).



The anthropogenic context for malaria in Imperial Italy

Proxies of the multi-causal pathway behind exposure and susceptibility to malaria are drawn from the Roman-era historical record and contemporary epidemiological knowledge to infer the scope of anthropogenic influences, as emphasized by Krieger (2001: 672), that “no aspect of our biology can be understood absent knowledge of history and individual and societal ways of living”. Accordingly, it is necessary to examine the influence of social and economic factors on the manifestation of malaria (e.g., population density, agriculture, construction activities, trade, and migration).

The foundation for the spread of malaria in Imperial Italy is attributed to not only optimum global and local climate, but also intensification of anthropogenic modification to the environment in the context of a burgeoning

Empire and its populations. The reshaping of the Roman economy during the Imperial period is attributed to resource transfers of taxes, tributes, and rents alongside increased trade and service sector development within climatic conditions enhancing agricultural output (Scheidel, 2004: 745). Demographic information for the city of Rome is variable, ranging from estimates of 150,000 to four million (Morley, 2013), with limited information for the periphery. Morbidity and mortality are presumed as similar to a contemporary third world country, with an excess of deaths in comparison to births and low life expectancy, although mortality patterns are inherently complex (Nutton, 2004; Scheidel, 2009; Oerlemans and Tacoma, 2014).

In this scenario, the pathogen burden is inferred as one of chronic infections (e.g., tuberculosis, leprosy), acute diseases (e.g., malaria, smallpox, cholera), and opportunistic infections (e.g., gastroenteritis), with associations from entangled biosocial variables (e.g., malnutrition, inadequate “sanitation” infrastructure, and overcrowded living conditions) (Grmek, 1991; Sallares, 2002; Scheidel, 2003; Nutton, 2004; Gowland and Garnsey, 2010). The distribution of pathogens within a locality is dynamic and responsive to not only such macro-scale factors (e.g., climate, stressors of life in an expanding Empire), but also micro-scale variables (e.g., temperature changes, anthropogenic activity). It is within this broad sociopolitical context of the Empire, that the distribution of malaria is evaluated as related to the ecological and social circumstances proliferating or mitigating its influence at Velia, Vagnari, and Portus Romae.

Accordingly, although malaria was not recovered from adults at Portus Romae, it does not mean it was absent, as malaria can presumptively be associated with any of these localities. The application of ecosocial theory (Krieger, 1994; 2011) functions as an explanatory device to frame the genomic results within potential causal pathways inferred from epidemiological, historical, and archaeological sources. It is recognized that unpredictable factors contribute to fluctuations in the malaria burden, and factors beyond the ones discussed below may also impact the proliferation of malaria.

Firstly, the complexity of malaria transmission and spectrum of responses to infection underscore the contextualization of the genomic results. With regards to the broad context of Imperial Italy, the nature of malaria transmission is equivocal. A stable malaria burden may be interpreted from the historical record (e.g., the Hippocratic Corpus references high mortality in children from periodic fevers) with the associated inference that immigrants from non-endemic areas were prone to severe infection, while the local population gained some measure of clinical immunity (e.g., Sallares, 2002; Scheidel, 2003; Retief and Cilliers, 2004). However, it is worth noting that acquiring complete (anti-parasitic) immunity is a long process, as the human host is required to create antibodies to multiple *P. falciparum* strains that may be circulating (e.g., due to regional variability from vectors or parasite responses to the host), leaving individuals highly prone to re-infection or acting as parasite reservoirs for subsequent recrudescence (Carter and Mendis, 2002; Crompton et al., 2014). An unstable or epidemic malaria burden

also fits with existing historical evidence for Imperial Italy, particularly in consideration of the weather fluctuations characterizing the varied Mediterranean ecology (i.e., floods from the Tiber River, excess rainfall, humid temperatures, or droughts) (e.g., Bruce-Chwatt and de Zulueta, 1980; Sallares, 2002; Scheidel, 2003, 2009). Similarly, under the auspices of a growing Empire, factors of migration, resettlement, the slave trade, and war campaigns may further risk the importation of malaria from other regions, thereby contributing to epidemic scenarios (e.g., Bruce-Chwatt and de Zulueta, 1980; de Zulueta, 1994; Carter and Mendis, 2002).

Underlying this uncertain complexity of transmission is the interplay of malaria pathogenesis as individuals can carry the parasites but not have the disease while variable responses such as acquired or inherited immunity means a spectrum of tolerance (Snow and Omumbo, 2006). For example, the frequency of resistance genes that mitigate severe outcomes of malaria, such as glucose-6-phosphate-dehydrogenase deficiency (G6PD), alpha and beta thalassemias as well as sickle cell anemia are unknown for Imperial period Italy, although there is molecular evidence of G6PD deficiency from an infant in 5th. c. A.D. Lugnano (Italy) noted by Sallares et al., (2004). The current frequencies of the thalassemias and G6PD polymorphisms in the Mediterranean region (e.g., 2-40%) as inferred outcomes of previously intense malaria do not provide direct association to the scope of malaria in the past, particularly as many genes are involved with genetic resistance to malaria and may vary across populations (e.g., presence or absence

of certain variants, strain and parasite diversity) (Cavalli-Sforza, 1994; Kwiatkowski, 2005; Hedrick, 2011). However, although *P. falciparum* was recovered from the Velia and Vagnari adults, but none at Portus Romae where it was expected, these complexities of inherited or acquired immunity may also undetectably influence malaria susceptibility and its recovery post-mortem using ancient DNA technology.

Ultimately, the genomic and historical evidence cannot address inferences of malaria endemicity or selection pressures of this pathogen at the localities of Velia, Vagnari, and Portus Romae. However, local epidemiological factors also impact the scope of malaria, leading to potentially uneven and fluctuating patterns in these localities, rather than a singular narrative of an endemic scourge. This multifaceted impact of malaria in a locality is connected to anthropogenic and ecological factors that alter the exposure pathways to anopheline reservoirs, which cannot be completely untangled despite using an integrated approach, but does highlight the richness of such a framework in systematically evaluating malaria in given locality to frame the experience of disease. In this manner, aspects of disease ecology (e.g., landscape, geomorphology, or vector breeding sites) and the human-environment interaction (e.g., land use patterns such as deforestation for agriculture and economic activities, or the sewage system and water supply) are discussed in connection with Velia, Vagnari, and Portus Romae.

The ecology of Velia (a coastal promontory between alluvial plains and marshes; Amato et al., 2010), Vagnari (a wooded river valley with lowland hills;

Small, 2011), and Portus Romae (a low-lying basin of woodlands near the Tiber River alongside marshes and lagoons; Keay and Paroli, 2011) frame the arenas of human interaction with a local epidemiological landscape. The responsiveness of these diverse ecosystems to human activity or climatological influences will be inherently dynamic in terms of structuring the potential distribution of *Anopheles* vectors. However, over-arching parameters that are important in shaping patterns of malaria are capable of being explored at these localities by integrating historical, archaeological, and epidemiological evidence.

A critical anthropogenic impact on the distribution of vector-borne diseases is deforestation. Deforestation is an ecosystem-wide modifier, influencing the microclimate (e.g., reducing shade, changing rainfall patterns) with increased water run-off, increased surface temperature, surface pooling, and altered air movement (creating aridity and humidity) (Sutherst, 2004; Yasuoka and Levins, 2007). Vector responses to this stressor variably impact disease distribution, increasing anopheline reservoirs as in eastern and southern Africa or eliminating such breeding sites, as in Thailand (Dutta et al., 2010). The reliance on timber as part of economic and construction activities, such as ship-building at Velia and Portus, or fuel for kilns at Vagnari, has implications for the alteration of the landscape and its conduciveness to parasite-vector proliferation. For example, harvesting timber from the woodland surrounding Vagnari and Portus may reduce available topsoil to prevent water run-off, thereby increasing the availability of surface pools and drawing humans into closer contact with vectors, while

considering the geomorphology of Velia (on a promontory with river valleys), deforestation may affect natural drainage patterns. The degree of ecosystem resilience to such anthropogenic intrusions is uncertain, as the exploitation of timber as part of intensified economic activity during the Imperial period may variably affect the distribution of anopheline reservoirs and malaria exposure.

The vector-parasite relationship is also variably influenced by intensified agriculture (as it directly affects land-use patterns). For example in 20th c. A.D. Italy, the practice eliminated available breeding sites in various regions (e.g., Massarosa) by reducing water proliferation with an increase in livestock offering an accessible food supply and shifting the anopheline balance towards primarily zoophilic *An. maculipennis* vectors (Hackett and Missiroli, 1931). The intensity of such opportunistic shifts in the *An. maculipennis* complex through diversification and expansion in regional areas is currently unknown (Loaiza et al., 2012), which supports a potentially dynamic distribution at the study localities that is equally responsive to diverse ecological and social factors. For example, despite the intensity of agricultural activity and transhumance offering abundant non-human blood meals for *Anopheles* at Vagnari, the recovery of *P. falciparum* aDNA suggests a degree of human preference between the vectors and human hosts in this location. Similarly, the use of the terrace system at Velia (Greco and Krinzing, 1994) as a means of cultivating crops on less steep slopes may enable increased water absorption by the soil and control soil erosion (acting to minimize surface pools), essentially mitigating exposure to vectors (Dyson, 2010); however,

irregular maintenance or neglect may detrimentally affect the distribution of infective vectors.

Broadly, agricultural development may lead to increased vector-borne diseases, due to the responsiveness of anophelines to changes in ecological conditions and available breeding sites (Yasuoka and Levins, 2007), and this may be connected to an unevenness of malaria patterns at Velia, Portus Romae, and Vagnari. For example, the use of irrigation canals as part of agricultural production in Fiumicino (Italy, 1928) proliferated anopheline reservoirs and led to a malaria epidemic (Hackett and Missiroli, 1931). The intensification of agriculture alongside animal husbandry is shown at Velia as an 80 ha area was under permanent cultivation (Greco, 1999; Sperduti et al., 2012), while those at Vagnari were similarly involved in agricultural production, animal husbandry and transhumance (Small, 2011, 2014). The functionality of irrigation canals or related water systems in propagating reservoirs is unknown; yet, potentially, the work of harvesting crops in the rich coastal plains and river valleys of Velia and Vagnari, may further expose individuals to malaria, if the summer harvest season coincided with peak infectivity (Snowden, 2008). Considering the ecology of Portus in terms of its proximity to the Tyrrhenian Sea with dunes and lagoons nearby, cultivable land is presumed to have been limited (Sperduti et al., 2012), suggesting the intensification of agriculture, arboriculture, and pasture lands may play a role in the uneven distribution of malaria at these three localities.

Infrastructure modifications to ensure the prosperity and health of a population are also connected to the distribution of malaria; however, the degree to which such factors are accessible using archaeological and historical evidence is variable, which underlies the inherent complexity of responsiveness to malaria at Velia, Vagnari, and Portus. Drainage systems and water supplies are critical factors in the distribution of vector-borne disease (Sutherst, 2004). Roman aqueducts were fed from freshwater reservoirs to transport water to towns/cities and the removal of wastewater was facilitated by underground pipes with connections to bathhouses, latrines, and residences, or drawing overflows from public fountains or cisterns (Hansen, 1983; Scobie, 1986; O’Sullivan et al., 2008). Evidence for aqueducts is indicated at Portus (along the *Via Portuensis*; Petriaggi et al., 1995), Velia (*Ascea Marina*; Krinzinger, 1986), and Vagnari (Silvium aqueduct in Gravina in Puglia; Parise et al., 2000). Sections were constructed underground in order to prevent contamination (Prowse et al., 2007); however, seepage or overflows are a relevant concern for vector proliferation in proximity to residential zones. The degree to which the maintenance of such infrastructure mitigated or proliferated anopheline reservoirs is uncertain, and will reflect the specific circumstances of a given locality.

The construction of roads as outgrowths of servicing a growing Empire may impact the natural drainage patterns in the landscape by cuttings (trenching to reach bedrock or a firm foundation) and embankments, where the surfaces ranged from beaten earth, compacted gravel, limestone or basalt (Chevallier,

1976; Laurence, 1999). The construction of the roads also varied (e.g., rubble foundation, edged by stones to assist with drainage, sand, and a surface material), but were structured by the natural topography of the landscape (Chevallier, 1976; Cicala, 2013). The *Via di Porta Rosa* at Velia was bound by the topography of the hillside and constructed from paving stones of various sizes with some sections on the upper terrace levels indicating adjacent channels for water removal (Cicala, 2013), potentially precluding the proliferation of standing water due to the natural drainage contours of the landscape. The *Via Appia* (connecting Rome to the southern coast) was near Vagnari, but the lowland hills of this landscape possibly facilitated efficient drainage (i.e., limited freshwater ditches). This is unlike the stretch of the *Via Appia* in the flat Pontine Plain that may have led to water accumulation in roadside ditches acting as reservoirs for vectors (Sallares, 2002; O’Sullivan, 2008). Similarly, the *Via Portuensis* (linking Rome and Portus) was constructed with small stones (Keay and Paroli, 2011), potentially proliferating the longevity of standing water due to inadequate absorption. Extreme climatic events such as droughts or floods also influence the development, longevity, and infectivity of vectors (Service and Townson, 2002) acting to eliminate vector breeding sites or enhance their availability (Dutta and Dutt, 1978; Sutherst, 2004). Flooding episodes are indicated at Velia by alluvial sedimentation in the stratigraphic layers of buildings in the southern quarter (1st c. B.C. (Amato et al., 2010), as well as a road (2nd c. A.D.) (Cicala, 2013). Similarly, the proximity of Portus to the Tiber River may have exposed this location to occasional flood

events (Keay and Paroli, 2011). For Vagnari, the ravine may have been affected by increased rainfall, and alluvial sedimentation is present in one region of the cemetery (posited to have occurred after its construction). The impact of climatic events on the human-vector-parasite interaction is important; however, these may variably contribute to changes in malaria proliferation at Velia, Portus, and Vagnari.

An underlying factor that structures these pathways of exposure to malaria is the proximity of humans to anopheline reservoirs. For example, in urban areas, there is the potential for reduced vector densities in comparison to rural environments, although it is recognized that within any district or location, this impact can vary considerably even over short distances (Trape et al., 1992). The reduction in open space and the spread of anophelines across a dense human population may lead to reduced exposure per person, as well as localizing transmission areas (Trape et al., 1992). Accordingly, as Portus is presumptively more “urban” than Velia and Vagnari, there is the potential for vector exposure to be differentially structured, and this may affect the recovery of *P. falciparum* molecular signatures from individuals associated with Portus (i.e., being more challenging to find from the subsample of 20 individuals that were tested from this location). Similarly, the potential for a gradient of transmission depending on the proximity to anopheline reservoirs in general, may further impact the dynamic distribution (or intensity) in response to anthropogenic and ecological factors at Velia, Vagnari, and Portus.

Hence, there is no single version of the “Roman malaria” due to the inherent complexity of the ecological and social substrates underlying this burden. This is shown with isotope data from the Velia and Vagnari individuals, relating to the implication that immigrants to Rome presumably experienced more severe infections in the absence of immunity (Sallares, 2002; Scheidel, 2009). Oxygen isotope analyses for the adult male (VAG F234) from Vagnari, indicates that he was born in the region around Vagnari (Prowse, 2016) while strontium and oxygen isotope analyses for the adult male from Velia (VEL186) similarly indicates he was born in the surrounding region (R. Stark, pers. comm., May 2016). The significance of recovering *P. falciparum* from “local” individuals emphasizes the importance of site-specific (contextual) epidemiological factors contributing to malaria, although whether this molecular signature reflects exposure, infection, or parasite tolerance is uncertain. But, rather than being simply endemic or epidemic, malaria reflects complexity in its distribution and responsiveness to the localized biosocial factors. The molecular evidence frames malaria at Velia, Vagnari, and Portus Romae as potentially embedded in a complex network of varied host and parasite interactions in diverse social and ecological scenarios.

Conclusions

Consistent with evidence from the historical record, evidence of *P. falciparum* malaria was recovered from different social, economic, and environmental contexts. This is the first study to implicate *P. falciparum* in adults

at multiple sites in Imperial period southern Italy. Confirmation of *P. falciparum* in Velia and Vagnari, but not at Portus (associated with the Isola Sacra necropolis), does not preclude its presence, but does lead to a significant question regarding the degree to which the diversely mobile population at this comparatively “urban” site impacted the dynamics of malaria. In terms of the biological narrative of the pathogen itself, the variable recovery of *P. falciparum* in two individuals from diverse contexts attests to the success of hybridization capture in the recovery of minute *Plasmodium* spp. genomic constituents that are embedded in a complex background of non-target (exogenous) molecules. However, the inability to recover low-level infections typically associated with *P. vivax* and *P. malariae*, does not preclude their presence in Imperial Italy, nor their respective capability to influence the pathogen pool.

Correlating archaeological evidence (e.g., paleoenvironmental or anthropogenic modifications) with the historical record (e.g., ancient Greek and Roman texts) remains an indirect measure of evaluating malaria presence, but functions to contextualize the methodological scope of the ancient DNA work. Ancient DNA analysis is the most direct way to find evidence of a causative *Plasmodium* species in archaeological remains, despite challenges broadly associated with recovering pathogen DNA from ancient skeletons as well as the recognition that pathogen presence is not equivalent to disease expression. It is part of a robust framework to explore the story of malaria at Velia, Vagnari, and Portus Romae through an integrated molecular and anthropological approach.

Although we may not know all aspects surrounding ancient malaria epidemiology, such as the exclusivity of vector anthropophily, ecosystem resilience to mitigating/proliferating exposure to vectors or the impact of anthropogenic modifications on disease distribution; through interweaving the bioarchaeological and historical records with the molecular evidence, we are able to propose various pathways relevant at the studied localities as potentially impacting the distribution of *P. falciparum*.

Exploring malaria in Imperial southern Italy or other regions in antiquity greatly benefits from a multi-faceted approach recognizing the entangled causality between humans, vectors, *Plasmodium* parasites, and the ecological environment in contributing to the dynamism of malaria. As a critical human pathogen, malaria is tied to the biosocial context within which humans survive and thrive, and merits further molecular investigation at other sites along the frontiers of the Roman Empire, as malaria is considered one of many contributing factors to the decline of this civilization.

Acknowledgements

We gratefully extend our appreciation to collaborators at the L. Pigorini Museum in the excavation and curation of these bioarchaeological remains. A special thanks goes to R. Stark for providing the isotope information. Past and current members of the McMaster Ancient DNA Centre are also recognized for supporting this work. This research was funded by a Social Sciences and Humanities Research Council of Canada Doctoral Fellowship awarded to S.

Marciniak (#752-2014-1849), and the Canada Research Chairs Program to H.N.

Poinar.

Literature Cited

- Ali H, Ahsan T, Mahmood T, Bakht SF, Farooq MU, Ahmed N. 2008. Parasite density and the spectrum of clinical illness in falciparum malaria. *J Coll Physicians Surg Pak* **8**:362-8.
- Altschul SF, Gish W, Miller W, Myers EW, Lipman DJ. 1990. Basic local alignment search tool. *J Mol Biol* **215**:403–410.
- Amato L, Bisogno G, Cicala L, Cinque A, Romano P, Ruello MR, Russo Ermolli E. 2010. Palaeo-environmental changes in the archaeological settlement of Elea-Velia: climatic and/or human impact signatures? In: Ciarallo A, Senatore MR, editors. *Scienze naturali e archeologia. Il paesaggio antico: interazione uomo/ambiente ed eventi catastrofici*. Rome: Aracne Editrice. p. 13-16.
- Angel JL. 1966. Porotic hyperostosis, anemias, malarial, and marshes in the prehistoric Eastern Mediterranean. *Science* **153**:60-763.
- Baldari M, Tamburro A, Sabatinelli G, Romi R, Severini C, Cuccagna G, Fiorilli G, Allegri MP, Buriani C, Toti M. 1998. Malaria in Maremma, Italy. *The Lancet* **351**:1246-1247.
- Bates M. 1940. The nomenclature and taxonomic status of the mosquitoes of the *Anopheles maculipennis* complex. *Ann Entomol Soc Am* **33**:343-56.
- Beauchesne PD. 2012. Physiological Stress, Bone Growth and Development in Imperial Rome. University of California, Berkley, unpublished PhD dissertation.
- Bei AK, Duraisingh MT. 2013. Invasion of host red blood cells by malaria parasites. In: Carlton JM, Perkins SL, Deitsch KW, editors. *Malaria Parasites: Comparative Genomics, Evolution and Molecular Biology*. United Kingdom: Caister Academic Press. p. 169-197.
- Bellotti P, Calderoni G, Di Rita F, D’Orefice M, D’Amico C, Esu D, Magri C, Martinez MP, Tortora P, Valeri P. 2011. The Tiber river delta plain (central Italy): coastal evolution and implications for the ancient Ostia Roman settlement. *The Holocene* **21**:1105-1116.
- Bianucci R, Mattutino G, Lallo R, Charlier P, Jouin-Spriet H, Peluso A, Higham T, Torre C, Rabino Massa E. 2008. Immunological evidence of *Plasmodium falciparum* infection in an Egyptian child mummy from the Early Dynastic Period. *J Archaeol Sci* **35**:1880-1885.

- Bondioli L, Macchiarelli R, Salvadei L, Passarelli P. 1995. Paleobiologia dell'eta` romana imperiale: il Progetto "Isola Sacra". In: Peretto C, Milliken S, editors. *XI Congresso degli Antropologi Italiani. L'Adattamento Umano all'Ambiente. Passato e Presente*. Cosmo Iannone Editore. p. 78-79.
- Breman JG. 2001. The ears of the hippopotamus: manifestations, determinants, and estimates of the malaria burden. *Am J Trop Med Hyg* **64**: 1-11.
- Bruce-Chwatt LJ. 1980. *Essential Malariology*. London: William Heinemann Medical Books Ltd.
- Bruce-Chwatt LJ, de Zulueta J. 1980. *The Rise and Fall of Malaria in Europe: A Historico-Epidemiological Study*. Oxford: Oxford University Press.
- Brunt PA. 1971. *Italian Manpower, 225 B.C.–A.D. 14*. London: Oxford University Press.
- Burbano HA, Hodges E, Green RE, Briggs AW, Krause J, Meyer M, Good JM, Maricic T, Johnson PLF, Xuan Z, Rooks M, Bhattacharjee A, Brizuela L, Albert FW, de la Rasilla M, Fortea J, Rosas A, Lachmann M, Hannon GJ, Pääbo S. 2010. Targeted investigation of the Neandertal genome by array based sequence capture. *Science* **328**:723-725.
- Buikstra JE, Ubelaker DH. 1994. *Standards for Data Collection from Human Skeletal Remains*. Fayetteville: Arkansas Archaeological Survey.
- Carpenter ML, Buenrostro JD, Valdiosera C, Schroeder H, Allentoft ME, Sikora M, Rasmussen M, Gravel S, Guillén S, Nekhrizov G, Leshtakov K, Dimitrova D, Theodossiev N, Pettener D, Luiselli D, Sandoval K, Moreno-Estrada A, Li Y, Wang J, Gilbert MTP, Willerslev E, Greenleaf WJ, Bustamante CD. 2013. Pulling out the 1%: whole-genome capture for the targeted enrichment of ancient DNA sequencing libraries. *Am J Hum Genet* **93**:1-13.
- Carter R, Mendis KN, Roberts D. 2000. Spatial targeting of interventions against malaria. *Bull World Health Organ* **78**:1401-1411.
- Carter R, Mendis KN. 2002. Evolutionary and historical aspects of the burden of malaria. *Clin Microbiol Rev* **15**:564-594.
- Cavalli-Sforza LL. 1994. *The History and Geography of Human Genes*. Princeton University Press: New Jersey.

- Chaves LF, Harrington LC, Keogh CL, Nguyen AM, Kitron UD. 2010. Blood feeding patterns of mosquitoes: random or structured? *Front Zoo* **7**:3-14.
- Chevallier R. 1976. *Roman Roads*. Field NH, Translator. Berkley: University of California Press.
- Cicala L. 2013. Il Quartiere occidentale di Elea-Velia. Un'analisi preliminare. *Mélanges de l'École française de Rome-Antiquité* **125**.
<http://mefra.revues.org/1300>
- Craig OE, Biazzo M, O'Connell TC, Garnsey P, Martinez-Labarga C, Lelli R, Salvadei L, Tartaglia G, Nava A, Renò L, Fiammenghi A, Rickards O, Bondioli L. 2009. Stable isotopic evidence for diet at the Imperial Roman coastal site of Velia (1st and 2nd Centuries AD) in Southern Italy. *Am J Phys Anthropol* **139**:572-83.
- Crompton PD, Moebius J, Portugal S, Waisberg M, Hart G, Garver LS, Miller LH, Barillas C, Pierce SK. 2014. Malaria immunity in man and mosquito: insights into unsolved mysteries of a deadly infectious disease. *Annu Rev Immunol* **32**:157-187.
- Crowe F, Sperduti A, O'Connell TC, Craig OE, Kirsanow K, Germoni P, Macchiarelli R, Garnsey P, Bondioli L. 2010. Water-related occupations and diet in two Roman coastal communities (Italy, first to third century AD): correlation between stable carbon and nitrogen isotope values and auricular exostosis prevalence. *Am J Phys Anthropol* **142**:355-366.
- Cunha CB, Cunha BA. 2008. Brief history of the clinical diagnosis of malaria: from Hippocrates to Osler. *J Vector Borne Dis* **45**:194-199.
- Cunnington A J. 2012. Malaria and Susceptibility to Other Infections. Ph.D. thesis, School of Hygiene & Tropical Medicine of London.
- Dermody BJ, de Boer HJ, Bierkens MFP, Weber SL, Wassen MJ, Dekker SC. 2011. Revisiting the humid Roman hypothesis: novel analyses depict oscillating patterns. *Clim Past Discuss* **7**:2355-2389.
- DeWitte SN, Stojanowski CM. 2015. The osteological paradox 20 years later: past perspectives, future directions. *J Archaeol Res* **23**:397-450.
- de Zulueta J. 1973. Malaria and Mediterranean history. *Parassitologia* **15**: 1-15.
- de Zulueta J. 1994. Malaria and ecosystems: from prehistory to posteradication. *Parassitologia* **36**:7-15.

- Di Rita F, Celant A, Magri D. 2010. Holocene environmental instability in the wetland north of the Tiber delta (Rome, Italy): sea-lake-man interactions. *J Paleolimnol* **44**:51-67.
- Druilhe P, Tall A, Sokhna C. 2005. Worms can worsen malaria: towards a new means to roll back malaria? *Trends Parasitol* **21**:359–362.
- Dutta HM, Dutt AK. 1978. Malarial ecology: a global perspective. *Soc Sci Med* **12**:69-84.
- Dutta P, Khan SA, Bhattarcharyya DR, Khan AM, Sharma CK, Mahanta J. 2010. Studies on the breeding habits of the vector mosquito *Anopheles baimai* and its relationship to malaria incidence in Northeastern region of India. *EcoHealth* **7**:498-506.
- Dyson SL. 2010. *Rome: A Living Portrait of an Ancient City*. Baltimore: John Hopkins University Press.
- Elena H, Peyron O, Bonnefille R, Jolly D, Cheddadi R, Guiot J, Andrieu V, Bottema S, Buchet G, de Beaulieu JL, Hamilton AC, Maley J, Marchant R, Perez-Obiol R, Reille M, Riollet G, Scott L, Straka H, Taylor D, Van Campo E, Vincens A, Laarif F, Jonson H. 2000. Pollen-based biome reconstruction for southern Europe and Africa 18,000 yr BP. *J Biogeo* **27**:621-634.
- Enk JM, Devault AM, Kuch M, Murgha YE, Rouillard JM, Poinar HN. 2014. Ancient whole genome enrichment using baits built from modern DNA. *Mol Biol Evol* **31**:1292-94.
- Ermolli R, Romano P, Liuzza V, Amato V, Ruello MR, Di Donato V. 2014. Evidence of human-induced morphodynamic changes along the Campania coastal areas (southern Italy) since the 3rd-4th cent. AD. *EGU General Assembly Conference, May*.
- Faure E. 2014. Malarial pathocoenosis: beneficial and deleterious interactions between malaria and other human diseases. *Front Physiol* **5**:441-454.
- Fiammenghi CA. 2003. La Necropoli di Elea-Velia: qualche osservazione preliminare. In Cicala L, Greco G, editors. *Elea-Velia. Le Nuove ricerche*. Quaderni del Centro Studi Magna Grecia 1: Naus Editoria. p. 49-61.
- Fornaciari G, Giuffra V, Ferroglio E, Gino S, Bianucci R. 2010. *Plasmodium falciparum* immunodetection in bone remains of members of the Renaissance Medici family (Florence, Italy, sixteenth century). *Trans R Soc Trop Med Hyg* **104**:583-587.

- Garcia LS. 2001. *Diagnostic Medical Parasitology*, ed 4. Washington: ASM Press.
- Giraudi C, Tata C, Paroli L. 2009. Late Holocene evolution of Tiber river delta and geoarchaeology of Claudius and Trajan harbor, Rome. *Geoarchaeol* **24**:371-382.
- Gowland R, Garnsey P. 2010. Skeletal evidence for health, nutritional status and malaria in Rome and the Empire. In: Eckardt H, editor. *Roman Diasporas: Archaeological Approaches to Mobility and Diversity in the Roman Empire*. Journal of Roman Archaeology, Portsmouth, Supplement 78. p. 131-156.
- Gowland RL, Western AG. 2012. Morbidity in the marshes: using spatial epidemiology to investigate skeletal evidence for malaria in Anglo-Saxon England (AD 410-1050). *Am J Phys Anthropol* **147**:301-311.
- Greco G, Krinzinger, F. 1994. *Velia: Studi E Ricerche*. Modena: F.C. Panini.
- Greco G. 1999. Velia: citta` delle acque. In: Krinzinger F, Tocco G, editors. *Neue Forschungen in Velia*. Vienna: Austrian Academy of Sciences Press. p. 73–84.
- Grmek MD. 1991. *Diseases in the Ancient Greek World*. Baltimore: Hopkins University Press.
- Grove AT, Rackham O. 2001. *The Nature of Mediterranean Europe: An Ecological History*. New Haven: Yale University Press.
- Hackett LW, Missiroli A. 1935. The varieties of *Anopheles maculipennis* and their relationship to the distribution of malaria in Europe. *Medicina de los Paises Calidos* **8**:1-60.
- Hansen RD. 1983. Water and wastewater systems in Imperial Rome. *J Am Water Resour Assoc* **19**:263-269.
- Hansheid T. 1999. Diagnosis of malaria: A review of alternatives to conventional microscopy. *Clin Lab Haematol* **21**:235-245.
- Hawass Z, Gad YZ, Ismail S, Khairat R, Fathalla D, Hasan N, Ahmed A, Elleithy H, Ball M, Gaballah F, Wasef S. 2010. Ancestry and pathology in King Tutankhamen's family. *J Am Med Assoc* **303**:638-647.
- Hedrick PW. 2011. Population genetics of malaria resistance in humans. *Heredity* **107**:283–304.

- Henneberg M, Henneberg RJ. 1998. Biological characteristics of the population based on analysis of skeletal remains. In Carter JC, editor. *The Chora of Metaponto: The Necropoleis, Vol. II*. Austin: University of Texas Press. p. 503–562.
- HersHKovitz I, Rothschild BM, Latimer B, Dutour O, Leonetti G, Greenwald CM, Rothschild C, Jellema LM. 1997. Recognition of sickle cell anemia in skeletal remains of children. *Am J Phys Anthropol* **104**:213-226.
- Hofreiter M, Paijmans JLA, Goodchild H, Speller CF, Barlow A, Fortes GG, Thomas JA, Ludwig A, Collins MJ. 2015. The future of ancient DNA: technical advances and conceptual shifts. *Bioessays* **37**:284-293.
- Holland TD, O'Brien MJ. 1997. Parasites, porotic hyperostosis and the implications of changing perspectives. *Am Antiq* **62**:183-193.
- Horsfall WR. 1955. *Mosquitoes: Their Bionomics and Relation to Disease*. New York: Ronald Press Company.
- Jetten TH, Takken W. 1994. Anophelism without malaria in Europe. A review of the ecology and distribution of the genus *Anopheles* in Europe. *Wageningen Agricultural University Papers*.
- Jouanna J. 1999. Hippocrates. DeBevoise, M.B. (Trans.) Baltimore: John Hopkins University Press.
- Keay S, Millett M. 2005. Integration and discussion. In: Keay S, Millett M, Paroli L, Strutt K, editors. *Portus: An Archaeological Survey of the Port of Imperial Rome*. London: Archaeological Monographs of the British School at Rome. p. 269-296.
- Keay S, Millett M, Paroli L, Strutt K, (editors). 2005. *Portus: An Archaeological Survey of the Port of Imperial Rome*. London: Archaeological Monographs of the British School at Rome.
- Keay SJ, Paroli L, (editors). 2011. *Portus and its Hinterland: Recent Archaeological Research*. Archaeological Monographs of the British School at Rome: London.
- Keay S, (editor). (2012) *Rome, Portus and the Mediterranean*. Archaeological London: Monographs of the British School at Rome.

- Kindt TJ, Goldsby RA, Osborne BA. 2007. *Kuby Immunology*, 6th ed. New York: WH Freeman and Company.
- Knapp M, Hofreiter M. 2010. Next generation sequencing of ancient DNA: requirements, strategies and perspectives. *Genes* **1**:227-243.
- Krieger N. 2001. Theories for social epidemiology in the 21st century: an ecosocial perspective. *Int J Epidemiol* **30**:668-677.
- Krieger N. 2008. Proximal, distal, and the politics of causation: what's level got to do with it? *Am J Public Health* **98**:221-230.
- Krieger N. 2011. *Epidemiology and the People's Health: Theory and Context*. Oxford: Oxford University Press.
- Krinzinger F. 1986. Velia. Grabungsbericht 1983-1986. *J Romische Historische Mitteilungen* **28**: 31-56.
- Kwiatkowski D, Nowak M. 1991. Periodic and chaotic host-parasite interactions in human malaria. *Proc Nat Acad Sci USA* **88**:5111-3.
- Kwiatkowski DP. 2005. How malaria has affected the human genome and what human genetics can teach us about malaria. *Am J Hum Genet* **77**:171-92.
- Lalremruata A, Ball M, Bianucci R, Welte B, Nerlich AG, Kun JF, Pusch CM. (2013). Molecular identification of falciparum malaria and human tuberculosis co-infections in mummies from the Fayum depression (Lower Egypt). *PLoS ONE* **8**:e60307.
- Laurence R. 1999. *The Roads of Roman Italy: Mobility and Cultural Change*. London: Routledge.
- Lewis ME. 2012. Thalassemia: its diagnosis and interpretation in past skeletal populations. *Int J Osteoarchaeol* **22**:685-693.
- Loaiza JR, Bermingham E, Sanjur OI, Scott ME, Bickersmith SA, Conn JE. 2012. Review of genetic diversity in malaria vectors (Culicidae: Anophelinae). *Infect Genet Evol* **12**:1-12.
- Macchiarelli R, Salvadei L, Catalano P. 1998. Biocultural changes and continuity throughout the first millennium B.C. in central Italy: anthropological evidence and perspectives. *Riv di Anthropol* **66**(Suppl):249-272.

- Mackinnon MJ, Marsh K. 2010. The selection landscape of malaria parasites. *Science* **328**:866-71.
- Manguin S, Carnevale P, Mouchet J, Coosemans M, Julvez J, Richard-Lenoble D, Sircoulon J. 2008. *Biodiversity of malaria in the world*. France: John Libbey Eurotext.
- Mannucci V, Verduchi P. 1996. Il porto imperiale di Roma: le vicende storiche, in: V. Mannucci (Ed.), *Il Parco Archeologico Naturalistico del Porto di Traiano*, Gangemi Editore, Roma, 1996, pp. 15–28.
- Marciniak S, Prowse TL, Herring DA, Klunk J, Kuch M, Duggan AT, Bondioli L, Holmes EC, Poinar HN. 2016. *Plasmodium falciparum* malaria in 1st-2nd c. A.D. southern Italy. *In Press*, Current Biology.
- Mazzini I, Faranda C, Giardini M, Giraudi C, Sadori L. 2011. Late Holocene palaeoenvironmental evolution of the Roman harbour of Portus, Italy. *J Paleolimnol* **46**:243-256.
- Miller LH, Baruch DI, Marsh K, Doumbo OK. 2002. The pathogenic basis of malaria. *Nature* **415**:673-9.
- Miller RL, Ikram S, Armelagos GJ, Walker R, Harer WB, Shiff CJ, Baggett D, Carrigan M, Maret SM. 1994. Diagnosis of *Plasmodium falciparum* infections in mummies using the rapid manual ParaSight-F Test. *Trans R Soc Trop Med Hyg* **88**:31–32.
- Molak M, Ho SYW. 2011. Evaluating the impact of post-mortem damage in ancient DNA: a theoretical approach. *J Mol Evol* **73**:244-255.
- Moody A. 2002. Rapid diagnostic tests for malaria parasites. *Clin Microbiol Rev* **15**: 66-78.
- Morel JP. 1999. Hyele revue a la lumiere de Massalia. In: Krinzinger F, Tocco G, editors. *Neue Forschungen in Velia*. Vienna: Austrian Academy of Sciences Press. p 11–22.
- Morley N. 2013. Population size and social structure. In: Erdkamp P, editor. *The Cambridge Companion to Ancient Rome*. Cambridge: Cambridge University Press. p. 29-44.
- Nerlich AG, Schraut B, Dittrich S, Jelinek TH, Zink A. 2008. *Plasmodium falciparum* in Ancient Egypt. *Emerg Infect Dis* **14**:1317–8.

- Nutton V. 2004. *Ancient Medicine*. London: Routledge.
- O’Sullivan L, Jardine A, Cook A, Weinstein P. 2008. Deforestation, mosquitoes, and ancient Rome: lessons for today. *BioScience* **58**:756-760.
- Oerlemans A, Tacoma LE. 2014. Three great killers: infectious diseases and patterns of mortality in Imperial Rome. *Anc Soc* **44**:213-241.
- Oxenham MF, Cavill I. 2010. Porotic hyperostosis and cribra orbitalia: the erythropoietic response to iron-deficiency anaemia. *Anthropol. Sci.* **118**:199-200.
- Pääbo S, Poinar HN, Serre D, Jaenicke-Despres V, Heble, J, Rohland N, Kuch M, Krause J, Vigilant L, Hofrieter, M. 2004. Genetic analyses from ancient DNA. *Ann Rev Genet* **38**:645-679.
- Parise M, Bixio R, Quinto G, Savino G. 2000. Ricerche geologic-speleologiche in cavita artificiali: gli impianti idrici sotterranei di Gravina in Puglia. Atti Convegno GeoBen 2000, Torino 7-9: 739-747.
- Paroli L. 2005. The Basilica Portuense. In: Keay S, Millet M, Paroli L, Strutt K (Eds). *Portus. An Archaeological Survey of the Port of Imperial Rome*. London: British School at Rome Archaeological Monographs. p. 258-268.
- Pattanayak SK, Yasuoka J. 2008. Deforestation and malaria: revisiting the human ecology perspective. In: Colfer CJP, editor. *Human Health and Forests: A Global Overview of Issues, Practice and Policy*. United Kingdom: Earthscan. p. 197-220.
- Perandin FN, Manca G, Piccolo A, Calderaro L, Galati L, Ricci MC, Medici C, Dettori G, Chezzi C. 2004. Development of a real-time PCR assay for detection of *Plasmodium falciparum*, *Plasmodium vivax*, and *Plasmodium ovale* for routine clinical diagnosis. *J Clin Microbiol* **42**:1214–1219.
- Petriaggi R, Bonacci G, Corbonara A, Vittori MC, Vivarelli ML, Vori P. 1995. Scavi a Ponte Galeria: nuove acquisizioni sull’acquedoto di Porto e sulla topografia del territorio Portuense. *Arch Laz* **12**:361–373.
- Prowse T, Schwarcz HP, Saunders S, Macchiarelli R, Bondioli L. 2004. Isotopic paleodiet studies of skeletons from the Imperial Roman-age cemetery of Isola Sacra, Rome, Italy. *J Archaeol Sci* **31**:259-72.

- Prowse TL, Schwarcz HP, Saunders SR, Macchiarelli R, Bondioli L. 2005. Isotopic evidence for age-related variation in diet from Isola Sacra, Italy. *Am J Phys Anthropol* 128:2-13.
- Prowse TL, Schwarcz HP, Garnsey P, Knyf M, Macchiarelli R, Bondioli L. 2007. Isotopic evidence for age-related immigration to Imperial Rome. *Am J Phys Anthropol* 132:510–519.
- Prowse TL, Barta JL, von Hunnius TE, Small AM. 2010. Stable isotope and mtDNA evidence for geographic origins at the site of Vagnari, south Italy. In: Eckardt H, editor. *Roman Diasporas: Archaeological Approaches to Mobility and Diversity in the Roman Empire*. Journal of Roman Archaeology, Portsmouth, Supplement 78. p. 175-198.
- Prowse TL, Nause C, Ledger M. 2014. Growing up and growing old on an imperial estate: preliminary palaeopathological analysis of skeletal remains from Vagnari. In: Small AM, editor. *Beyond Vagnari: New Themes in the Study of Roman South Italy*. Italy: Edipuglia. p. 111-122.
- Prowse TL. 2016. Isotopes and mobility in the ancient Roman world. In: de Ligt L, Tacoma LE, eds. *Migration and Mobility in the Early Roman Empire*. Leiden: Brill. p. 205-233.
- Rabino Massa E, Cerutti N, Savoia AMD. 2000. Malaria in ancient Egypt: paleo-immunological investigations in predynastic mummified remains. *Chungara (Arica)* 32:7–9.
- Retief F, Cilliers L. 2004. Malaria in Graeco-Roman Times. *Acta Classica* 47:127-137.
- Riley EM, Wahl S, Perkins DJ, Schofield L. 2006. Regulating immunity to malaria. *Parasite Immunol* 28:35-49.
- Sacco G. 1984. *Iscrizioni Greche d'Italia: Porto*. Rome: Edizioni di Storia e Letteratura.
- Sacks D, Sher A. 2002. Evasion of innate immunity by parasitic protozoa. *Nat Immunol* 3:1041-1047.
- Sadori L, Giardini M, Giraudi C, Mazzini I. 2010. The plant landscape of the imperial harbour of Rome. *J Archaeol Sci* 37:3294-3305.
- Sallares R, Gomzi S. 2001. Biomolecular archaeology of malaria. *Anc Biomol* 3:195-213.

- Sallares R. 2002. *Malaria and Rome: A History of Malaria in Ancient Italy*. Oxford: Oxford University Press.
- Sallares R, Bouwman A, Anderung C. 2004. The spread of malaria to southern Europe in antiquity: new approaches to old problems. *Med Hist* **48**:311-328.
- Sallares R. 2006. Role of environmental changes in the spread of malaria in Europe during the Holocene. *Quat Int* **150**:21-27.
- Salomon F, Delile H, Goiran JP, Bravard JP, Keay S. 2012. The Canale di Comunicazione Traverso in Portus: the Roman sea harbour under river influence (Tiber delta, Italy). *Geomorphologie* 18: 75-90.
- Scheidel W. 2003. Germs for Rome. In: Edwards C, Woolf G, editors. *Rome the Cosmopolis*. Cambridge: Cambridge University Press. p. 158-176.
- Scheidel W. 2004. Demographic and economic development in the ancient Mediterranean world. *J Inst Theoretical Econ* **160**:743-757.
- Scheidel W. 2009. Disease and death in the ancient city of Rome. Stanford University: Princeton/Stanford Working Papers in Classics.
- Schofield L, Grau GE. 2005. Immunological processes in malaria pathogenesis. *Nat Rev Immunol* **5**:722-735.
- Scobie A. 1986. Slums, sanitation, and mortality in the Roman world. *Klio* **68**:399-433.
- Service MW, Townson H. 2002. The Anopheles vector. In: Warrell DA, Gilles HM, editors. *Essential Malariology*, 4th edition. London: Arnold. p. 59-84.
- Shaw BD. 1996. Seasons of death: aspects of mortality in imperial Rome. *J Roman Studies* **94**:1-26.
- Sherman IW. 1998. *Malaria: parasite biology, pathogenesis, and protection*. Washington: ASM Press.
- Small AM, (editor). 2011. *Vagnari. The village, the industries the imperial property*. Italy: Edipuglia.
- Small AM, editor. 2014. *Beyond Vagnari: New Themes in the Study of Roman South Italy*. Italy: Edipuglia.

- Smith-Guzman NE. 2015a. The skeletal manifestation of malaria: An epidemiological approach using documented skeletal collections. *Am J Phys Anthropol* **158**:624-635.
- Smith-Guzman NE. 2015b. Cribra orbitalia in the ancient Nile Valley and its connection to malaria. *Int J Paleopathol* **10**:1-12.
- Snow RW, Omumbo JA. 2006. Malaria. In: Jamison DT, Feachem RG, Makgoba MW, Bos ER, Baingana FK, Hofman KJ, Rogo KO, editors. *Disease and Mortality in Sub-Saharan Africa*. Washington: The International Bank for Reconstruction and Development. p. 195-214.
- Snowden F. 2008. *The conquest of malaria: Italy, 1900-1962*. Yale University Press.
- Soren D, Soren N. 1999. *A Roman Villa and a Late Roman Infant Cemetery: Excavation at Poggio Gramignano, Lugnano in Teverina*. Rome: L'Erma di Bretschneider.
- Sperduti, A. 1995. I resti scheletrici umani della necropoli di età romano imperiale di Isola Sacra (i-iii sec. d. C.): analisi paleodemografica. PhD dissertation.
- Sperduti A, Bondioli L, Garnsey P. 2012. Skeletal evidence for occupational structure at the coastal towns of Portus and Velia (1st-3rd c. AD). In: Schrufer-Kolb I, editor. *More Than Just Numbers? The Role of Science in Roman Archaeology*. Portsmouth: Journal of Roman Archaeol (Suppl 91). p.53-70.
- Stuart-Macadam P. 1991. Anaemia in Roman Britain: Poundbury Camp. In: Bush H, Zvelebil M, editors. *Health in Past Societies. Biocultural Interpretations of Human Skeletal Remains in Archaeological Contexts*. Oxford: British Archaeological Reports. p. 101-113.
- Stuart-Macadam P. 1992. Porotic hyperostosis: a new perspective. *Am J Phys Anthropol* **87**:39-47.
- Sutherst RW. 2004. Global change and human vulnerability to vector-borne diseases. *Clin Microbiol Rev* **17**:136-173.
- Taylor GM, Rutland P, Molleson T. 1997. A sensitive polymerase chain reaction method for the detection of *Plasmodium* species DNA in ancient human remains. *Anc Biomol* **1**:193-203.

- Trape JF, Lefebvre-Zante E, Legros F, Ndiaye G, Bouganali H, Druilhe P, Salem G. 1992. Vector density gradients and the epidemiology of urban malaria in Dakar, Senegal. *Am J Trop Med Hyg* **47**:181-189.
- Wagner DM, Klunk J, Harbeck M, Devault A, Waglechner N, Sahl JW, Enk J, Birdsell DN, Kuch M, Lumibao C, Poinar D, Pearson T, Fourment M, Golding B, Riehm JM, Earn DJ, DeWitte S, Rouillard JM, Grupe G, Wiechmann I, Bliska JB, Keim PS, Scholz HC, Holmes EC, Poinar H. 2014. *Yersinia pestis* and the plague of Justinian 541-543 AD: a genomic analysis. *Lancet Infect Dis* **14**:319-326.
- Walker PL, Bathurst RR, Richman R, Gjerdrum T, Andrushko VA. 2009. The causes of porotic hyperostosis and cribra orbitalia: A reappraisal of the iron-deficiency-anemia hypothesis. *Am J Phys Anthropol* **139**:109-125.
- White BJ, Collins FH, Besansky NJ. 2011. Evolution of *Anopheles gambiae* in relation to humans and malaria. *Ann Rev Ecol Evol Syst* **42**: 111-132.
- Wilkinson RJ, Brown JL, Pasvol G, Chiodini PL, Davidson RN. 1994. Severe falciparum malaria: predicting the effect of exchange transfusion. *Q J Med* **87**:553-557.
- Wood JW, Milner GR, Harpending HC, Weiss KM. 1992. The osteological paradox: problems of inferring prehistoric health from skeletal samples. *Curr Anthropol* **33**:343-370.
- Wright LE, Yoder CJ. 2003. Recent progress in bioarchaeology: approaches to the osteological paradox. *J Archaeol Res* **11**:43-70.
- Yasuoka J, Levins R. 2007. Impact of deforestation and agricultural development on Anopheline ecology and malaria epidemiology. *Am J Trop Med Hyg* **76**:450-460.
- Zink A, Haas CJ, Herberth K, Nerlich AG. 2001. PCR amplification of Plasmodium DNA in ancient human remains. *Anc Biomol* **3**:293.

**CHAPTER 4: PARALLEL HYBRIDIZATION CAPTURE OF MULTIPLE
PATHOGENS IN ARCHAEOLOGICAL SAMPLES: TOWARDS
INTEGRATED PALEOPATHOLOGICAL INVESTIGATIONS**

By: Stephanie Marciniak¹, Ana T. Duggan¹, Shea Gardner², Crystal Jaing²,
Jonathan Allen², Kevin McLoughlin², Monica Borucki², Tracy L. Prowse⁴,
Hendrik N. Poinar^{1,3}

¹McMaster Ancient DNA Centre, Department of Anthropology, McMaster
University, Hamilton, ON, L8S 4L9, Canada

²Lawrence Livermore National Laboratory, Livermore, CA

³Michael G. DeGroote Institute for Infectious Disease Research, McMaster
University

⁴ Department of Anthropology, McMaster University, Hamilton, ON, L8S 4L9,
Canada

Abstract

The molecular investigation of disease in ancient human remains is complicated by the lack of exclusive evidence (e.g., skeletal, historical, or archaeological) that connects a burial assemblage to a given pathogen. In such scenarios, it is critical to effectively prioritize pathogens that are contextually relevant, as disease is a multi-faceted process, influenced by interactions with other pathogens, as well as ecological and anthropogenic modifiers. Here we report results of an in-solution RNA bait set designed to detect 1,152 human pathogenic species using hybridization capture combined with high-throughput sequencing. Previously verified bacterial pathogens in archaeological samples (e.g., *Yersinia pestis* and *Staphylococcus saprophyticus*) were successfully confirmed with our parallel pathogen capture technique. In addition, samples of unknown pathogenic constituents were evaluated (e.g., from Imperial period Italy, medieval Europe, and North America) and demonstrate the versatility of this technique in characterizing the minute pathogen fraction to the exclusion of non-target DNA. The stringency of bait design, capture protocol efficiency, and algorithmic assessment of sequence reads leads to few false positive and false negative outcomes. Further work on recovering low abundance pathogenic taxa within dynamic ancient DNA extracts is crucial to paleopathological applications focused on the complexity of synergistic disease interactions in diverse archaeological contexts.

Introduction

Paleopathological approaches of examining health in the past are at the crossroads of skeletal manifestations of physiological stress and the experience of disease in a given context (as influenced by ecology and the biocultural environment). As such, the challenges of investigating disease are outcomes of the archaeological record, in particular, poor preservation of skeletal remains, sample representativeness (i.e., biases in survival or mortuary practices) and small sample sizes (see Jackes, 2011; Ortner, 1992, 2009; Saunders, Herring & Boyce, 1995; Waldron, 1994). However, the most confounding factor is that not all diseases will manifest skeletally, as the disease process is multi-causal (i.e., not a relationship of a singular pathogen to a singular disease; Dutour, 2013), and individuals are heterogeneous in their susceptibility to infectious agents (underlying the “Osteological Paradox” and the challenges of inferring “health” from dead individuals; see DeWitte & Stojanowski, 2015; Wood et al., 1992; Wright & Yoder, 2003).

This impacts integrated ancient DNA and anthropological approaches of exploring disease-associated pathogens as it is rare to have exclusive evidence (e.g., skeletal, historical or archaeological) that links a specific disease to a given burial assemblage. For example, skeletal evidence of infectious diseases can be diagnostic in the case of leprosy (e.g., *facies leprosa*; Andersen & Manchester, 1992) or tuberculosis (e.g., thoracic kyphosis; Ortner, 2003), yet there is a scope of responses ranging from non-specific or even absent due to individual variation

in vulnerability and immune response to infectious agents. This requires exercising caution when interpreting visible skeletal lesions, whether due to chronic exposure (e.g., specific lesions associated with tuberculosis or non-specific lesions due to physiological stressors) or even the absence of skeletal lesions (spontaneous recovery or acute mortality) (DeWitte & Stojanowski, 2015; Roberts & Manchester, 2005; Wood et al., 1992). With respect to the non-specificity of skeletal lesions, it is difficult to associate skeletal evidence to a specific pathological process, particularly when considering the inability to differentiate between risk of exposure (susceptibility) and individual (physiological) responses in the manifestation of associated lesions (Ortner, 2011).

Similarly, using other evidentiary sources to assess the presence of potential pathogens, such as the historical record (e.g., textual sources) or archaeological evidence, provide varied perspectives on contextually relevant disease-associated pathogens. Evidence of catastrophic events (i.e., epidemics or pandemics) as noted in surviving literary records are rare in terms of providing candidate pathogens to evaluate in a given context. For example, Galen's documentation of the Antonine Plague (Bruun, 2003; Duncan-Jones, 1996; Littman & Littman, 1973), although not providing a clear causative agent, does provide potential candidates (e.g., smallpox, measles, epidemic typhus, noted in Cunha & Cunha, 2008) to explore within an integrated framework. This level of information, however, is relatively uncommon. A common scenario is that burial

assemblages are not often connected to catastrophic events and historical sources do not provide a consensus about diseases present at the time. In shifting from focusing on a singular causative pathogen in a given context that is presumably connected to catastrophic events, it is also critical to investigate everyday morbidity and mortality that is characteristic of a dynamic pathogen pool in contributing to the biosocial context of disease. It is at this point where ancient DNA is an ideal methodological complement to address these challenges of identifying pathogens of interest from diverse archaeological contexts.

Our study focuses on the evaluation of a capture strategy that targets low abundant pathogens in parallel in a single archaeological sample, since it is critical to recover only the desired pathogen fraction from complex ancient DNA extracts in order to prioritize candidates for downstream analyses and create comprehensive pathogen profiles of the constituents. The primary purpose of the pathogen capture bait set is to provide researchers with a quantitative and qualitative assessment of candidate pathogens likely present in the sample in order to determine the feasibility of following-up with specific pathogen hybridization capture. The second application of the bait set is to identify the presence or absence of key pathogens at various times and places (e.g., prior to, during or after pandemics) to further elucidate the dynamic picture of co-infection and host-pathogen evolution over time.

Pathogen detection strategies

In integrating ancient DNA in the detection of pathogens, it is critical to note that ancient DNA comes with its own challenges. Ancient DNA exhibits signatures of molecular and chemical degradation alongside idiosyncratic preservation (both within and between specimens), resulting in an abundance of short fragments (e.g., 30-60 bp) with characteristic damage signals (C>T and G>A transitions on the 5' and 3' ends, respectively) (see reviews by Hofreiter et al., 2015; Molak & Ho, 2011; Orlando, Gilbert, & Willerslev, 2015). The exogenous burial environment (e.g., geochemistry of soil, pH, temperature, manner of burial) and endogenous specimen-specific factors (e.g., rate of post-mortem decay, DNA survivability and recoverability post-mortem), create a dynamic context of DNA “preservation”. The resultant damaged DNA molecules are subsequently a mixture of environmental (e.g., macro-organisms, such as plants or fungi), modern contaminant (e.g., post-excavation specimen handling), and non-target molecules with a typically low endogenous component (i.e., 0-5%) (Burbano et al., 2010; Carpenter et al., 2013; Pääbo et al., 2004). Ancient pathogen DNA is essentially embedded in this complex molecular pool, which poses a significant challenge to resolving historical pathogen presence.

In archaeological contexts where there is conflicting or an absence of information regarding presumed pathogen presence, previous molecular approaches relied on metagenomic (“shotgun”) sequencing (no selection of genomic targets such as loci, genes, or genomes) as a means to prioritize potential

candidates to further pursue (i.e., via hybridization capture or the sequestration of known DNA targets with probes or “baits”). A related strength with a shotgun metagenomic approach is that since the expression of disease is multifaceted (e.g., heterogeneity of risk within a dynamic epidemiological environment), the capability of sequencing the entire (individual) microbial content circumvents issues surrounding the use of skeletal lesions to prioritize specimens. Shotgun sequencing demonstrates significant successes in ancient DNA research, such as a 6.5-fold coverage of a *Brucella melitensis* genome from a medieval specimen by Kay et al. (2014). The approach is relatively unbiased in comparison to hybridization capture which requires a presumed (singular) pathogen to target, and depending on the sequence depth, is able to resolve the distribution and abundance of the microbial DNA content of a sample (Devault et al., 2014a; Warinner et al., 2015; Whatmore, 2014).

The limitations of shotgun metagenomics are connected to the inherent properties of ancient DNA itself as part of the paleopathological toolkit. A caveat is that low abundant human pathogens are often undetectable within these substantial metagenomic datasets due to the overabundance of the exogenous components (environmental, contaminant, and non-target molecules), where for example, *Yersinia pestis* sequence reads were approximately 0.08% of metagenomic data set in Devault et al. (2014a) while *Plasmodium* spp. reads were 0.006% of taxonomically identifiable constituents indicated in Marciniak et al. (2016). Currently, it is cost-prohibitive to deeply sequence samples for diagnostic

pathogen identification (defined as greater than 30X for meaningful genome coverage). When there is no knowledge of a presumed disease and considering the pathogen fraction is often less than 1% of the entire molecular constituents, this creates a significant methodological obstacle. The inability to fully exploit metagenomic profiles for pathogen prioritization or subsequent identification necessitates the use of hybridization capture techniques capable of detecting multiple pathogens in parallel.

Hybridization capture strategies are successful in the identification of historically significant ancient pathogens such as *Yersinia pestis* associated with the 14th c. A.D. Black Death (e.g., Bos et al., 2011; Schuenemann et al., 2011) or the Plague of Justinian (541-543 A.D.) (Wagner et al., 2014), and medieval *Mycobacterium leprae* (10th-14th c. A.D.) (Schuenemann et al., 2013), but this approach requires a presumed pathogen in order to be applied. The goal of capture strategies focused on ancient DNA recovery is to maximize *sensitivity* (i.e., diversity/complexity of target molecules recovered) at the cost of *specificity* (i.e., on-target sequence reads) in order to capture as many unique molecules of the rare target as possible, since the target molecules will be degraded, and at a lower frequency than the overall non-target constituents, which leads to fewer chances for a specific bait to encounter its target (Enk, 2016). With this strategy, the caveat is that “*you only find what you’re looking for*”, which is a complicating factor when assessing pathogen presence in uncharacterized skeletal assemblages. With the growing emphasis on synergistic interactions and the interplay between

multiple co-existing pathogens as part of the disease burden, the ability to detect a suite of human pathogens in a single ancient DNA extract is important to explore this landscape of disease.

Recently, parallel pathogen detection is emerging as a way forward to screen and prioritize pathogens from inherently complex archaeological samples (e.g., Bos et al., 2015; Devault et al., 2014a). For example, Devault et al. (2014a) compared metagenomic detection of known pathogens with the Lawrence Livermore Microbial Detection Array or LLMDA (fluorescence-based) for *Vibrio cholerae* (19th c. A.D., Philadelphia epidemic) and *Yersinia pestis* (14th c. A.D., Black Death), ultimately demonstrating parallel microbial detection as an effective approach to screen and construct microbial profiles for archaeological samples. Similarly, Bos et al. (2015) utilized solid platform hybridization capture for the detection of 92 pathogens in parallel, with success in capturing known *Mycobacterium leprae* sequences in a medieval specimen while limiting exogenous (background) capture. In pursuing parallel pathogen detection as part of the historical reconstruction of disease(s) in the past, it grounds the concept of pathocenosis (Grmek, 1969) in a given spatiotemporal context. The concept of pathocenosis involves considering the diseases of a given population in its entirety, as different diseases differentially contribute to morbidity and mortality, which speaks to synergistic pathogen interactions in a specific historical geographical context (Faure, 2014; Grmek, 1969, 1991; Ortner, 2011). The frequency and distribution of each disease in a given biocultural environment

depends on pathogen specific factors (infectivity, virulence, mode of transmission), ecological factors (climate, land use patterns) and pathogen-pathogen interactions (frequency and distribution of all other diseases) (Faure, 2014; Grmek, 1969, 1991). Even with targeting single pathogens (i.e., *Y. pestis*, *M. leprae*), each pathogen is embedded in a dynamic biosocial context and by integrating the detection of multiple pathogens at once, the aims of bioarchaeological research may be further integrated in molecular explorations of such pathogen interactions.

Pathogen capture overview

The basis for the pathogen capture baits evaluated in this research is drawn from the LLMDA, which contains probes from the genes, genomes, and plasmid sequences of all bacteria, viruses, protozoa, and fungi from various databanks (e.g., National Center for Biotechnology Information GenBank, LLNL microbial database) (Gardner et al., 2010; McLoughlin et al., 2011). The selection of regions was based on taxonomic relationships identified in the genomic databases where compatibility among the probe sequences (e.g., avoiding cross-hybridization) was evaluated with melt temperature, self-complementarity, and entropy (Gardner et al., 2010). To confirm the sequences were conserved among the Family and unique relative to other Families, each was screened via BLAST (Basic Local Alignment Search Tool), which compares the similarity of a given sequence to all others in the NCBI databases (Gardner et al., 2010). The selection of probes proceeded via two strategies: 1) “*Discovery*” probes that are taxonomically unique

within a Family, but are also shared among species within that Family (assists in detecting novel variants) and represent a conservative measure; and 2) “*Detection*” or “*census*” probes that represent highly variable regions for the precise characterization of species or strains (Gardner et al., 2010; McLoughlin et al., 2011).

Essentially, the probes target conserved and unique regions among all currently known and sequenced Family, Genus, Species and strains of human pathogens, whereby the unique combinations of the probes enable species-level identification based on the distribution of probe matches across the sequence reads. In order to facilitate accurate and stringent identification of the reads, a likelihood maximization algorithm (Composite Likelihood Maximization or CLiMax) compares the sequence reads to the LLNL microbial genomic databases, evaluating the expected (total number of probes for a given target) versus detected hits (number of reads from the sample that match the known probes) and characterizes the likelihood of target presence (McLoughlin et al., 2011).

It is a hierarchical identification process to predict the series of targets represented by the specific sample, where the level of similarity determines the “best fit” at the particular taxonomic level (e.g., Family, Genus, Species, strain). With this high stringency approach, the ability to target the human pathogens in parallel without the “noise” from exogenous non-target DNA enhances the prioritization of disease-associated pathogens. One drawback, however, is that pathogen detection is limited to the diversity and abundance of taxa available in

the genomic databases, which also includes related non-pathogens (e.g., opportunistic or microbiome constituents).

In order to test the specificity and sensitivity of our pathogen capture technique, previously verified bacterial pathogen samples (“knowns”) were included alongside a range of samples that were not previously characterized via shotgun or capture (“unknowns”) to further demonstrate the versatility of this capture approach. The “known” specimens included: 1) a tooth from a 1348 A.D. Black Death plague victim (specimen 8291) associated with *Yersinia pestis* (Bos et al., 2011; Devault et al., 2014a); 2) a tooth from a Plague of Justinian victim (541-543 A.D.) (Wagner et al., 2014) associated with a terminal strain of *Yersinia pestis*; 3) a tissue sample from a 19th c. A.D. victim of the cholera epidemic in Philadelphia (*Vibrio cholerae*) (Devault et al., 2014b); and 4) a calcified nodule from Troy (Bronze Age to 13th c. A.D., Turkey) associated with *Staphylococcus saprophyticus* (Devault et al., n.d.). These samples were previously evaluated with high-throughput shotgun sequencing, which was available for the pathogen capture analysis. The “unknown” samples spanned from Imperial Italy (1st-4th c. A.D.), Newfoundland (5,000-4,000 B.C., Canada), and medieval Italy (16th c. A.D.). Sediments from late-medieval Greece and Italy were also included as a means to demonstrate the specificity of the pathogen baits to human-only pathogens (e.g., avoiding environmental contaminants). Our study assessed whether multiple pathogen detection was specific and sensitive in: 1) confirming the primary pathogenic agent for the positive pathogen samples; 2) enabling

prioritization of potential pathogens for further downstream analyses (i.e., hybridization capture); and 3) limiting exogenous (non-target) DNA signals in the detection of the minute pathogen fraction. The goal of integrating this molecular approach is to enhance the complementarity of disparate evidentiary sources (e.g., literary records, skeletal data, and archaeological evidence) to ground the molecular pathogen data in a historical-geographical space.

Methods

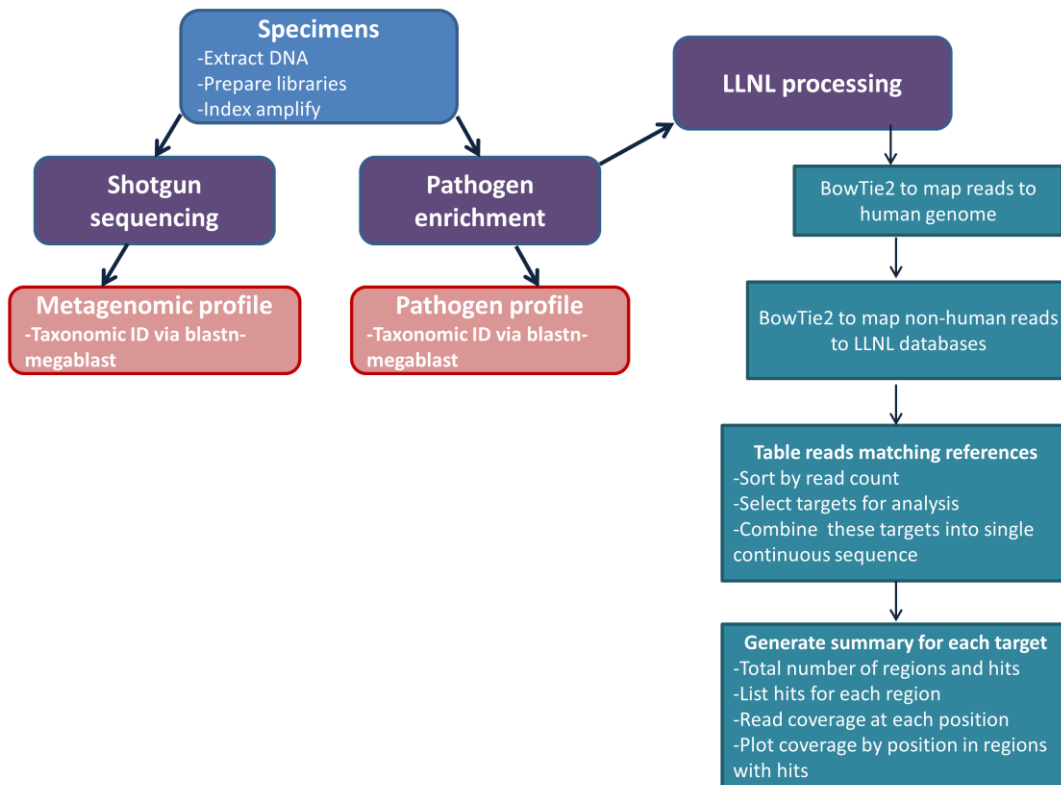
The specimens were sub-sampled, with DNA extracted and converted into libraries specific for Illumina sequencing as described for: Black Death specimen 8291 (Bos et al., 2011; Devault et al., 2014a), Plague of Justinian (Wagner et al., 2014), 19th c. cholera (Devault et al., 2014b), and the calcified nodule from Troy along with the sediments (Devault et al., n.d.). For the remaining samples (Maritime Archaic, Imperial Italian adults and juveniles), sub-sampling, DNA extraction and library conversion were performed as described in Marciniak et al. (2016). Accordingly, existing libraries were used where possible for the known samples, while extracts from the unknown samples were converted into double-stranded libraries followed by indexing amplification (using protocols described in Kircher et al., 2012, and Meyer & Kircher, 2010, with modifications). Refer to the Supplementary Appendix for additional methodological details.

In-solution pathogen capture was performed according to the manufacturer's protocol (MYcroarray, Ann Arbor, MI) for two rounds with modifications for maximizing sensitivity to ensure high target complexity in

capture (e.g., 55°C hybridization temperature, 16-24h hybridization capture, bait concentration from 50-100 ng) (Enk, 2016). The pathogen-enriched libraries were sequenced and bioinformatically processed in two ways: 1) reads were trimmed, merged, and mapped to the pathogen baits reference; and 2) reads were processed but not mapped in order to apply the CLiMax algorithm. Shotgun sequence data was previously available for the known pathogen samples, and was also generated as part of this project, processed alongside the pathogen-enriched libraries via blastn-megablast (Altschul et al., 1990) and parsed with MEGAN (MEtaGenome ANalyzer; Huson et al., 2007) to taxonomically identify the microbial constituents.

A brief overview of the LLNL analysis is as follows: the iterative process of the CLiMax algorithm searches for matches from the pathogen enriched data sets against the context database (i.e., LLNL microbial database), with the hits filtered by Bowtie2 (Langmead & Salzberg, 2012), and subsequent matching of the hits to the sequence Family, Genus, and Species annotations. A log-likelihood score is constructed for each reference genome that has hits, that reflects the mean coverage of each region that is expected to be enriched, the number of enriched regions in the genome that have hits, and the distribution of hits within each region. Refer to Figure 1 for the analysis workflow and the Supplementary Appendix for detailed methods.

Figure 1. Workflow summary.



Results

Our experiments showed the in-solution parallel pathogen capture technique was successful in enriching the pathogen DNA fraction from both the known and unknown samples (Tables 1, 2, and 3). For the known pathogen samples, after enrichment with the pathogen baits, 1-519 reads (2-81%) were alignable to their respective reference (Figure 2 and Table 2), versus the pre-capture alignable reads of 0-50% (Table 1). In previous work on the known samples, the percent of pre-capture reads alignable to the primary targets were: 0.09% (*Y. pestis*, the Plague of Justinian in Wagner et al., 2014), 0.08% (*Y. pestis*, Black Death in Devault et al., 2014a), 0.03% (*V. cholerae* in Devault et al.,

2014a) and 50% (*S. saprophyticus*, Troy nodule in Devault et al., n.d.). For the shotgun sequencing performed to evaluate the pathogen capture strategy, discrepancies in the metagenomic identification of the primary targets for *Y. pestis* associated with the Plague of Justinian (Wagner et al., 2014) and *V. cholerae* associated with the 19th c. A.D. epidemic in Philadelphia (Devault et al., 2014b), were attributed to the differences in sequence depth (as well as stochastic variation of sequencing or library re-amplification). For the unknown samples, a range of reads were alignable to the pathogen baits reference post-capture (Figure 3 and Table 3). The low background in the experiment controls (reagent blanks and sediments) suggested that the capture protocol and specificity of the pathogen probes yields a low number of false-positives (Figure 4, as well as Tables 2 and 3). Despite the power of this capture approach, a caution is that the comprehensiveness of a specimen's pathogen (or microbial) profile depends on characteristics of the ancient DNA extract and sample itself (e.g., amount of endogenous DNA, inhibition, DNA loss throughout processing or the type of sample used). See Table S1 in the Supplementary Appendix for the Family-level probe calls for the entire data set.

Figure 2. Number of reads taxonomically identified to respective primary targets for "known" samples (after mapping to pathogen baits).

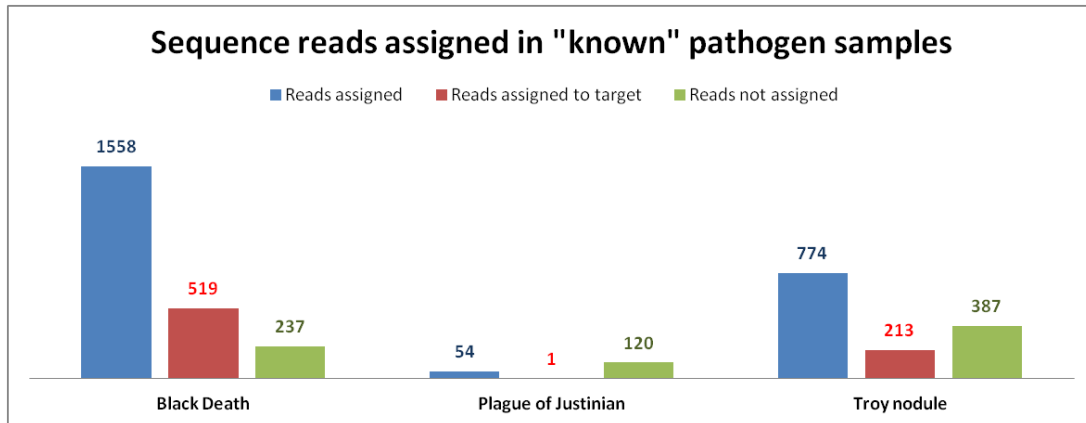


Figure 3. Number of reads taxonomically identified for "unknown" samples (after mapping to pathogen baits).

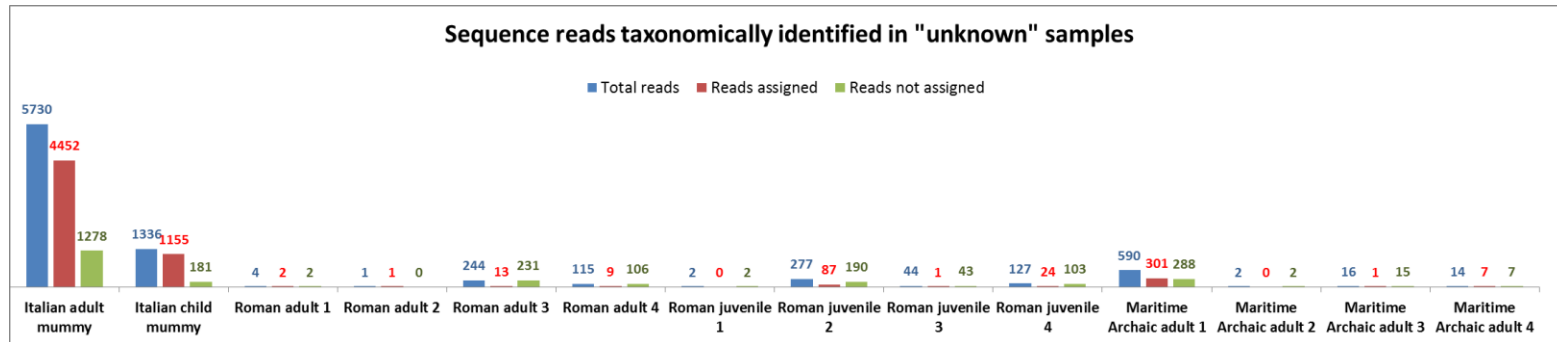


Figure 4. Number of reads taxonomically identified for reagent controls and sediment samples (after mapping to pathogen baits).

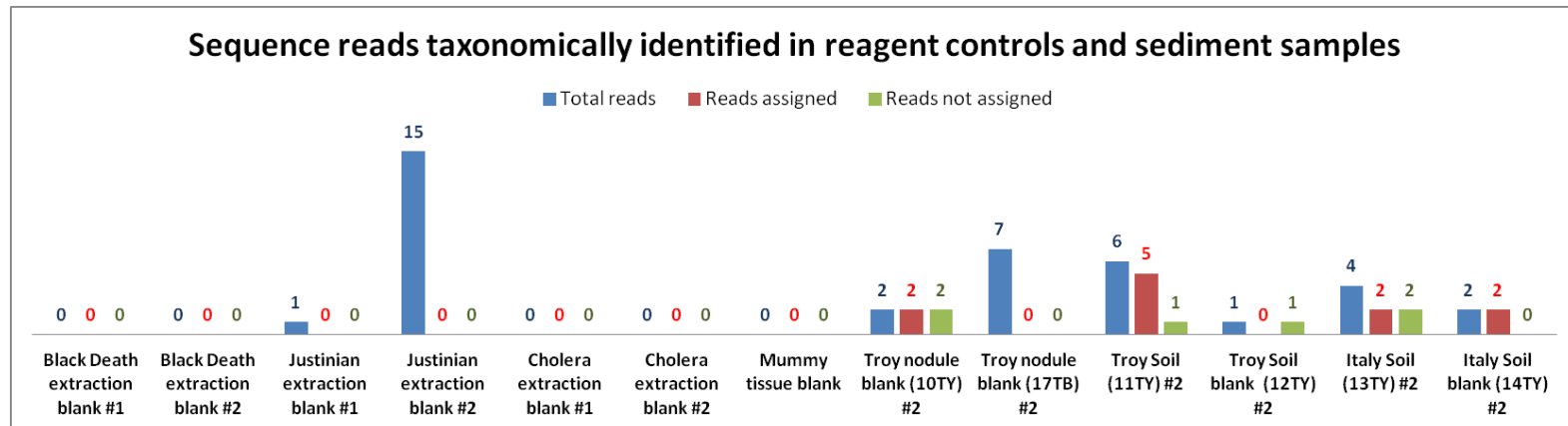


Table 1. Pre-capture shotgun data for primary pathogen constituents.

Library ID	Pre-capture shotgun				
	<i>Total reads (processed)</i>	<i>Total assigned (MEGAN)</i>	<i># reads taxonomically identifiable to known target</i>	<i>% taxonomically identifiable to known target</i>	<i>% taxonomically identifiable to known target from previous data</i>
Black Death	1,096,353	160,624	151	0.094	0.08% (Devault et al., 2014a)
Plague of Justinian	1,217,835	72,518	0	0	0.09% (Wagner et al., 2014)
Cholera	1,456,591	202,834	0	0	0.03% (Devault et al., 2014a)
Troy nodule	21,765,064	5,031,654	2,110,081	41.94	50.0% (Devault et al., n.d.)

Table 2. Post-capture summary for “known” samples.

Library ID	Post-capture (MEGAN for taxonomic ID mapped to pathogen baits)						
	# raw (unprocessed) reads	Total reads (processed)	Total mapped	Total mapped (24bp, MQ 20)	% on-target	# reads taxonomically identifiable to known target	% taxonomically identifiable to primary pathogen
Black Death #1 (P06BD)	2,156,924	212,412	282	103	0.048	32	35.96
Black Death extraction blank (P07BD) #1	67,638	0	0	0	0	0	N/A
Black Death #2 (P07BD)	2,131,039	62,374	3,620	1,795	2.878	519	33.31
Justinian #1 (P01JT)	2,385,398	5,881	248	16	0.272	1	33.33
Justinian extraction blank (P02JT) #1	17,894	48	2	1	2.083	0	N/A
Justinian (P01JT) #2	2,378,229	43,862	2,074	174	0.397	1	1.85
Justinian extraction blank (P02JT) #2	22,502	7,623	46	15	0.197	0	N/A
Cholera (P08CH) #1	104	3	0	0	0.000	0	0
Cholera extraction blank (P09CH) #1	60,458	396	18	16	4.040	0	N/A
Cholera (P18CH) #2	14	5	0	0	0.000	0	0
Cholera (P19CH) #2	14	3	0	0	0.000	0	0
Cholera (P20CH) #2	5,685	1,972	35	0	0.000	0	0
Cholera (P21CH) #2	237	87	2	0	0.000	0	0
Cholera extraction blank (P22CH) #2	1,140	401	0	0	0.000	0	N/A
Troy nodule (P09TY) #2	1,178,436	30,366	2,390	2,306	7.594	241	11.03
Troy nodule blank (P10TY) #2	12,848	4,244	322	2	0.047	0	N/A
Troy nodule (15TB) #2	2,546,489	160,058	2,686	1,968	1.230	287	17.05
Troy nodule (16TB) #2	6,458,859	238,618	2,143	1,161	0.487	213	27.52
Troy nodule extraction blank (17TB) #2	44,402	15,623	171	7	0.045	0	N/A

Table 3. Post-capture summary for “unknown” samples.

Library ID	Post-capture (MEGAN for taxonomic ID mapped to pathogen baits)						
	<i># raw (unprocessed) reads</i>	<i>Total reads (processed)</i>	<i>Total mapped</i>	<i>Total mapped (24bp, MQ 20)</i>	<i>% on-target</i>	<i># reads taxonomically identifiable</i>	<i>% taxonomically identifiable</i>
Mummy - child (P03MM) #1	1,845,984	140	18	18	12.857	18	100
Mummy - child (P03MM) #2	1,625,926	49,556	238	45	0.091	24	53.33
Mummy - child (P04MM) #2	3,981,932	143,160	1,878	1,336	0.933	1,155	86.45
Mummy - adult (P05MM) #2	3,055,843	78,024	1,493	514	0.659	387	75.29
Mummy - adult (P06MM) #2	3,686,358	77,142	6,143	5,730	7.428	4,452	77.70
Mummy tissue extraction blank (P05MM)	560	85	0	0	0	0	0
Roman adult (P16RM) #1	311,562	461	17	4	0.868	2	50
Roman adult (P17RM) #1	1,615,528	365	2	1	0.274	1	100
Roman adult (P23RM) #2	5,491,909	107,106	4,281	244	0.228	13	5.33
Roman adult (P24RM) #2	2,354,687	36,040	865	115	0.319	9	7.83
Roman juvenile (P19JV) #1	2,363,782	1,680	119	1	0.060	0	0
Roman juvenile (P20JV) #1	2,275,146	282,930	11,695	277	0.098	87	31.41
Roman juvenile extraction blank (P21JV) #1	2,298	10	0	0	0.000	0	0

	<i># raw (unprocessed reads)</i>	<i>Total reads (processed)</i>	<i>Total mapped</i>	<i>Total mapped (24bp, MQ 20)</i>	<i>% on- target</i>	<i># reads taxonomically identifiable</i>	<i>% taxonomically identifiable</i>
Roman juvenile (P25JV) #2	286,307	3,636	1,630	44	1.210	1	2.27
Roman juvenile (P26JV) #2	1,751,529	23,946	3,956	127	0.530	24	18.90
Maritime Archaic (P22BT) #1	9,980,810	212,745	3,414	590	0.277	301	51.02
Maritime Archaic (P23BT) #1	10,939,776	3,301	57	2	0.061	0	0
Maritime Archaic extraction blank (P24BT) #1	1,632	13	0	0	0	0	0
Maritime Archaic (P27BT) #2	260,827	4,436	111	16	0.361	1	6.25
Maritime Archaic (P28BT) #2	1,228,219	60,626	94	14	0.023	7	50
Troy sediment (P11TY) #2	57,403	3,098	84	6	0.194	5	83.33
Troy sediment extraction blank (P12TY) #2	256	68	1	1	1.471	0	0
Italy sediment (P13TY) #2	666,075	59,192	634	4	0.007	2	50
Italy sediment extraction blank (P14TY) #2	14,870	672	30	2	0.298	2	100

Known pathogen samples

The number of reads mapping to the pathogen probes and the specific number of reads mapping to the primary target (post-capture) demonstrate the specificity and sensitivity of the capture baits. The established authenticity (i.e., fragment length distribution, damage profiles, phylogenetic placement) of the specimens used to evaluate the pathogen capture strategy is indicated in previous publications – Wagner et al. (2014), Devault et al. (2014a, 2014b, n.d.) and Bos et al. (2011). However, the cholera specimen under-performed in the capture, with no reads successfully identified (*V. cholerae* or otherwise), which is attributed to the sequence depth obtained for this sample (further explained in the Discussion section below). Broadly, the results confirm the primary target for each of the known samples to a degree that demonstrates the specificity of the pathogen baits to identify predominant microbial taxa, and sensitivity of detection (e.g., limited exogenous DNA). See Figure 5 for the post-capture comparisons of microbial taxa for the known samples.

Unknown pathogen samples

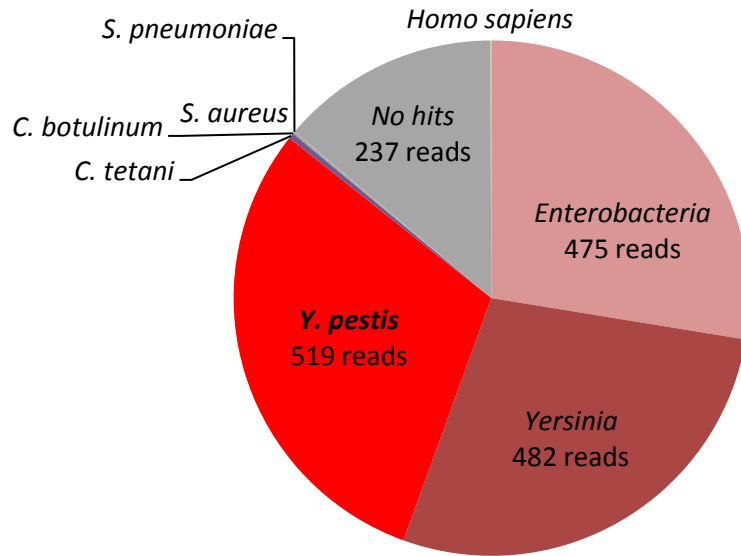
The versatility of parallel pathogen detection is successfully demonstrated in the unknown samples; however, a wide range of reads were taxonomically identifiable, in comparison to the known samples. The proportion of reads alignable to the pathogen probe regions varied from 0-86% (as indicated in Figure 3), but, even with as few as 31% of reads aligning, a microbial profile could still be rendered. For example, a Vagnari juvenile (P20JV) has 277 reads mapped to

the pathogen baits (Figure 6), but still provides potential microbial targets for further analyses. Of the 87 reads that are taxonomically identified, 10-14 reads are assigned to dental pathogens (e.g., *Tannerella forsythia*, *Porphyromonas gingivalis*) (which is not unexpected as this was a tooth sample) and 22 reads to the genus *Neisseria* (12 reads to *N. lactamica*). *N. lactamica* is typically associated with childhood infections and acquired immunity to meningococcal disease (*N. meningitidis*) (Cartwright et al., 1987; Gold et al., 1978), and presents an intriguing candidate for downstream analyses.

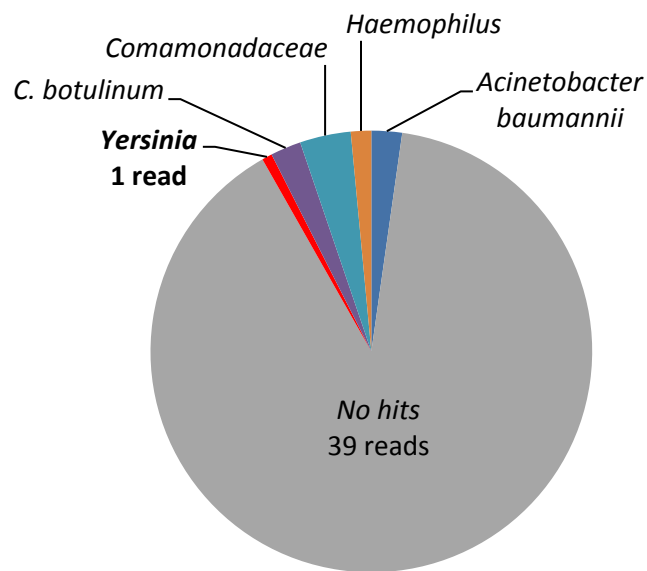
The strength of our parallel capture approach to prioritize pathogen targets is successfully indicated with the Italian child mummy specimen (16th c. A.D., Naples, Italy). A presumption of Hepatitis B virus (HBV) was paleopathologically informed by the presence of small lesions, as chronic infection may involve dermatological manifestations, such as a deep tissue rash that leads to the necrosis of small blood vessels (Kappus & Sterling, 2013). The metagenomic profile for the child mummy indicated an absence of taxonomically identifiable reads to HBV; however, 70% of the sequence reads were identifiable to HBV post-capture, which led to the reconstruction of an entire viral genome (Figure 7 for post-capture taxa identified).

Figure 5. Post-capture comparisons for primary pathogenic targets in the known samples. (a) Black Death (*Yersinia pestis*), (b) Plague of Justinian (*Yersinia pestis*), and (c) Troy nodule (*Staphylococcus saprophyticus*).

(a) Black Death (*Y. pestis*)



(b) Plague of Justinian (*Y. pestis*)



(c) Troy nodule (*S. saprophyticus*)

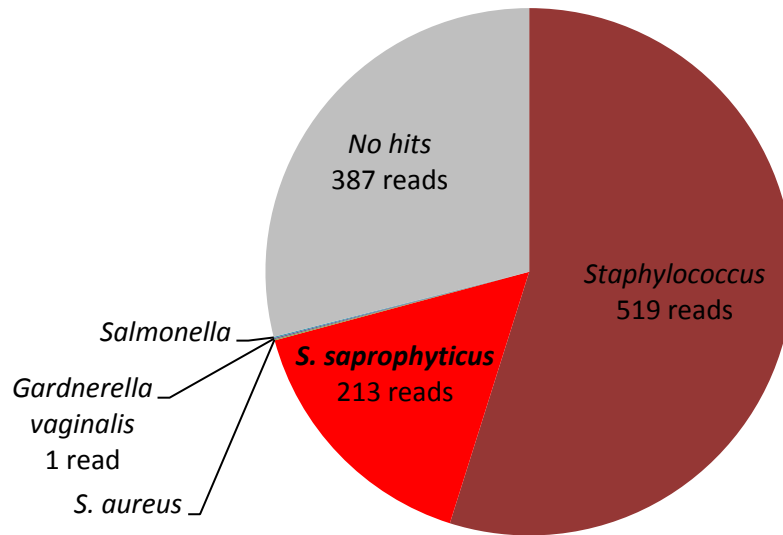


Figure 6. Microbial profile for Imperial Italian (Vagnari) juvenile (P20JV), 87 reads assigned

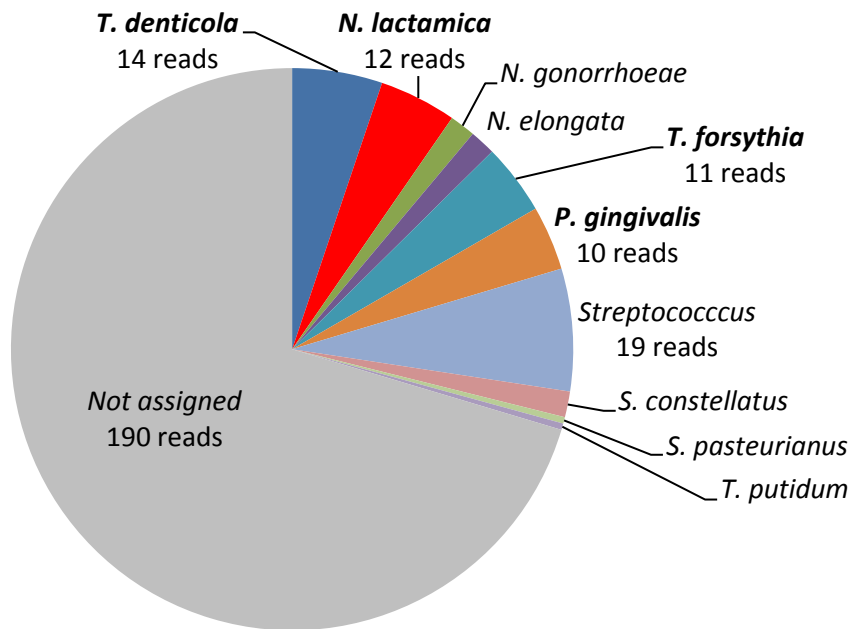


Figure 7. Post-capture microbial profile for the Italian child mummy

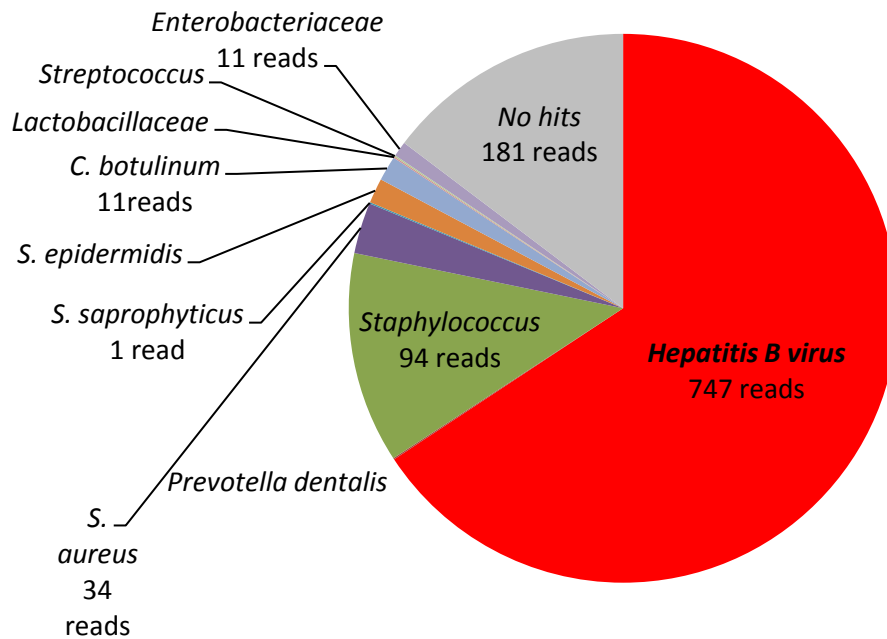
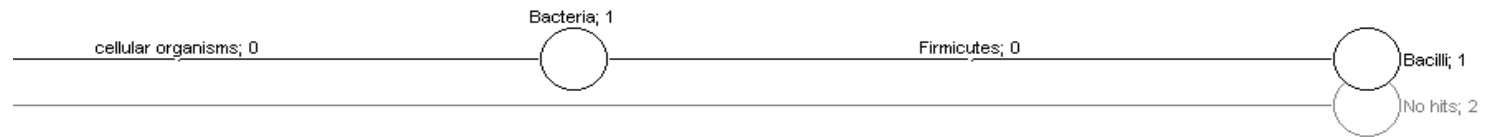
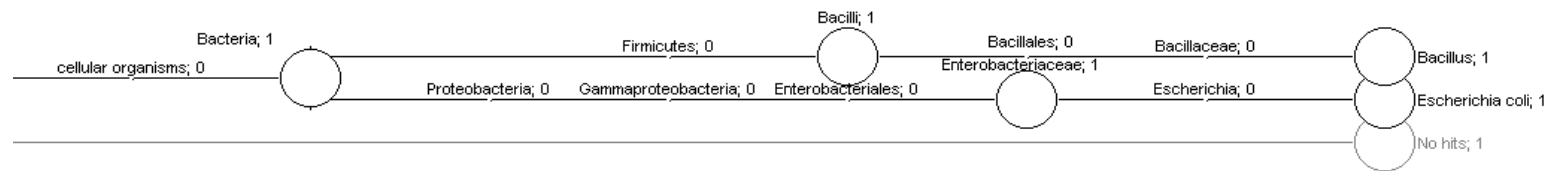


Figure 8. Post-capture comparison of sediments from (a) Italy, and (b) Greece (visualized in MEGAN; Huson et al., 2007).

(a) Italy



(b) Greece



Characterization of reagent controls and sediments

Post-capture, the reads alignable to the pathogen bait set ranged from 0 to 15 for the reagent controls, with alignments to Family-level taxa including *Comamonadaceae*, *Burkholderiaeeceae*, *Enterobacteriaceae*, *Papillomaviridae*, *Moraxellaceae*, and *Streptococcaceae*. However, there were no taxonomically identifiable reads in these data sets (except for the Troy nodule extraction blank, P10TY), meaning the sequence depth may not have been sufficient for detection, or the pathogen baits are highly specific. For the sediments, 1 to 6 reads mapped to the pathogen bait set, with predominant Family-level taxa as *Bacillaceae*, *Enterobacteriaceae*, and *Staphylococcaceae* with *Clostridiaceae* and *Enterobacteriaceae* characterizing the sediment extraction blanks (Tables 2 and 3, Figure 8); although most reads were not taxonomically identifiable upon blastn-megablast analysis (Altschul et al., 1990) and parsing with MEGAN (Huson et al., 2007). The ubiquity of commensal organisms that are within the environment but can become pathogenic in susceptible individuals were identified at low levels within the reagent controls and sediments (e.g., *Clostridiaceae*, *Enterobacteriaceae*, *Staphylococcaceae*). Despite this, the overall low genomic signals in the reagent controls and sediments indicate few false positives.

Black Death and Cholera samples as examples for the efficacy of CLiMax in confirming primary pathogenic agents

The initial testing of the CLiMax algorithm as modified for these in-solution pathogen baits, indicates a computational approach that is promising in qualitatively assessing the likelihood of pathogen (microbial) presence. In assessing the likelihood of presence for individual species/strains, two parameters were evaluated: first, the number of regions covered by the pathogen baits that have hits from the sequence reads, and second, whether those high coverage regions are close to the positions of the bait probes (i.e., coverage peaks must line up with the probe signal to be considered present).

Black Death (P06BD)

In the Black Death sample (P06BD), there are hits to 25 of 77 total regions (105 reads) in the *Y. pestis* 91001 chromosome, 13 of 21 total regions in plasmid pCD1 (99 reads), and 1/1 total region in plasmid pPCP1 (470 reads) (see Table 4 for the probe hits summary). Accordingly, *Y. pestis* is considered a “present” target. The distribution of reads across the specific *Y. pestis* regions (rather than only a single probe showing a signal) attest to the confirmation of this target in the sequenced library and the sensitivity of the *Y. pestis* capture regions used in this bait set. There are also hits to the *Plasmodium vivax* genome (43/747 regions); however, upon examination of the probe coverage plots (see Figure 9) the coverage peaks are not aligned on the probe positions, rendering this signal

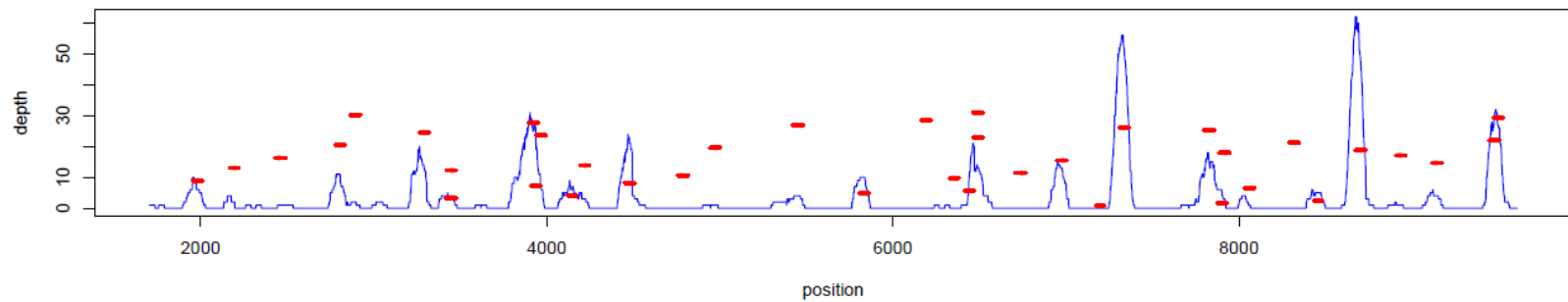
unreliable. In terms of assessing the likelihood of other targets present alongside *Y. pestis*, the following are identified (based on alignment of coverage peaks with the probe signals): *Amphibacillus jilinenis* (a soda lake-dwelling bacterium) (Cheng et al., 2013), *Escherichia coli*, human immunodeficiency virus, and *Klebsiella pneumoniae*.

Table 4. Summary of probe hits for Black Death specimen (P06BD).

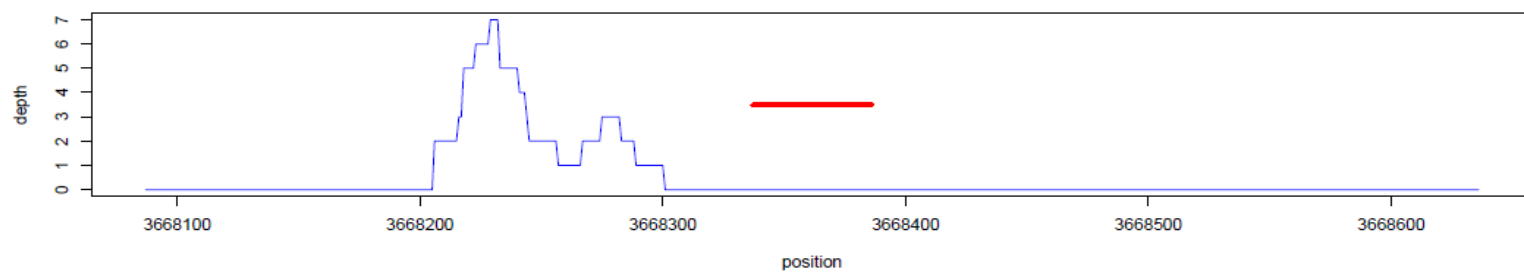
Species	# probe regions	# probe regions with hits	% probe regions with hits	Total # hits summed across regions	Aligns with probes?
<i>Amphibacillus jilinenis</i>	3	3	100.0	468	Yes
<i>Babesia bigemina</i>	9	2	22.2	14	No
<i>Bacillus thuringiensis</i>	43	2	4.7	46085	No
<i>Burkholderia</i> sp.	2	1	50.0	38	No
<i>Clostridium difficile</i>	4	2	50.0	27151	No
<i>Clostridium drakei</i>	42	3	7.1	9568	No
<i>Escherichia coli</i> KTE16	59	3	5.1	90	Yes
Hepatitis C virus	3	1	33.3	28	No
Human immunodeficiency virus	6	1	16.7	14	Yes
<i>Klebsiella pneumoniae</i>	70	2	2.9	35	Yes
<i>Listeria monocytogenes</i>	66	3	4.5	26	No
<i>Mycoplasma mycoides</i> subsp. <i>capri</i>	4	1	25.0	14	No
<i>Plasmodium vivax</i> Salvador-1	747	43	5.8	456	No
<i>Rhodococcus wratislaviensis</i>	3	2	66.7	47	No
<i>Salmonella enterica</i>	578	3	0.5	36812	No
<i>Streptococcus agalactiae</i>	21	1	4.8	311	No
<i>Yersinia pestis</i> Angola plasmid pMT-pPCP	31	10	32.3	504	Yes
<i>Yersinia pestis</i> (chromosome)	77	25	32.5	105	Yes
<i>Yersinia pestis</i> (plasmid pCD1)	21	13	61.9	99	Yes
<i>Yersinia pestis</i> (plasmid pPCP1)	1	1	100.0	470	Yes
<i>Yersinia pseudotuberculosis</i>	60	21	35.0	92	Yes
<i>Yersinia</i> sp.	26	9	34.6	36752	Yes

Figure 9. CLiMax algorithm applied to Black Death sample (P06BD) indicating target presence (a), and (b) exclusion of false positive (*Plasmodium vivax* Sal-1) by examination of probe alignment. Probe signals are indicated in red.

(A) Black Death, and positive *Y. pestis* signal example (probes align with sequence data coverage)



(B) *Plasmodium vivax* Sal-1, false signal (probes not aligned with sequence data coverage)



Cholera (P20CH)

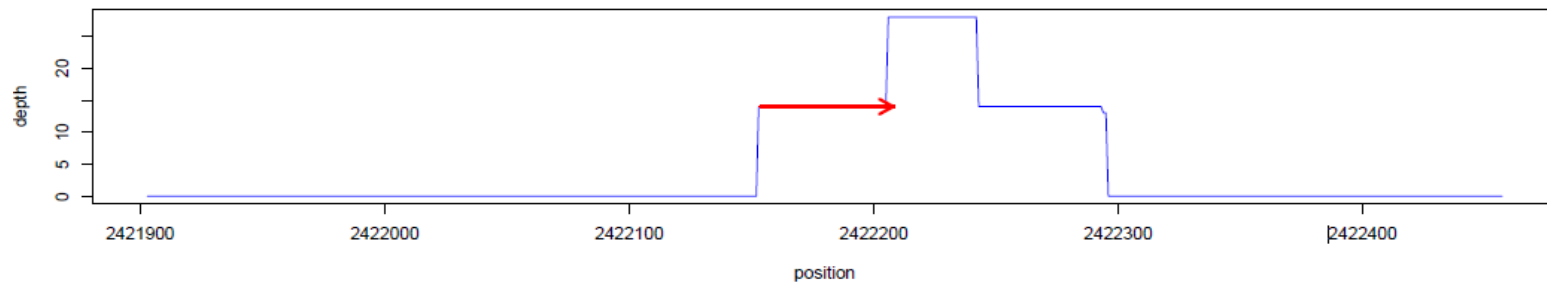
The *Vibrio cholerae* species genomic regions are represented by 41 probes, and cholera sample P20CH has 23 reads matching this region, with 28 reads assigned to *Vibrio* sp., but all of these reads are in one region (see Table 5 for the probe hits summary). Although this is one of the “pathogen-positive” samples, it is unlikely that one out of 41 *V. cholerae* species-specific bait probes is more effective than the others in terms of identifying the target. This is poor evidence for concluding *V. cholerae* presence (Figure 10); however, the previously successful shotgun and capture of *V. cholerae* (Devault et al., 2014b) was sequenced to a greater depth than the pathogen-enriched library (i.e., 180X compared to less than 1X), and remains a likely cause of this discrepancy. It is similarly significant to note that despite reads matching other probe regions (e.g., *Bacillus thuringiensis*, *Salmonella enterica*), no other hits align with the probe regions, leading to a probable assessment of *Vibrio* sp. presence.

Table 5. Summary of probe hits for cholera specimen (P20CH).

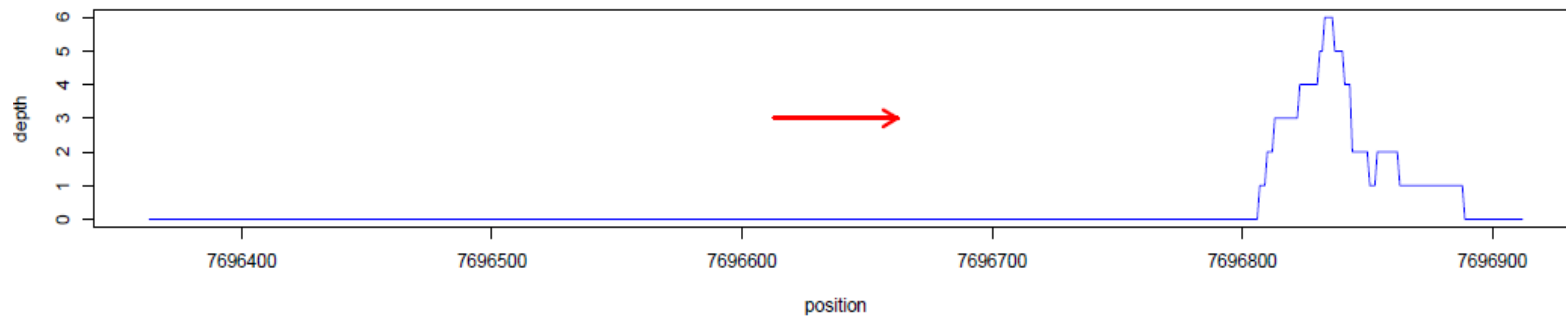
Species	# probe regions	# probe regions with hits	% probe regions with hits	Total # hits summed across regions	Aligns with probes?
<i>Bacillus thuringiensis</i>	43	1	2.3	593	No
<i>Burkholderia</i> sp.	2	1	50.0	59	No
<i>Clostridium difficile</i>	4	1	25.0	271	No
<i>Clostridium drakei</i>	42	1	2.4	186	No
Dengue virus	5	1	20.0	4	No
<i>Enterobacter cloacae</i>	17	1	5.9	54	No
<i>Escherichia coli</i>	52	1	1.9	4	No
Gallid herpesvirus 2 strain RB-1B	36	1	2.8	2	No
Hepatitis C virus RNA	73	2	2.7	36	No
<i>Leishmania donovani</i>	1139	2	0.2	8	No
<i>Lelliottia amnigena</i>	60	1	1.7	54	No
<i>Neisseria meningitidis</i>	49	1	2.0	5	No
<i>Plasmodium vivax</i> Salvador-I	747	44	5.9	259	No
<i>Rhodococcus wratislaviensis</i>	3	1	33.3	83	No
<i>Salmonella enterica</i>	578	1	0.2	457	No
<i>Staphylococcus aureus</i>	100	1	1.0	17	No
<i>Streptococcus agalactiae</i>	21	1	4.8	4	No
<i>Vibrio cholerae</i>	41	1	2.4	23	Yes
<i>Vibrio</i> sp.	48	1	2.1	28	Yes
<i>Yersinia</i> sp.	26	1	3.8	439	No

Figure 10. CLiMax algorithm applied to cholera sample (P20CH) indicating minimal target presence (a), and (b) exclusion of false positive (*Plasmodium vivax* Sal-1) by examination of probe alignment. Probe signals are in red.

(A) *V. cholerae* reads (few within expected probe distribution)



(B) *Plasmodium vivax* Sal-1, false signal (probes not aligned with sequence data)



Discussion

The stringency of bait design, efficiency of the capture protocol and downstream processing of reads demonstrate the capability of our parallel pathogen capture technique to identify microbial constituents, with minimal interference from non-target DNA (i.e., environmental or contaminant) and thus, enables prioritization of candidate pathogens for hybridization capture. To evaluate the evidence that each target shown is truly present, the following parameters are recommended. First, in the summary and hit count tables generated through the analysis pipeline (detailed in the Supplementary Appendix), it is necessary to identify the number of regions covered by the pathogen bait probes that have hits from the sequence reads. Although, a caveat is that the number of reads alone is not sufficient to demonstrate target presence. It is necessary to further evaluate the probe coverage and distribution of regions across the probe set. Secondly, in the coverage plots, identifying whether the positions with high coverage depth are close to the positions of the bait probes is necessary to determine the likelihood of target presence. In order to be assessed as present, the resultant signals (from the sequence reads) must align with the probes. At this point in our analyses, the parallel pathogen capture technique successfully provides a qualitative assessment of sample representativeness for a particular target species.

Limitations of the approach are broadly related to the array of challenges recognized when working with ancient DNA (variable preservation within and

between specimens, exogenous contamination affecting endogenous DNA recovery, and sequencing depth). As such, the resolution of the microbial profile largely depends on a sample's idiosyncrasies and complexity (e.g., preservation, amount of endogenous DNA). Accordingly, due to these limitations, cautious interpretations of results in their specific context is critical alongside comparisons of the probe signals as part of the probe hits summary when using the CLiMax algorithm. The distribution of targets across a given genome is also an important consideration, as the concentration of reads within narrow genomic regions is presumptively identified as false positives (and removed from analyses). The next task ahead is turning the qualitative data into a quantitative measure of evidence supporting species presence or absence. The overarching goal is the development of a novel pipeline for rapid interpretation with statistical support for determining pathogenic targets of high interest (and are reasonable) to pursue.

Through the integration of parallel pathogen detection within paleopathological research, the focus is comparing not only pathogen presence in diverse biocultural environments, but also the dynamic changes of the pathogen pool over significant historical events (i.e., climatic fluctuations, human migrations or pandemics). The specificity and sensitivity of parallel capture in confirming and prioritizing pathogen candidates is amenable to integration alongside the scope of multidisciplinary approaches within paleopathological disease identification. Broadly, we have demonstrated the applicability of parallel pathogen capture using probes designed for the LLMDA across diverse

archaeological samples of known and unknown microbial constituents. Parallel pathogen detection further overcomes the limitations of metagenomics, which critically under-predicts the pathogenic component of ancient extracts and cannot facilitate inclusion or exclusion of disease-associated pathogens. By removing the “noise” associated with metagenomic (microbial) profiles, the narrow targeting of the human-only pathogen component will further facilitate informed capture strategies and increase the likelihood of post-capture success. Overall, this strategy provides a means of reconstructing detailed profiles of primary and co-infecting pathogenic/opportunistic agents within and across spatiotemporal contexts. The success of this molecular approach exploits the historical and geographical context within which ancient DNA is embedded, ultimately providing a window to explore the multi-faceted aspects of the disease process (as influenced by the environment, by human activity and other pathogens). In this manner, the integration of parallel pathogen detection alongside paleopathological analyses enhances the investigation of synergistic disease landscapes far removed in space and time.

References

- Altschul, S.F., Gish, W., Miller, W., Myers, E.W., Lipman, D.J. (1990). Basic local alignment search tool. *Journal of Molecular Biology*, 215(3), 403–410.
- Andersen, J.G., & Manchester, K. (1992). The rhinomaxillary syndrome in leprosy: a clinical, radiological, and paleopathological study. *International Journal of Osteoarchaeology*, 2(2), 121-129.
- Bos, K. I., Schuenemann, V. J., Golding, G. B., Burbano, H. A., Waglechner, N., Coombes, B. K., ... & Krause, J. (2011). A draft genome of *Yersinia pestis* from victims of the Black Death. *Nature*, 478(7370), 506-510.
- Bos, K. I., Jäger, G., Schuenemann, V. J., Vågane, Å. J., Spyrou, M. A., Herbig, A., ... & Krause, J. (2015). Parallel detection of ancient pathogens via array-based DNA capture. *Philosophical Transactions of the Royal Society of London B: Biological Sciences*, 370(1660), 20130375.
- Bruun, C. (2007). The Antonine plague and the 'third-century crisis'. In Hekster, O., de Kleijn, G., & Sliotjes, D. (Eds.), *Crises and the Roman Empire* (pp. 201-218). Leiden: Brill.
- Burbano, H. A., Hodges, E., Green, R. E., Briggs, A. W., Krause, J., Meyer, M., ... & Pääbo, S. (2010). Targeted investigation of the Neandertal genome by array-based sequence capture. *Science*, 328(5979), 723-725.
- Carpenter, M. L., Buenrostro, J. D., Valdiosera, C., Schroeder, H., Allentoft, M. E., Sikora, M., ... & Bustamante, C.D. (2013). Pulling out the 1%: whole-genome capture for the targeted enrichment of ancient DNA sequencing libraries. *American Journal of Human Genetics*, 93(5), 852-864.
- Cartwright, K.A.V., Stuart, J.M., Jones, D.M., & Noah, N.D. (1987). The Stonehouse survey: nasopharyngeal carriage of meningococci and *Neisseria lactamica*. *Epidemiology and Infection*, 99(3), 591-601.
- Cheng, H., Fang, M. X., Jiang, X. W., Wu, M., Zhu, X. F., Zheng, G., & Yang, Z. J. (2013). Draft genome sequence of *Amphibacillus jilinensis* Y1T, a facultatively anaerobic, alkaliphilic and halotolerant bacterium. *Standards in Genomic Sciences*, 8(3), 491-499.
- Cunha, C.B., Cunha, B.A. (2008). Brief history of the clinical diagnosis of malaria: from Hippocrates to Osler. *Journal of Vector Borne Diseases*, 45(3), 194-199.

- Devault, A.M., McLoughlin, K., Jaing, C., Gardner, S., Porter, T. M., Enk, J., ... & Poinar, H.N. (2014a). Ancient pathogen DNA in archaeological samples detected with a Microbial Detection Array. *Nature Scientific Reports*, 4, 42-45.
- Devault, A.M., Golding, B., Waglechner, N., Enk, J.M., Kuch, M., Tien, J.H., ... & Poinar, H.N. (2014b). Second-pandemic strain of *Vibrio cholerae* from the Philadelphia cholera outbreak of 1849. *New England Journal of Medicine*, 370(4), 334-340.
- Devault, A.M., Mortimer, T.D., Kitchen, A., Kiesewetter, H., Enk, J.M., Golding, G.B., ... & Pepperell, C.S. (n.d.). An ancient emerging infection as a cause of maternal sepsis in Late Byzantine Troy (In Review).
- DeWitte, S.N., & Stojanowski, C.M. (2015). The Osteological Paradox 20 years later: past perspectives, future directions. *Journal of Archaeological Research*, 23(4), 397-450.
- Duncan-Jones, R.P. (1996). The impact of the Antonine plague. *Journal of Roman Archaeology*, 9, 108-136.
- Dutour, O. (2013). Paleoparasitology and paleopathology. Synergies for reconstructing the past of human infectious diseases and their pathocenosis. *International Journal of Paleopathology*, 3(3), 145-149.
- Enk, J. (2016). Target capture for ancient DNA: temperature, time, and tiling density. 81st Annual Meeting of the Society for American Archaeology (Orlando, FL).
- Faure, E. (2014). Malarial pathocenosis: beneficial and deleterious interactions between malaria and other human diseases. *Frontiers in Physiology*, 5, 441-454.
- Gardner, S., Jaing, C., McLoughlin, K., & Slezak, T. (2010). A microbial detection array (MDA) for viral and bacterial detection. *BMC Genomics*, 11(1), 668-689.
- Gold, R., Goldschneider, I., Lepow, M.L., Draper, T.F., & Randolph, M. (1978). Carriage of *Neisseria meningitidis* and *Neisseria lactamica* in infants and children. *Journal of Infectious Diseases*, 137(2), 112-121.
- Grmek, M.D. (1969). Préliminaires d'une étude historique des maladies. *Annales. Histoire, Sciences Sociales*, 24(6), 1473-1483.

- Grmek, M.D. (1991). *Diseases in the Ancient Greek World*. Baltimore: John Hopkins University Press.
- Hofreiter, M., Paijmans, J. L., Goodchild, H., Speller, C. F., Barlow, A., Fortes, G. G., ... & Collins, M.J. (2015). The future of ancient DNA: technical advances and conceptual shifts. *BioEssays*, 37(3), 284-293.
- Huson, D.H., Auch, A.F., Qi, J., Schuster, S.C. (2007). MEGAN analysis of metagenomic data. *Genome Research*, 17, 377-386.
- Jackes, M. (2011). Representativeness and bias in archaeological skeletal samples. In Agarwal, S. C., Glencross, B. A., Eds. *Social Bioarchaeology* (pp.107-146). Chichester: Wiley-Blackwell.
- Kappus, M. R., & Sterling, R. K. (2013). Extrahepatic manifestations of acute hepatitis B virus infection. *Gastroenterology & Hepatology*, 9(2), 123-126.
- Kay, G. L., Sergeant, M. J., Giuffra, V., Bandiera, P., Milanese, M., Bramanti, B., ... & Pallen, M. J. (2014). Recovery of a medieval *Brucella melitensis* genome using shotgun metagenomics. *mBio*, 5(4), e01337-14.
- Kircher, M., Sawyer, S., Meyer, M. (2012). Double indexing overcomes inaccuracies in multiplex sequencing on the Illumina platform. *Nucleic Acids Research*, 40(1), e3.
- Langmead, B., & Salzberg, S. (2012). Fast gapped-read alignment with Bowtie 2. *Nature Methods*, 9,357-359.
- Littman, R.J., & Littman, M.L. (1973). Galen and the Antonine plague. *American Journal of Philology*, 94(3), 243-255.
- Marciniak, S., Prowse, T.L., Herring, D.A., Klunk, J., Kuch, M., Duggan, A.T., ... & Poinar, H. N. (2016). *Plasmodium falciparum* malaria in 1st-2nd c. A.D. southern Italy. *In Press*, Current Biology.
- Meyer, M., Kircher, M. (2010). Illumina sequencing library preparation for highly multiplexed target capture and sequencing. *Cold Spring Harbor Protocol*, 6, t5448.
- McLoughlin, K. S. (2011). Microarrays for pathogen detection and analysis. *Briefings in Functional Genomics*, 10(6), 342–353.

- Molak, M., Ho, S.Y.W. (2011). Evaluating the impact of post-mortem damage in ancient DNA: a theoretical approach. *Journal of Molecular Evolution*, 73(3-4), 244-255.
- Orlando, L., Gilbert, M.T.P., Willerslev, E. (2015). Reconstructing ancient genomes and epigenomes. *Nature Reviews Genetics*, 16(7), 395-408.
- Ortner, D. J. (1992). Skeletal paleopathology: Probabilities, possibilities, and impossibilities. In Verano, J. W., Ubelaker, D. H., (Eds.). *Disease and Demography in the Americas* (pp. 5–13). Washington: Smithsonian Institution Press.
- Ortner, D.J. (2003). *Identification of Pathological Conditions in Human Skeletal Remains*. San Diego: Academic Press.
- Ortner, D. J. (2009). Issues in paleopathology and possible strategies for dealing with them. *Anthropologischer Anzeiger*, 67, 323–340.
- Ortner, D.J. (2011). Human skeletal paleopathology. *International Journal of Paleopathology*, 1(1), 4-11.
- Pääbo, S., Poinar, H., Serre, D., Jaenicke-Després, V., Hebler, J., Rohland, N., ...& Hofreiter, M. (2004). Genetic analyses from ancient DNA. *Annual Review of Genetics*, 38, 645-679.
- Roberts, C., & Manchester, K. (2005). *The Archaeology of Disease, 3rd ed.* Ithaca: Cornell University Press.
- Saunders, S. R., Herring, D. A., & Boyce, G. (1995). Can skeletal samples accurately represent the living populations they come from? The St. Thomas' Cemetery site, Belleville, Ontario. In Grauer, A.L., (Ed.). *Bodies of Evidence: Reconstructing history through skeletal analysis* (pp. 69-89). Chichester: Wiley-Liss.
- Scheidel, W. (2002). A model of demographic and economic change in Roman Egypt after the Antonine plague. *Journal of Roman Archaeology*, 15, 97-114.
- Schuenemann, V. J., Singh, P., Mendum, T. A., Krause-Kyora, B., Jäger, G., Bos, K. I., ...& Krause, J. (2013). Genome-wide comparison of medieval and modern *Mycobacterium leprae*. *Science*, 341(6142), 179-183.

- Schuenemann, V. J., Bos, K., DeWitte, S., Schmedes, S., Jamieson, J., Mittnik, A., ... & Poinar, H.N. (2011). Targeted enrichment of ancient pathogens yielding the pPCP1 plasmid of *Yersinia pestis* from victims of the Black Death. *Proceedings of the National Academy of Sciences*, 108(38), E746-E752.
- Wagner, D. M., Klunk, J., Harbeck, M., Devault, A., Waglechner, N., Sahl, J. W., ... & Poinar, H.N. (2014). *Yersinia pestis* and the plague of Justinian 541-543 AD: a genomic analysis. *The Lancet Infectious Diseases*, 14(4), 319-326.
- Waldron, T. (1994). *Counting the Dead: The Epidemiology of Skeletal Populations*. Chichester: Wiley.
- Warinner, C., Speller, C., & Collins, M.J. (2015). A new era in palaeomicrobiology: prospects for ancient dental calculus as a long-term record of the human oral microbiome. *Philosophical Transactions of the Royal Society London B*, 370(1660), 20130376.
- Whatmore, A.M. (2014). Ancient-pathogen genomics: coming of age? *mBio*, 5(5), e01676-14.
- Wood, J. W., Milner, G. R., Harpending, H. C., & Weiss, K. M. (1992). The Osteological Paradox: problems of inferring prehistoric health from skeletal samples. *Current Anthropology*, 33(4), 343–370.
- Wright, L.E., & Yoder, C.J. (2003). Recent progress in bioarchaeology: approaches to the osteological paradox. *Journal of Archaeological Research*, 11(1), 43-70.

Supplementary Appendix

Parallel hybridization capture of multiple pathogens in archaeological samples: towards integrated paleopathological investigations

By: Stephanie Marciniak¹, Ana T. Duggan¹, Shea Gardner², Crystal Jaing², Jonathan Allen², Kevin McLoughlin², Monica Borucki², Tracy L. Prowse⁴, Hendrik N. Poinar^{1,3}

¹McMaster Ancient DNA Centre, Department of Anthropology, McMaster University, Hamilton, ON, L8S 4L9, Canada

²Lawrence Livermore National Laboratory, Livermore, CA

³Michael G. DeGroote Institute for Infectious Disease Research, McMaster University

⁴ Department of Anthropology, McMaster University, Hamilton, ON, L8S 4L9, Canada

Supplementary Methods

A. Sample preparation

Known pathogen specimens were sub-sampled, DNA extracted and converted into libraries appropriate for the Illumina platform were prepared as previously described: Black Death tooth from specimen 8291 of the East Smithfield cemetery (London, 1348-1349 A.D.) (Bos et al., 2011); intestinal specimen from a cholera victim of the Philadelphia 19th c. epidemic (Devault et al., 2014a); Plague of Justinian tooth specimen (Bavaria, Germany, 541-543 A.D.) (Wagner et al., 2014); and a calcified nodule with associated sediments from a cemetery in Troy (Bronze Age to 13th c. A.D., Turkey) (Devault et al., n.d.). For the unknown specimens, sub-sampling, DNA extraction and library conversion are also previously described in Marciniak et al. (2016) for the Imperial Italian adults (1st-4th c. A.D., from the cemeteries of Isola Sacra, Velia, and Vagnari in Italy), juveniles from Vagnari, Italy (1st-4th c. A.D.), and Maritime Archaic individuals (5,000-4,000 B.C., Newfoundland, Canada). For the Italian mummies (adult female and associated juvenile), extraction proceeded with a modified protocol (Schwarz et al., 2009), followed by double-stranded library preparation (Meyer and Kircher, 2010) and indexing amplification (Kircher et al., 2012).

B. Parallel pathogen capture

The published MYbaits protocol was followed for two rounds of enrichment, alongside modifications to bait concentration (50-100 ng), hybridization time (18-24h), and temperature (55°C). The reamplification after each round of enrichment used the primer combination IS5_long_amp.P5 (5'-AATGATACGGCGACCACCGA-3') and IS6_long_amp.P7 (5'-CAAGCAGAAGACGGCATAACGA-3') (150 nM each), and KAPA SYBR® FAST qPCR Master Mix (2X). The parameters of the thermal program for all reamplifications were the following: a 95°C activation (5 minutes), followed by 11-13 cycles of 95°C (30 seconds), 60°C (45 seconds), ending with 60°C (3 minutes). Following this amplification, each sample was purified with the modified MinElute PCR Purification (Qiagen) protocol described above, and eluted in 18 µL of EB.

C. Sequencing

Sequencing was performed on the Illumina HiSeq 1500 platform at the Farncombe Family Digestive Health Research Institute (McMaster University, Hamilton ON, Canada). The samples were pooled in equimolar ratios and sequenced using 2 x 90 bp read chemistry. The previously verified bacterial pathogen samples were already subjected to shotgun sequencing as described for:

Black Death 8291 (Devault et al., 2014b; Bos et al., 2011), Plague of Justinian (Wagner et al., 2014), cholera (Devault et al., 2014a) and the calcified nodule along with the sediments (Devault et al., n.d.). The Maritime Archaic, Imperial Italian adults and juveniles, and medieval Italian mummies were shotgun sequenced (2,000,000 paired-end reads).

D. Bioinformatic processing of data

As described in Marciniak et al. (2016), the bioinformatic processing of the sequence data proceeded as described below.

i. Trimming and merging of enriched libraries. CASAVA processed reads were trimmed and merged with leeHom [<https://github.com/greanud/leeHom>], using ancient DNA parameters (--ancientdna), then mapped with a modified version of BWA [<https://github.com/udo-stenzel/network-aware-bwa>] with a maximum edit distance of 0.01 (-n 0.01), allowing a maximum of two gap openings (-o 2) and with seeding effectively disabled (-l 16500). Mapped reads were further filtered to those which were either merged or unmerged but properly paired [<https://github.com/greanud/libbam>] as well as unique based on both 5' and 3' coordinates [<https://github.com/udo-stenzel/biohazard>]. For all further analyses, we restricted reads to those where the minimum length of inserts was 24 bp a minimum mapping quality of 20. The mapped bam files were also converted to a fasta file for blastn-megablast analysis (v.2.2.29) (Altschul et al., 1990).

ii. Trimming and merging of shotgun libraries. CASAVA processed reads were trimmed and merged with leeHom [<https://github.com/greanud/leeHom>], using ancient DNA parameters (--ancientdna). Reads in unmapped bam files (i.e., contains all reads and no mapping to a reference), were then converted to a fasta file for blastn-megablast analysis (v.2.2.29) (Altschul et al., 1990).

E. Taxonomic analysis

The shotgun and pathogen-enriched data were processed to identify taxonomic assignments by comparison to a nucleotide sequence database (blastn-megablast, v.2.2.29) (Altschul et al., 1990). Each BLAST (Basic Local Alignment Search Tool) output was parsed using MEGAN5 (v.5.11.3) (Huson et al., 2007) in order to assign a taxon.

F. LLNL pathogen baits analysis

i. Pathogen baits design. Complete and draft sequences for all viruses, bacteria, fungi, archaea and human pathogenic protozoa were obtained from public and proprietary genomic databases (Gardner et al., 2010). The design for the in-solution probes followed previous iterations of the LLMDA by using

Family-specific regions among all available sequences (genes, genomes, plasmids), then identifying conserved and unique (discriminatory) probes within these regions for targeting specific species and strains (Gardner et al., 2010; McLoughlin et al., 2011). Probes that detected more targets in a Family were selected over probes that detected fewer, and the selected candidate probe had to be 85% similar to the target sequence, with 100% matches to 29 continuous base pairs in the middle of each 80-bp probe (Gardner et al., 2010).

ii. *Analysis pipeline.* The CLiMax algorithm facilitates a hierarchical identification process, by identifying to the Family, Genus, Species, and strain level, using an iterative procedure to predict the likelihood of the targets in the sample. First, the target that likely explains the largest portion of observed reads is identified, and in subsequent iterations, the next target selected is one that explains the largest part of the reads not already explained by the previous target (Gardner et al., 2010; McLoughlin et al., 2011). This continues until the maximum number of targets that explain the signals are identified (Gardner et al., 2010; McLoughlin et al., 2011). A log-likelihood score is also constructed for each iteration of a read based on its match to the target database, computing a log-odds score for each subsequent target, where the target with the highest log-likelihood is appended to the series (Devault et al., 2014b; McLoughlin et al., 2011). This process continues until there are no additional targets to improve the likelihood by predicting additional targets (Devault et al., 2014b; McLoughlin et al., 2011). Broadly, the analysis constructs a log-likelihood score for each reference genome that has hits, that reflects the mean coverage of each region (context sequence) expected to be enriched, the number of enriched regions in the genome that have hits, and the distribution of hits within each region. In this iterative manner, the possibility of identification of a target remains hierarchical, depending on the likelihood of target presence (i.e., the reads may not be stringently identified to the species, but can be to the Genus-level). See Table 1 for the Family-level calls for the data set and Figure 1 in the main text for the analysis pipeline.

Supplementary Results

A. Taxonomic distributions for select samples

Figure S1. Maritime Archaic adult (P22BT) post-capture microbial profile

Figure S2. Plague of Justinian sample #2 (P01JT) post-capture microbial profile

Figure S3. Italian adult mummy (P06MM) post-capture microbial profile

Figure S4. Italian child mummy #2 (P04MM) post-capture microbial profile

Figure S5. Imperial Italian adult (P24RM) post-capture microbial profile

Figure S6. Vagnari juvenile (P20JV) post-capture microbial profile

Figure S7. Troy sediment (P11TY) post-capture microbial profile

B. LLNL and HTS analysis

Table S1. Family-level probes identified from alignments to the sequence data, full results.

Table S2. Taxonomic assessment of sequence data, full results.

Figure S1. Maritime Archaic adult (P22BT) post-capture microbial profile.

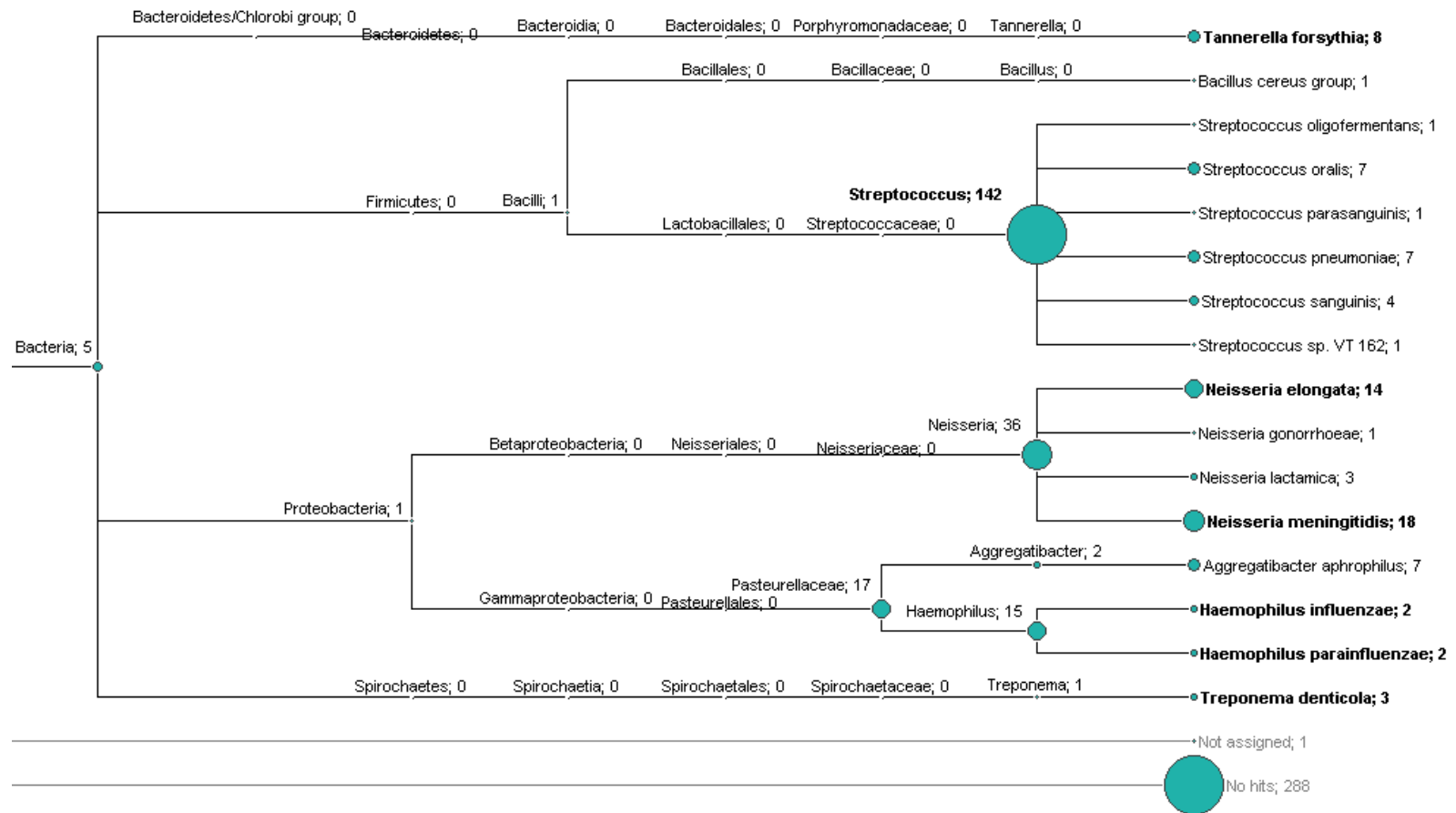


Figure S2. Plague of Justinian #2 (P01JT) post-capture microbial profile.

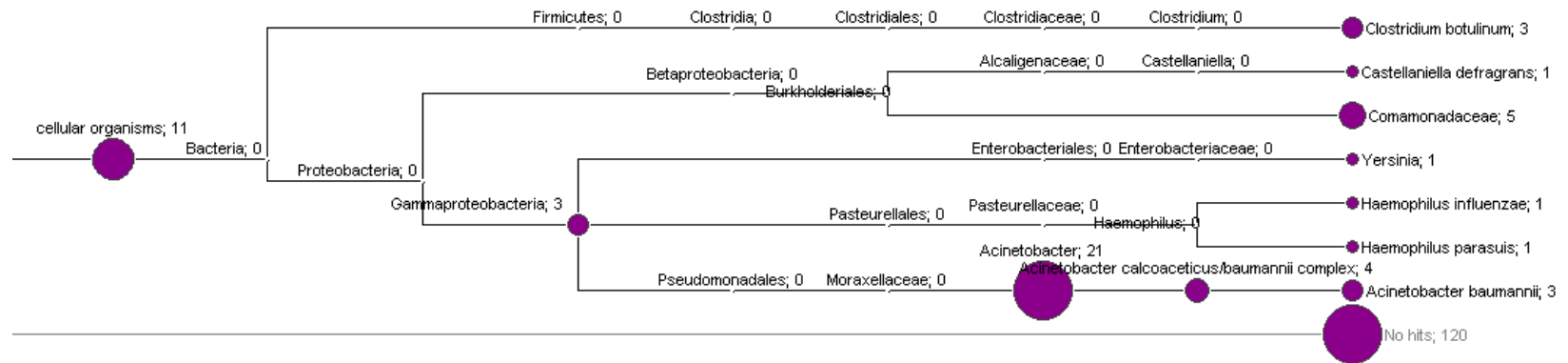


Figure S3. Italian adult mummy (P06MM) post-capture microbial profile.

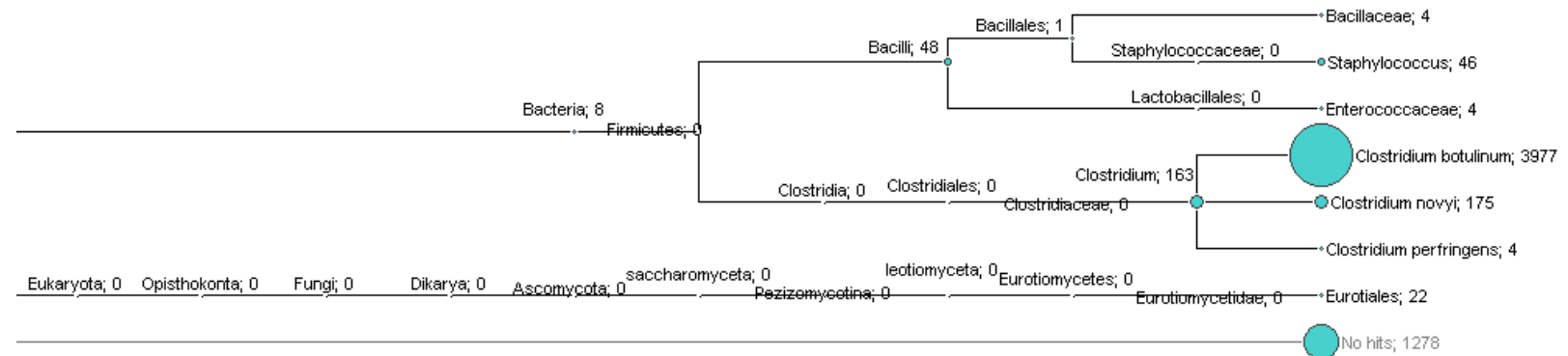


Figure S4. Italian child mummy #2 (P04MM) post-capture microbial profile.

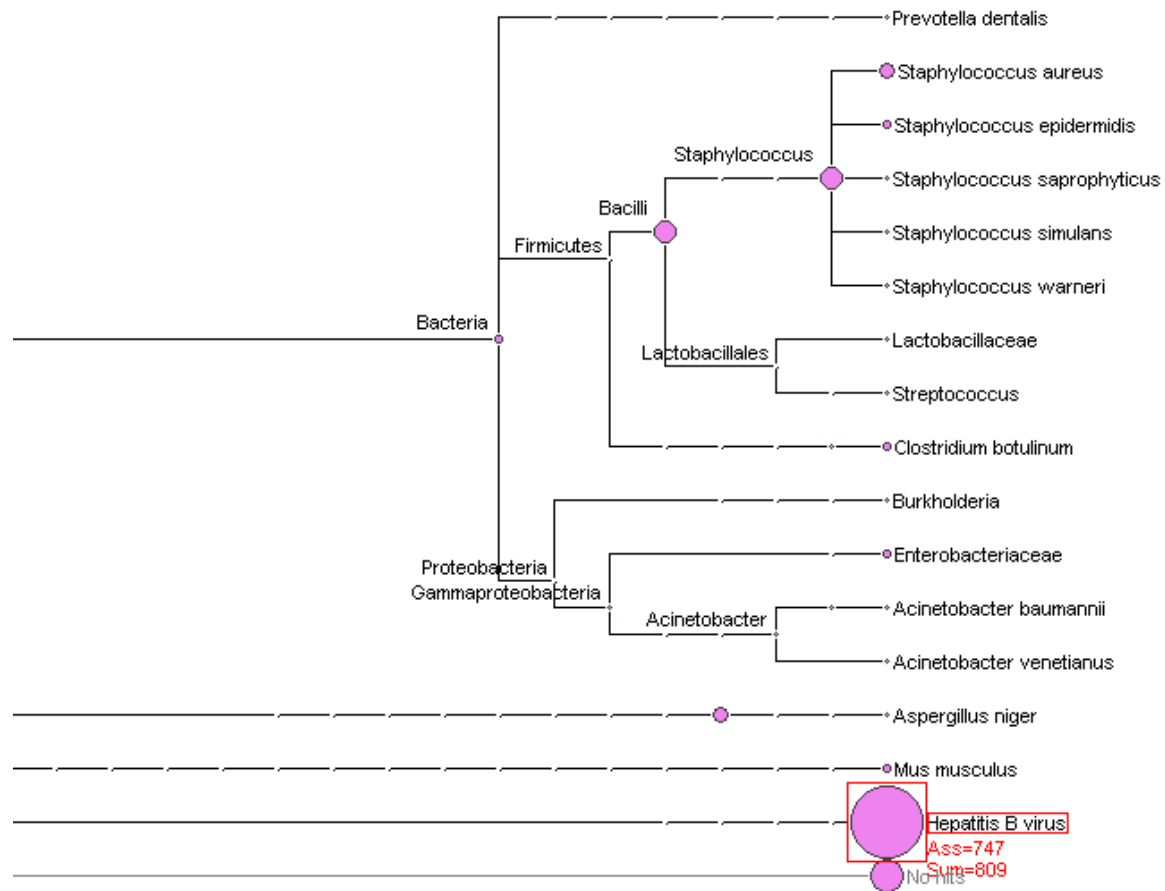


Figure S5. Imperial Italian adult (P24RM) post-capture microbial profile.

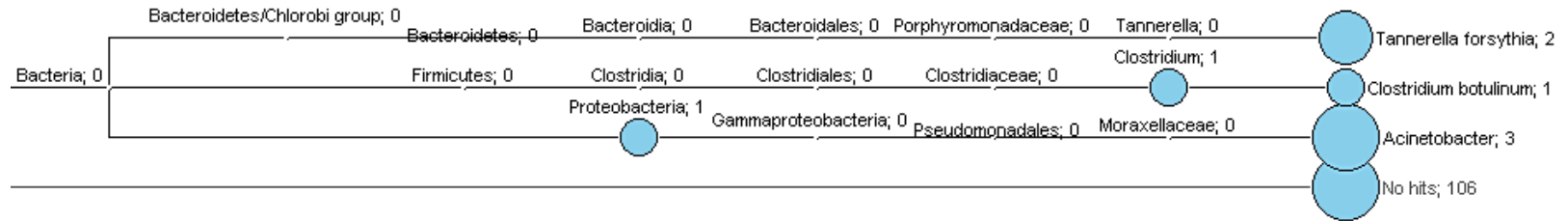


Figure S6. Vagnari juvenile (P20JV) post-capture microbial profile.

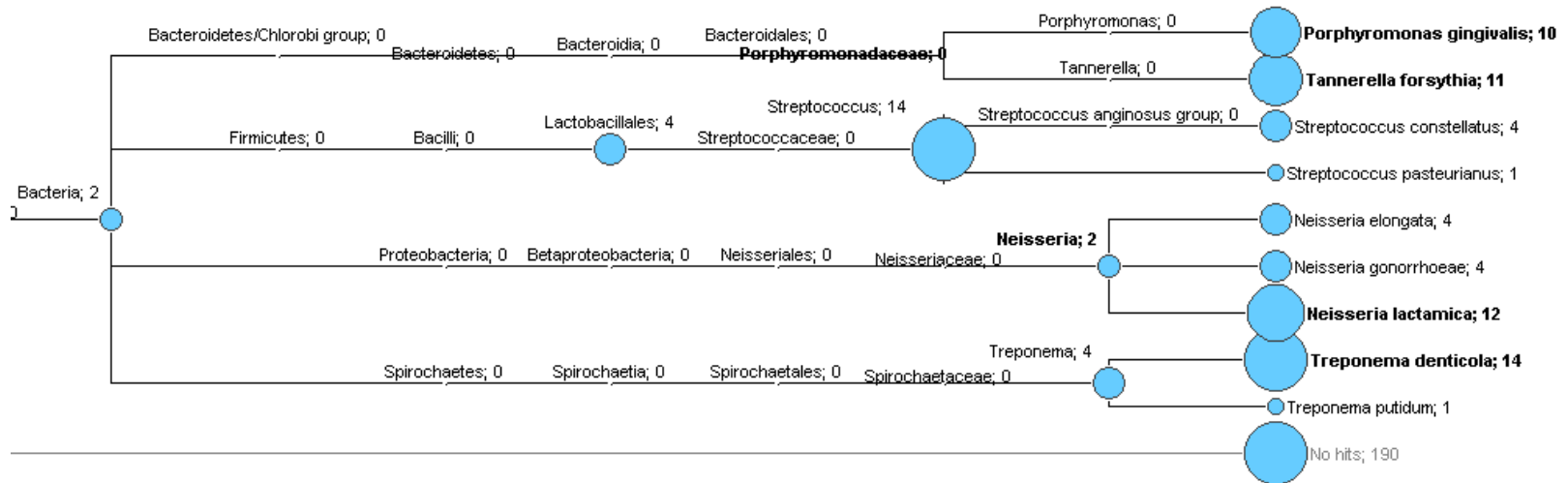


Figure S7. Troy sediment (P11TY) post-capture microbial profile.

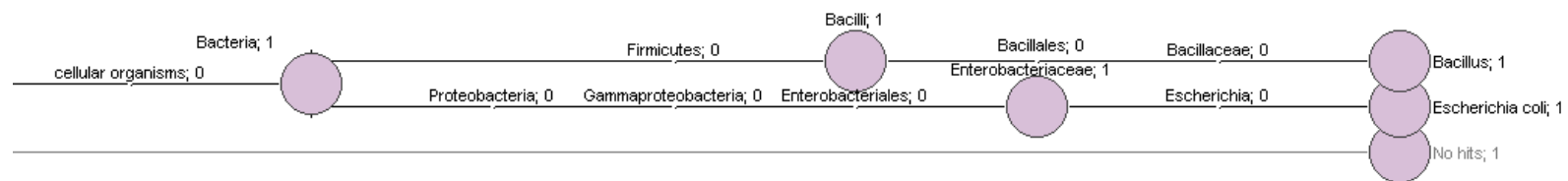


Table S1. Family-level probes identified from alignments to the sequence data, full results.

Sample ID	Probe ID	# Reads matching probes	bp range
Black Death (P06BD) #1	Enterobacteriaceae	93	24-59
	Clostridiaceae_1110	1	32
	Bacillaceae_2108	1	24
	all_protozoa_1293	1	24
	Flaviviridae_5111	1	24
	Helicobacteraceae_296	1	24
	Herpesviridae_1586	1	24
	Inoviridae_434	1	24
	Papillomiviridae	2	24
	Pasteurellaceae_616	1	24
Black Death (P07BD) #2	Enterobacteriaceae	1,648	24-64
	Clostridiaceae	24	25-57
	Protozoa	12	24-29
	Aurantimonadaceae_14	1	32
	Bacillaceae_1015	1	26
	Brucellaceae_105	1	24
	Campylobacteraceae_114v6	1	24
	Enterococcaceae	2	25-35
	Flaviviridae	18	24-28
	Helicobacteraceae	3	25
	Hepadnaviridae	3	24-25
	Herpesviridae	3	24-26
	Moraxellaceae	5	24-41
	Mycobacteriaceae	1	26
	Myoviridae	7	26-34
	Neisseriaceae	3	25-30
	Orthomyxoviridae_7153	1	24
	Papillomiviridae	15	24-27
	Pasteurellaceae_106v6	1	26
	Polyomaviridae_874	1	26
	Porphyromonadaceae_207	1	24
Retroviridae	19	24-31	
Sarcocystidae_25v6	1	24	
Spirochaetaceae	12	24-26	

	Probe ID	# Reads matching probes	bp range
	Staphylococcaceae	9	25-48
	Vibrionaceae	2	25-32
Justinian (P01JT) #1	Enterobacteriaceae	2	31-49
	Clostridiaceae	3	33-53
	Flaviviridae_5704	1	24
	Hepadnaviridae_598	1	25
	Neisseriaceae_625	1	24
	Papillomiviridae	3	24
	Retroviridae_11471	1	24
	Spirochaetaceae_3361	1	27
	Protozoa	3	24-25
	Justinian extraction blank (P02JT) #1	Comamonadaceae_230	1
Justinian (P01JT) #2	Enterobacteriaceae	18	24-47
	Flaviviridae	14	24-26
	Hepadnaviridae	14	24-26
	Moraxellaceae	45	37-63
	Retroviridae	12	24-28
	Protozoa	26	24-26
	Brucellaceae	5	24-50
	Burkholderiaceae	3	24-35
	Papillomiviridae	9	24-28
	Clavicipitaceae_97v6	1	24
	Clostridiaceae	5	37-53
	Comamonadaceae_230	5	34-53
	Helicobacteraceae_525	1	25
	Herpesviridae	6	24-28
	Myoviridae	3	24-30
	Neisseriaceae	2	24-26
	Pasteurellaceae	2	24-38
	Spirochaetaceae_3278	1	24
	Streptococcaceae_3129	1	24
	Vibrionaceae_2548	1	24
Justinian extraction blank (P02JT) #2	Burkholderiaceae	7	29-40
	Comamonadaceae_230	23	25-59
	Enterobacteriaceae_3879	1	42
	Papillomiviridae	12	27-61

Sample ID	Probe ID	# Reads matching probes	bp range
Mummy - child (P03MM) #1	Hepadnaviridae	14	36-51
	Staphylococcaceae	3	45-52
	Clostridiaceae_1444	1	42
Mummy - child (P03MM) #2	Hepadnaviridae	3	27-45
	Protozoa	2	24
	Bacillaceae_1015	1	25
	Brucellaceae_61	1	24
	Clostridiaceae	3	31-58
	Enterobacteriaceae	2	25-48
	Flaviviridae_5806	1	25
	Moraxellaceae	2	47-52
	Papillomiviridae	4	24-26
	Pasteurellaceae_132v6	1	24
	Retroviridae	2	24
	Spirochaetaceae_3347	1	24
	Staphylococcaceae	15	27-60
	Trichocomaceae_1429	6	36-53
Mummy - child (P04MM) #2	Hepadnaviridae	850	24-63
	Protozoa	30	24-45
	Bacillaceae	2	25-26
	Bartonellaceae_150v6	1	24
	Brucellaceae_6	1	24
	Burkholderiaceae	5	27-39
	Clostridiaceae	37	32-58
	Enterobacteriaceae	16	24-49
	Flaviviridae	10	24-25
	Herpesviridae	3	24-25
	Lactobacillaceae	2	24-45
	Listeriaceae_207	1	24
	Moraxellaceae	10	36-56
	Papillomiviridae	10	24-27
	Plasmodiidae_106v6	1	35-44
	Porphyromonadaceae_520	1	25
	Retroviridae	17	24-56
	Spirochaetaceae	9	24-27
	Staphylococcaceae	255	25-62
Streptococcaceae_2193	1	54	

	Probe ID	# Reads matching probes	bp range
	Trichocomaceae	69	24-56
	Trypanosomatidae_70v6	1	25
	Vibrionaceae	2	24-26
Mummy - adult (P05MM) #2	Protozoa	9	24-26
	Bacillaceae_878	1	25
	Enterobacteriaceae	261	24-59
	Enterococcaceae_213	1	24
	Flaviviridae	16	24-31
	Francisellaceae_347	1	24
	Helicobacteraceae	2	25-27
	Hepadnaviridae_1440	1	25
	Herpesviridae_16	1	16
	Listeriaceae_194	1	24
	Microviridae_172	1	27
	Moraxellaceae_19	1	54
	Myoviridae	3	25-35
	Papillomiviridae	14	24-27
	Retroviridae	12	24
	Rickettsiaceae_292	1	24
	Spirochaetaceae	12	24-26
	Staphylococcaceae	7	24-52
	Streptococcaceae	3	25-26
	Trichocomaceae	164	31-59
Vibrionaceae	2	25-31	
Mummy - adult (P06MM) #2	Protozoa	4	24-25
	Bacillaceae	8	26-48
	Clostridiaceae	5,538	24-68
	Enterobacteriaceae	6	24-44
	Enterococcaceae	3	53-66
	Flaviviridae	6	24
	Inoviridae_513	1	25
	Papillomiviridae	2	24-26
	Pasteurellaceae_1219	1	24
	Podoviridae_1365	1	24
	Porphyromonadaceae_323	1	24
	Retroviridae	6	24-26
	Spirochaetaceae_3342	1	25

	Probe ID	# Reads matching probes	bp range
	Staphylococcaceae	116	32-62
	Streptococcaceae_2265	3	30-32
	Trichocomaceae_1429	33	40-56
Troy nodule (P09TY) #2	Staphylococcaceae	2,272	24-65
	Bacillaceae	19	24, 42
	Enterobacteriaceae	5	24-43
	Flaviviridae_7789	1	27
	Hepadnaviridae_1043	1	27
	Herpesviridae_1046	1	25
	Orthomyxoviridae_8498	1	26
	Papillomaviridae_351	1	25
	Retroviridae_8361	1	30
	Spirochaetaceae_3347	4	24-26
Troy nodule extraction blank (P10TY) #2	Moraxellaceae	2	40
Troy nodule (P15TB) #2	Protozoa	19	24-28
	Staphylococcaceae	1,796	24-65
	Bacillaceae_1015	76	24-43
	Brucellaceae_6	1	27
	Burkholderiaceae_273	1	24
	Campylobacteraceae_146v6	1	28
	Clostridiaceae_2945	1	26
	Corynebacteriaceae_357	1	24
	Enterobacteriaceae	9	24-34
	Flaviviridae	17	24-29
	Hepadnaviridae	2	24-29
	Herpesviridae	4	24-27
	Inoviridae_347	1	25
	Listeriaceae	2	26-27
	Moraxellaceae_792	1	39
	Mycobacteriaceae_251	1	24
	Orthomyxoviridae	3	24-27
	Papillomaviridae	6	24-27
	Pasteurellaceae_796	1	24
	Podoviridae_716	1	24
Polyomaviridae	2	24	
Retroviridae	5	24-25	

	Probe ID	# Reads matching probes	bp range
	Sarcocystidae_78v6	1	27
	Siphoviridae_2801	1	25
	Spirochaetaceae	10	24-28
	Vibrionaceae	2	24-25
Troy nodule (P16TB) #2	Staphylococcaceae	850	24-58
	Protozoa	27	24-29
	Bacillaceae	51	24-42
	Brucellaceae	9	24-26
	Burkholderiaceae_2548	1	25
	Campylobacteraceae_670	1	24
	Enterobacteriaceae	22	24-35
	Flaviviridae	37	24-29
	Helicobacteraceae_95	1	26
	Hepadnaviridae	3	24
	Herpesviridae	10	24-26
	Inoviridae_512	1	25
	Listeriaceae_3v6	1	26
	Moraxellaceae	3	25-26
	Mycobacteriaceae	3	24-31
	Myoviridae_1173	1	24
	Neisseriaceae_969	1	26
	Orthomyxoviridae	3	24-29
	Papillomaviridae	35	24-30
	Pasteurellaceae	3	24-58
	Retroviridae	53	24-30
	Rickettsiaceae	2	26-27
	Sarcocystidae	3	24-26
	Siphoviridae	2	26-27
	Spirochaetaceae	36	24-30
	Streptococcaceae_968	1	27
	Vibrionaceae_108v6	1	24
	Troy nodule extraction blank (P17TB) #2	Enterobacteriaceae	2
Moraxellaceae_801		1	54
Papillomaviridae_15		1	35
Streptococcaceae		3	41
Roman adult (P16RM) #1	Clostridiaceae	3	27-54
	Myoviridae_1725	1	40

Sample ID	Probe ID	# Reads matching probes	bp range	
Roman adult (P17RM) #1	Streptococcaceae_1794	1	50	
Roman adult (P23RM) #2	Protozoa	41	24-29	
	Bacillaceae_1205	1	24	
	Brucellaceae	6	24-27	
	Burkholderiaceae	3	24-51	
	Campylobacteraceae	3	24	
	Clostridiaceae	6	33-54	
	Corynebacteriaceae_93	1	24	
	Enterobacteriaceae	28	24-46	
	Flaviviridae	23	24-30	
	Hepadnaviridae	7	24-25	
	Herpesviridae	12	24-27	
	Lactobacillaceae_197	2	24-28	
	Listeriaceae	2	24-25	
	Methylococcaceae_168	1	24	
	Moraxellaceae	2	30-42	
	Mycobacteriaceae	7	24	
	Myoviridae	9	24-32	
	Neisseriaceae_918	1	24	
	Papillomaviridae	17	24-27	
	Paramyxoviridae_417	1	26	
	Pasteurellaceae_1346	1	26	
	Podoviridae_1676	8	24-29	
	Retroviridae	33	24-27	
	Rickettsiaceae_286	1	25	
	Siphoviridae_4767	2	24-25	
	Spirochaetaceae	16	24-27	
	Staphylococcaceae_1296	1	32	
	Streptococcaceae_1911	1	26	
	Trypanosomatidae	2	24	
	Vibrionaceae	6	24-44	
	Roman adult (P24RM) #2	Protozoa	10	24-29
		Brucellaceae_336	2	25-26
		Burkholderiaceae_2886	1	29
Clostridiaceae		5	24-50	
Enterobacteriaceae		32	24-28	

	Probe ID	# Reads matching probes	bp range
	Flaviviridae	8	24-27
	Herpesviridae	6	24-25
	Moraxellaceae	4	29,52
	Myoviridae_1661	3	27-35
	Neisseriaceae_712	1	27
	Papillomaviridae	10	24-28
	Pasteurellaceae	2	24
	Podoviridae_1971	1	24
	Porphyromonadaceae	2	38-53
	Poxviridae_675	1	24
	Retroviridae	20	24-26
	Spirochaetaceae	6	24-26
	Vibrionaceae_1455	1	26
Roman juvenile (P19JV) #1	Protozoa	1	24
	Enterobacteriaceae_8557	1	24
Roman juvenile (P20JV) #1	Protozoa	32	24-29
	Bacillaceae	3	24-25
	Brucellaceae	3	24
	Burkholderiaceae	5	24-27
	Enterobacteriaceae	27	24-27
	Flaviviridae	24	24-28
	Helicobacteraceae_469	1	24
	Hepadnaviridae	6	24-25
	Herpesviridae	15	24-26
	Listeriaceae	2	24-26
	Moraxellaceae	4	24-26
	Mycobacteriaceae	3	24
	Neisseriaceae	30	26-54
	Orthomyxoviridae_8239	1	24
	Papillomaviridae	12	24-26
	Paramyxoviridae	2	25-26
	Pasteurellaceae	4	24-41
	Porphyromonadaceae	24	31-57
	Retroviridae	11	24-28
	Rickettsiaceae_20v6	1	24
Siphoviridae_6684	1	24	
Spirochaetaceae	33	24-60	

	Probe ID	# Reads matching probes	bp range
	Staphylococcaceae	4	24-25
	Streptococcaceae	26	26-55
	Vibrionaceae_1987	1	24
Roman juvenile (P25JV) #2	Protozoa	3	24-25
	Bacillaceae_1015	1	24
	Burkholderiaceae_351	1	52
	Enterobacteriaceae	8	24-28
	Flaviviridae	5	24-26
	Helicobacteraceae_32v6	1	28
	Hepadnaviridae	2	25-26
	Herpesviridae_1067	1	25
	Moraxellaceae	2	42-43
	Myoviridae_2159	1	32
	Papillomaviridae	5	24-27
	Retroviridae	9	24-28
	Spirochaetaceae	3	26-27
	Staphylococcaceae	1	26
	Vibrionaceae_1826	1	24
Roman juvenile (P26JV) #2	Protozoa	13	24-27
	Brucellaceae_123	1	24
	Burkholderiaceae	2	24
	Enterobacteriaceae	24	24-43
	Flaviviridae	15	24-27
	Hepadnaviridae	9	24-27
	Herpesviridae	2	24
	Moraxellaceae	7	24-51
	Mycobacteriaceae_874	1	26
	Myoviridae	2	24,35
	Neisseriaceae	4	29-48
	Papillomaviridae	10	24-27
	Podoviridae_7v6	1	24
	Porphyromonadaceae	2	24
	Retroviridae	13	24-28
	Siphoviridae_4767	1	26
	Spirochaetaceae	2	24
	Staphylococcaceae	15	34-64
	Streptococcaceae	2	38-41

	Probe ID	# Reads matching probes	bp range
	Vibrionaceae_842	1	24
Maritime Archaic (P22BT) #1	Protozoa	28	24-26
	Bacillaceae	7	25-42
	Burkholderiaceae_549	1	24
	Clostridiaceae_1016	1	24
	Enterobacteriaceae	20	24-28
	Flaviviridae	15	24-25
	Hepadnaviridae	2	24
	Herpesviridae	9	24-26
	Inoviridae_511	1	25
	Methylococcaceae_276	1	24
	Moraxellaceae_792	1	54
	Mycobacteriaceae	3	24
	Myoviridae_1661	1	31
	Neisseriaceae	183	24-59
	Orthomyxoviridae_7622	1	26
	Papillomaviridae	16	24-28
	Pasturellaceae	54	24-57
	Podoviridae	2	24-25
	Porphyromonadaceae	9	34-56
	Retroviridae	11	24-27
	Rickettsiaceae_18v6	1	24
	Spirochaetaceae	6	24-57
	Staphylococcaceae	3	24-26
Streptococcaceae	210	24-62	
Vibrionaceae_842	4	24-26	
Maritime Archaic (P23BT) #1	Brucellaceae_58	1	24
	Enterobacteriaceae_6675	1	25
Maritime Archaic (P27BT) #2	Protozoa	4	24-26
	Burkholderiaceae_2282	1	24
	Enterobacteriaceae_10507	1	27
	Flaviviridae_5207	1	26
	Herpesviridae_198	1	25
	Moraxellaceae_259_	1	32
	Mycobacteriaceae_462	1	24
	Papillomaviridae_3940	1	24
	Podoviridae_412	1	26

	Probe ID	# Reads matching probes	bp range
	Retroviridae	4	24-28
Maritime Archaic (P28BT) #2	Burkholderiaceae_1154	1	24
	Enterobacteriaceae	4	26-46
	Flaviviridae_5941	1	24
	Herpesviridae_445	1	25
	Moraxellaceae	4	34-47
	Retroviridae	3	24
Troy sediment (P11TY) #2	Bacillaceae_327	1	38
	Enterobacteriaceae	3	48-56
	Staphylococcaceae	2	40-44
Troy sediment extraction blank (P12TY) #2	Clostridiaceae_1165	1	45
Italy sediment (P13TY) #2	Protozoa	2	25-30
	Enterobacteriaceae_4933	1	43
	Staphylococcaceae_1296	1	43
Italy sediment extraction blank (P14TY) #2	Enterobacteriaceae	2	41-42

Table S2. Taxonomic assessment of sequence data, full results.

Sample ID	MEGAN reads total	MEGAN assigned reads	Taxonomic IDs (Family, Genus, Species)	# reads assigned
Black Death (P06BD) #1	103	89	<i>Enterobacteriaceae</i>	86
			<i>Yersinia</i>	58
			<i>Y. pestis</i>	32
			No hits	14
Black Death (P07BD) #2	1,795	1,558	<i>Enterobacteriaceae</i>	475
			<i>Yersinia</i>	482
			<i>Y. pestis</i>	519
			<i>Clostridiaceae</i>	0
			<i>Clostridium</i>	2
			<i>C. tetani</i>	2
			<i>C. botulinum</i>	1
			<i>Staphylococcaceae</i>	0
			<i>Staphylococcus</i>	2
			<i>S. aureus</i>	1
			<i>S. pneumoniae</i>	1
			<i>Moraxellaceae</i>	0
			<i>Acinetobacter</i>	1
			<i>A. baumannii</i>	1
<i>Homo</i>	0			
<i>Homo sapiens</i>	1			
No hits	237			
Justinian (P01JT) #1	16	3	<i>Clostridiaceae</i>	0
			<i>Clostridium</i>	1
			<i>C. botulinum</i>	1
			<i>Enterobacteriaceae</i>	1
No hits	13			
Justinian (P01JT) #2	174	54	<i>Clostridiaceae</i>	0
			<i>Clostridium</i>	3
			<i>C. botulinum</i>	3
			<i>Alcaligenaceae</i>	0
			<i>Castellaniella</i>	0
			<i>C. defragrans</i>	1
			<i>Commamonadaceae</i>	5
<i>Enterobacteriaceae</i>	0			
<i>Yersinia</i>	1			

			<i>Pasturellaceae</i>	0
			<i>Haemophilus</i>	0
			<i>H. influenzae</i>	1
			<i>H. parasuis</i>	1
			<i>Moraxellaceae</i>	0
			<i>Acinetobacter</i>	21
			<i>A. baumannii</i>	2
			No hits	120
Mummy - child (P03MM) #1	18	18	<i>Hepadnaviridae</i>	0
			<i>Orthohepadnavirus</i>	0
			Hepatitis B virus	14
			<i>Staphylococcaceae</i>	0
			<i>Staphylococcus</i>	1
			<i>S. aureus</i>	1
			<i>Clostridiaceae</i>	0
<i>Clostridium</i>	0			
			<i>C. botulinum</i>	1
Mummy - child (P03MM) #2	45	24	<i>Staphylococcaceae</i>	0
			<i>Staphylococcus</i>	8
			<i>Clostridiaceae</i>	0
			<i>Clostridium</i>	0
			<i>C. botulinum</i>	2
			<i>C. novyi</i>	1
			<i>Enterobacteriaceae</i>	1
			<i>Moraxellaceae</i>	0
			<i>Acinetobacter</i>	0
			<i>A. baumannii</i>	1
			<i>Hepadnaviridae</i>	0
			<i>Orthohepadnavirus</i>	0
			Hepatitis B virus	3
No hits	21			
Mummy - child (P04MM) #2	1,336	1,155	<i>Staphylococcaceae</i>	0
			<i>Staphylococcus</i>	94
			<i>S. aureus</i>	34
			<i>S. saprophyticus</i>	1
			<i>S. epidermidis</i>	18
			<i>S. simulans</i>	2
			<i>S. warneri</i>	1
			<i>Prevotellaceae</i>	0

			<i>Prevotella</i>	0
			<i>Prevotella dentalis</i>	1
			<i>Clostridiaceae</i>	0
			<i>Clostridium</i>	0
			<i>C. botulinum</i>	18
			<i>Streptococcaceae</i>	0
			<i>Lactobacillaceae</i>	1
			<i>Streptococcus</i>	1
			<i>Enterobacteriaceae</i>	11
			<i>Burkholderiaceae</i>	0
			<i>Burkholderia</i>	1
			<i>Moraxellaceae</i>	0
			<i>Acinetobacter</i>	1
			<i>A. baumannii</i>	2
			<i>A. venetianus</i>	1
			<i>Aspergillaceae</i>	0
			<i>Aspergillus</i>	0
			<i>A. niger</i>	1
			<i>Hepadnaviridae</i>	0
			<i>Orthohepadnavirus</i>	0
			Hepatitis B virus	747
			No hits	181
Mummy - adult (P05MM) #2	514	387	<i>Staphylococcaceae</i>	0
			<i>Staphylococcus</i>	2
			<i>Enterobacteriaceae</i>	133
			<i>Proteus</i>	17
			<i>P. mirabilis</i>	75
			<i>P. vulgaris</i>	2
			<i>Moraxellaceae</i>	0
			<i>Acinetobacter</i>	1
			<i>Aspergillaceae</i>	0
			<i>Aspergillus</i>	3
			<i>A. niger</i>	2
<i>A. fumigatus</i>	6			
<i>A. ustus</i>	1			
			No hits	127
Mummy - adult (P06MM) #2	5,730	4,452	<i>Bacillaceae</i>	4
			<i>Staphylococcaceae</i>	0
			<i>Staphylococcus</i>	46

			<i>Enterococcaceae</i>	4
			<i>Clostridiaceae</i>	0
			<i>Clostridium</i>	163
			<i>C. botulinum</i>	3,977
			<i>C. novyi</i>	175
			<i>C. perfringens</i>	4
			No hits	1,278
Troy nodule (P09TY) #2	2,306	2,185	<i>Staphylococcaceae</i>	2
			<i>Staphylococcus</i>	1,856
			<i>S. aureus</i>	4
			<i>S. haemolyticus</i>	4
			<i>S. saprophyticus</i>	241
			No hits	120
Troy nodule extraction blank (P10TY) #2	2	2	<i>Moraxellaceae</i>	0
			<i>Acinetobacter</i>	0
			<i>A. venetianus</i>	2
Troy nodule (P15TB) #2	1,968	1,683	<i>Staphylococcaceae</i>	7
			<i>Staphylococcus</i>	1,340
			<i>S. aureus</i>	1
			<i>S. epidermidis</i>	1
			<i>S. saprophyticus</i>	3
			<i>Enterobacteriaceae</i>	1
			No hits	285
Troy nodule (P16TB) #2	1,161	774	<i>Bifidobacteriaceae</i>	0
			<i>Gardnerella</i>	0
			<i>G. vaginalis</i>	1
			<i>Staphylococcaceae</i>	5
			<i>Staphylococcus</i>	519
			<i>S. aureus</i>	1
			<i>S. saprophyticus</i>	213
			<i>Enterobacteriaceae</i>	0
			<i>Salmonella</i>	1
			<i>Pasturellaceae</i>	0
			<i>Haemophilus</i>	0
			<i>H. influenzae</i>	1
			<i>Homo</i>	0
			<i>Homo sapiens</i>	1
			No hits	387
	4	2	<i>Clostridiaceae</i>	0

Roman adult (P16RM) #1			<i>Clostridium</i>	1
			<i>Myoviridae</i>	0
			<i>Clostridium</i> phage c-st	1
			No hits	2
Roman adult (P17RM) #1	1	1	<i>Streptococcaceae</i>	0
			<i>Streptococcus</i>	1
Roman adult (P23RM) #2	244	13	<i>Streptococcaceae</i>	0
			<i>Streptococcus</i>	0
			<i>S. pneumoniae</i>	1
			<i>Clostridiaceae</i>	0
			<i>Clostridium</i>	0
			<i>C. botulinum</i>	4
			<i>C. novyi</i>	1
			<i>Enterobacteriaceae</i>	2
			<i>Serratia</i>	1
			No hits	231
Roman adult (P24RM) #2	115	9	<i>Porphyromonadaceae</i>	0
			<i>Tannerella</i>	0
			<i>T. forsythia</i>	2
			<i>Clostridiaceae</i>	0
			<i>Clostridium</i>	1
			<i>C. botulinum</i>	1
			<i>Moraxellaceae</i>	0
			<i>Acinetobacter</i>	3
			No hits	106
Roman juvenile (P19JV) #1	2	0	No hits	2
Roman juvenile (P20JV) #1	277	87	<i>Porphyromonadaceae</i>	0
			<i>Porphyromonas</i>	0
			<i>P. gingivalis</i>	10
			<i>Tannerella</i>	0
			<i>T. forsythia</i>	11
			<i>Streptococcaceae</i>	0
			<i>Streptococcus</i>	14
			<i>S. constellatus</i>	4
			<i>S. pasteurianus</i>	1
			<i>Neisseriaceae</i>	0
			<i>Neisseria</i>	2
			<i>N. elongata</i>	4

			<i>N. gonorrhoeae</i>	4
			<i>N. lactamica</i>	12
			<i>Spirochaetaceae</i>	0
			<i>Treponema</i>	4
			<i>T. denticola</i>	14
			<i>T. putidum</i>	1
			No hits	190
Roman juvenile (P25JV) #2	44	1	<i>Moraxellaceae</i>	0
			<i>Acinetobacter</i>	0
			<i>A. baumannii</i>	1
			No hits	43
Roman juvenile (P26JV) #2	127	24	<i>Staphylococcaceae</i>	
			<i>Staphylococcus</i>	9
			<i>S. aureus</i>	1
			<i>Streptococcaceae</i>	0
			<i>Streptococcus</i>	0
			<i>S. oralis</i>	1
			<i>Neisseriaceae</i>	0
			<i>Neisseria</i>	1
			<i>Moraxellaceae</i>	0
			<i>Acinetobacter</i>	2
			<i>A. baumannii</i>	1
			<i>A. oleivorans</i>	1
			No hits	103
Maritime Archaic (P22BT) #1	590	301	<i>Neisseriaceae</i>	0
			<i>Neisseria</i>	72
			<i>N. meningitidis</i>	14
			<i>N. elongata</i>	14
			<i>N. lactamica</i>	3
			<i>N. gonorrhoeae</i>	1
			<i>Streptococcaceae</i>	0
			<i>Streptococcus</i>	142
			<i>S. oralis</i>	7
			<i>S. pneumoniae</i>	5
			<i>S. oligofermentans</i>	1
			<i>S. parasanguinis</i>	1
			<i>S. sanguinis</i>	2
			<i>Pasturellaceae</i>	17
			<i>Haemophilus</i>	19

			<i>H. influenzae</i>	2
			<i>H. parainfluenzae</i>	2
			<i>Spirochaetaceae</i>	0
			<i>Treponema</i>	1
			<i>T. denticola</i>	3
			<i>Porphyromonadaceae</i>	0
			<i>Tannerella</i>	0
			<i>T. forsythia</i>	8
			No hits	288
			Not assigned	1
Maritime Archaic (P23BT) #1	2	0	No hits	2
Maritime Archaic (P27BT) #2	16	1	Gammaproteobacteria (Class)	1
Maritime Archaic (P28BT) #2	14	7	<i>Enterobacteriaceae</i>	3
			<i>Moraxellaceae</i>	0
			<i>Acinetobacter</i>	1
			<i>A. baumannii</i>	1
			No hits	7
Troy sediment (P11TY) #2	6	5	<i>Bacillaceae</i>	0
			<i>Bacillus</i>	1
			<i>Enterobacteriaceae</i>	1
			<i>Escherichia</i>	0
			<i>E. coli</i>	1
			No hits	1
Troy sediment extraction blank (P12TY) #2	1	0	No hits	1
Italy sediment (P13TY) #2	4	2	Bacilli (Class)	1
			No hits	2
Italy sediment extraction blank (P14TY) #2	2	2	Bacteria (Super Kingdom)	2

Supplementary References

- Altschul, S.F., Gish, W., Miller, W., Myers, E.W., Lipman, D.J. Basic local alignment search tool. *J. Mol. Biol.* **215**, 403–410, (1990).
- Bos, K.I. *et al.* A draft genome of *Yersinia pestis* from victims of the Black Death. *Nature* **478**, 506-510, (2011).
- Devault, A.M. *et al.* Second-pandemic strain of *Vibrio cholerae* from the Philadelphia cholera outbreak of 1849. *New Engl. J. Med.* **370**, 334-340 (2014a).
- Devault, A.M. *et al.* Ancient pathogen DNA in archaeological samples detected with a Microbial Detection Array. *Sci. Rep.* **4**, 42-45, (2014b).
- Devault, A.M. *et al.* An ancient emerging infection as a cause of maternal sepsis in Late Byzantine Troy (In Review) (n.d.).
- Huson, D.H., Auch, A.F., Qi, J., Schuster, S.C. MEGAN analysis of metagenomic data. *Genome Res.* **17**(3), 377-386 (2007).
- Kircher, M., Sawyer, S., Meyer, M. Double indexing overcomes inaccuracies in multiplex sequencing on the Illumina platform. *Nucleic Acids Res.* **40**, e3, (2012).
- Langmead B, Salzberg S. Fast gapped-read alignment with Bowtie 2. *Nature Methods* **9**, 357-359, (2012).
- Marciniak, S. *et al.* *Plasmodium falciparum* malaria in 1st-2nd c. A.D. southern Italy. *Curr. Biol.*, In press, (2016).
- McLoughlin, K. S. Microarrays for pathogen detection and analysis. *Brief. Funct. Genom.* **10**, 342–353, doi: 10.1093/bfgp/elr027, (2011).
- Meyer, M., Kircher, M. Illumina sequencing library preparation for highly multiplexed target capture and sequencing. *Cold Spring Harb. Protoc.* **6**, 1-7, (2010).
- Schwarz. C. *et al.* New insights from old bones: DNA preservation and degradation in permafrost preserved mammoth remains. *Nucleic Acids Res.* **37**, 3215–3229, (2009).

Wagner, D.M. *et al.* *Yersinia pestis* and the plague of Justinian 541-543 AD: a genomic analysis. *Lancet Infect. Dis.*14, 319-326, (2014).

CHAPTER 5: DISCUSSION AND CONCLUSIONS

The three papers of this thesis encompass critical questions surrounding the integration of ancient DNA as part of a multi-faceted framework to explore disease in the past. The fundamental questions addressed here are: 1. Is the presumption of catastrophic malaria in Imperial period Italy (1st-5th c. A.D.) amenable to investigation using molecular evidence from different localities in the southern peninsula? If so, is it possible to identify a causative species? 2. To what degree is it possible to identify factors contributing or hindering the emergence and maintenance of malaria within specific localities in Imperial southern Italy? 3. How effective is ancient DNA for assisting researchers to address pathogen-pathogen interactions for a range of endemic (or acute) diseases under conditions of non-catastrophic morbidity and mortality? I address these questions through the framework of an integrated biocultural and ecosocial epidemiological approach that grounds the ancient pathogen DNA data in socio-historical and geographical contexts. Most notably, my research demonstrates through the successful recovery of a partial *P. falciparum* mitochondrial genome that malaria was present in two adults from Velia and Vagnari during the Imperial period (1st-2nd c. A.D.) and contributes to highlighting the biosocial context of this disease in the studied localities.

Although there is incomplete knowledge surrounding the broad evolutionary history of malaria in Europe, and more specifically, the extent of its influence in ancient Rome, the predominant discourse (largely informed by

classical literary sources) infers that malaria had disastrous effects on morbidity and mortality in a period of socio-political and economic change for the Empire (Bruce-Chwatt & de Zulueta 1980; Brunt 1971; Sallares, 2002; Scheidel, 2004). This lack of evidence led me to ask whether the scope of malaria's influence could be detected using an anthropological and ancient DNA approach that integrated molecular results with literary and archaeological evidence.

The answer is inherently complex. Ancient textual sources do not provide evidence for the specific species of “malaria” broadly referenced therein, and so, the ancient DNA results directly implicate a causative *Plasmodium* agent. The confirmation of only *P. falciparum* in two individuals (out of 58), one from Vagnari (a remote rural agricultural site) and one from Velia (a minor port city) attests to not only idiosyncrasies in retrieving minute pathogen fractions using ancient DNA technology, but confounding complexities from clinical to inherited immunity that frames individual susceptibility alongside unknown transmission patterns in Imperial period Italy (e.g., endemic to epidemic). However, this is the first successful recovery of a genomic signature of *P. falciparum* malaria from adults in Imperial southern Italy, and from more than one site. The absence of *Plasmodium* genomic signatures in individuals from Portus (which does not preclude its presence), a presumably ideal site to “expect” malaria due to its unique ecology (e.g., coastal marshes and lagoons) and relatively “urban” context (e.g., economically associated with the core of the Roman Empire and sustained higher population densities due to immigration) suggests a potentially dynamic

epidemiology of this “Roman malaria” in these study locations. As discussed in Chapter 3, the influences of acquired or inherited immunity (e.g., the thalassemiias or G6PD deficiency) function under complex pathways of malaria transmission that may undetectably influence the post-mortem detection of *Plasmodium* parasites from the individuals associated with Velia, Vagnari, and Portus Romae. The molecular results are consistent with the historical record, in so far as confirming malaria was present; however, inferences of endemicity, (e.g., a stable or unstable malaria burden) cannot be addressed with the available evidentiary sources for the studied localities (e.g., molecular, archaeological, historical). Accordingly, I argue that ancient DNA evidence, considered in an ecosocial context, complements the historical narrative and provides insights about the lived experience of malaria in diverse social, economic, and ecological contexts. Further to this, I address the importance of distinguishing pathogen exposure from disease manifestation when applying ancient DNA methods to investigate “invisible” pathogens.

This research also addresses methodological and theoretical issues surrounding the identification of pathogens in skeletal assemblages where multiple evidentiary sources provide limited information on disease-associated pathogens. For example, infectious diseases were presumed as a significant structuring force in the Roman world; however, the documentation of epidemics or outbreaks is scarce due to the fragmentary survival of textual sources (Nutton, 2004). The Antonine Plague (165-180 A.D.) is an excellent case in point, as its

origin or spread is not traceable due to an absence of demographic evidence, while documentation of the plague was incomplete, and multiple causative agents have been proposed (i.e., smallpox, measles, bubonic plague, yellow fever, or typhoid fever) (Littman & Littman, 1973; Cunha & Cunha, 2008). Thus, the historical record may indicate that particular diseases were significant, in a sense “expected” in a given context (such as ideas of the “Roman malaria”), but much of the evidence remains undocumented, largely owing to the preservation biases in the surviving literary, skeletal, and archaeological records. The application of molecular approaches capable of targeting a suite of pathogens without *a priori* knowledge of their presence in a locality further expands the scope of identifying pathogens, and pathogen-pathogen interactions, within dynamic biosocial landscapes.

Catastrophic Malaria and the Molecular Evidence

As discussed in Chapter 3, malaria is an ancient disease that has long impacted human populations, but is difficult to directly identify in the skeletal record. However, the causative *Plasmodium* agent can be investigated in antiquity, as shown by the detection of *P. falciparum* in two Imperial period Italian adults. Even with the use of ancient DNA methods to demonstrate the presence of *Plasmodia* in human tissue, these methods cannot determine whether the individual was exposed to the pathogen or had malaria (i.e., a given expression of a particular symptomology). However, paleopathological evidence can provide additional evidence to address this, as active cribra orbitalia and

porotic hyperostosis indicated in the Vagnari individual, and cribra orbitalia in the remodelling phase for the Velia individual, are suggestive of non-specific physiological perturbations. Ultimately, detecting specific pathogenic signatures demonstrates presence, but says nothing about the cause of death of the individual or the prevalence of the pathogen within a particular skeletal assemblage. In this sense, it is necessary to move beyond a conceptual model of “single pathogen, single host, single disease” (Dutour, 2013: 148) to characterize the human-pathogen relationship. In order to frame the molecular results, it is beneficial to consider the interplay of individual immunity and susceptibility in malaria pathogenesis.

Malaria pathogenesis impacts its post-mortem recovery

The biological pathways affecting malaria transmission, vector efficiency, and host response are structured not only within the complex genomic landscape of *P. falciparum* (as it extends to its human host and vector), but the epidemiological environment as well. The *Plasmodium* parasite adapts in response to constant feedback within the human host (e.g., antibody type, antigenic repertoire, virulence) and epidemiological environment (e.g., vector abundance, persistence of infected gametocytes for uptake within the host) (Mackinnon & Marsh, 2010). The pathogenesis of malaria, as related to immune system functionality, duration of infection, or severity of symptoms, is inherently an individual biological response. As *P. falciparum* genomic signatures were only recovered from two Imperial Italian adults, this is a salient point. The level

of parassitaemia (parasitized red blood cells) and stage of infection (e.g., parasite sequestration in the liver or haematogenous spread) impacts the “abundance” of mitochondrial genomes accessible from *Plasmodium* parasites in the bloodstream, not only during the course of infection, but after parasite clearance. In clinical scenarios, the amount of host and parasite DNA directly affects the recovery of *Plasmodium* genomic data (DeBarry et al., 2013), where for example, Melnikov et al. (2011) show *P. falciparum* was 0.1% of the total DNA in a one-year old blood clot sample. Depending on the stage of infection and host immune system functionality, the efficacy of parasite clearance by the spleen (whether dead/dying parasites remain in the peripheral blood) or sequestration of infected red blood cells (less effective with increasing parassitaemia) (Chotivanich et al., 2002), impacts the post-mortem detection of parasitic genomic signatures, as the level of infection (i.e., high parasite load) does not necessarily correlate with successful recovery of genomic signatures.

Such low fractions of surviving *P. falciparum* DNA within human genomic constituents are greatly magnified in ancient human samples, as evident in Chapter 2 of this thesis. *P. falciparum* was less than 0.006% of the taxonomically identifiable sequence reads of the metagenomic pool in the Imperial Italian adults. The novel techniques used in my research, primarily *Plasmodium* spp. mitochondrial genome capture, demonstrates it is successful in recovering these signatures; however, the caveat is that (as with any pathogen), ancient parasites may go undetected not only in individuals with low-levels of

infection as typical of *P. vivax* and *P. malariae*, but even among those who died at the peak of infectivity. It stands to reason that the “actual” prevalence of malaria in these Imperial period Italian samples is under-represented.

Similarly, the molecular results cannot equate *P. falciparum* (the causative species) to malaria (i.e., clinical symptomology). Essentially, this rests on an inability to differentiate between “malaria-infection” (asymptomatic carriage of the parasite) and “malaria-disease” (carriage of the parasite and manifests symptoms) (Manguin et al., 2008). Individual immune status and the nature of malaria transmission whether it is stable, unstable (fluctuates), or epidemic, structures this individual risk, which is further dependent on local epidemiological conditions – all of which affect the parasite load tolerated by an individual (Manguin et al., 2008). This complexity is at the core of exploring the dynamics of malaria at Velia, Vagnari, and Portus Romae.

As illustrated in Chapter 3, I suggest the complexity of human responses to malaria via acquired or inherited immunity alongside anthropogenic activity and ecology differentially influence exposure pathways to malaria that are inherently local, particularly as the nature of malaria transmission is unknown for Imperial period Italy. Interpretations of textual descriptions are equivocal, such as the Hippocratic Corpus referencing high mortality rates in children from periodic fevers (Retief & Cilliers, 2004), generally the susceptible cohort in high intensity malaria transmission regions, which suggests stable scenarios where adults subsequently acquire clinical immunity (i.e., asymptomatic carriers) (Ali et al.,

2008; Carter & Mendis, 2002). Conversely, unstable and epidemic malaria as fluctuations in exposure affect all age groups, and is inferred from atypical weather events (e.g., Tiber River floods, excess humidity), and the migration of non-immune individuals to an endemic area (e.g., from the slave trade or war campaigns) (Bruce-Chwatt & de Zulueta, 1980; Carter & Mendis, 2002; Sallares, 2002; Scheidel, 2003, 2009).

A further complicating factor is the number of bites by vectors, which is not detectable in antiquity, can create a spectrum of possibilities for the malaria burden in the disparate ecological and social contexts of Vagnari, Velia, and Portus Romae (Carter & Mendis, 2002). This directly affects individual parasite tolerance, as individuals with greater (continued) exposure to infectious vectors may only manifest symptoms at higher parasite densities than those with less or infrequent exposure (Ali et al., 2008; Carter & Mendis, 2002; Wilairatana et al., 2013). Even with repeated exposure, individuals may remain susceptible to infection as pre-blood stage infection (parasites invading the liver) does not induce host immune responses, and being an asymptomatic carrier may lead to recrudescence (Carter & Mendis, 2002; Crompton et al., 2014). Accordingly, as noted by Carter, Mendis and Roberts (2000, p. 1408) the intensity of transmission and risk of malaria are “distributed in a highly uneven way across any malarious landscape”. Thus, although the nature of malaria at the localities of Velia, Vagnari, and Portus Romae is undetectable, I propose an alternative scenario of potentially uneven (multifaceted) intensity and distribution that is highly

responsive to the contextual determinants at these localities, rather than the narrative of a singular scourge across ancient Italy. Essentially, in this scenario, instability may be introduced by seasonal changes or weather events, alongside the possibility for epidemics, and accordingly, complexity in immunity acquisition (i.e., parasite tolerance). In consideration of “malaria-infection” and “malaria-disease” as dynamic outcomes of the epidemiological setting, it merits recognition that it is possible the individuals at the study sites were not necessarily widely decimated by a malarious scourge and thus, requires open-ended interpretations of the molecular evidence as part of this historical record.

Reconciling the genomic evidence with the historical record

The recovery of *P. falciparum* genomic signatures is direct evidence of this causative agent in the specific geographical and historical contexts of Velia and Vagnari (1st-2nd c. A.D.), to a degree that is not possible with the literary record. The molecular data complements the textual sources; however, attempting to address the catastrophic nature of this disease in Imperial Italy is equivocal, as alluded to in the above discussion on the dynamics of the malaria burden.

The richness of the Roman historical narrative about “malaria” is not in dispute; however ancient texts are products of a specific sociocultural context of understanding and experiencing disease (Rosenberg, 1992). The diversity of medical sects that existed during this time (Dogmatist, Empiricist, Methodist, and Pneumatic) complicates the interpretation of disease descriptions (e.g., causation, significant symptoms, and prognosis) as such theoretical conceptualizations or

cultural meanings are not necessarily explicit or transmitted through literary evidence (Cruse, 2004; Scarborough, 1969).

The etiological designation of a causative *Plasmodium* species based on modern understandings of the disease is confounded by ancient descriptions of fever symptomology, geographical association, and epidemiological patterns. Within the Hippocratic tradition, for instance, fevers were considered to be a disease, rather than a symptom, as the focus was on humoral imbalances or pre-existing vulnerable constitutions (Nutton, 2004). Fevers were broadly attributed to imbalances in humoral fluids, blockage of pores trapping heat, or breathing in noxious vapours (Nutton, 2004; Scarborough, 1969). Although Hippocrates first described periodic fevers (e.g., tertian, semi-tercian, quartan, quotidian), there were also descriptions of septans and nonans (Cunha & Cunha, 2008). Accordingly, I suggest that the category of “fevers” is a dynamic entity in the Roman experience of disease, and not simply a unique correlation to “malaria” in the biomedical sense.

Ascribing a species-specific label to these periodic fevers (as *P. falciparum*, *P. vivax* or *P. malariae*) fixes the nature of malaria as solely a biological phenomenon. For example, the death of Philiscus in Hippocrates’ “*Of the Epidemics*” has been ascribed to *P. falciparum* due to descriptions of black urine with acute tertian fever (as noted by Grmek, 1991). This inference, however, projects modern clinical diagnoses of complications from malaria onto the past; as “blackwater fever” was only noted as a complication of malaria in

1898 (Grmek, 1991). A related challenge is the non-specificity of periodic fevers, as other febrile illnesses may show similar symptomology, such as typhoid, brucellosis, pneumonia, and other protozoan diseases (Orsel et al., 2015), while not all individuals will manifest the “classic” symptomology of febrile paroxysms (e.g., chills, fever, sweats, remission) (Sykes & Mabunda, 2002). Overall, this may lead to potential conflation (or over-representation) in the documentation of “malaria” historically.

The idea that “malaria” is ancient has been perpetuated in retrospective diagnoses of the disease in literary texts and paleopathological inquiries. The word “mal’aria” derives from “mal aere” in the 15th c. A.D., meaning bad or corrupted air. The term “mal’aria” was popularized by Walpole in 1740, as “a horrid thing called the ‘mal’aria’ which comes to Rome every summer and kills one” (MacArthur, 1951: 199; Neghina et al., 2010). “Malaria” is written without the apostrophe in the 19th c. A.D. and the mode of transmission and infection remained entrenched in 17th c. A.D. miasma theory as noxious vapours emanating from decaying matter in swamps and marshes (Major, 1978; Neghina et al., 2010). Translating ancient texts constructed in a specific context of experiencing disease, and equating these periodic fevers arising from noxious vapours to the biomedical epidemiology of malaria remains challenging.

As an outcome of the permanence of malaria as a disease entity, it has also been naturalized and described in a static epidemiological pattern. In particular, the seasonal pattern of occurrence (i.e., late summer and early autumn) is

emphasized as inherent to the Imperial context and placed alongside Roman cultural beliefs that connect the environment to health (Cunha & Cunha, 2008; Sallares, 2002). For example, marshes were pestilential in the summer but healthy in winter, while those with seawater connections were comparatively healthier than ones isolated from such infiltrations (Sallares, 2002). This view disconnects malaria from its complex biological, social, and ecological context, as Shaw (1996) argues contemporary concerns of malaria elimination programmes increased attention to the disease in antiquity. The diverse ecological environment of ancient Greece and Rome were simplified to have been broadly conducive to malaria, even though it is evident today that the distribution of malaria is heterogeneous (see Bejon et al., 2010).

This tendency to naturalize malaria epidemiology is also common to contemporary settings. For example, biomedical definitions of malaria emphasize measurable biological components (e.g., a particular set of symptoms, such as fevers, chills, and anemia) separated from unpredictable factors that contribute to dynamic transmission potential, such as demography (e.g., population movement, migration), economic activities (e.g., trade, resource use), social circumstances (e.g., urbanization, land use patterns), and biological factors (e.g., regional variation among strains, vectors or hosts) (Martens, 2002; NCBI, 2011; Packard & Brown, 1997).

Together, these lines of thinking have emphasized that malaria was a scourge upon the Roman Empire; yet, the alternative scenario merits recognition:

I suggest that complex dynamics in the transmission of malaria potentially created multifaceted epidemiological patterns. Accordingly, the “meaning” of the genomic results for malaria outlined in this thesis are considered alongside the literary record to explore how entangled biosocial pathways potentially framed the distribution of this pathogen within the political and economic context of the Roman Empire.

The Epidemiological Context of Malaria in Imperial Southern Italy

As a case in point, I emphasize the application of an ecosocial epidemiological approach to contextualize malaria within the Imperial period contexts of Velia, Vagnari, and Portus Romae. This extends to the proximate causal relationship between the pathogen and its vector (*Anopheles*) and the biosocial interactions from which the infections largely derive (Krieger, 1994, 2008, 2011; Singer, 2010). Scales of the ecosocial epidemiological framework as applied to the “Roman malaria” emphasize differential susceptibility framed within socio-political realms where humans “are shaped by and shape their environment” (Krieger, 2011: p. 208). In this sense, one of the purposes of my research is to propose pathways that may have connected the particular biosocial context of the study sites in Imperial Italy to the proliferation or hindrance of malaria.

Essentially, within the human population, susceptibility to malaria is heterogeneous, owing to host factors (immune response or protective polymorphisms), variable parasite virulence (e.g., parasitizing susceptible host

cells), and nature of malaria transmission (endemic, epidemic, or hyperendemic) (Bei & Duraisingh, 2013). By applying ecosocial epidemiological theory, it enables contextualization of the ancient DNA results within the diverse social and ecological localities of Velia, Vagnari, and Portus Romae, functioning as a multi-faceted explanatory framework of pathways differentially impacting malaria, rather than a singular vision of the “Roman malaria”. The inspiration for applying an ecosocial epidemiological framework in this manner is Snowden’s (2008, p. 3) reference to malaria in Italy from 1880-1962 as a “social disease, an occupational disease, and a disease of poverty and social neglect”. In this sense, I emphasize malaria as part of overarching social or economic circumstances that are dynamically manifested at Portus Romae, Vagnari, and Velia.

Snowden (2008) notes that the unification of Italy (in 1861) enhanced malaria transmission in the South compared to the North, due to intensification of the agricultural economy, resulting in ecological degradation (e.g., deforestation of the Apennines), while urbanization activities, such as railway construction, altered land use patterns and perpetuated marshes (Snowden, 2008).

Disproportionately, those in the South suffered from the perniciousness of malaria, as labourers risked exposure by working in the low-lying agricultural fields that were predisposed to malaria, and these farming regions lacked investments by leaseholders (malaria rendered these untenable for development), leading to reduced standards of living (e.g., deteriorated buildings, roads, and soil conditions) (Snowden, 2008). This scourge drastically affected life expectancy in

the malarious regions, with an average life span of 22.5 years, compared to 35.7 elsewhere in 19th c. A.D. Italy, and was structured within a complex sociopolitical web (Snowden, 2008). This suggests that malaria is not solely a biological phenomenon, but is entangled with social, economic or political networks that contribute to a highly “uneven” distribution in a given locality. Accordingly, it is possible to consider this dynamic relationship at Velia, Portus Romae, and Vagnari.

Malaria intensification under a burgeoning Empire

These contemporaneous sites of the Imperial period (1st-4th c. A.D.) were outgrowths of a burgeoning Empire that ushered in significant social and environmental changes during the 3rd c. B.C. and 2nd c. A.D. (Scheidel, 2004) with potential consequences on disease distribution. In order to explore malaria at the site-level of Velia, Vagnari, and Portus Romae, it is necessary to frame the macro-level socio-political context of the Roman Empire itself during this period. The demographic and economic expansion of the Roman state (central Italy) facilitated rapid unregulated urbanization, such as intensified agriculture (particularly in rural regions), enrichment of the Roman elite through the transfer of slaves to Italy, and public infrastructure investments creating new cities, such as the western provinces of the Empire with archaeological evidence of temples, marketplaces, and villas (Scheidel, 2004; Woolf, 1998). Increased production, trade, and the influx of people in the Mediterranean more broadly, enabled the proliferation of commercial activity (e.g., mass production of pottery for non-

elites) due to reduced transaction costs (Scheidel, 2004). However, population growth outpaced the scale of urbanization and associated infrastructure, as by the 2nd c. A.D. the population of the Empire was estimated at 60-70 million while the 2,000 cities accounted for 10-15% of this population (Scheidel, 2004). The presumed increase of malaria during this time of social, political, and economic change in the Imperial period (1st-5th c. A.D.) (as noted by Brunt, 1971; Sallares, et al., 2004; Scheidel, 2009), parallels the unification of Italy in 1861.

Accordingly, I suggest that the pattern of malaria may have been influenced from the conditions embedded within the demographic and economic expansion of the Empire during the Imperial period, with local causal factors dynamically manifested at Velia, Vagnari, and Portus Romae. The expectation for malaria in urban coastal settings, such as Portus Romae (noted by Sallares, 2002; Scheidel, 2009) is discordant with the recovery of *P. falciparum* in the minor port town of Velia and the remote rural locale of Vagnari. However, the previously noted complexity of transmission and pathogenesis alongside the challenges of recovering this minute molecular fraction, underlie these genomic results, as malaria can presumptively be present in any of these localities. Accordingly, ecosocial theory functions as an explanatory device to explore the facets of host and parasite biology alongside ecological and social circumstances at the study sites. Although a range of factors related to disease ecology and the human-environment interaction were identified, unknown factors will also have contributed to the impact of this pathogen. The unpredictability and entangled

nature of factors affecting malaria epidemiology influences the contextualization at the three localities using an integrated ancient DNA approach. However, it is still possible to explore the host-parasite-vector-environment interaction at Velia, Vagnari, and Portus Romae. Thus, I emphasize a potentially “uneven” distribution of malaria in these localities is further framed by deforestation and intensified agriculture; proximity to anopheline reservoirs; heterogeneity in susceptibility to infection, complemented by rough anti-prophylactic measures to malaria; and local individuals as similarly vulnerable to malaria, rather than a disproportionate effect on non-local “non-immune” individuals.

A) Intensification of the agricultural economy

Within changing land-use patterns that were intensified during the Imperial period, alterations of the natural landscape via deforestation (e.g., for agriculture, construction, or fuel) or developing infrastructure to support a population (e.g., aqueducts, roadways) may affect the dynamic between humans and *Anopheles* vectors. Deforestation is the most critical impact on the local environment, as it results in disruptions to the microclimate (e.g., reducing shade, changing rainfall patterns) alongside increases in water run-off and surface temperature, leading to the proliferation of surface pools (Sutherst, 2004; Yasuoka & Levins, 2007). For example, exploiting woodlands to acquire timber for use in construction activities (e.g., houses, estates, shops), ship-building at Velia and Portus (Craig et al., 2010; Crowe et al., 2009; Sperduti et al., 2012), or as a fuel source, for industrial processes at Vagnari (Small, 2014), may undetectably alter

the ecosystem resilience to vector-borne diseases. Similarly, modifications of the landscape as part of infrastructure-building, such as creating roads, canals or aqueducts, may variably affect the exposure pathways between humans and potential anopheline reservoirs, as the topographical landscapes of Velia, Vagnari or Portus Romae may differentially proliferate or hinder the distribution of malaria. However, deforestation related to agricultural development and intensified anthropogenic activity is noted to disproportionately alter the vector-parasite-human-environment relationship (O'Sullivan et al., 2008; Yasuoka & Levins, 2007).

Land clearing (deforestation) for agricultural development contributes to increases in mosquito-borne disease by promoting breeding sites (e.g., solar exposure, changes in the micronutrients of the soil, water runoff and changes to the water table), although this relationship is not always correlated (O'Sullivan et al., 2008; Yasuoka & Levins, 2007). However, the density of anophelines is significantly greater in human modified agricultural land than in forested areas (Yasuoka & Levins, 2007); while animal grazing (e.g., goats, sheep, cattle, pigs) may also contribute to the destruction of vegetation and resultant soil erosion (Hughes, 1994), which may be important in potentially influencing malaria at Velia, Vagnari, and Portus Romae. For example, at Vagnari, intensified agriculture, animal husbandry and transhumance were practiced; and the river valleys of Velia sustained agriculture, arboriculture, and pasture land, with 80 hectares under permanent cultivation (Greco, 1999; Sperduti et al., 2012). In

contrast, the proximity of Portus to the Tyrrhenian Sea with its natural ecology of dunes and lagoons, limited its available cultivable area, with the associated inference that relatively few of the citizenry were required to work the land (Sperduti et al., 2012). The uneven exposure to malaria leads to a potential suggestion that occupational activities as part of the intensity of agricultural or animal husbandry practices, preferentially exposed individuals at Velia and Vagnari to malaria, particularly due to the necessity of a significant labour force to cultivate and harvest the land. Further, if the summer harvest season coincided with a peak in malaria infectivity, as demonstrated in 19th c. A.D. Italy (see Snowden, 2008), the farmhands and labourers at Velia and Vagnari may have faced heightened risks during this time. The potential for soil erosion due to intense agriculture within a densely settled locale, as inferred for the city of Rome (Sallares, 2002), is unknown for Velia and Vagnari, although these localities were presumably not densely populated. Ultimately, the agricultural intensification at Velia and Vagnari potentially contributed to a disproportionate (uneven) risk of malaria, while Portus' connection to the core of the Empire through its trading and mercantile activities perhaps precluded such instability.

B) Spatial heterogeneity framing exposure

The location of dwellings directly reflects the stratification of Roman society and disproportionately impacts exposure pathways to infectious diseases as well as malaria co-infections. The proximity of humans to anopheline reservoirs in urban settings, such as Portus, may result in reduced exposure per

person, and promote localized areas of exposure, whereas the mixed landscapes of Velia and Vagnari may promote greater contact per person to infectious vectors. For example, the proximity of the Portus administrative centre to the canals is a parameter I initially hypothesized to influence exposure to infective vectors due to the greater frequency with which humans may contact *Anopheles* in the brackish freshwater canals (see Mazzini et al., 2011). However, this sector may have also precluded the proliferation of ecologically suitable habitats by reducing available breeding sites (e.g., replacing vegetation with roads, buildings, and shops).

Similarly, the location of human settlements within a landscape also structures the risk of malaria, since *Anopheles* are presumed to establish breeding sites in proximity to their human food source (Carter et al., 2000). For example, the Roman upper classes had imperial palaces and senatorial residences on the hills of Italy, which may have afforded some measure of protection due to ventilation, natural drainage, and an inability of *Anopheles* to fly at altitudes of 500 meters (Jetten & Takken, 1994; Sallares, 2002; Scobie, 1986). Conversely, the middle- or lower-status individuals at Portus, Vagnari and Velia, may have occupied a range of dwellings. Archaeological evidence indicates *insulae* (subdivided apartments) and mud-brick habitations at Velia (Cicala, 2013), and residential buildings at the inner harbour of Portus (Keay, 2012); while as of yet, there is no evidence for residences at Vagnari. Potentially, the lower floors of *insulae* are inferred to risk greater vector contact (e.g., via open windows or standing rain water pools at the centre) (Sallares, 2002). Similarly, the proximity

of settled areas (e.g., houses, workshops, administrative complexes) to aqueducts and sewage systems raises the issue of exposure to stagnant reservoirs from overflows or surface pools (e.g., due to seepage, floods, or increased rainfall) (Keay et al., 2005; Keiser et al., 2005). For example, the districts in Velia are bisected by streets where surface pools could proliferate (Cicala, 2013); the commercial centre near the inner harbour of Portus risks contact with stagnant pools depending on the degree of drain or sewage connections in this urban core (Keay et al., 2005); and the large complexes and range of buildings at the industrial processing centre of Vagnari may similarly affect the degree of contact with surface cesspools (Small, 2011). The distribution of vector breeding sites and human settlements may disproportionately influence the range of malaria transmission (i.e., proximity of humans to infective reservoirs) creating differential or uneven exposure (regardless of social class) (Carter, Mendis & Roberts, 2000).

It merits recognition that proximity to vector reservoirs, although highly variable within a given locality, influences the degree of risk and exposure to malaria. This important epidemiological factor is not detectable at the localities studied, but spatial heterogeneity should be considered as a factor that unpredictably alters the human-parasite-vector-environment relationship.

Confounding influences from co-infections may also predispose individuals with an existing malaria infection to heightened mortality. For example, helminth infections (e.g., as caused by fecal-transmitted contamination

in soil or water in areas of poor “sanitation”) frequently co-occur in malarious regions (Mwangi et al., 2013) and compromise the immune system response to malaria, thereby increasing its severity (Druilhe et al., 2005). This may not be uncommon in the Roman-era context, in regards to the “sanitation” infrastructure inferred from the Roman capital, as the waste removal and water-providing functions of pipes were presumed to be ineffective (O’Sullivan et al., 2008; Sallares, 2002; Scobie, 1986).

An existing malaria infection enhances host susceptibility to waterborne diseases (e.g., arising from receding floodwaters, stagnant pools, or seepage) such as gastrointestinal disorders due to *Salmonella* spp., *Shigella* spp. and *Vibrio cholerae*, by increasing permeability of the gut to invasive bacteria and/or suppressing the immune response (Cunnington, 2012; Faure, 2014; Sallares 2002). For example, the disproportionate risk of flood events at Portus due to its proximity to the Tiber River (Keay et al., 2005) and stratigraphic evidence for floods at Velia (Amato et al., 2010), may expose individuals at these localities to not only water-borne diseases, but potential worsening of an existing malaria infection. On a related note, the effect of crowd diseases as an outcome of population density, may have been more likely at Portus, as it was more “urban” than Velia, with an estimated population of 11,000 to 17,000 (Keay, 2012), leading to the potential for co-infection of tuberculosis, which exacerbates malaria due to reduced host immune response (Li & Zhou, 2013). The deleterious interactions between malaria and co-infecting pathogens is complex to infer at

Velia, Vagnari and Portus, as each will be structured according to the local conditions.

C) “Preventative” measures of malaria

In terms of responses to “malaria” or at least “fevers”, the Roman cultural emphasis on avoiding unhealthy environments (e.g., marshes, swamps) may only have been possible for the elite; however malaria is lethal regardless of class (Sallares, 2002; Scheidel, 2009). The ability to leave the city during the peak infectivity of malaria (e.g., July to October) to hillside villas provides some measure of protection against *Anopheles* vectors, as the elite were able to afford not only such villas but the loss of income from abandoning businesses (O’Sullivan et al., 2008). This was not necessarily a possibility for the middle- and low-status individuals or slaves (Sallares, 2002). Although there is no evidence for an aristocracy at Portus (Prowse et al., 2004, 2007), the migratory merchants and traders may not have remained in this region during the presumably high peaks of the malaria burden (i.e., Keay, 2012 infers a reduced population between autumn and spring when shipping activities were lessened). In contrast, the labourers at Velia and Vagnari were connected to the economic output of their relative activities, potentially affecting exposure to malaria.

D) “Local” and “non-local” individuals’ vulnerability to malaria

As a lead-in from the above argument, the presumption of increased vulnerability among non-local (“non-immune”) individuals to a malaria-endemic

region is addressed in the context of intensified agricultural activity at Velia and Vagnari. If malaria was exerting a toll on economic productivity (as was the case for Italy from 1880-1962), the Roman elite were able to import large numbers of slaves to cultivate agricultural land in the valleys or coastal areas as a form of seasonal labour during the harvest season, when the effects of malaria were intense (Sallares, 2002). However, at the imperial estate at Vagnari, oxygen isotope evidence indicates a predominantly “local” constituent, not an imported workforce (Prowse et al., 2016) and the Vagnari individual from which *P. falciparum* was recovered is isotopically identified as “local”, thereby providing a counter-argument to the vulnerability of non-immune (non-local) individuals to malaria. Similarly, the Velian individual with *P. falciparum* is also presumptively “local” based on strontium and oxygen isotopic analyses (R. Stark, personal communication, May 2016). This preliminarily supports loose inferences of local individuals at Velia and Vagnari as similarly vulnerable to malaria infection, and not just a non-local constituent pre-disposed to malaria. However, whether the *P. falciparum* signature from these individuals is indicative of exposure, infection or tolerance cannot be discerned, but the emphasis remains that contextual determinants unpredictably contribute to multifaceted experiences of malaria at these localities. Similarly, the extent of individuals migrating to Portus, whether as merchants, traders or short-term visitors is presumed as essential to sustaining the population in this “hyperendemic” region (e.g., Scheidel, 2003). Thus, I propose the flux of individuals both into and out of this region (e.g., as one-third

of individuals at Isola Sacra identified by Prowse et al., 2007 were not from the region around Rome), may not only preclude the stationary population necessary to complete the *Plasmodium* lifecycle in situ (in the vector and human), but also potentially manifest confounding factors in detecting malaria signatures in this locality if a presumptively intense degree of malaria exposure led to greater levels of parasite tolerance.

Ultimately, the recovery of *P. falciparum* from ecologically and socially disparate locations at Velia and Vagnari, demonstrates that the expectation for Portus as a malarial hotbed (Sallares, 2002; Scheidel, 2003) is not simply a factor of suitable ecology or an “urban” context, there are inherently nuanced factors that affect the pattern of malaria in a given locality. Although I posit a dynamic scenario of an uneven malaria distribution at Velia, Vagnari, and Portus, this is also unpredictably influenced by heterogeneous susceptibility (e.g., acquired or inherited immunity) and the nature of malaria transmission, which are undetectable. Further, the interconnection of contextual determinants of malaria related to disease ecology and the human-environment interaction, dynamically influence the pathways of exposure in these localities.

Consequently, there is no singular version of the “Roman malaria” as evidenced by the entangled biosocial pathways at Velia, Vagnari, and Portus, involved in enhancing or dampening the burden of malaria. Accordingly, in these heterogeneous environments, it is possible for other pathogens to enhance susceptibility to malaria, or for malaria to enhance susceptibility to other

pathogens. Malaria does not occur on its own, it is part of a dynamic pathogen pool that is embedded within a particular biosocial context structuring the lived experience of disease.

Synergistic Pathogen Interactions and Ancient DNA

Ancient pathogen DNA represents a largely minute fraction within the pool of non-target molecules, and as such it is critical to emphasize its integration across complementary evidentiary sources to expand investigations of pathogen-pathogen interactions in dynamic social and ecological landscapes. It is evident from Chapter 3 that malaria (as an infection or disease), is not only an outcome of the biosocial context, but interacts with other co-circulating diseases that may contribute to overall morbidity and mortality. While Chapter 4 shows that in the success of parallel pathogen detection, it is important to expand this approach as a measure of evaluating shifts in the pathogen burden to explore synergistic interactions. As part of an integrated framework, I emphasize through the following discussion, that ancient DNA is increasingly applicable to elucidate the dynamic interactions of pathogens in a given spatio-temporal context.

Co-infections may be more common than infection by a single pathogen, as the cascading effect of infection with one agent may reduce immunity to subsequent invasions (Cox, 2001; Graham et al., 2007). Accordingly, it is not simply the correlation of a single pathogen with a single disease, but unravelling the interactive causalities that embed these pathogen-pathogen interactions and the multi-faceted process of disease manifestation. The interactions of this

pathogen-pathogen relationships are framed as antagonistic, where one disease hinders the effects of another; synergistic or when one disease facilitates the invasion and subsequent “contagiousness” of another; while independent interactions involve two diseases that do not influence one another (Gonzalez et al., 2010; Singer, 2010). I specifically use the example of malaria as it exemplifies the concept of pathocenosis (see Faure, 2014; Sallares, 2005) to highlight the scope of pathogen interactions for this singular parasite as a means to demonstrate the spectrum of pathogen-pathogen relationships that ancient DNA methodologies are increasingly able to explore.

Although negative pathogen interactions are rare (noted by Faure, 2014), these antagonistic relationships are an intriguing example, specifically for the molecular detection of *P. falciparum* protective variants. These variants are not “pathogens” but function to mitigate severity of the disease process and merit consideration as a negative interaction with malaria. Protective polymorphisms such as the thalassemias and glucose-6-phosphate dehydrogenase deficiency (G6PD) may cause lower parasite loads in individuals (Dronamraju, 2006), thereby complicating detection of *P. falciparum* post-mortem. The geographic distribution of G6PD deficiency and the thalassemias is argued to coincide with the historical record of intense *P. falciparum* transmission in Greece and Italy, as these variants presumably arose 1,500-6,000 years ago (Arese et al., 2006; Tishkoff et al., 2001). For example, putative paleopathological indicators of thalassemia (e.g., porotic hyperostosis on the occipital and parietals, hypertrophic

metacarpals and phalanges) were found in a juvenile skeleton (5th-7th c. A.D.) at *Piazza dei Miracoli* in Pisa (Italy), which is located near a swamp and presumptively, a malarious area (Baggeri & Mallegni, 2001). Molecular evidence of G6PD is similarly reported from one infant at Lugnano (5th c. A.D.) in a burial where previous PCR-based detection yielded a *P. falciparum* 18S rRNA fragment (Sallares & Gomzi, 2001; Sallares et al., 2004). Due to the complexity of immunity acquisition and transmission in antiquity, a molecular investigation of these interactive variants with *P. falciparum* may facilitate characterizing the selection landscape of *Plasmodium* parasites in key localities.

Similarly, a pre-existing malaria infection may hinder the severity of invading pathogens. For example, malarial fevers may inhibit the effects of syphilis (*Treponema pallidum*) or gonorrhea, as the bacteria are temperature sensitive (Snounou & Perignon, 2013). Archaeologically, malaria precludes skeletal identification, whereas syphilis is amenable to paleopathological evaluation (in the minority of cases where tertiary stage lesions manifest), and so, examining the relationship between the degree of co-infection between these pathogens is intriguing using aDNA approaches. Conversely, the relationship between tuberculosis and malaria (or other parasitic diseases) is complex, as the decreased immune response exacerbates tuberculosis infections (Li & Zhou, 2013). A malaria endemic region does not preclude the simultaneous presence of tuberculosis, as for example, Lalremruata et al. (2013) molecularly identified (via PCR) a presumptive co-infection of *P. falciparum* and *Mycobacterium*

tuberculosis in Egyptian mummies, attributed to dense crowding and intensified crop cultivation within an ancient Fayum population. In consideration of the spectrum of skeletal responses upon infection with tuberculosis, the potential to simultaneously target such co-infections molecularly has significant implications for understanding the biosocial context of crowd diseases and parasitic infections.

As previously noted, the interaction between malaria and helminthes is a crucial consideration in ancient Rome broadly, particularly due to the recovery of parasitological remains of whipworm and roundworm across countries of the Empire (e.g., Italy, Egypt, France, Britain) (reviewed by Mitchell, 2016) since these co-infections can be antagonistic or synergistic with malaria (Nacher, 2008). The Imperial period environment (at least in the capital and perhaps cities) indicates the potential for parasitic agents due to ineffective sanitation measures (e.g., latrines, sewage systems, water from aqueducts) (Scobie, 1986). Accordingly, the parasitological remains of helminthes could be further explored through integrated molecular approaches to investigate the coincidence with malaria or other protozoan parasites.

Synergistic interactions are more common than antagonistic ones, as an already compromised immune system is advantageous for invading pathogens (Faure, 2014; Gonzalez et al., 2010). Archaeologically, the investigation of viruses is important in exploring malaria, particularly as viral infections are not detectable paleopathologically, but are also challenging to recover using ancient DNA technology. Respiratory illnesses, such as influenza and pneumonia are

deleterious upon interaction with malaria. For example, individuals with existing malaria infections were more severely affected during the Spanish influenza pandemic (1918-1920) in Iran due a confluence of factors in addition to malaria, such as famine, opium consumption, and anemia contributing to higher mortality rates (Afkhani, 2003), arguing for the potential of influenza to enhance underlying malaria mortality in antiquity. There are even potential strain differences between the human malaria species, as influenza exacerbates *P. falciparum* infections, but not those of *P. vivax* (Shanks & White, 2013). Broadly, malaria-induced immunosuppression may contribute to the severity of such respiratory illnesses, including pneumonia (Bruneel et al., 2003).

Bacterial infections are also adverse upon interaction with malaria, as susceptibility to bacteremia draws on immune system impairment induced by malaria (e.g., red blood cell destruction and anemia, levels of parasitaemia) (Cunnington, 2012; Faure, 2014). Malaria (*P. vivax* or *P. falciparum*) may exacerbate gastrointestinal diseases caused by *Vibrio cholerae*, *Shigella* spp., and *Salmonella* spp. (Cunnington, 2012). For example, previously malaria endemic areas or regions in France encountered greater impacts from cholera (e.g., Dubreuil & Rech, 1836), as it is presumed the ecological conditions favouring the sustainability of malaria may also benefit cholera (Faure, 2014).

Archaeologically, these enteric pathogens are not detectable and may arise from ancient environments without an efficient “sanitation” infrastructure, such as Imperial Italy, and in order to explore the interaction between malaria and these

infections, molecular detection provides a complementary measure to attempt to investigate these “invisible” microbial constituents. As malaria mortality may also be attributable to co-infection from an enteric pathogen in a suitable environment, these co-infections are important due to the potential to shape the mortality pattern.

Similarly as an extension of the heightened mortality from malaria, in consideration of the probable co-circulation of *P. vivax* and *P. falciparum* in malarious environments of the past, the dormant stage of a *P. vivax* infection may be re-activated upon systemic parasitic or bacterial infection (e.g., typhoid fever, brucellosis, epidemic louse-borne typhus) (Shanks & White, 2013). As *P. vivax* is generally of lower parasitaemia than *P. falciparum*, the potential remains for mortality attributed to a relapse triggered by such pathogens. Ultimately, presumptions of catastrophic mortality in malarious environments of the past need not solely be attributed to malaria, due to the potential for other pathogen interactions (e.g., respiratory or gastrointestinal diseases) to heighten mortality from an existing infection, particularly in consideration that malaria mortality broadly ranges from a few percent to 30% in non-immune individuals (Carter & Mendis, 2002).

Necessarily, pathogens are in flux and dynamically respond to the surrounding social, ecological, and economic contexts within which they are embedded. By understanding a singular pathogen, such as malaria (e.g., epidemiology, symptomology, cellular responses), it further enables

understanding the scope of its interactions with other pathogens. For example, seasonal peaks of *P. falciparum*, pneumonia, gastroenteritis and malnutrition following the rainy season (September to October) increased morbidity and mortality among children in Gambia (Brewster & Greenwood, 1992), and further demonstrates the cascading effects of pathogen-pathogen interactions in changing biosocial contexts. The interaction of pathogens with one another and the degree to which this interaction is moderated by antagonistic, synergistic or independent relationships affects the distribution of disease-associated pathogens at any one point in time. Although it is possible to broadly infer such interactions as antagonistic or synergistic, the manner in which these host-microbe interactions manifested in a particular individual will not be known, due to heterogeneous vulnerability and susceptibility.

Accordingly, in order to explore the complex circumstances surrounding exposure to pathogens, the identification of constituents from these microbial pools are important to integrate with the particular biosocial context that constructs this disease distribution. Challenges associated with the skeletal record (e.g., limited and infrequent responses to infectious agents), archaeological evidence (e.g., non-catastrophic burials may not be informative about primary pathogens), and textual sources (e.g., socially constructed descriptions and the inability to ascribe a “species” designation) benefit from the integration of a comprehensive anthropological and ancient DNA strategy. By recognizing the scope of pathogen-pathogen interactions in affecting individual responsiveness

and subsequent distribution of disease, this facilitates framing interactive causalities of health and disease in holistic contexts.

Conclusions

Using a biocultural lens as a means of integrating ancient DNA with the historical record, I have investigated malaria as an important human pathogen in sites from Imperial southern Italy both from a genomics perspective and an ecosocial epidemiological framework, alongside methodological innovations in the detection of multiple pathogens as a shift towards exploring the synergistic infectious disease landscape. The integration of disparate data sets emphasizes the complementarity of each in terms of elucidating historical pathogen presence in its spatiotemporal context, where the challenges of ancient DNA, such as idiosyncratic preservation, variable recovery, molecular damage, and degradation are informed by the literary record which frames the disease experience at a given time and by archaeological evidence for land use patterns and the structures of daily life.

My research focused on the context of Imperial southern Italy to explore the central narrative that malaria was an important part of the experience of people who lived during this period through an innovative approach: first, using ancient DNA analysis to definitively establish the presence of *P. falciparum* malaria in ancient human skeletal remains; and second, using the molecular results to investigate the potential factors framing the relationship between this pathogen, humans, and the environment through an examination of archaeological

and ancient literary sources. From a molecular perspective, the successful recovery of a partial *P. falciparum* mitochondrial genome to the exclusion of all other *Plasmodia* and Apicomplexa demonstrates the capability of hybridization capture to detect the minute remnants of this parasitic infection in ancient human skeletal remains. Given that *Plasmodium* signatures were identified in only two individuals, it was not possible to contribute to the debate surrounding the timing of *Plasmodium* spp. entry into Europe, or to determine the relationship of this Imperial period malaria strain to currently circulating *P. falciparum* isolates. To my knowledge, however, this is the first application of targeted enrichment coupled with high-throughput sequencing to detect genomic signatures of malaria in adults from multiple Imperial period sites in southern Italy. The contextualization of malaria relies on emphasizing its complexity within the human-vector-parasite-environment relationship, where varied factors proliferate or hinder its presence or distribution. Still, much remains uncertain about the pressures exerted by malaria upon the Imperial Italian populace.

Although the recovery of *P. falciparum* is outlined in this thesis, there are implications for further targeting this pathogen in ancient skeletal samples, due to its “invisibility” in the historical record. By “invisibility”, I mean situations in the archaeological record where there is an absence of skeletal changes, no catastrophic or epidemic burials, and where literary sources present challenges in interpreting diseases and epidemics, as is the case for the Greek and Roman literary records (noted by Scheidel, 2009). Not since Sallares and Gomzi (2001)

has malaria been molecularly investigated in Imperial period Italy. It is critical to further evaluate the scope of interactions among adults, due to malaria's potential impact on the social and economic fabric of a society (Snowden, 2008).

Accordingly, there are significant challenges involved in extending the scope of this research in antiquity, which is bound by the limitations in prioritizing skeletal assemblages to maximize the successful recovery of this ancient human parasite. However, this research contributes new knowledge and perspectives to the historical narrative of malaria presence in Velia and Vagnari during the Imperial period (1st-2nd c. A.D.) when the disease was presumed to be at its height (Sallares 2002; Soren, 2003; Scheidel 2009). From the vantage point of an ecosocial epidemiological framework, I suggest that the distribution of malaria was uneven in the studied localities, capable of fluctuations and dynamic influences from contextual determinants associated with disease ecology and the human-environment interaction. Malaria is at once a biological and a cultural entity, with neither separate from the other.

Parallel pathogen detection provides a means of addressing limitations associated with the paleopathological identification of disease (e.g., a spectrum of skeletal responses to infection, equivocal historical record) as not all evidentiary sources combine to provide a consensus on disease-associated pathogens.

Although ancient DNA itself is not without its challenges, the shift towards exploring pathocenosis in a given spatiotemporal context (Faure, 2014; Gonzalez et al., 2010; Grmek, 1969, 1997) illuminates the dynamics of the pathogen burden

(within an individual or population) as responsive to other pathogens, anthropogenic modifiers, and ecological fluctuations (Faure, 2014; Grmek, 1969; Singer, 2010). This research confirms the promise of previous parallel detection approaches (Bos et al., 2015; Devault et al., 2014b) and provides a feasible method to screen for multiple pathogens in a single DNA extract from an ancient specimen, with the complement of qualitative measures (e.g., pathogen probe alignment to sequences, algorithmic assessment) to prioritize the pathogens likely represented in a given sample. This stream of research offers a stringent approach to identify pathogens of interest in the commonly encountered archaeological scenario where the scope of disease-associated pathogens is uncertain. This research contributes to the investigatory trend that the disease process is not singular and the interaction of pathogens with one another, with humans, and local ecology are critical determinants in structuring pathways of risk and exposure.

Future Research Directions

As the cemeteries included in this thesis were from southern Italy, it is ideal to extend the biomolecular search for human *Plasmodium* species in regions beyond. For example, during the malarious period of Italy's history (1880-1962), *P. vivax* was predominant in the northern regions, with *P. falciparum* in the southern regions (Snowden, 2008). This is relevant in consideration that the three species of malaria (*P. vivax*, *P. falciparum*, and *P. malariae*) are presumed to

have entered Europe together, highlighting the potential for co-infection of these species (Sallares, 2002; Sykes & Mabunda, 2002).

This is salient in the discussion surrounding the implication of malaria as one of many factors precipitating the downfall/decline/transformation of the Western Roman Empire (Ward-Perkins, 2005). Ward-Perkins (2005) noted over 210 reasons put forward as contributing to the collapse of the Empire (including malaria), while Cary (1963: 105) presumes malaria was a “local disease” lacking far-reaching effects. The gradual collapse of Rome as a world power may be interpreted as a succession of events (e.g., internal wars, financial and political crises, invasions) (Bury, 1963) that led to an impoverished state of affairs. The categorization of the Imperial period as one of increasing infectious disease and insalubrious living conditions, alongside periodic pestilences (e.g., Antonine Plague in 160 A.D., the Plague of Cyprian in 251 A.D., the Plague of Justinian in 541-543 A.D.) (Harper, 2016; Scheidel, 2003), demonstrate the impact of dynamic factors that ruptured the fabric of Roman civilization over a significant time scale. The impact of malaria within this period of Roman history merits further evaluation from social, environmental, and molecular perspectives, particularly in consideration of the heterogeneity of the disease experience and the challenges of inferring the presence of this pathogen.

Ancient DNA as a molecular approach to the paleopathological investigation of disease is increasingly amenable to integration with complementary evidentiary sources that characterize the historical record of

human disease. Enhancing the screening and prioritization of pathogens from complex samples using novel techniques (e.g., Bos et al., 2015; Devault et al., 2014b) or bioinformatics approaches (e.g., Herbig et al., 2016; Peltzer et al., 2016), emphasizes the necessity of further exploring the contribution of ancient DNA to understanding the dynamics of disease in varied scenarios. One such potential is the application of ancient DNA through a parallel capture approach to elucidate the temporal and spatial progression of disease-associated pathogens in the equilibrium or breakdown of the European pathocenosis before, during and after the Black Death.

The integration of ancient DNA data alongside the historical record is critical to continue exploring questions surrounding the synergistic landscape of disease in a biosocial context. Moving beyond one pathogen as causing one disease and emphasizing the multi-faceted nature of pathogen interactions is significant, and the limitations of evidentiary sources are improved by the inherent complementarity of those same data sets.

REFERENCES

- Adams, F. (1891). *The Genuine Works of Hippocrates*. New York: William Wood and Company.
- Afkhami, A. (2003). Compromised constitutions: the Iranian experience with the 1918 influenza pandemic. *Bulletin of the History of Medicine*, 77(2), 367-392.
- Ali, H., Ahsan, T., Mahmood, T., Bakht, S.F., Farooq, M.U., & Ahmed, N. (2008). Parasite density and the spectrum of clinical illness in falciparum malaria. *Journal of the College of Physicians and Surgeons Pakistan*, 18(6), 362-368.
- Amato, L., Bisogno, G., Cicala, L., Cinque, A., Romano, P., Ruello, M.R., & Russo Ermolli, E. (2010). Palaeo-environmental changes in the archaeological settlement of Elea-Velia: climatic and/or human impact signatures? In Ciarallo, A., Senatore, M.R., (Eds.). *Scienze naturali e archeologia. Il paesaggio antico: interazione uomo/ambiente ed eventi catastrofici* (pp. 13-16). Rome: Aracne Editrice.
- Armelagos, G.J., & Harper, K.N. (2005). Genomics at the origins of agriculture. *Evolutionary Anthropology*, 14, 109-21.
- Arese, P., Ayi, K., Skorokhod, A., & Turrini, F. (2006). Removal of early parasite forms from circulation as a mechanism of resistance against malaria in widespread red blood cell mutations. In Dronamraju, K.R., Arese, P., (Eds.), *Malaria: Genetic and Evolutionary Aspects* (p. 25-55). New York: Springer.
- Arrizabalaga, J. (2002). Problematizing retrospective diagnosis in the history of disease. *Asclepio*, LIV(1), 51-70.
- Baggieri, G., & Mallegni, F. (2001). Morphopathology of some osseous alterations of thalassic nature. *Paleopathology Newsletter*, 116, 10–16
- Baldari, M., Tamburro, A., Sabatinelli, G., Romi, R., Severini, C., Cuccagna, G., ...& Toti, M. 1998. Malaria in Maremma, Italy. *The Lancet*, 351,1246-1247.
- Baron, H., Hummel, S., & Herrmann, B. (1996). *Mycobacterium tuberculosis* complex DNA in ancient human bones. *Journal of Archaeological Science*, 23(5), 667-671.

- Beauchesne, P.D. (2012). Physiological Stress, Bone Growth and Development in Imperial Rome. University of California, Berkley, unpublished PhD dissertation.
- Bei, A.K., & Duraisingh, M.T. (2013). Invasion of host red blood cells by malaria parasites. In Carlton, J.M., Perkins, S.L., Deitsch, K.W., (Eds.), *Malaria Parasites: Comparative Genomics, Evolution and Molecular Biology* (p. 169-197). United Kingdom: Caister Academic Press.
- Bejon, P., Williams, T. N., Liljander, A., Noor, A. M., Wambua, J., Ogada, E., ... & Marsh, K. (2010). Stable and unstable malaria hotspots in longitudinal cohort studies in Kenya. *PLoS Medicine*, 7(7), e1000304.
- Bellotti, P., Calderoni, G., Di Rita, F., D'Orefice, M., D'Amico, C., Esu, D., ... & Valeri, P. 2011. The Tiber river delta plain (central Italy): coastal evolution and implications for the ancient Ostia Roman settlement. *The Holocene*, 21, 1105-1116.
- Bianucci, R., Mattutino, G., Lallo, R., Charlier, P., Jouin-Spriet, H., Peluso, A., ... & Rabino Massa, E. (2008). Immunological evidence of *Plasmodium falciparum* infection in an Egyptian child mummy from the Early Dynastic Period. *Journal of Archaeological Science*, 35,1880-1885.
- Bos, K. I., Schuenemann, V. J., Golding, G. B., Burbano, H. A., Waglechner, N., Coombes, B. K., ... & Krause, J. (2011). A draft genome of *Yersinia pestis* from victims of the Black Death. *Nature*, 478(7370), 506-510.
- Bos, K. I., Jäger, G., Schuenemann, V. J., Vågane, Å. J., Spyrou, M. A., Herbig, A., ... & Krause, J. (2015). Parallel detection of ancient pathogens via array-based DNA capture. *Philosophical Transactions of the Royal Society of London B: Biological Sciences*, 370(1660), 20130375.
- Bouwman, A.S., & Brown, T.A. (2005). The limits of biomolecular palaeopathology: ancient DNA cannot be used to study venereal syphilis. *Journal of Archaeological Science*, 32, 703-715.
- Brewster, D. R., & Greenwood, B. M. (1992). Seasonal variation of paediatric diseases in The Gambia, West Africa. *Annals of Tropical Paediatrics*, 13(2), 133-146.
- Bruce-Chwatt, L.J., & de Zulueta, J. (1980). *The Rise and Fall of Malaria in Europe: A Historico-Epidemiological Study*. Oxford: Oxford University Press.

- Bruneel, F., Hocqueloux, L., Alberti, C., Wolff, M., Chevret, S., Bédos, J. P., ... & Vachon, F. (2003). The clinical spectrum of severe imported falciparum malaria in the intensive care unit: report of 188 cases in adults. *American Journal of Respiratory and Critical Care Medicine*, 167(5), 684-689.
- Brunt, P.A. (1971). *Italian Manpower, 225 B.C.–A.D. 14*. London: Oxford University Press.
- Burbano, H. A., Hodges, E., Green, R. E., Briggs, A. W., Krause, J., Meyer, M., ... & Pääbo, S. (2010). Targeted investigation of the Neandertal genome by array-based sequence capture. *Science*, 328(5979), 723-725.
- Bury, J.B. (1963). The Later Roman Empire. In Chambers, M. (Ed.), *The Fall of Rome: Can it be Explained?* (p 13-20). New York: Holt, Rinehart and Winston.
- Carpenter, M. L., Buenrostro, J. D., Valdiosera, C., Schroeder, H., Allentoft, M. E., Sikora, M., ... & Bustamante, C.D. (2013). Pulling out the 1%: whole-genome capture for the targeted enrichment of ancient DNA sequencing libraries. *American Journal of Human Genetics*, 93(5), 852-864.
- Carter, R., Mendis, K.N., & Roberts, D. (2000). Spatial targeting of interventions against malaria. *Bulletin of the World Health Organization*, 78, 1401-1411.
- Carter, R., & Mendis, K.N. (2002). Evolutionary and historical aspects of the burden of malaria. *Clinical Microbiology Reviews*, 15, 564-594.
- Cary, M. (1963). The Roman Empire: Retrospect and Prospect. In Chambers, M. (Ed.), *The Fall of Rome: Can it be Explained?* (p 103-11). New York: Holt, Rinehart and Winston.
- Chevallier, R. (1976). *Roman Roads*. Field, N.H., Translator. Berkeley: University of California Press.
- Chotivanich, K., Udomsangpetch, R., McGready, R., Proux, S., Newton, P., Pukrittayakamee, S., ... & White, N. J. (2002). Central role of the spleen in malaria parasite clearance. *Journal of Infectious Diseases*, 185(10), 1538-1541.
- Cicala, L. (2013). Il Quartiere occidentale di Elea-Velia. Un'analisi preliminare. *Mélanges de l'École française de Rome-Antiquité*, 125.
<http://mefra.revues.org/1300>

- Conway, D. J., Fanello, C., Lloyd, J. M., Ban, M. S., Baloch, A. H., Somanath, S. D., ... & Thomas, A.W. (2000). Origin of *Plasmodium falciparum* malaria is traced by mitochondrial DNA. *Molecular and Biochemical Parasitology*, *111*(1), 163-171.
- Cox, F.E.G. (2001). Concomitant infections, parasites and immune response. *Parasitology*, *122*, S23–S28.
- Craig, O.E., Biazzo, M., O'Connell, T.C., Garnsey, P., Martinez-Labarga, C., Lelli, R., ... & Bondioli, L. (2009). Stable isotopic evidence for diet at the Imperial Roman coastal site of Velia (1st and 2nd Centuries AD) in Southern Italy. *American Journal of Physical Anthropology*, *139*, 572-83.
- Crompton, P. D., Moebius, J., Portugal, S., Waisberg, M., Hart, G., Garver, L. S., ... & Pierce, S. K. (2014). Malaria immunity in man and mosquito: insights into unsolved mysteries of a deadly infectious disease. *Annual Review of Immunology*, *32*, 157-187.
- Crowe, F., Sperduti, A., O'Connell, T.C., Craig, O.E., Kirsanow, K., Germoni, P., ... & Bondioli, L. (2010). Water-related occupations and diet in two Roman coastal communities (Italy, first to third century AD): correlation between stable carbon and nitrogen isotope values and auricular exostosis prevalence. *American Journal of Physical Anthropology*, *142*, 355-366.
- Cruse, A. (2004). *Roman Medicine*. Gloucestershire: Tempus Publishing Ltd.
- Cucina, A., Vargiu, R., Mancinelli, D., Ricci, R., Santandrea, E., Catalano, P., & Coppa, A. (2006). The necropolis of Vallerano (Rome, 2nd–3rd century AD): an anthropological perspective on the ancient Romans in the Suburbium. *International Journal of Osteoarchaeology*, *16*(2), 104-117.
- Cunha, C.B., & Cunha, B.A. (2008). Brief history of the clinical diagnosis of malaria: from Hippocrates to Osler. *Journal of Vector Borne Disease*, *45*, 194-199.
- Cunnington, A. J. (2012). Malaria and Susceptibility to Other Infections. Ph.D. thesis, School of Hygiene & Tropical Medicine of London.
- DeBarry, J.D., Fatumo, S., & Kissinger, J.C. (2013). The Apicomplexan Genomic Landscape: The Evolutionary Context of *Plasmodium*. In Carlton, J.M., Perkins, S.L., Deitsch, K.W., (Eds.), *Malaria Parasites: Comparative Genomics, Evolution and Molecular Biology* (p. 17-34). United Kingdom: Caister Academic Press.

- Dermody, B.J., de Boer, H.J., Bierkens, M.F.P., Weber, S.L., Wassen, M.J., & Dekker, S.C. (2011). Revisiting the humid Roman hypothesis: novel analyses depict oscillating patterns. *Climate of the Past Discussion*, 7, 2355-2389.
- Devault, A.M., Mortimer, T.D., Kitchen, A., Kieseewetter, H., Enk, J.M., Golding, G.B., Southon, J., Kuch, M., Duggan, A.T.D., Aylward, W., Gardner, S.N., Allen, J.E., King, A.M., Wright, G.D., Kuroda, M., Kato, K., Briggs, D.E.G., Fornaciari, G., Holmes, E.C., Poinar, H.N., Pepperell, C.S. (n.d.). An ancient emerging infection as a cause of maternal sepsis in Late Byzantine Troy (In Review).
- Devault, A.M., Golding, B., Waglechner, N., Enk, J.M., Kuch, M., Tien, J.H., ... & Poinar, H.N. (2014a). Second-pandemic strain of *Vibrio cholerae* from the Philadelphia cholera outbreak of 1849. *New England Journal of Medicine*, 370(4), 334-340.
- Devault, A.M., McLoughlin, K., Jaing, C., Gardner, S., Porter, T. M., Enk, J., ... & Poinar, H.N. (2014b). Ancient pathogen DNA in archaeological samples detected with a Microbial Detection Array. *Nature Scientific Reports*. 4, 42-45.
- Di Rita, F., Celant, A., & Magri, D. (2010). Holocene environmental instability in the wetland north of the Tiber delta (Rome, Italy): sea-lake-man interactions. *Journal of Paleolimnology*, 44, 51-67.
- Dobson, M.J. (1997). *Contours of Death and Disease in Early Modern England*. Cambridge: Cambridge University Press.
- Donoghue, H.D., & Spigelman, M. (2006). Pathogenic microbial ancient DNA: a problem or an opportunity? *Proceedings of the Royal Society of London B: Biological Sciences*, 273, 641-642.
- Drancourt, M., Aboudharam, G., Signoli, M., Dutour, O., & Raoult, D. (1998). Detection of 400-year-old *Yersinia pestis* DNA in human dental pulp. An approach to the diagnosis of ancient septicaemia. *Proceedings of the National Academy of Sciences*, 95, 12637-12640.
- Drancourt, M., & Raoult, D. (2005). Palaeomicrobiology: current issues and perspectives. *Nature Reviews Microbiology*, 3(1), 23-35.
- Dronamraju, K.R. (2006). Introduction. In Dronamraju, K.R., Arese, P., (Eds.), *Malaria: Genetic and Evolutionary Aspects* (p. 2-15). New York: Springer.

- Druilhe, P., Tall, A., & Sokhna, C. (2005). Worms can worsen malaria: towards a new means to roll back malaria? *Trends in Parasitology*, 21(8), 359–362.
- Dubreuil, J., & Rech, A. (1836). *Rapport sur le Choléra-Morbus Asiatique qui a Régné dans le midi de la France en 1835*. Montpellier: Martel.
- Dutour, O. (2013). Paleoparasitology and paleopathology. Synergies for reconstructing the past of human infectious diseases and their pathocenosis. *International Journal of Paleopathology*, 3(3), 145-149.
- Dyson, S.L. (2010). *Rome: A Living Portrait of an Ancient City*. Baltimore: John Hopkins University Press.
- Eckardt, H., (Ed.). (2010). *Roman Diasporas: Archaeological Approaches to Mobility and Diversity in the Roman Empire*. Portsmouth: Journal of Roman Archaeology, Supplement 78.
- Ehrhardt, S., Burchard, G. D., Mantel, C., Cramer, J. P., Kaiser, S., Kubo, M., ... & Mockenhaupt, F. P. (2006). Malaria, anemia, and malnutrition in African children—defining intervention priorities. *Journal of Infectious Diseases*, 194(1), 108-114.
- Enk, J.M., Devault, A.M., Kuch, M., Murgha, Y.E., Rouillard, J.M., & Poinar, H.N. (2014). Ancient whole genome enrichment using baits built from modern DNA. *Molecular Biology and Evolution*, 31, 1292-94.
- Facchini, F., Rastelli, E., & Brasili, P., (2004). Cribra orbitalia and cribra cranialia in Roman skeletal remains from the Ravenna area and Rimini (I-IV century AD). *International Journal of Osteoarchaeology*, 14, 126-136.
- Faerman, M., Jankauskas, R., Gorski, A., Bercovier, H., & Greenblatt, C.L. (1997). Prevalence of human tuberculosis in a Medieval population of Lithuania studied by ancient DNA analysis. *Ancient Biomolecules*, 1, 205–214.
- Faure, E. (2014). Malarial pathocenosis: beneficial and deleterious interactions between malaria and other human diseases. *Frontiers in Physiology*, 5, 441-454.
- Fiammenghi, C.A. (2003). La Necropoli di Elea-Velia: qualche osservazione preliminare. In Cicala, L., Greco, G., (Eds.), *Elea-Velia. Le Nuove ricerche*. Quaderni del Centro Studi Magna Grecia 1 (p. 49-61). Italy: Naus Editoria.

- Fornaciari, G., Giuffra, V., Ferroglia, E., Gino, S., & Bianucci, R. (2010). *Plasmodium falciparum* immunodetection in bone remains of members of the Renaissance Medici family (Florence, Italy, sixteenth century). *Transactions of the Royal Society of Tropical Medicine and Hygiene*, 104, 583-587.
- Giraudi, C., Tata, C., & Paroli, L. (2009). Late Holocene evolution of Tiber river delta and geoarchaeology of Claudius and Trajan harbor, Rome. *Geoarchaeology*, 24, 371-382.
- Gonzalez, J. P., Guiserix, M., Sauvage, F., Guitton, J. S., Vidal, P., Bahi-Jaber, N., ... & Pontier, D. (2010). Pathocenosis: a holistic approach to disease ecology. *EcoHealth*, 7(2), 237-241.
- Gowland, R., & Garnsey, P. (2010). Skeletal evidence for health, nutritional status and malaria in Rome and the Empire. In Eckardt, H. (Ed.), *Roman Diasporas: Archaeological Approaches to Mobility and Diversity in the Roman Empire* (p. 131-156). Portsmouth: Journal of Roman Archaeology, Supplement 78.
- Graham, A.L., Cattadori, I.M., Lloyd-Smith, J.O., Ferrari, M.J., & Bjørnstad, O.N. (2007). Transmission consequences of coinfection: cytokines writ large? *Trends in Parasitology*, 23(6), 284–291.
- Greco, G., & Krinzinger, F. (1994). *Velia: Studi E Ricerche*. Modena: F.C. Panini.
- Greco, G. (1999). Velia: citta` delle acque. In Krinzinger, F., Tocco, G., (Eds.), *Neue Forschungen in Velia* (p. 73-84). Vienna: Austrian Academy of Sciences Press.
- Grmek, M.D. (1969). Préliminaire d'une étude historique des maladies. *Annales. Histoire, Sciences Sociales*, 24(6), 1437–1483.
- Grmek, M.D. (1991). *Diseases in the Ancient Greek World*. London: Hopkins University Press.
- Grmek, M.D. (1997). *Histoire de la Pensée Médicale en Occident: Tome 2, De la Renaissance aux Lumières*. Paris: Le Seuil.
- Haensch, S., Bianucci, R., Signoli, M., Rajerison, M., Schultz, M., Kacki, S., ... & Bramanti, B. (2010). Distinct clones of *Yersinia pestis* caused the Black Death. *PLoS Pathogens*, 6, e1001134.

- Hansen, R.D. (1983). Water and wastewater systems in Imperial Rome. *Journal of the American Water Resources Association*, 19, 263-269.
- Harper, K. (2016). The Environmental Fall of the Roman Empire. *Daedalus*, 145(2), 101-111.
- Hartl, D.L. (2004). The origin of malaria: mixed messages from genetic diversity. *Nature Reviews Microbiology*, 2, 15-22.
- Hawass, Z., Gad, Y.Z., Ismail, S., Khairat, R., Fathalla, D., Hasan, N., ... & Wasef, S. (2010). Ancestry and pathology in King Tutankhamen's family. *Journal of the American Medical Association*, 303, 638-647.
- Herbig, A., Maixner, F., Bos, K. I., Zink, A., Krause, J., & Huson, D. H. (2016). MALT: Fast alignment and analysis of metagenomic DNA sequence data applied to the Tyrolean Iceman. *bioRxiv*, 050559.
- Horsfall, W.R.. (1955). *Mosquitoes: Their Bionomics and Relation to Disease*. New York: Ronald Press Company.
- Hughes, A. L., & Vierra, F. (2001). Very large long-term effective population size in the virulent human malaria parasite *Plasmodium falciparum*. *Proceedings of the Royal Society of London B: Biological Sciences*, 268(1478), 1855-1860.
- Hughes, D.J. (1994). *Pan's Travail: Environmental Problems of the Ancient Greeks and Romans*. Maryland: John Hopkins University Press.
- Inhorn, M. C., & Brown, P. J. (1990). The anthropology of infectious disease. *Annual review of Anthropology*, 19, 89-117.
- Jetten, T.H., & Takken, W. (1994). Anophelism without malaria in Europe. A review of the ecology and distribution of the genus *Anopheles* in Europe. *Wageningen Agricultural University Papers*.
- Jones, W.H.S. (1909). *Malaria and Greek History*. Historical Series No. VIII. Manchester: Manchester University Press.
- Jouanna, J. (1999). *Hippocrates*. (M.B. DeBevoise, Trans). Baltimore: John Hopkins University Press.
- Joy, D. A., Feng, X., Mu, J., Furuya, T., Chotivanich, K., Krettli, A. U., ... & Su, X. (2003). Early origin and recent expansion of *Plasmodium falciparum*. *Science*, 300(5617), 318-321.

- Kay, G. L., Sergeant, M. J., Giuffra, V., Bandiera, P., Milanese, M., Bramanti, B., ... & Pallen, M. J. (2014). Recovery of a medieval *Brucella melitensis* genome using shotgun metagenomics. *mBio*, 5(4), e01337-14.
- Keay, S., & Millett, M. (2005). Integration and discussion. In Keay, S., Millett, M., Paroli, L., Strutt, K., (Eds.), *Portus: An Archaeological Survey of the Port of Imperial Rome* (pp. 269-296). London: Archaeological Monographs of the British School at Rome.
- Keay, S., Millett, M., Paroli, L., & Strutt, K., (Eds.). (2005). *Portus: An Archaeological Survey of the Port of Imperial Rome*. London: Archaeological Monographs of the British School at Rome.
- Keay, S.J., & Paroli, L., (Eds.). (2011). *Portus and its Hinterland: Recent Archaeological Research*. London: Archaeological Monographs of The British School at Rome.
- Keay, S.J. (2012). The port system of Imperial Rome. In Keay, S.J., (Ed.), *Rome, Portus and the Mediterranean* (p. 33-67). London: Archaeological Monographs of the British School at Rome.
- Keiser, J., de Castro, M.C., Maltese, M.F., Bos, R., Tanner, M., Singer, B.H., & Utzinger, J. (2005). Effect of irrigation and large dams on the burden of malaria on a global and regional scale. *American Journal of Tropical Medicine and Hygiene*, 72, 392-406.
- Killgrove, K. (2010). Migration and mobility in Imperial Rome. University of North Carolina at Chapel Hill, Chapel Hill, unpublished PhD dissertation.
- Kindt, T.J., Goldsby, R.A., & Osborne, B.A. (2007). *Kuby Immunology*, 6th edition. New York: W.H. Freeman and Company.
- Knapp, M., & Hofreiter, M. (2010). Next generation sequencing of ancient DNA: requirements, strategies and perspectives. *Genes*, 1, 227-243.
- Krieger, N. (1994). Epidemiology and the web of causation: has anyone seen the spider? *Social Science and Medicine*, 39(7), 887-903.
- Krieger, N. (2001). Theories for social epidemiology in the 21st century: an ecosocial perspective. *International Journal of Epidemiology*, 30, 668-677.
- Krieger, N. (2008). Proximal, distal, and the politics of causation: what's level got to do with it? *American Journal of Public Health*, 98(2), 221-230.

- Krieger, N. (2011). *Epidemiology and the People's Health: Theory and Context*. Oxford: Oxford University Press.
- Krinzinger, F. (1986). Velia. Grabungsbericht 1983-1986. *Journal Romische Historische Mitteilungen*, 28, 31-56.
- Kwiatkowski, D.P. (2005). How malaria has affected the human genome and what human genetics can teach us about malaria. *American Journal of Human Genetics*, 77, 171-92.
- Lalremruata, A., Ball, M., Bianucci, R., Welte, B., Nerlich, A.G., Kun, J.F.J., & Pusch, C.M. (2013) Molecular Identification of Falciparum Malaria and Human Tuberculosis Co-Infections in Mummies from the Fayum Depression (Lower Egypt). *PLoS ONE*, 8, e60307.
- Langholf, V. (1990). *Medical Theories in Hippocrates: Early Texts and "The Epidemics"*. New York: Walter de Gruyter.
- Laurence, R. (1999). *The Roads of Roman Italy: Mobility and Cultural Change*. London: Routledge.
- Lebel, J. (2003). *Health: An Ecosystem Approach*. International Development Research Centre: Canada.
- Leven, K.H. (2004). "At times these ancient facts seem to lie before me like a patient on a hospital bed" – retrospective diagnosis and ancient medical history. In Horstmannshoff, H.F.J., Stol, M., van Tilburg, C.R. (Eds.), *Magic and Rationality in Ancient Near Eastern and Graeco-Roman Medicine* (p. 369-380). Boston: Brill Academic Publishers.
- Li, X. X., & Zhou, X. N. (2013). Co-infection of tuberculosis and parasitic diseases in humans: a systematic review. *Parasites & Vectors*, 6(1), 79-91.
- Littman, R. J., & Littman, M. L. (1973). Galen and the Antonine plague. *The American Journal of Philology*, 94(3), 243-255.
- Loy, D. E., Liu, W., Li, Y., Learn, G. H., Plenderleith, L. J., Sundararaman, S. A., Sharp, P.M., & Hahn, B. H. (2016). Out of Africa: origins and evolution of the human malaria parasites *Plasmodium falciparum* and *Plasmodium vivax*. *International Journal for Parasitology*, doi: 10.1016/j.ijpara.2016.05.008
- MacArthur, W. (1951). A brief story of English malaria. *British Medical Bulletin*, 8, 76-79.

- Mackinnon, M.J., & Marsh, K. (2010). The selection landscape of malaria parasites. *Science*, 328, 866-71.
- Maixner, F., Krause-Kyora, B., Turaev, D., Herbig, A., Hoopmann, M. R., Hallows, J. L., ... & Zink, A. (2016). The 5300-year-old *Helicobacter pylori* genome of the Iceman. *Science*, 351(6269), 162-165.
- Major, R.H. (1978). *Classic Descriptions of Disease: With Biographical Sketches of the Authors*, 3rd edition. Springfield: Charles C. Thomas.
- Manguin, S., Carnevale, P., & Mouchet, J. (2008). *Biodiversity of Malaria in the World*. United Kingdom: John Libbey Eurotext Limited.
- Marciniak, S., Prowse, T.L., Herring, D.A., Klunk, J., Kuch, M., Duggan, A.T., Bondioli, L. Holmes, E. C. and Poinar, H. N. (2016). *Plasmodium falciparum* malaria in 1st-2nd c. A.D. southern Italy. *In Press*, *Current Biology*.
- Martens, P. (2002). Of Malaria and models: challenges in modeling global climate change and malaria risk. In Casman, E.A., Dowlatabadi, H., (Eds.), *The Contextual Determinants of Malaria* (p. 14-26). Washington: RFF Press.
- Mazzini, I., Faranda, C., Giardini, M., Giraudi, C., & Sadori, L. (2011). Late Holocene palaeoenvironmental evolution of the Roman harbour of Portus, Italy. *Journal of Paleolimnology*, 46(2), 243-256.
- Melnikov, A., Galinsky, K., Rogov, P., Fennell, T., Van Tyne, D., Russ, C., ... & Neafsey, D. E. (2011). Hybrid selection for sequencing pathogen genomes from clinical samples. *Genome Biology*, 12(8), R73.
- Miller, R.L., Ikram, S., Armelagos, G.J., Walker, R., Harer, W.B., Shiff, C.J., ... & Maret, S.M. (1994). Diagnosis of *Plasmodium falciparum* infections in mummies using the rapid manual ParaSight-F Test. *Transactions of the Royal Society of Tropical Medicine and Hygiene*, 88, 31–32.
- Mitchell, P.D. (2011). Retrospective diagnosis and the use of historical texts for investigating disease in the past. *International Journal of Paleopathology*, 1, 81-88.
- Mitchell, P.D. (2016). Human parasites in the Roman world: health consequences of conquering an empire. *Parasitology*, 1-11, doi:10.1017/S0031182015001651.

- Molak, M., & Ho, S.Y.W. (2011). Evaluating the impact of post-mortem damage in ancient DNA: a theoretical approach. *Journal of Molecular Evolution*, 73(3-4), 244-255.
- Morley, N. (2005). The salubrioness of the Roman city. In King, H., (Ed.), *Health in Antiquity* (p. 192-204). London: Routledge.
- Morley, N. (2013). Population size and social structure. In Erdkamp, P., (Ed.), *The Cambridge Companion to Ancient Rome* (p. 29-44). Cambridge: Cambridge University Press.
- Mu, J., Duan, J., Makova, K. D., Joy, D. A., Huynh, C. Q., Branch, O. H., ... & Su, X. Z. (2002). Chromosome-wide SNPs reveal an ancient origin for *Plasmodium falciparum*. *Nature*, 418(6895), 323-324.
- Mwangi, T. W., Bethony, J. M., & Brooker, S. (2013). Malaria and helminth interactions in humans: an epidemiological viewpoint. *Annals of Tropical Medicine and Parasitology*, 100, 551-570.
- Nacher, M. (2002). Worms and malaria: noisy nuisances and silent benefits. *Parasite Immunology*, 24(7), 391-393.
- National Center for Biotechnology Innovation (NCBI). 2011. PubMed Health: Malaria. <http://www.ncbi.nlm.nih.gov/pubmedhealth/PMH0001646/> Accessed 10 February 2013.
- Neghina, R., Neghina, A.M., Marincu, I., & Iacobiciu, I. (2010). Malaria, a journey in time: in search of the lost myths and forgotten stories. *The American Journal of the Medical Sciences*, 340(6), 492-498.
- Nerlich, A.G., Schraut, B., Dittrich, S., Jelinek, T.H., & Zink, A. (2008). *Plasmodium falciparum* in Ancient Egypt. *Emerging Infectious Diseases*, 14, 1317-1318.
- Nutton, V. (2004). *Ancient Medicine*. London: Routledge.
- O'Sullivan, L., Jardine, A., Cook, A., & Weinstein, P. (2008). Deforestation, mosquitoes, and ancient Rome: Lessons for today. *BioScience*, 58, 756-760.
- Oerlemans, A., & Tacoma, L.E. (2014). Three Great Killers. *Ancient Society*, 44, 213-241.
- Orlando, L., Gilbert, M.T.P., & Willerslev, E. (2015). Reconstructing ancient genomes and epigenomes. *Nature Reviews Genetics*, 16(7), 395-408.

- Orsel, K., Ho, J., Hatfield, J., Manyama, M., Ribble, C., & van der Meer, F. (2015). Brucellosis serology as an alternative diagnostic test for patients with malaria-like symptoms. *Tanzania Journal of Health Research*, 17(4), 1-10.
- Ortner, D.J. (2011). Human skeletal paleopathology. *International Journal of Paleopathology*, 1(1), 4-11.
- Pääbo, S., Poinar, H.N., Serre, D., Jaenicke-Despres, V., Heble, J., Rohland, N., ..& Hofrieter, M. (2004). Genetic analyses from ancient DNA. *Annual Review of Genetics* 38, 645-679.
- Packard, R.M., & Brown, P.J. (1997). Rethinking health, development and malaria: historicizing a cultural model in international health. *Medical Anthropology*, 17(3), 181-194.
- Parise, M., Bixio, R., Quinto, G., & Savino, G. (2000). Ricerche geologic-speleologiche in cavita artificiali: gli impianti idrici sotterranei di Gravina in Puglia. *Atti Convegno GeoBen 2000*, Torino 7-9: 739-747.
- Pattanayak, S.K., & Yasuoka, J. (2008). Deforestation and malaria: revisiting the human ecology perspective. In Colfer, C.J.P., (Ed.). *Human Health and Forests: A Global Overview of Issues, Practice and Policy* (pp. 197-220). United Kingdom: Earthscan.
- Peltzer, A., Jäger, G., Herbig, A., Seitz, A., Kniep, C., Krause, J., & Nieselt, K. (2016). EAGER: efficient ancient genome reconstruction. *Genome biology*, 17(1), 1.
- Petriaggi, R., Bonacci, G., Carbonara, A., Vittori, M.C., Vivarelli, M.L., & Vori, P. (1995). Scavi a Ponte Galeria: nuove acquisizioni sull'acquedoto di Porto e sulla topografia del territorio Portuense. *Archeologia Laziale*, 12, 361–373.
- Prowse, T.L., Schwarcz, H.P., Saunders, S., Macchiarelli, R., & Bondioli, L. (2004). Isotopic paleodiet studies of skeletons from the Imperial Roman-age cemetery of Isola Sacra, Rome, Italy. *Journal of Archaeological Science*, 3, 259-72.
- Prowse, T.L., Schwarcz, H.P., Garnsey, P., Knyf, M., Macchiarelli, R., & Bondioli, L. (2007). Isotopic evidence for age-related immigration to Imperial Rome. *American Journal of Physical Anthropology*, 132, 510–519.

- Prowse, T.L., Barta, J.L., von Hunnius, T.E., & Small, A.M. (2010). Stable isotope and mtDNA evidence for geographic origins at the site of Vagnari, south Italy. In Eckardt, H., (Ed.), *Roman Diasporas: Archaeological Approaches to Mobility and Diversity in the Roman Empire* (p. 175-198). Portsmouth: Journal of Roman Archaeology, Supplement 78.
- Prowse, T.L., Nause, C., & Ledger, M. (2014). Growing up and growing old on an imperial estate: preliminary palaeopathological analysis of skeletal remains from Vagnari. In Small, A.M., (Ed.), *Beyond Vagnari: New Themes in the Study of Roman South Italy* (p. 111-122). Italy: Edipuglia.
- Prowse, T.L. (2016). Isotopes and mobility in the ancient Roman world. In de Ligt, L., Tacoma, L.E., (Eds.), *Migration and Mobility in the Early Roman Empire* (p. 205-233). Leiden: Brill.
- Rabino Massa, E., Cerutti, N., & Savoia, A.M.D. (2000). Malaria in ancient Egypt: paleo-immunological investigations in predynastic mummified remains. *Chungara (Arica)*, 32, 7–9.
- Raoult, D., Aboudharam, G., Crubezy, E., Larrouy, G., Ludes, B., & Drancourt, M. (2000). Molecular identification by “suicide PCR” of *Yersinia pestis* as the agent of medieval Black Death. *Proceedings of the National Academy of Sciences USA*, 97, 12800-12803.
- Rapport, D.J., Costanza, R., & McMichael, A.J. (1998). Assessing ecosystem health. *TREE*, 13(10), 397-402.
- Retief, F., & Cilliers, L. (2004). Malaria in Graeco-Roman Times. *Acta Classica*, 47, 127-37.
- Rich, S. M., Licht, M. C., Hudson, R. R., & Ayala, F. J. (1998). Malaria’s Eve: evidence of a recent population bottleneck throughout the world populations of *Plasmodium falciparum*. *Proceedings of the National Academy of Sciences*, 95(8), 4425-4430.
- Rich, S.M., & Ayala, F.J. (2006). Evolutionary Origins of Human Malaria Parasites. In Dronamraju, K.R., Arese, P., (Eds.), *Malaria: Genetic and Evolutionary Aspects* (p. 125-146). New York: Springer.
- Roberts, C., & Manchester, K. (2005). *The Archaeology of Disease*, (3rd ed). Ithaca: Cornell University Press.

- Rollo, F., & Marota, I. (1999). How microbial ancient DNA, found in association with human remains, can be interpreted. *Philosophical Transactions of the Royal Society of London B: Biological Sciences*, 354, 111-119.
- Rosenberg, C.E. (1992). Framing disease: illness, society and history. In Rosenberg, C.E., Golden, J., (Eds.), *Framing Disease: Studies in Cultural History* (p. iii-xxvi). New Jersey: Rutgers University Press.
- Sallares, R., & Gomzi, S. (2001). Biomolecular archaeology of malaria. *Ancient Biomolecules*, 3, 195-213.
- Sallares, R. (2002). *Malaria and Rome: A History of Malaria in Ancient Italy*. Oxford: Oxford University Press.
- Sallares, R., Bouwman, A., & Anderung, C. (2004). The spread of malaria to southern Europe in antiquity: new approaches to old problems. *Medical History*, 48(3), 311-328.
- Sallares, R. (2005). Pathocoenoses ancient and modern. *History and Philosophy of the Life Sciences*, 27, 221-240.
- Sallares, R. (2006). Role of environmental changes in the spread of malaria in Europe during the Holocene. *Quaternary International*, 150(1), 21-27.
- Scarborough, J. (1969). *Roman Medicine*. Ithaca: Cornell University Press.
- Scheidel, W. (2003). Germs for Rome. In Edwards, C., Woolf, G., (Eds), *Rome the Cosmopolis* (p. 158-176). Cambridge: Cambridge University Press.
- Scheidel, W. (2004). Demographic and economic development in the ancient Mediterranean world. *Journal of Institutional and Theoretical Economics*, 16, 743-757.
- Scheidel, W. (2009). Disease and death in the ancient city of Rome. Stanford University: Princeton/Stanford Working Papers in Classics.
- Scheidel, W. (2010). Physical wellbeing in the Roman world. Stanford University: Prince/Stanford Working Papers in Classics.

- Schuenemann, V. J., Bos, K., DeWitte, S., Schmedes, S., Jamieson, J., Mittnik, A., ... & Poinar, H.N. (2011). Targeted enrichment of ancient pathogens yielding the pPCP1 plasmid of *Yersinia pestis* from victims of the Black Death. *Proceedings of the National Academy of Sciences*, 108(38), E746-E752.
- Scobie, A. (1986). Slums, sanitation, and mortality in the Roman world. *Klio*, 68, 399-433.
- Service, M.W., Townson, H. (2002). The *Anopheles* vector. In Warrell, D.A., Gilles, H.M., (Eds.) *Essential Malariology*, 4th edition (p. 59-84). London: Arnold.
- Setzer, T.J. (2010). Malaria in prehistoric Sardinia (Italy): an examination of skeletal remains from the middle Bronze Age. Unpublished PhD. University of South Florida.
- Shanks, G. D., & White, N. J. (2013). The activation of vivax malaria hypnozoites by infectious diseases. *The Lancet Infectious Diseases*, 13(10), 900-906.
- Shaw, B.D. (1996). Seasons of death: aspects of mortality in imperial Rome. *Journal of Roman Studies*, 94, 1-26.
- Singer, M. (2010). Pathogen-pathogen interaction: a syndemic model of complex biosocial processes in disease. *Virulence*, 1(1), 10-18.
- Small, A.M., (Ed.). (2011). *Vagnari. The village, the industries the imperial property*. Italy: Edipuglia.
- Small, A.M., (Ed.). (2014). *Beyond Vagnari: New Themes in the Study of Roman South Italy*. Italy: Edipuglia.
- Smith-Guzman, N.E. (2015). Cribra orbitalia in the ancient Nile Valley and its connection to malaria. *International Journal of Paleopathology*, 10, 1-12.
- Snounou, G., Perignon, J.L. (2013). Malariotherapy – insanity at the service of malariology. *Advances in Parasitology*, 81, 223-255.
- Snow, R.W., & Omumbo, J.A. (2006). Malaria. In Jamison, D.T., Feachem, R.G., Makgoba, M.W., Bos, E.R., Baingana, F.K., Hofman, K.J., & Rogo, K.O., (Eds.). *Disease and Mortality in Sub-Saharan Africa* (p. 195-214). Washington: The International Bank for Reconstruction and Development.

- Snowden, F. (2008). *The Conquest of Malaria: Italy, 1900-1962*. New Haven: Yale University Press.
- Soren, D. (2003). Can archaeologists excavate evidence of malaria? *World Archaeology*, 35, 193-209.
- Sperduti, A. (1995). I resti scheletrici umani della necropoli di età romano imperiale di Isola Sacra (i-iii sec. d. C.): analisi paleodemografica. PhD dissertation.
- Sperduti A, Bondioli L, Garnsey P. (2012). Skeletal evidence for occupational structure at the coastal towns of Portus and Velia (1st-3rd c. AD). In Schrufer-Kolb, I., (Ed.). *More Than Just Numbers? The Role of Science in Roman Archaeology* (p. 53-70). Portsmouth: Journal of Roman Archaeology (Supplement 91).
- Sutherst, R.W. (2004). Global change and human vulnerability to vector-borne diseases. *Clinical Microbiology Reviews*, 17, 136-173.
- Sykes, R., & Mabunda, G. (2002). Malaria. In Lashley, F.R., Durham, J.D. (Eds.), *Emerging Infectious Diseases: Trends and Issues* (p.193-202). New York: Springer Publishing Company.
- Taylor, G.M., Rutland, P., & Molleson, T. (1997). A sensitive polymerase chain reaction method for the detection of *Plasmodium* species DNA in ancient human remains. *Ancient Biomolecules*, 1, 193-203.
- Tishkoff, S. A., Varkonyi, R., Cahinhinan, N., Abbas, S., Argyropoulos, G., Destro-Bisol, G., ... & Clark, A.G. (2001). Haplotype diversity and linkage disequilibrium at human G6PD: recent origin of alleles that confer malarial resistance. *Science*, 293(5529), 455-462.
- Tito, R.Y., Knights, D., Metcalf, J., Obregon-Tito, A.J., Cleeland, L., Najjar, F., ... & Foster, M. (2012). Insights from characterizing extinct human gut microbiomes. *PLoS ONE*, 7(12), e51146.
- Tran, T.N.N., Aboudharam, T.G., Raoult, D., & Drancourt, M. (2011). Beyond ancient microbial DNA: nonnucleotide biomolecules for paleomicrobiology. *Biotechniques*, 50, 370-380.
- Tyagi, B.K., Chaudhary, R.C. (1997). Outbreak of falciparum malaria in the Thar Desert (India), with particular emphasis on physiographic changes brought about by extensive canalization and their impact on vector density and dissemination. *Journal of Arid Environments*, 36, 541-555.

- von Hunnius, T.E., Yang, D., Eng, B., Wayne, J.S., & Saunders, S.R. (2007). Digging deeper into the limits of ancient DNA research on syphilis. *Journal of Archaeological Science*, 34, 2091-2100.
- Wagner, D. M., Klunk, J., Harbeck, M., Devault, A., Waglechner, N., Sahl, J. W., ... & Poinar, H.N. (2014). *Yersinia pestis* and the plague of Justinian 541-543 AD: a genomic analysis. *The Lancet Infectious Diseases*, 14(4), 319-326.
- Waltner-Toews, D. (2001). An ecosystem approach to health and its applications to tropical and emerging diseases. *Reports in Public Health*, 17, 7-36.
- Ward-Perkins, B. (2005). *The Fall of Rome and the End of Civilization*. Oxford: Oxford University Press.
- Warinner, C., Rodrigues, J. F. M., Vyas, R., Trachsel, C., Shved, N., Grossmann, J., ... & Cappellini, E. (2014). Pathogens and host immunity in the ancient human oral cavity. *Nature Genetics*, 46(4), 336-344.
- White, K.D. (1976). Food requirements and food supplies in classical times in relation to the diets of the various classes. *Progress in Food Nutrition and Science*, 2, 143–191.
- Wilairatana, P., Tangpukdee, N., & Krudsood, S. (2013). Definition of hyperparasitemia in severe falciparum malaria should be updated. *Asian Pacific Journal of Tropical Biomedicine*, 3, 586.
- Wood, J.W., Milner, G.R., Harpending, H.C., & Weiss, K.M. (1992). The osteological paradox: problems of inferring prehistoric health from skeletal samples. *Current Anthropology*, 33, 343-370.
- Woolf, G. (1998). *Becoming Roman: The Origins of Provincial Organization in Gaul*. Cambridge: Cambridge University Press.
- Wright, L.E., & Yoder, C.J. (2003). Recent progress in bioarchaeology: approaches to the osteological paradox. *Journal of Archaeological Research*, 11, 43-70.
- Yasuoka, J., Levins, R. (2007). Impact of deforestation and agricultural development on Anopheline ecology and malaria epidemiology. *American Journal of Tropical Medicine and Hygiene*, 76, 450-460.
- Zink, A., Haas, C.J., Herberth, K., & Nerlich, A.G. (2001). PCR amplification of *Plasmodium* DNA in ancient human remains. *Ancient Biomolecules*, 3, 293.